

PB293542



Report to

THE NATIONAL SCIENCE FOUNDATION (RANN)  
Grant No. ENV74-14766

EARTHQUAKE RESISTANT STRUCTURAL WALLS -  
TESTS OF COUPLING BEAMS

by

G. B. Barney  
K. N. Shiu  
B. G. Rabbat  
A. E. Fiorato  
H. G. Russell  
W. G. Corley

Any opinions, findings, conclusions,  
or recommendations expressed in this  
publication are those of the author(s)  
and do not necessarily reflect the views  
of the National Science Foundation.

Submitted by  
PORTLAND CEMENT ASSOCIATION  
RESEARCH AND DEVELOPMENT  
CONSTRUCTION TECHNOLOGY LABORATORIES  
5420 Old Orchard Road  
Skokie, Illinois 60077

January 1978





<b>REPORT DOCUMENTATION PAGE</b>	1. REPORT NO. NSF/RA-780501	2.	3. Recipient's Accession No. <b>PB293542</b>
4. Title and Subtitle Earthquake Resistant Structural Walls - Tests of Coupling Beams		5. Report Date January 1978	
7. Author(s) G.B. Barney, K.N. Shiu, B.G. Rabbat, et al.		8. Performing Organization Rept. No. PCA R/D Ser. 1583	
9. Performing Organization Name and Address Portland Cement Association 5420 Old Orchard Road Skokie, Illinois 60077		10. Project/Task/Work Unit No.  11. Contract(C) or Grant(G) No. (C) (G) ENV7414766	
12. Sponsoring Organization Name and Address Applied Science and Research Applications (ASRA) National Science Foundation 1800 G Street, N.W. Washington, D.C. 20550		13. Type of Report & Period Covered Final (1974-1977) 14.	
15. Supplementary Notes			
16. Abstract (Limit: 200 words) Eight model reinforced concrete coupling beam specimens were subjected to reversing loads representing those that would occur in beams of coupled structural walls during a severe earthquake. Effects of selected variables on hysteretic response were determined. Controlled variables included shear span-to-effective depth ratio of the beams, reinforcement details, and size of the confined concrete core. Tests indicated that hysteretic performance of beams with conventional reinforcement is limited by deterioration that results in sliding in the hinging region. Full-length diagonal reinforcement significantly improved the performance of short beams. The improvement for long-span beams was less significant. Larger concrete core size improved load retention capacity.			
17. Document Analysis a. Descriptors Bend properties                      Earthquake resistant structures                      Tests Concrete structures                      Energy dissipation                      Ultimate strength Cyclic loads                      Plastic deformation                      Yield strength Ductility                      Shear properties                      Beams (supports) b. Identifiers/Open-Ended Terms                      Concrete construction                      Buildings  Shear walls Structural walls  c. COSATI Field/Group			
18. Availability Statement NTIS		19. Security Class (This Report)	21. No. of Pages 152
		20. Security Class (This Page)	22. Price PC F708 MF701



## TABLE OF CONTENTS

	<u>Page No.</u>
HIGHLIGHTS . . . . .	1
INTRODUCTION . . . . .	2
Previous Investigations . . . . .	2
Objectives and Scope . . . . .	4
OUTLINE OF EXPERIMENTAL PROGRAM . . . . .	6
Test Specimens . . . . .	6
Specimen Design . . . . .	6
Specimens C2, C5, and C7 . . . . .	9
Specimens C1, C3, and C4 . . . . .	9
Specimens C6 and C8 . . . . .	9
Test Procedure . . . . .	11
GENERAL RESPONSE CHARACTERISTICS . . . . .	15
Conventional Longitudinal Reinforcement . . . . .	15
Diagonal Reinforcement in Hinging Regions . . . . .	16
Full-Length Diagonal Reinforcement . . . . .	25
STRENGTH CHARACTERISTICS . . . . .	29
Observed Strengths . . . . .	29
Calculated Strengths . . . . .	31
DEFORMATION CHARACTERISTICS . . . . .	33
Load Versus Deflection Envelopes . . . . .	33
Ductility . . . . .	39
Energy Dissipation Capacity . . . . .	39
SUMMARY AND CONCLUSIONS . . . . .	49
Conventional Longitudinal Reinforcement . . . . .	49
Diagonal Reinforcement in Hinging Region . . . . .	50
Full-Length Diagonal Reinforcement . . . . .	50
Final Remarks . . . . .	51
ACKNOWLEDGMENTS . . . . .	52
REFERENCES . . . . .	53

TABLE OF CONTENTS (Continued)

	<u>Page No.</u>
APPENDIX A - EXPERIMENTAL PROGRAM . . . . .	A-1
Test Specimens . . . . .	A-1
Details of Reinforcement . . . . .	A-1
Materials . . . . .	A-9
Fabrication . . . . .	A-12
Supporting and Loading Systems . . . . .	A-12
Instrumentation . . . . .	A-15
Test procedure . . . . .	A-17
APPENDIX B - TEST RESULTS . . . . .	B-1
Specimen C1 . . . . .	B-1
Specimen C2 . . . . .	B-11
Specimen C3 . . . . .	B-19
Specimen C4 . . . . .	B-29
Specimen C5 . . . . .	B-39
Specimen C6 . . . . .	B-47
Specimen C7 . . . . .	B-55
Specimen C8 . . . . .	B-63
APPENDIX C - CALCULATION OF LOAD VERSUS DEFLECTION ENVELOPES . . . . .	C-1
Basic Calculations . . . . .	C-1
Modified Calculations . . . . .	C-4
APPENDIX D - NOTATION . . . . .	D-1

EARTHQUAKE RESISTANT STRUCTURAL WALLS -  
TESTS OF COUPLING BEAMS

by

G. B. Barney, K. N. Shiu, B. G. Rabbat,  
A. E. Fiorato, H. G. Russell, and W. G. Corley\*

HIGHLIGHTS

Eight model reinforced concrete coupling beam specimens were subjected to reversing loads representing those that would occur in beams of coupled structural walls during a severe earthquake. Effects of selected variables on hysteretic response were determined. Controlled variables included shear span-to-effective depth ratio of the beams, reinforcement details, and size of the confined concrete core. Load versus deflection, strength, energy dissipation, and ductility characteristics were the basic parameters used to evaluate performance.

Beams had shear span-to-effective depth ratios of either 1.4 or 2.8. This corresponds to span-to-total depth ratios of 2.5 or 5.0, respectively. Tests indicated that hysteretic performance of beams with conventional reinforcement is limited by deterioration that results in sliding in the hinging region. Full-length diagonal reinforcement significantly improved the performance of short beams. The improvement for long-span beams was less significant. Larger concrete core size improved load retention capacity.

---

\*Respectively, Structural Engineer, Associate Structural Engineer, Structural Engineer, Structural Development Section; Manager, Construction Methods Section; Manager, Structural Development Section; and Director, Engineering Development Department, Portland Cement Association, Skokie, Illinois.

## INTRODUCTION

The Portland Cement Association is carrying out a program to develop design criteria for reinforced concrete structural walls used as lateral bracing in earthquake-resistant buildings. The program includes both analytical and experimental investigations of isolated walls, coupled walls, and frame-wall systems. Of primary concern is the strength, energy dissipation capacity, and ductility of the walls and wall systems.

As part of the experimental program, tests were conducted to evaluate the behavior of reinforced concrete coupling beams under inelastic load reversals. The tests were done prior to the investigation of coupled walls. Coupling beams are used to join adjacent structural walls. Therefore, understanding hysteretic response of coupling beams is a prerequisite to understanding coupled wall response.

This report describes the results of tests on eight reinforced concrete coupling beam specimens subjected to static reversing loads.

### Previous Investigations

Several investigations by other researchers provided background information for this test series.

Brown and Jirsa<sup>(1)</sup> tested doubly-reinforced cantilever beams. These tests indicated that under inelastic load reversals intersecting cracks formed vertical slip planes through the beams. The formation of these planes led to an eventual breakdown in shear transfer as loading progressed. The breakdown was intensified as residual tensile strains developed in the longitudinal reinforcement. Decreasing stirrup spacing improved hysteretic response, but did not eliminate "sliding shear" as the limiting condition. The beams tested had shear span-to-effective depth ratios of either 6.0 or 3.0. Maximum nominal shear stresses ranged from  $2 \sqrt{f'_c}$  to  $7 \sqrt{f'_c}$  psi ( $0.17 \sqrt{f'_c}$  to  $0.58 \sqrt{f'_c}$  MPa).

---

\*Numbers in parentheses refer to the list of references at the end of this report.



Tests by Paulay and Binney<sup>(2)</sup> on deep coupling beams with conventional reinforcement also resulted in sliding shear failures. To prevent sliding shear, Paulay and Binney used full-length diagonal reinforcement. This arrangement changed the load transfer mechanism to that of a Mesnager hinge. For similar load histories, diagonally reinforced beams sustained their load capacity over a greater number of load cycles and dissipated more energy than conventionally reinforced beams. The beams had shear span-to-effective depth ratios of approximately 0.9. Maximum nominal shear stresses ranged from  $9\sqrt{f'_c}$  to  $1.4\sqrt{f'_c}$  psi ( $0.75\sqrt{f'_c}$  to  $1.16\sqrt{f'_c}$  MPa).

Bertero and Popov<sup>(3)</sup> investigated other arrangements of special reinforcement using cantilever beams with a shear span-to-effective depth ratio of 3.1. Maximum loads on the beams were equivalent to nominal shear stresses of approximately  $6\sqrt{f'_c}$  psi ( $0.5\sqrt{f'_c}$  MPa).

In addition to closely spaced confinement hoops with supplementary cross-ties, Bertero and Popov tested beams with supplementary diagonal reinforcement within the hinging region. Their results showed that the ability of the beams to maintain load and dissipate energy was significantly improved by reducing tie spacing. They also found that diagonal web reinforcement in combination with vertical ties minimized stiffness loss and stabilized hysteretic response under increasing inelastic loading cycles.

Wight and Sozen<sup>(4)</sup> tested a series of columns under large deflection reversals. The specimens were tested as cantilevers with and without axial compressive forces. The shear span-to-effective depth ratio for the tests was 3.5. Maximum nominal shear ranged from  $4\sqrt{f'_c}$  to  $6\sqrt{f'_c}$  psi ( $0.33\sqrt{f'_c}$  to  $0.5\sqrt{f'_c}$  MPa). These tests verified that progressive decrease in strength and stiffness occurs with cycling in the inelastic range. Transverse reinforcement used to confine the concrete core and carry the total shear improved the hysteretic response. However, provision of transverse reinforcement to carry the entire shear did not eliminate the possibility of shear failure with large load reversals. Rather the concrete core must remain intact

for shear to be transferred. Therefore, effective confinement of the core is essential.

Although the tests described in this report are an extension of previous investigations, they were planned as a part of the overall program on structural walls. Therefore, the specimens were designed to have the same details planned for the test program on coupled wall systems.

### Objectives and Scope

The objectives of this investigation were:


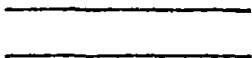
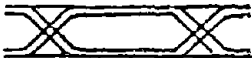



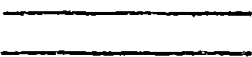
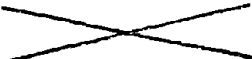
1. To provide information for selecting details of coupling beams for use in tests of structural wall systems.
2. To determine strengths of coupling beams subjected to reversing loads.
3. To determine load versus deflection characteristics of coupling beams with various reinforcing details.
4. To determine ductility and energy dissipation capacities of coupling beams subjected to reversing loads.

Eight specimens were tested. They represented approximately 1/3-scale models although no specific prototypes were considered. Specimens were subjected to in-plane reversing loads simulating those in beams of coupled structural walls.

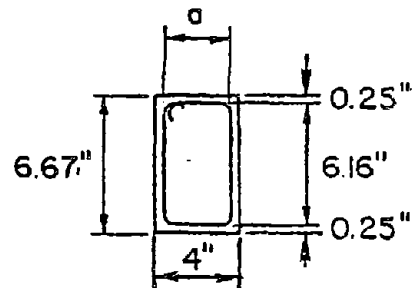
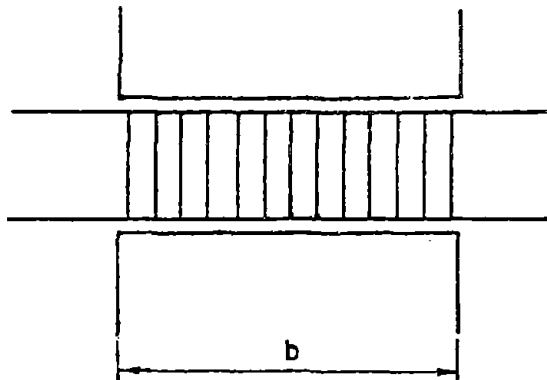
Controlled variables included in the program were the type and arrangement of primary reinforcement, span-to-depth ratio and size of confined concrete core. Details of specimens tested are listed in Table 1.

This report includes a description of the experimental program and the observed response of the test specimens. Effects of controlled variables are analyzed. Strength, load versus deflection relationships, energy dissipation and ductility are the basic parameters used to evaluate performance.

Table 1 Test Program Variables

Specimen	Core Width a (in.)	Span Length b (in.)	Primary Reinforcement
C1	2.63	16.67	
C2	2.63	16.67	
C3	2.63	16.67	
C4	3.50	16.67	
C5	3.50	16.67	
C6	3.50	16.67	
C7	3.50	33.33	
C8	3.50	33.33	

1 in. = 25.4 mm



## OUTLINE OF EXPERIMENTAL PROGRAM

This section includes a brief description of the test specimens and test procedure. A more detailed description is given in Appendix A.

### Test Specimens

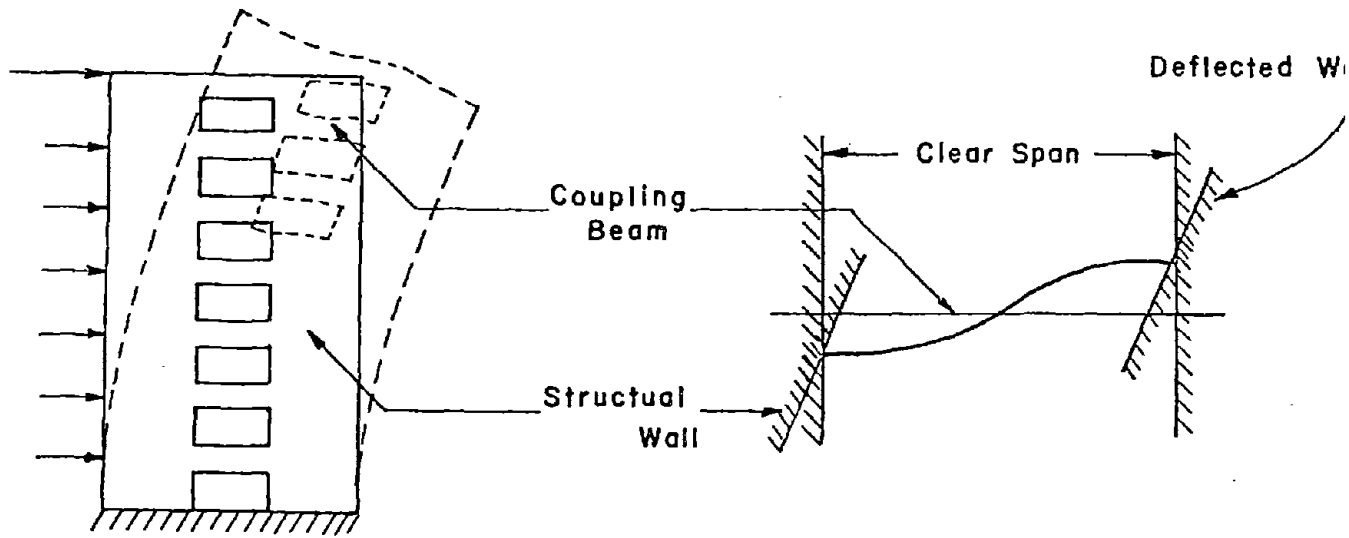
The configuration of the test specimens was selected so that applied loads represented those on beams in coupled walls subjected to lateral forces. Beam deformations were idealized as shown in Fig. 1. The test specimen is shown in Fig. 2. Each specimen consisted of two coupling beams framing into abutment walls at each end. End conditions imposed by the abutments represented those at the beam-wall intersection of coupled walls.

The beams had rectangular cross sections 4-in. (102 mm) wide and 6.67-in. (169 mm) deep. The effective depth of the main longitudinal reinforcement was 6.1-in. (155 mm). Beam lengths were 16.67-in. (423 mm) or 33.33-in. (847 mm). These corresponded to shear span-to-effective depth ratios of 1.4 and 2.8, respectively. The L-shaped abutment walls were 4-in. (102 mm) thick. Overall dimensions of the specimens are given in Fig. 3.

### Specimen Design

The short coupling beams were designed to carry maximum forces corresponding to nominal shear stresses of approximately  $9\sqrt{F'_C}$  psi ( $0.75\sqrt{F'_C}$  MPa). For design, concrete strength was taken as 3,000 psi (20.7 MPa) and steel yield strength as 60 ksi (414 MPa). Steel strain hardening of 50% was assumed. Primary reinforcement was selected to develop capacities corresponding to the desired maximum shear stress levels. To avoid anchorage failures, development lengths were taken 50% greater than those required by the 1971 ACI Building Code.<sup>(5)</sup>

Transverse hoop reinforcement was provided in all specimens to resist shear and to confine the concrete core. The hoops consisted of D-3 deformed wire spaced 1.33-in. (34 mm) on centers. Design of the reinforcement was such that stresses in



a) Deformed Wall System

b) Deformed Beam

Fig. 1 Idealized Coupling Beam Deformations

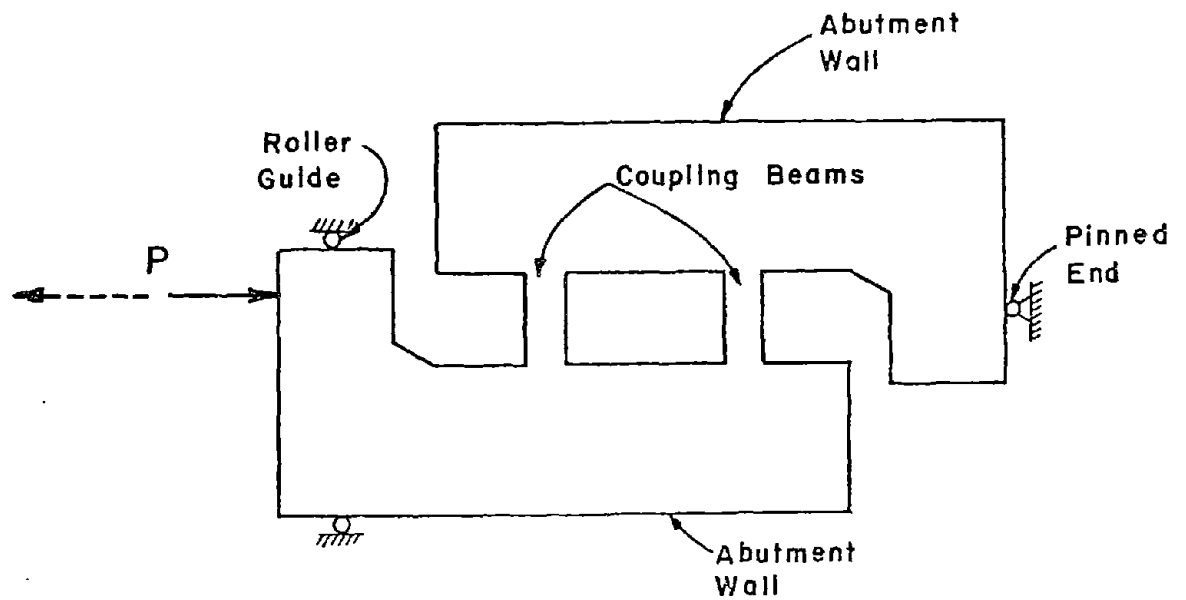


Fig. 2 Test Specimen

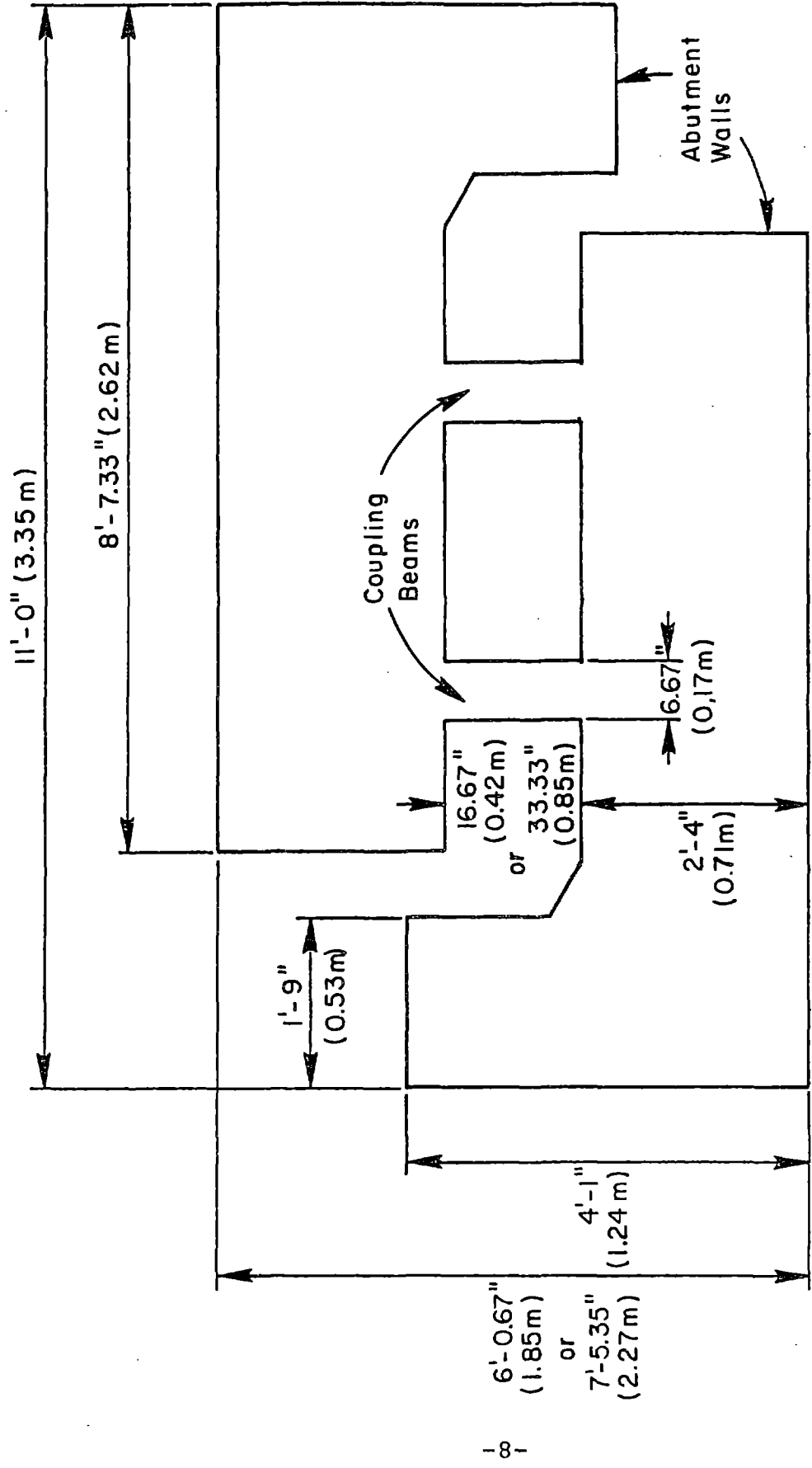


Fig. 3 Specimen Geometry

the hoops were below yield at forces corresponding to the maximum capacity of the beams. Shear stresses were calculated using Eq. 11-3 of the 1971 ACI Building Code<sup>(5)</sup> with the capacity reduction factor  $\phi = 1.0$ . Shear reinforcement was proportioned according to Eq. 11-13 of the 1971 ACI Building Code.<sup>(5)</sup> Nominal concrete shear stress capacity was neglected. The hoops also met the requirements for transverse reinforcement in flexural members of special ductile frames in Section A.5 of the 1971 ACI Building Code.<sup>(5)</sup>

#### Specimens C2, C5, and C7

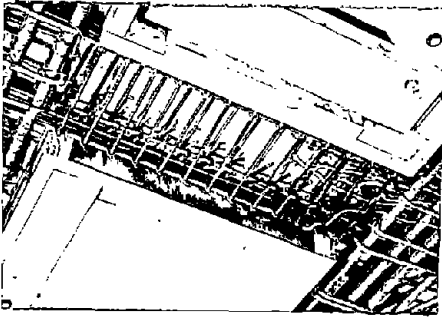
Specimens C2, C5, and C7 had straight longitudinal reinforcement, consisting of four 6-mm bars top and bottom. Photographs of the reinforcement are shown in Figs. 4(a) and 4(b). A larger confined concrete core was provided for Specimens C5 and C7. Shear span-to-effective depth ratio of Specimen C2 and C5 was 1.4. For Specimen C7, this ratio was 2.8.

#### Specimens C1, C3, and C4

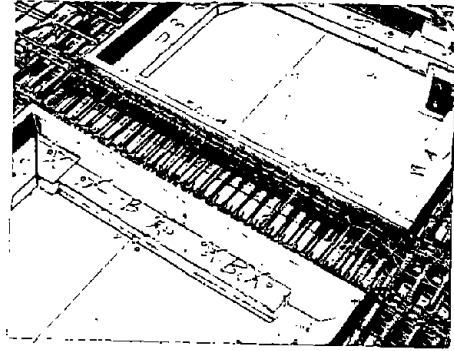
Specimens C1, C3, and C4 had diagonal bars in the hinging regions. This reinforcement was provided to reduce shear deterioration as suggested in tests by Bertero and Popor.<sup>(3)</sup> Design of these bars was based on the assumption that they would behave as diagonal truss members after the concrete deteriorated under repeated load reversals. They were designed to carry the maximum shear force without yielding. For Specimen C1, two 6-mm bars from both top and bottom were bent at 45 degrees starting at the face of the wall at each end of the beam as shown in Fig. 4(c). Specimens C3 and C4 contained two additional 6-mm bars top and bottom bent at 45 degrees. A photograph of this reinforcement is shown in Fig. 4(d) for Specimen C4. Additional reinforcement details are presented in Appendix A.

#### Specimens C6 and C8

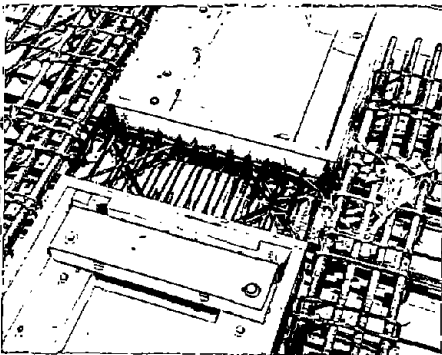
Specimens C6 and C8 had full-length diagonal reinforcement. This detail was used by Paulay and Binney<sup>(2)</sup> for coupling beams with shear span-to-effective depth ratios less



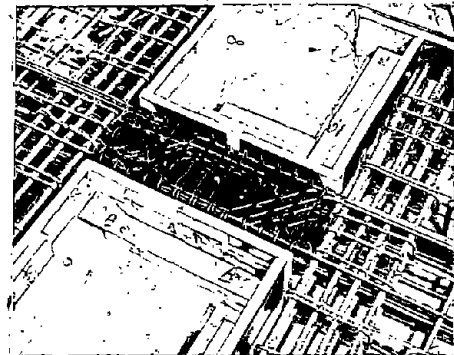
a) Specimen C2



b) Specimen C7



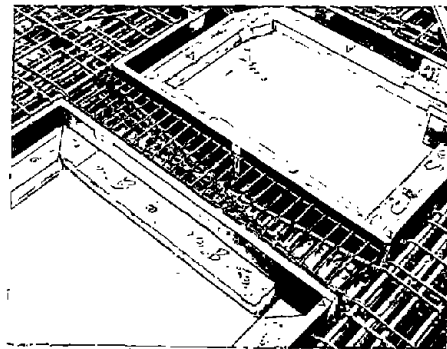
c) Specimen C1



d) Specimen C4



e) Specimen C6



f) Specimen C8

Fig. 4 Reinforcement for Test Specimens



than 0.9. Specimens C6 and C8 had shear span-to-effective depth ratios of 1.4 and 2.8, respectively.

Full-length diagonals for short beam specimens were designed to carry the maximum shear force corresponding to a nominal stress of  $9\sqrt{f'_c}$  psi ( $0.76\sqrt{f'_c}$  MPa). The area of diagonal reinforcement,  $A_s$ , was calculated as:

$$A_s = \frac{V_u}{2f_s \sin\alpha} \quad (1)$$

where:

$V_u$  = maximum shear force

$f_s$  = stress in diagonal reinforcement (90 ksi;  
621 MPa)

$\alpha$  = angle between diagonal bar and horizontal

Using this approach, a single No. 4 bar was provided in one direction and two No. 3 bars were used in the opposite direction.

Transverse hoops were provided to contain concrete in the core during reversals and to prevent buckling of the diagonal bars. Longitudinal bars supporting transverse hoops were not anchored in the abutment walls.

The reinforcement details used for Specimens C6 and C8 are shown in Figs. 4(d) and 4(f), respectively.

#### Test Procedure

The test setup is shown in Fig. 5. Specimens were placed parallel to the laboratory floor and supported on thrust bearings. Loads were applied by hydraulic rams at one end and resisted by a fixed support at the opposite end. The line of action of forces passed through the mid-length of the coupling beams.

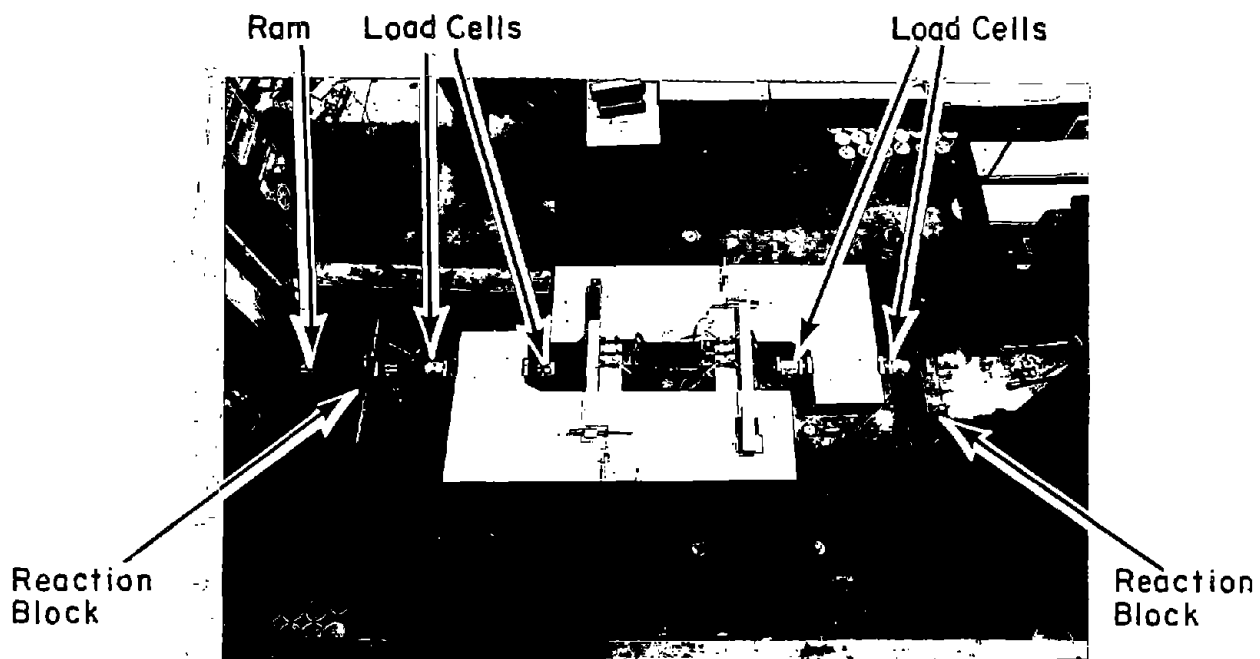


Fig. 5 Test Setup

Loading was controlled by the magnitude of applied force prior to yielding and by imposed deflections after yielding. For each increment of applied load or deflection, three completely reversed load cycles were applied. This is illustrated in Fig. 6. Deflections in successive increments were increased until the specimen was destroyed.

Instrumentation was provided to measure applied loads, deflections, beam elongations, and reinforcing steel strains.

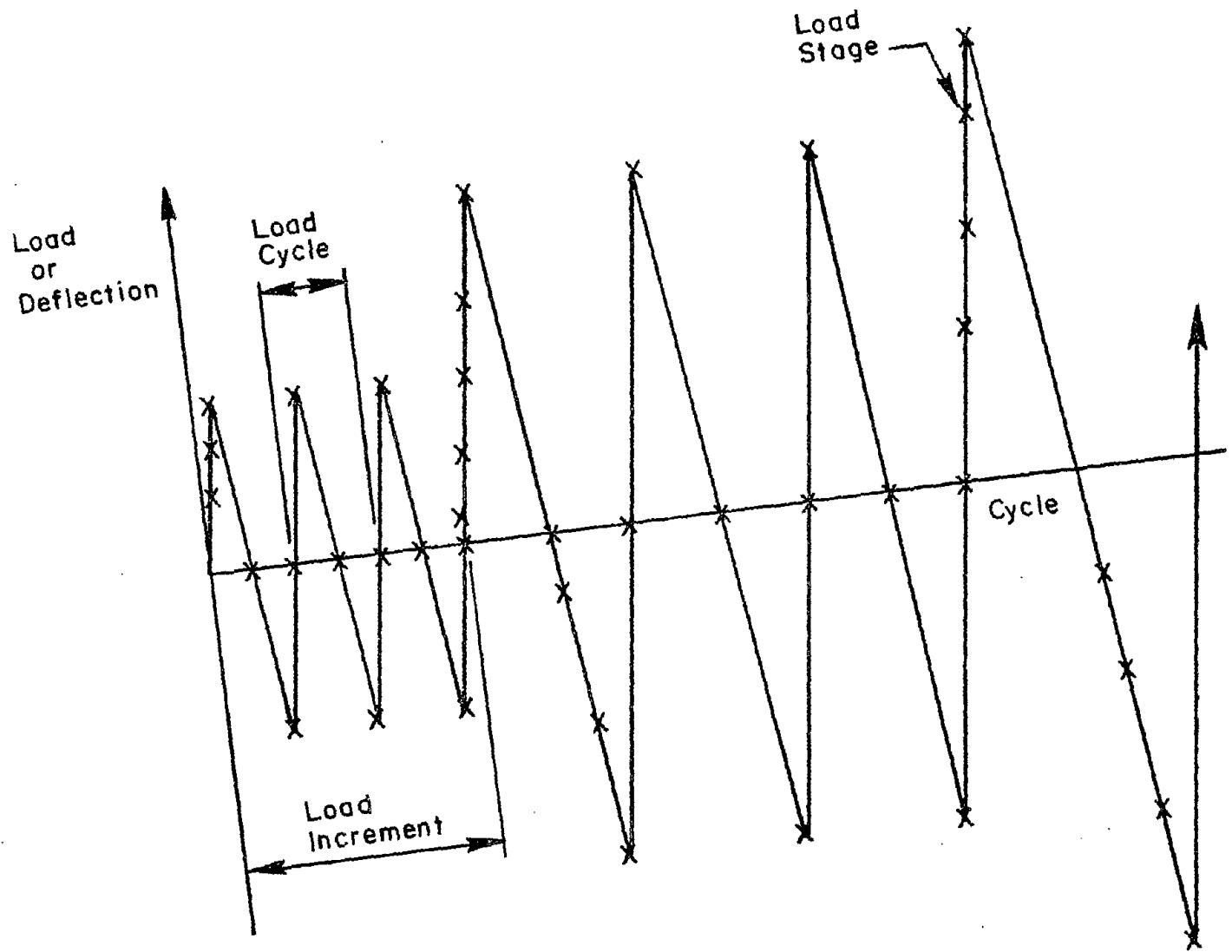


Fig. 6 Load or Deflection History

## GENERAL RESPONSE CHARACTERISTICS

In evaluating the test results, applied load was assumed to be divided equally between the two beams in each specimen. This assumption was checked by comparing companion measurements from each beam and by visual observation of the beams during testing. Except for Specimen C3, the performance of the two beams in each specimen was similar. In Specimen C3 one of the beams deteriorated much more rapidly than the other after the maximum load was reached. Test results for this specimen must be considered accordingly.

### Conventional Longitudinal Reinforcement

Specimens C2, C5, and C7 had conventional longitudinal reinforcement. Specimens C2 and C5, had short-span beams and core widths of 2.63- and 3.50-in. (67 and 89 mm), respectively. Specimen C7 had long-span beams and a core width of 3.50 in. (89 mm). Load versus deflection relationships for the specimens are shown in Figs. 7, 8, and 9. Photographs inset in these figures show the beams after testing. Plotted loads are those for each beam. Deflections are the relative displacements between ends of the beams.

Performance of the beams with conventional straight longitudinal reinforcement was limited by deterioration of the shear resisting mechanism in the hinging region. Under reversing loads, intersecting cracks propagated across the entire depth of the beams at their ends. As subsequent inelastic load reversals were applied, concrete at the ends was destroyed by cracking, abrasion, and spalling. With the concrete destroyed, shear transfer by "truss action" was not possible and the transverse hoops became ineffective. Interface shear transfer was also lost. Eventually, dowel action of longitudinal reinforcement provided the primary shear resistance. This loss of shear transfer is often termed "sliding shear" behavior. Because sliding was developed along a plane parallel to the transverse reinforcement, even the closely spaced hoops become

inefficient in transmitting shear. However, the hoops provided confinement of the concrete core.

Deterioration of the concrete at the ends of the beams was intensified by elongation of the beams, caused by residual tensile strains in the longitudinal reinforcement. These strains developed with successive load reversals into the inelastic range. In addition, partial slip of reinforcement anchored in the abutment walls contributed to widening cracks at the ends of the beams. Slip developed as bond between concrete and reinforcement deteriorated under inelastic load reversals.

Degradation of the shear transfer mechanism and deterioration of the confined concrete core were associated with "pinching" of the load versus deflection hoops as shown in Figs. 7, 8, and 9. The pinching occurred because, as loads were reversed, slip along the interface took place with little increase in load. Eventually, concrete surfaces on either side of the interface were brought into contact and the load resistance increased. In addition, shear transfer by dowel action of the longitudinal reinforcement increased. As the number of load cycles increased, continued abrasion and crushing of concrete in the critical region resulted in a complete breakdown of the shear transfer mechanism at the interface.

Both short and long-span coupling beams exhibited pinching. However, it was relatively less severe for the long-span beams.

#### Diagonal Reinforcement in Hinging Regions

To improve the performance of short-span beams, diagonal reinforcement was provided in the hinging region of several specimens. This reinforcement was patterned after details tested by Bertero and Popor.<sup>(3)</sup> However, modifications were made to simplify fabrication.

Specimens C1, C3, and C4 had diagonal reinforcement in the hinging regions as indicated in Fig. 4 and Table 1. Specimens C1 and C3, with the smaller core size, had single and double

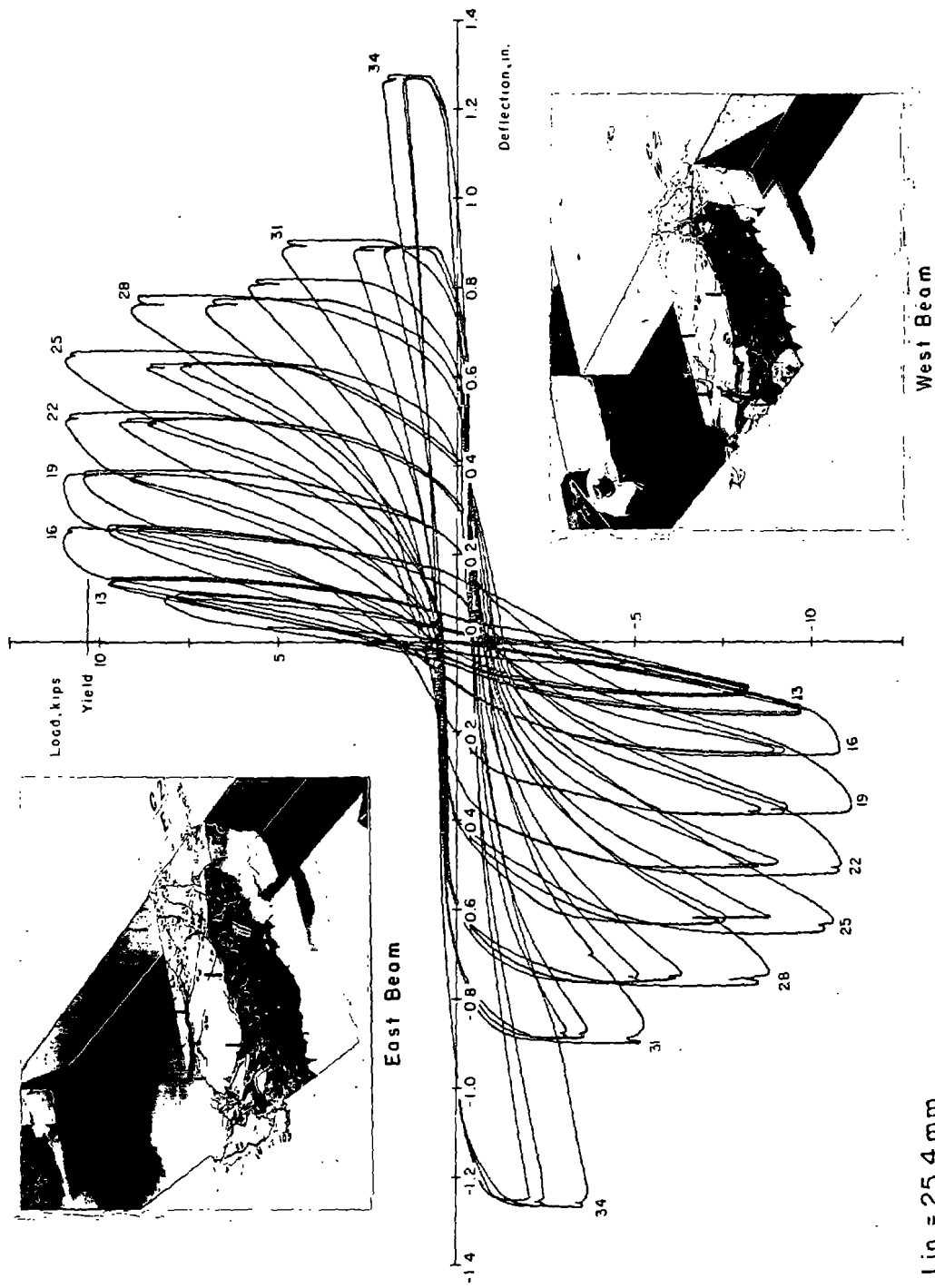


Fig. 7 Load versus Deflection Relationship for Specimen C2

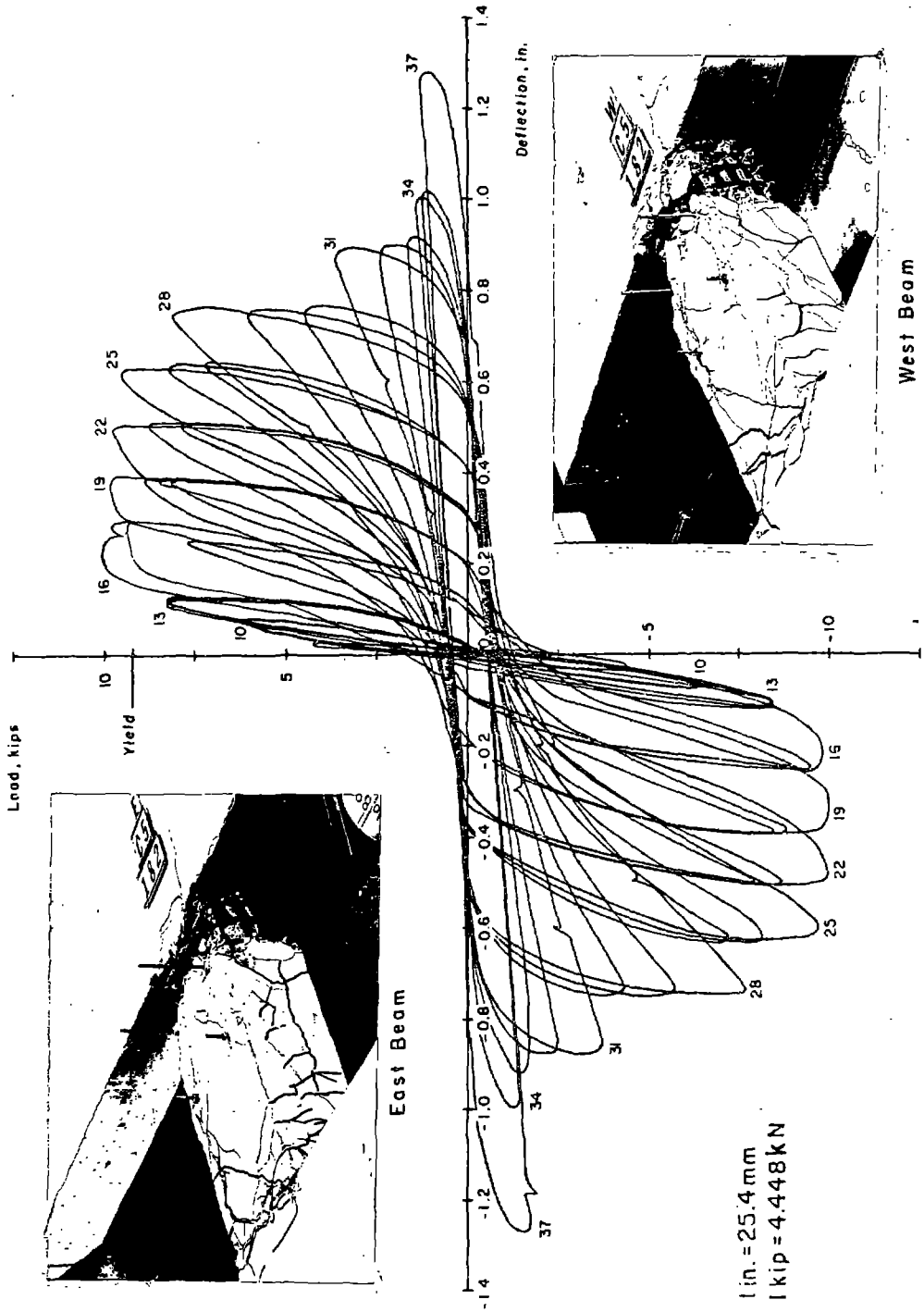


Fig. 8 Load versus Deflection Relationship for Specimen C5



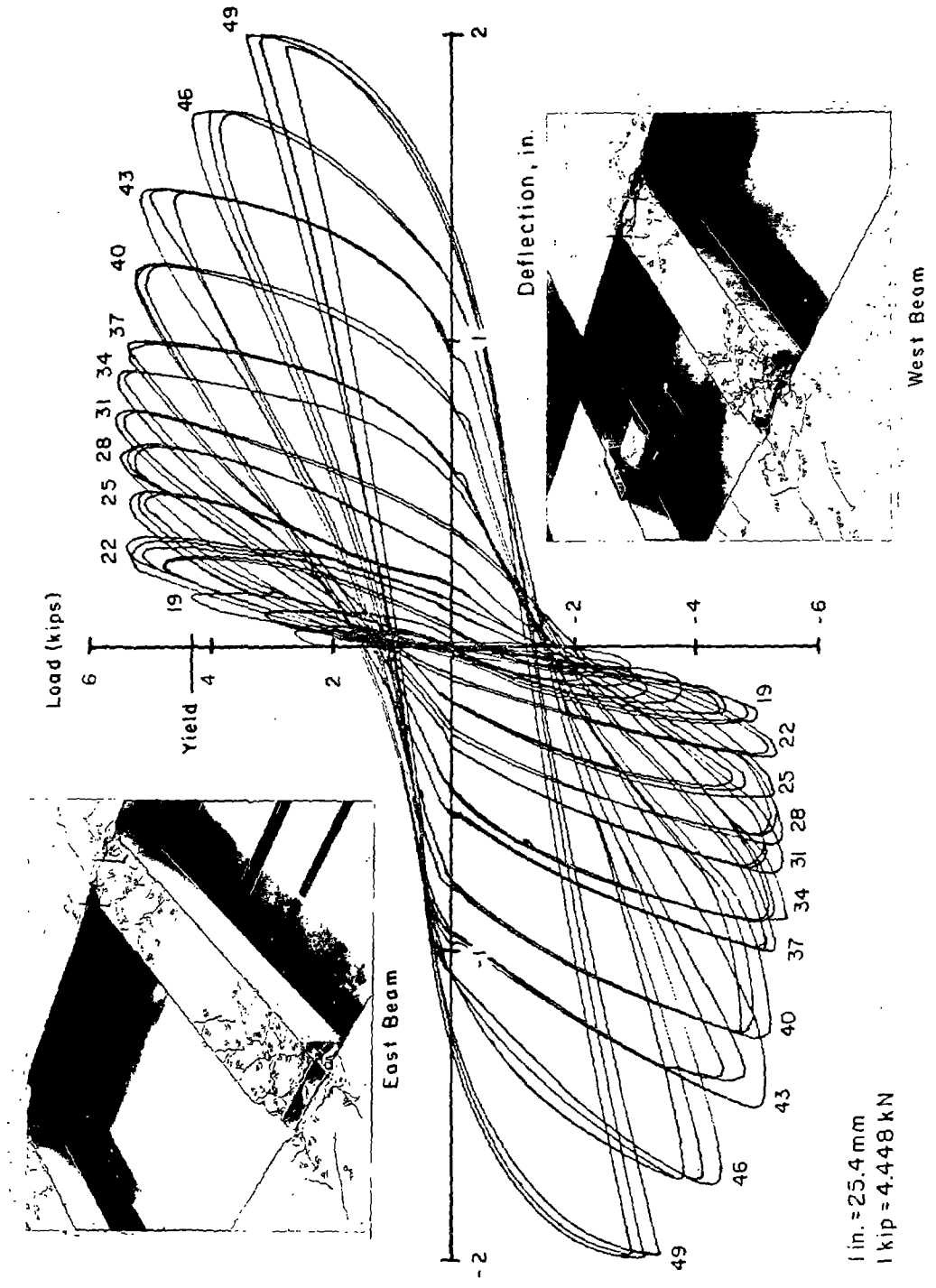


Fig. 9 Load versus Deflection Relationship for Specimen C7

diagonal bars, respectively. Specimen C4, with the larger core size, had double diagonal bars.

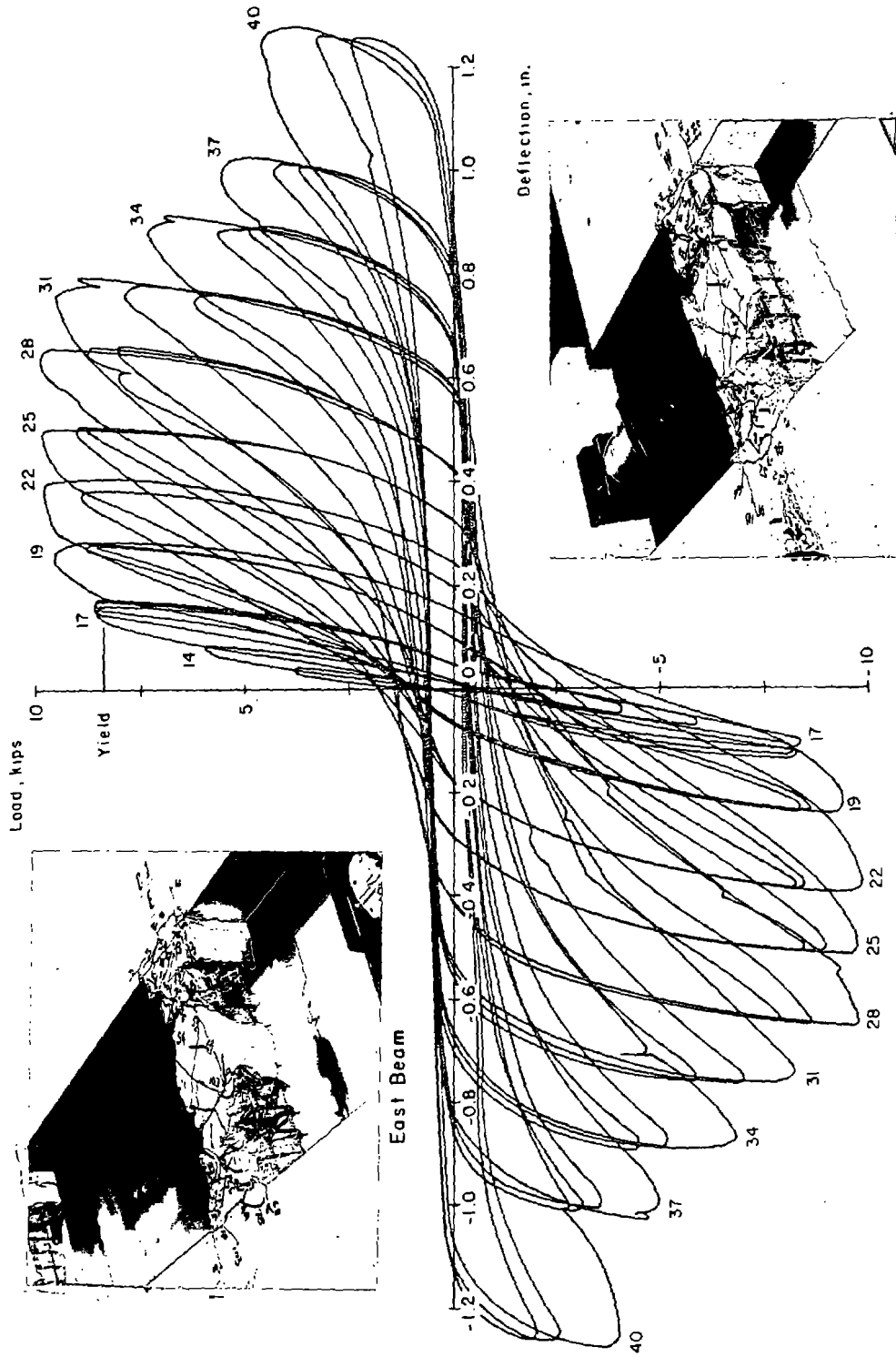
The intended function of the diagonal reinforcement was to eliminate the sliding shear that limited inelastic response of the beams with conventional horizontal reinforcement. The diagonal reinforcement was designed to provide an internal truss system to resist shear and to spread the critical plastic hinge location away from the face of the wall.

Use of diagonal reinforcement in the hinging regions did not result in the anticipated improvement in performance. The unsatisfactory performance was caused by a number of factors that are discussed below.

The hysteretic response of Specimens C1, C3, and C4 is illustrated in the load versus deflection relationships of Figs. 10, 11, and 12, respectively. Comparison of these figures with those shown previously for short-span beams with conventional reinforcement indicates that the special diagonals did not significantly improve the hysteretic response characteristics. While some improvements in energy dissipation and load retention capacities were attained, the added complexity and cost of the diagonals do not appear to be warranted.

The primary reason that the diagonals within the hinging region did not perform satisfactorily was the details for tying the "truss" together. Initially, the beams behaved as expected. Tensile yielding of the flexural reinforcement at the face of the wall and at the intersection of the diagonals occurred almost simultaneously. As loading cycles progressed into the inelastic range, concrete within the region of the diagonals deteriorated by spalling and crushing as can be seen in Fig. 10.

In principle, loss of concrete should not have affected the ability of the diagonal trusses to resist load as long as the diagonal bars did not buckle. However, as loading progressed and concrete was lost, the support points for the diagonals worked loose allowing the corners of the diagonal bars to displace. This is illustrated in Fig. 13. Once the supports for the diagonal truss softened, efficient truss action could



1 in. = 25.4 mm  
 1 kip = 4.448 kN

Fig. 10 Load versus Deflection Relationship for Specimen C1

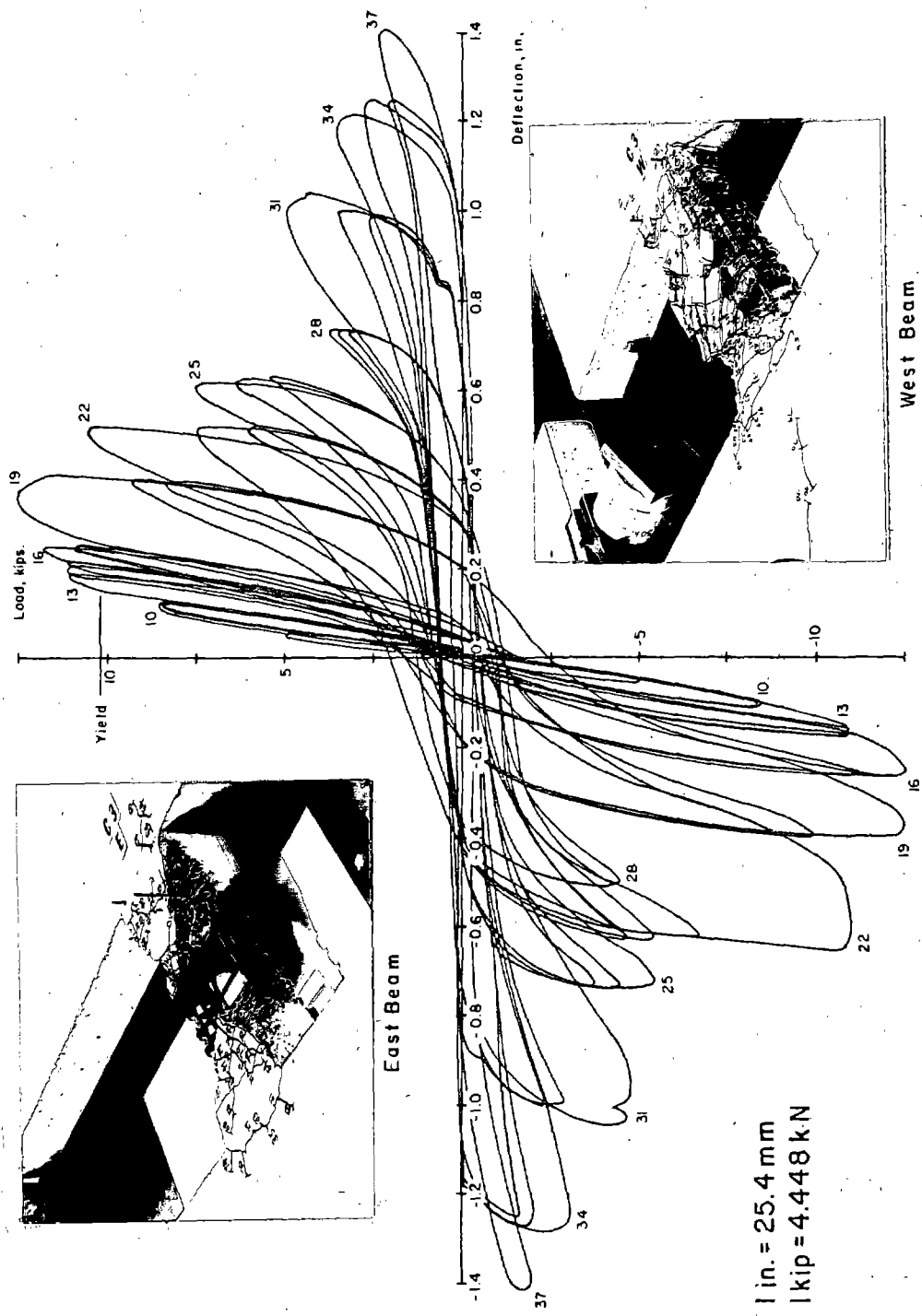


Fig. 11 Load versus Deflection Relationship for Specimen C3

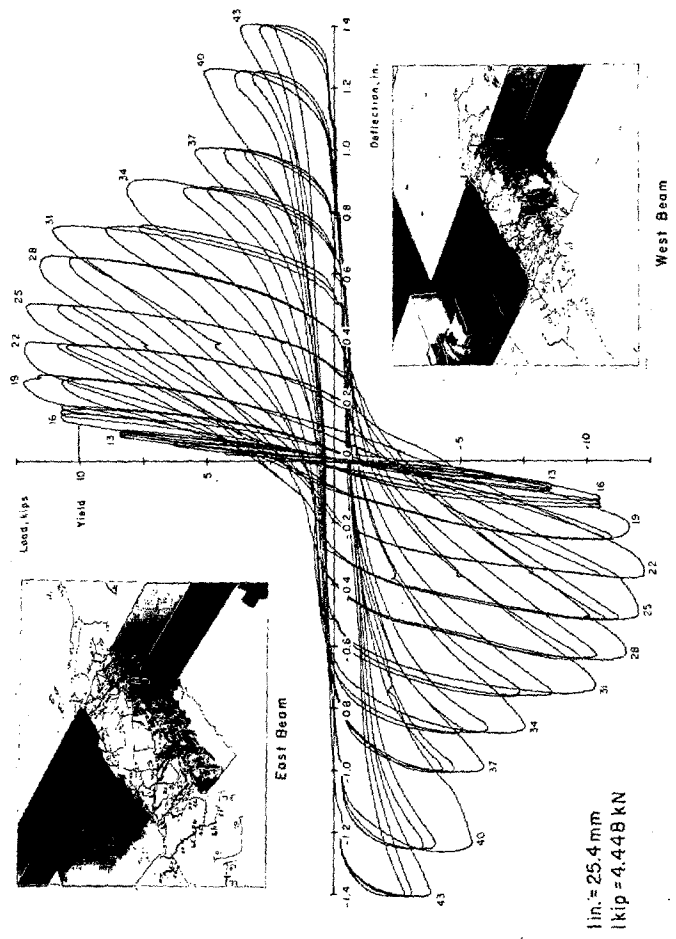
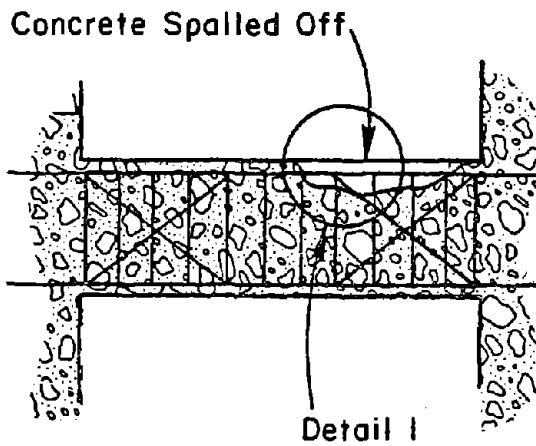
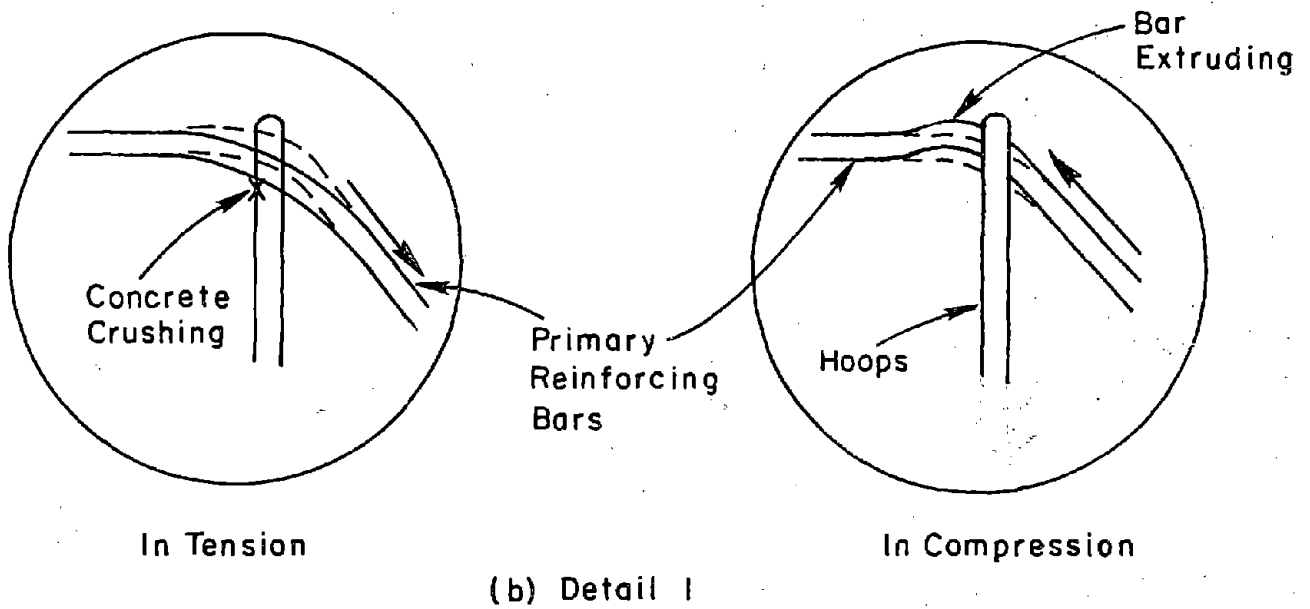


Fig. 12 Load versus Deflection Relationship for Specimen C4



(a) General Location



(b) Detail I

Fig. 13 Loss of Support for Diagonals in Hinging Region

not be developed. Therefore, the diagonals were not effective in carrying the applied shear.

It should be noted that the transverse hoops located at the corners of the diagonal were adequate to resist the outward thrust of the diagonal bars. Strain measurements indicated that these hoops did not yield. The problem encountered was that the force in the diagonal was not effectively transmitted to the transverse hoop.

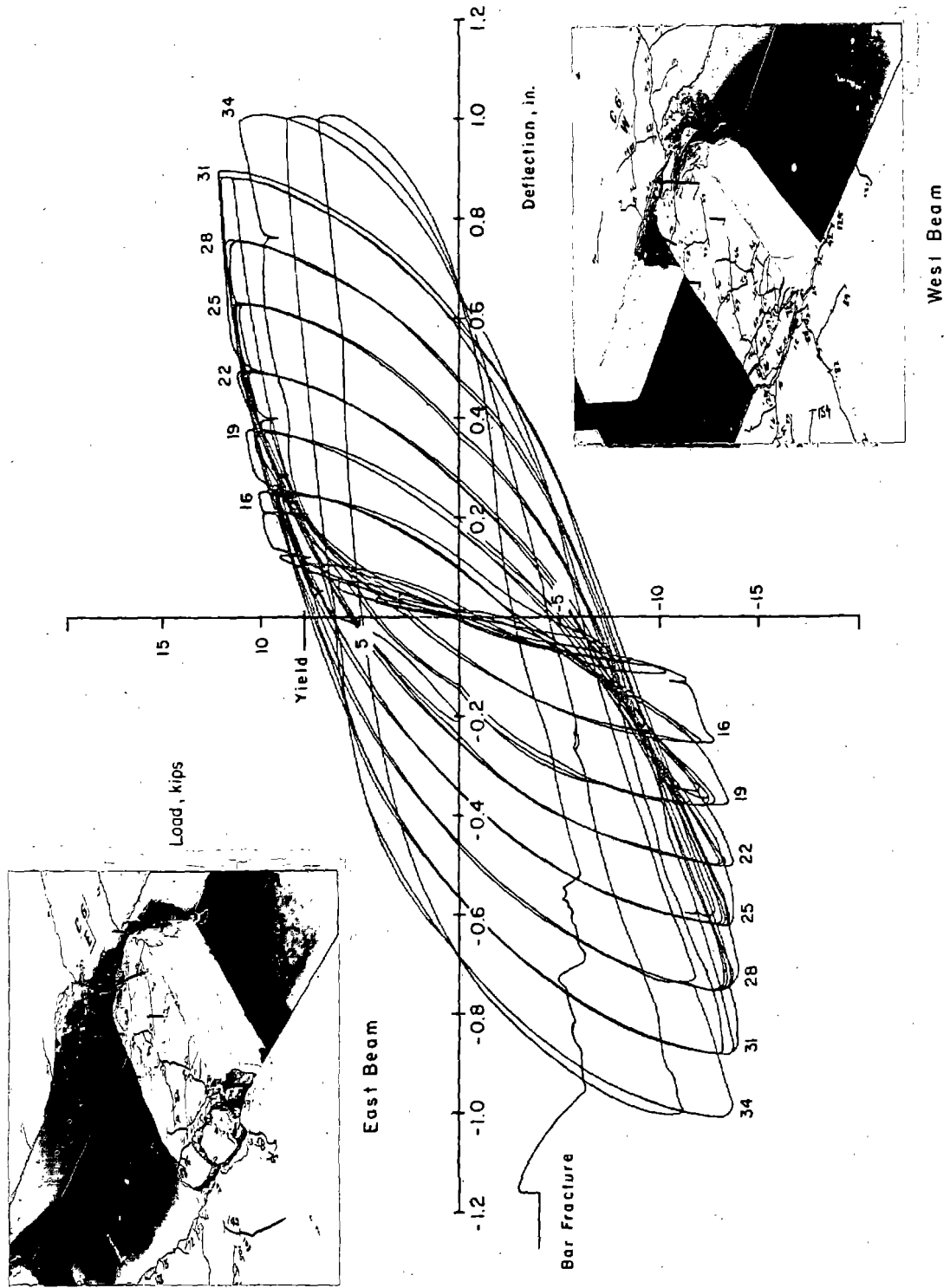
The addition of a second set of diagonals, as was done for Specimens C3 and C4, was tried to lower the force levels in the diagonal bars. However, the result was not satisfactory. It is apparent that to use this type of diagonal reinforcement, extreme caution must be used in securing the bars. The effectiveness and cost-benefit ratio of this detail is questionable.

One possibility to improve this detail would be to eliminate the bend in the diagonals at the intersection of the beam with the wall. However, this would cause additional problems in fabrication of the beam and wall reinforcement.

#### Full-Length Diagonal Reinforcement

Because of the ineffectiveness of diagonals located in the hinging regions and the sliding shear limitation with conventional reinforcement, Specimens C6 and C8 were tested with full-length diagonal reinforcement. The beams had shear span-to-effective depth ratios of 1.4 and 2.8, respectively. Reinforcement details are given in Fig. 4 and Table 1. The straight longitudinal bars that supported the transverse hoops were not anchored in the abutment walls. They were not considered to contribute to the load resisting mechanism.

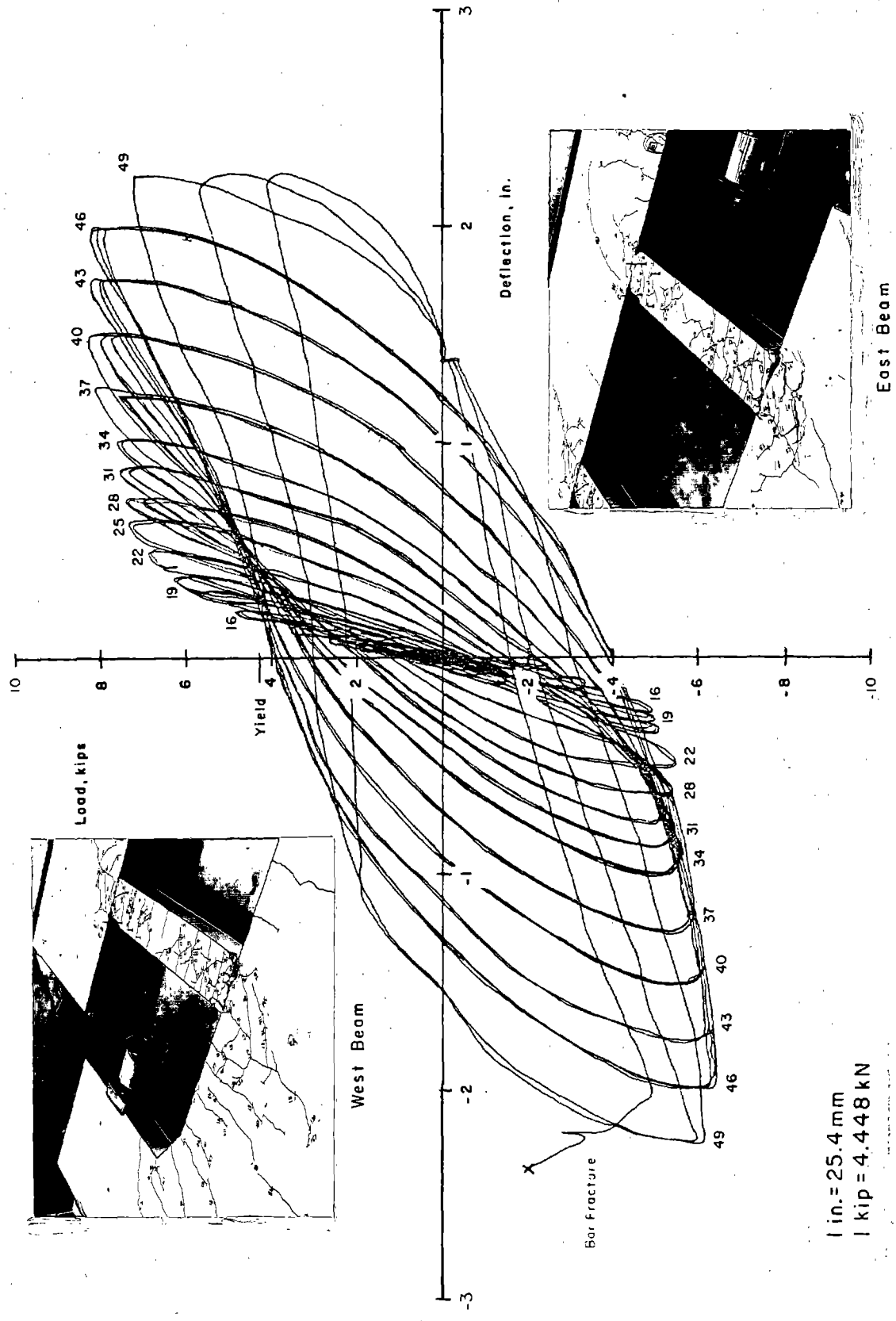
Load versus deflection relationships for Specimens C6 and C8 are shown in Figs. 14 and 15. Full-length diagonals effectively increased the load retention and energy dissipation capacity of these coupling beams. The load versus deflection curves do not exhibit the "pinching" that results from deterioration of the shear resisting mechanism. Also, the "sliding



1 in. = 25.4 mm  
 1 kip = 4.448 kN

Fig. 14 Load versus Deflection Relationship for Specimen C6





1 in. = 25.4 mm  
 1 kip = 4.448 kN

Fig. 15 Load versus Deflection Relationship for Specimen C8

shear" mechanism leading to loss of stiffness and strength was not observed.

Initial cracking in the beams with full-length diagonals was similar to that observed in the beams with conventional reinforcement. As inelastic load cycles were applied, concrete at the beam-wall interface crushed and spalled. This deterioration, however, was not reflected in the load versus deflection relationships. Forces on the beams were effectively resisted by truss action of the diagonal bars. The transverse hoops contained the concrete core over most of the beam thus supporting the diagonal bars against buckling.

Performance of test beams with full-length diagonals was eventually limited by inelastic buckling and subsequent fracture of the diagonal bars. At later stages of the test, concrete spalling at the beam-wall intersection exposed the diagonal bars within the abutment wall. In this region no reinforcement was provided to prevent the diagonals from buckling.

The mechanism that develops using full-length diagonals is essentially that of a Mesnager hinge. It was expected, based on Paulay and Binney's tests,<sup>(2)</sup> that significant improvement in response would be observed in the short-span beams. The shear span-to-effective depth ratio of these beams was 1.4 as compared to a maximum ratio of 0.9 in the beams noted by Paulay and Binney.<sup>(2)</sup> The use of full-length diagonals in longer span beams had not been tested previously. Therefore, Specimen C8 was tested with a shear span-to-depth ratio of 2.8.

Based on the behavior of Specimens C7 and C8, the improvement obtained using full-length diagonals in beams with a shear span-to-effective depth ratio of 2.8 (span-to-depth ratio of 5.0) was relatively small. In addition, gravity loads within the span take on greater significance for longer span beams. These loads cannot be resisted efficiently by diagonal reinforcement. Considering these findings, full-length diagonal bars do not appear to be justified for coupling beams with shear span-to-effective depth ratios of 2.8 or greater.

## STRENGTH CHARACTERISTICS

Table 2 is a summary of yield and maximum loads for the test specimens. Observed and calculated values are given. They represent the load on each beam based on the assumption that the total load was distributed equally. The area used to calculate the nominal shear stress was the width of the beam times its effective depth.

### Observed Strengths

Yield loads given in Table 2 are those observed when the main flexural reinforcement first reached its yield strain. For most specimens, the main flexural reinforcement was the straight longitudinal bars. For Specimens C6 and C8, which had full-length diagonals, yield load is that observed when the diagonal bars reached their yield strain.

Maximum observed loads correspond to the maximum value measured in either direction of loading. The last column in Table 2 gives the ratio of observed maximum load to the observed yield load for each specimen.

Several observations can be made regarding the strengths of the test specimens. For the short-span beams with conventional longitudinal reinforcement, Specimens C2 and C5, maximum load was only one percent higher than the yield load. This is indicative of the sliding shear deterioration that occurred in the cycles subsequent to yield.

Beams in Specimen C7, which had long spans with conventional reinforcement, reached a maximum load 21% greater than yield load.

Specimens C1, C3, and C4, which were short-span beams with diagonal reinforcement in the hinging regions, reached maximum loads 13 to 17% greater than yield loads.

Specimens with full-length diagonals C6 and C8, had ultimate strengths 73 to 77% greater than their yield strengths. This indicates that the diagonal bars efficiently developed strain hardening. In designing coupled wall systems differences between ultimate and yield strengths must be recognized

TABLE 2 - SPECIMEN STRENGTHS

Specimen No.	Yield Load						Maximum Load						Obs. Max. Obs. Yield
	Observed		Calculated*		Obs.	Calc.	Observed		Calculated*		Obs.	Calc.	
	kips	f' <sub>C</sub>	kips	f' <sub>C</sub>			kips	f' <sub>C</sub>	kips	f' <sub>C</sub>			
C1	8.1	6.2	9.0	6.9	0.90	9.2	7.0	10.8	8.2	0.85	1.13		
C2	10.2	7.6	9.8	7.3	1.04	10.3	7.7	12.8	9.6	0.80	1.01		
C3	10.2	7.7	9.8	7.4	1.04	11.8	9.0	12.4	9.4	0.95	1.17		
C4	10.0	7.0	9.5	6.7	1.05	11.5	8.0	11.7	8.2	0.98	1.14		
C5	9.2	6.7	8.8	6.5	1.05	9.4	6.8	11.4	8.4	0.82	1.01		
C6	7.8	6.3	7.4	6.0	1.05	13.4	10.9	14.4	11.6	0.93	1.73		
C7	4.3	2.9	4.4	3.0	0.98	5.2	3.5	5.6	3.8	0.93	1.21		
C8	4.3	3.0	4.0	2.8	1.08	7.5	5.3	8.7	6.1	0.86	1.77		

1 kip = 4.448 kN;  $1-\sqrt{f'_C}$  (psi) = 0.0830  $(\sqrt{f'_C})$  (MPa)

\*Based on monotonic flexural response

because forces developed in the beams influence the performance of the walls.

As indicated previously, the hoop reinforcement was designed such that it would not yield at loads corresponding to the capacity of the beams. Strain measurements, presented in Appendix B, confirmed that the hoops did not yield. This was the case for conventionally reinforced beams and those with special reinforcement. It is apparent that transverse hoops cannot prevent sliding shear in short conventionally reinforced beams when repeated inelastic load reversals are applied. However, this is very much dependent on load history. The laboratory loading on the beams was intentionally severe.

#### Calculated Strengths

Calculated values of yield and maximum load, shown in Table 2, are based on measured material properties. Calculations are described in detail in Appendix C. The calculated values are estimates of monotonic flexural strength. They do not account for effects of load reversals. Loads for Specimens C6 and C8, with full-length diagonals, were estimated using Eq. (1).

Calculated flexural yield values are in reasonable agreement with observed values. Observed maximum loads range from 80 to 98% of calculated. Besides the normal variations expected in such calculations, the differences reflect the effects of load reversals and shear deterioration.

Nominal shear stresses given in Table 2 were based on the effective depth of the section and the overall beam width. Observations of the beams during testing indicated that as inelastic load cycles were applied the concrete shell surrounding the confined core was lost. At this stage, nominal shear stresses based on the area of the confined core are more realistic. For Specimens C1, C2, and C3 the core area was 66% of the nominal area. Thus, nominal shear stresses based on the area of the confined core are 1.5 times those in Table 2. Based on the core area, maximum nominal stresses observed in C1, C2,

and C3 were  $10.7\sqrt{f'_c}$ ,  $11.7\sqrt{f'_c}$ , and  $13.7\sqrt{f'_c}$  psi ( $0.89\sqrt{f'_c}$ ,  $0.97\sqrt{f'_c}$  and  $1.14\sqrt{f'_c}$  MPa).

For all other specimens the core area was 88% of the nominal area. The corresponding maximum nominal shear stress for short-span beams ranged from  $7.8\sqrt{f'_c}$  to  $12.5\sqrt{f'_c}$  psi ( $0.65\sqrt{f'_c}$  to  $1.04\sqrt{f'_c}$  MPa). For long-span beams, the range was from  $4.0\sqrt{f'_c}$  to  $6.1\sqrt{f'_c}$  psi ( $0.33\sqrt{f'_c}$  to  $0.52\sqrt{f'_c}$  MPa).

## DEFORMATION CHARACTERISTICS

Because of potential excursions into the inelastic range of response, deformation characteristics of coupling beams are of considerable interest. For the beams tested, these characteristics have been quantified in terms of overall load versus deflection relationships, energy dissipation, and ductility.

### Load Versus Deflection Envelopes

Figures 16 and 17 show envelopes of the load versus deflection relationships for the short and long-span beams, respectively.

Except for Specimen C6, beams with shear span-to-effective depth ratios of 1.4 reached their maximum load capacities at deflections between 0.4 and 0.5 in. (10 and 13 mm). These deflections corresponded to overall rotations of 0.02 and 0.03 rad. Overall rotations were calculated as deflection divided by length of beam.

Specimen C7, which had conventional longitudinal reinforcement and a shear span-to-effective depth ratio of 2.8, reached its maximum load at a deflection of 0.9 in. (23 mm). This corresponded to an overall rotation of 0.03 rad.

Specimens with full-length diagonals, C6 and C8, reached maximum load capacities at deflections of 0.8 in. (20 mm) and 1.5 in. (38 mm), respectively. Corresponding rotations were 0.05 rad. for both the short- and long-span specimens. Although the beams with full-length diagonals reached higher rotations at maximum load than other beams, final load loss in these beams was more sudden. This is because their load capacity was limited by bar fracture.

It is evident in Figs. 16 and 17 that the envelopes for Specimens C6 and C8 are not symmetrical for opposite directions of loading. This results because the areas of the diagonals are not equal. Two No. 3 bars were used in one diagonal direction and one No. 4 bar was used in the other direction. The areas for these bars were 0.22 sq.in. and 0.20 sq.in. (142 and 129 sq.mm).

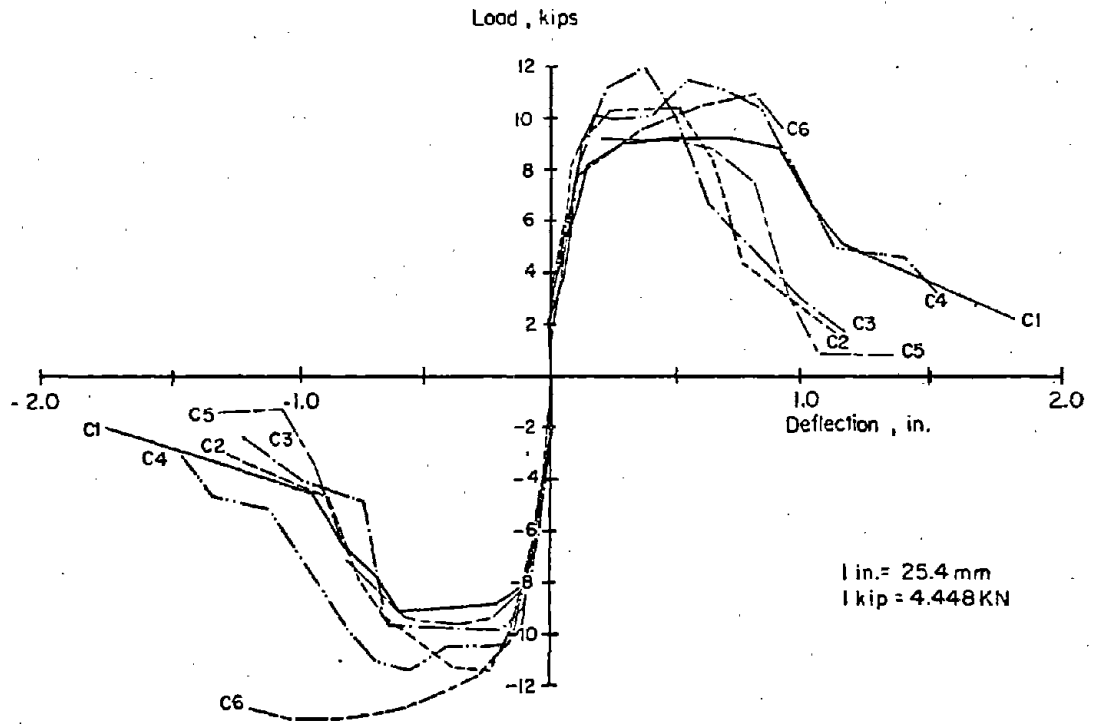


Fig. 16 Load versus Deflection Envelopes for Specimens with Short-Span Beams

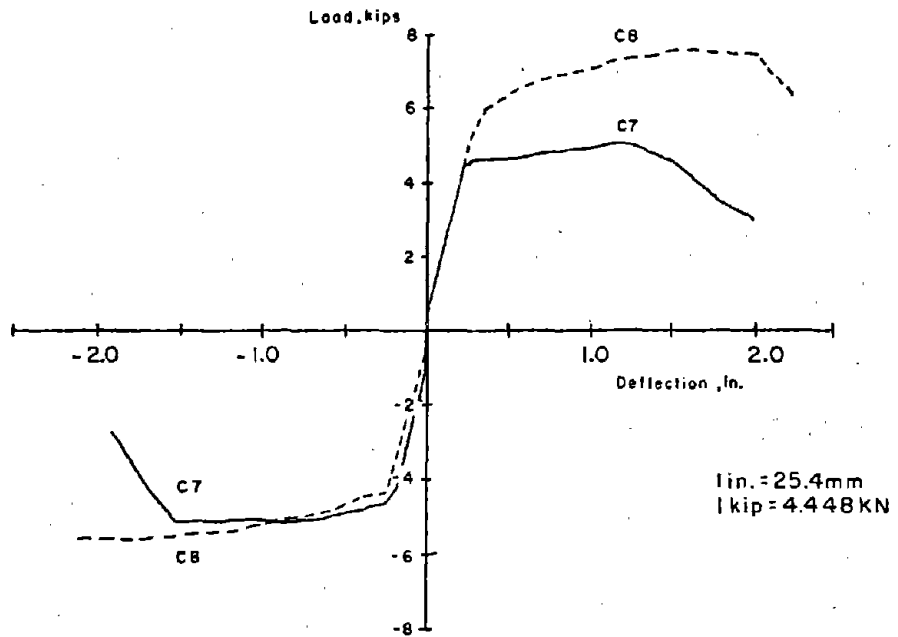


Fig. 17 Load versus Deflection Envelopes for Specimens with Long-Span Beams



Measured load versus deflection envelopes are compared in Figs. 18 and 19 with those calculated. The calculated curves represent first order approximation for monotonically loaded beams. Only flexural deformations were considered as described in detail in Appendix C. Calculated curves are presented to illustrate that the beam deformations are made up of a number of components, not all quantifiable.

Measured deflections are considerably in excess of calculated values. This is particularly the case for the short-span beams. The following factors were not included in the calculations:

1. Shearing distortions
2. Slip of main reinforcement anchored in abutment walls
3. Load reversals.

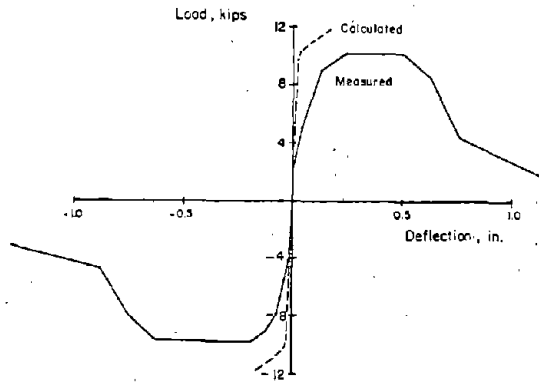
Each of these factors could make a major contribution to the deflection. This is in addition to the normal limitations on the accuracy of deflection calculations.

As an indication of the influence of shearing distortions, it is evident from Figs. 18 and 19 that calculated deflections for Specimen C7 are in better agreement with measured values than those for Specimen C5. It would be expected that shearing distortions would have less influence on Specimen C7 with more slender beams.

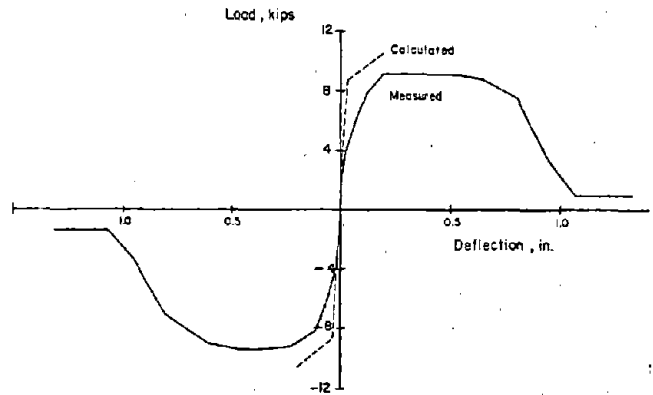
For the short beams with conventional reinforcement, contribution of the shearing distortions was estimated using the procedure developed by Bachmann.<sup>(6)</sup> The modified calculations are a better approximation to the envelope as can be seen in Fig. 20 and 21. Again, load reversals were not taken into account.

To be more than just a relative measure of performance, the calculation of load versus deflection relationships for beams under load reversals requires extensive refinement. Such refinement was outside the scope of this project.

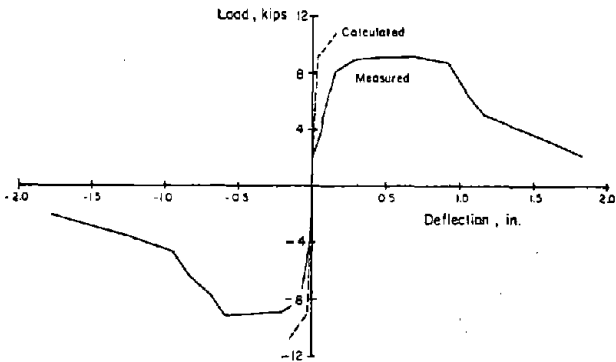
1 in. = 25.4mm  
1 kip = 4.448 kN



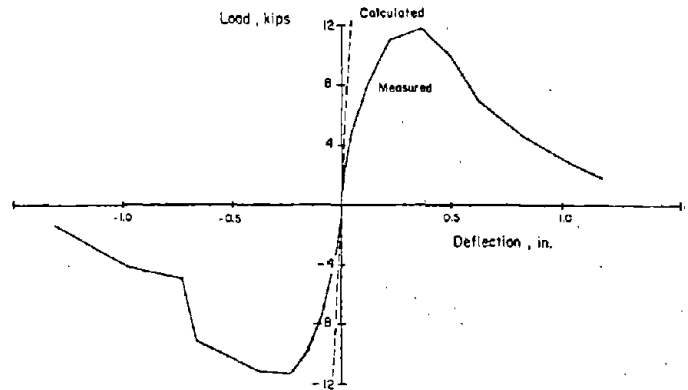
a) Specimen C2



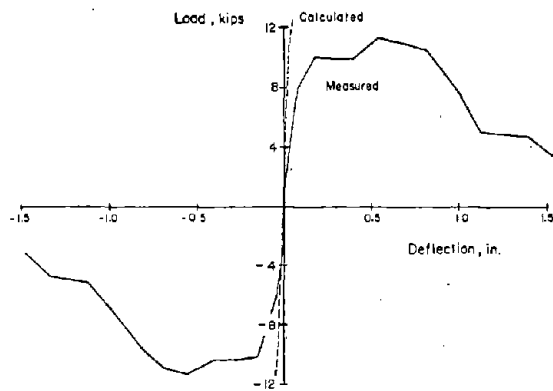
b) Specimen C5



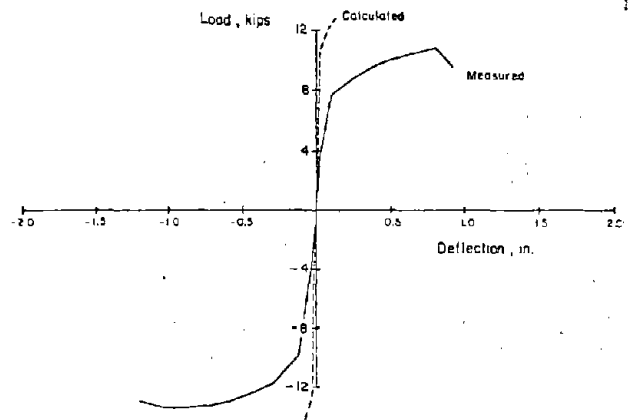
c) Specimen C1



d) Specimen C3

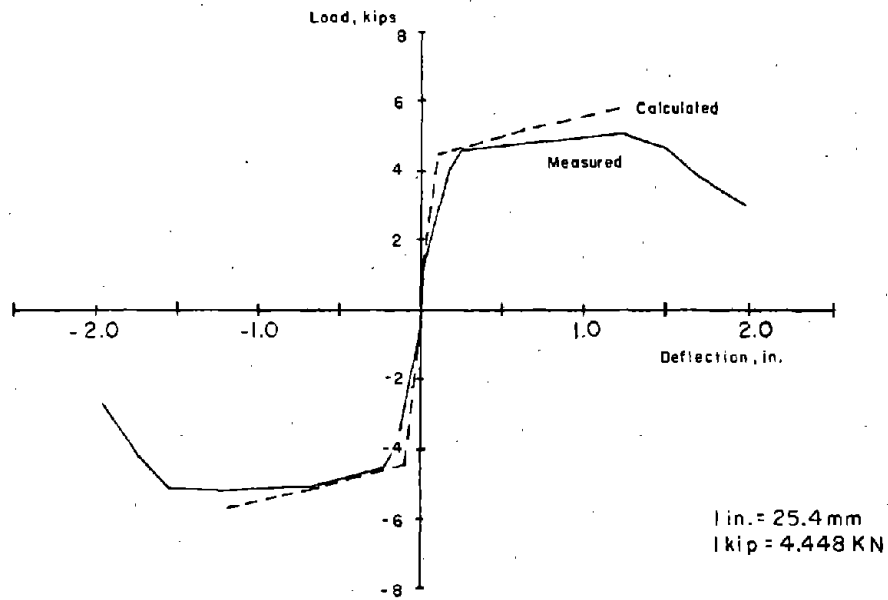


e) Specimen C4

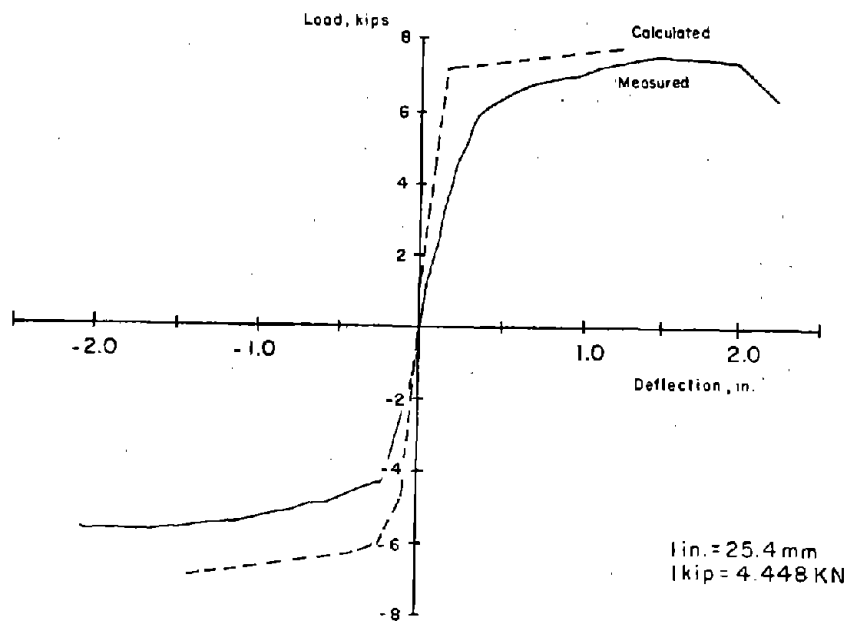


f) Specimen C6

Fig. 18 Calculated and Measured Load versus Deflection Envelope for Short-Span Beams



a) Specimen C7



b) Specimen C8

Fig. 19 Calculated and Measured Load versus Deflection Envelopes for Long-Span Beams

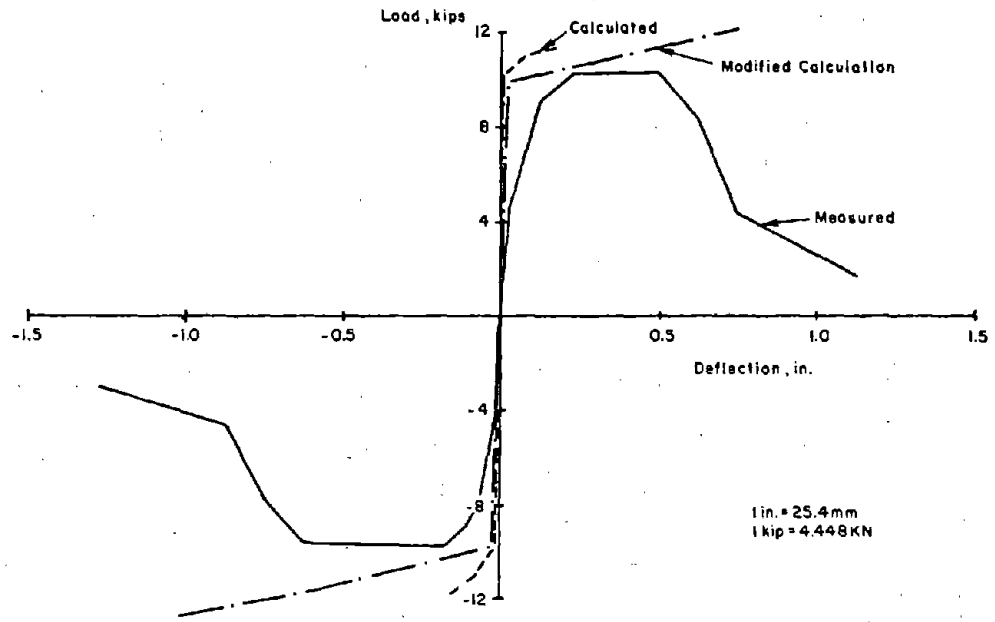


Fig. 20 Influence of Diagonal Crackings in the Calculation of Deflection for Specimen C2

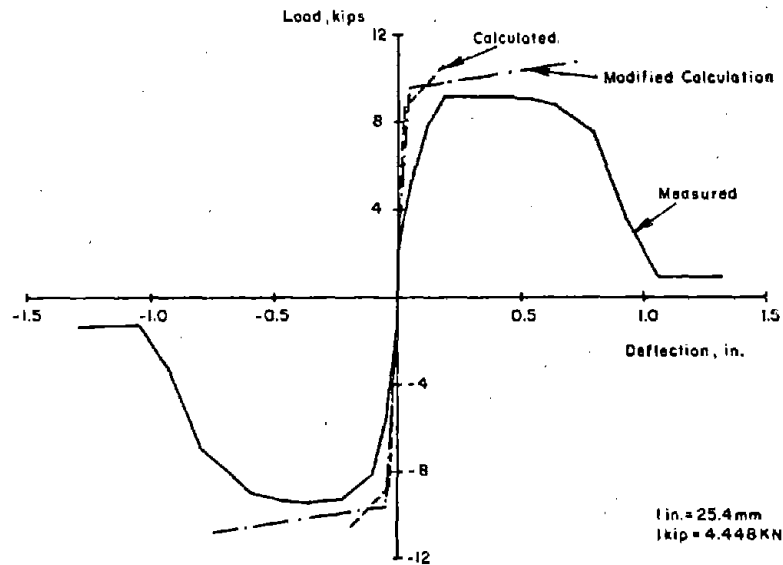


Fig. 21 Influence of Diagonal Crackings in the Calculation of Deflection for Specimen C5

### Ductility

Ductility of a structure is commonly used as a measure of its inelastic performance. Deflection ductility ratio is defined in this report as the ratio of the deflection of the beams to the deflection measured at yield. Cumulative deflection ductility ratio is the summation of ductility ratios for each cycle of loading. This is illustrated in Fig. 22. Ductility ratios for positive and negative loadings are summed separately.

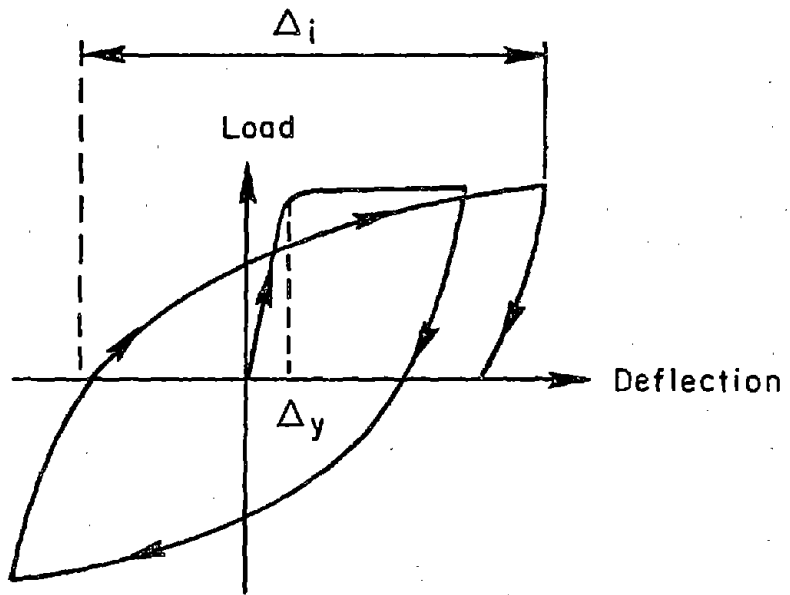
Comparisons of the performance of the specimens based on ductility are shown in Fig. 23. In this figure the load is plotted as percentage of the maximum, observed in either loading direction.

Specimens C2 and C5 with short-span beams and conventional reinforcement were tested with confined core area equal to 66% and 88% of the effective section area, respectively. As shown Fig. 23(a), the larger confined core area improved behavior. Under load reversals, the concrete shell was lost. Thus, nominal shear stresses on the smaller core were larger and lower cumulative ductility was attained by Specimen C2.

The effects of different reinforcement arrangements on ductility are shown in Figs. 23(b) and 23(c) for the short-span and long-span beams, respectively. For the short-span beams, the specimen with full-length diagonals maintained its load capacity for a significantly larger ductility than the other specimens. The difference was not as significant for the long-span beams.

### Energy Dissipation Capacity

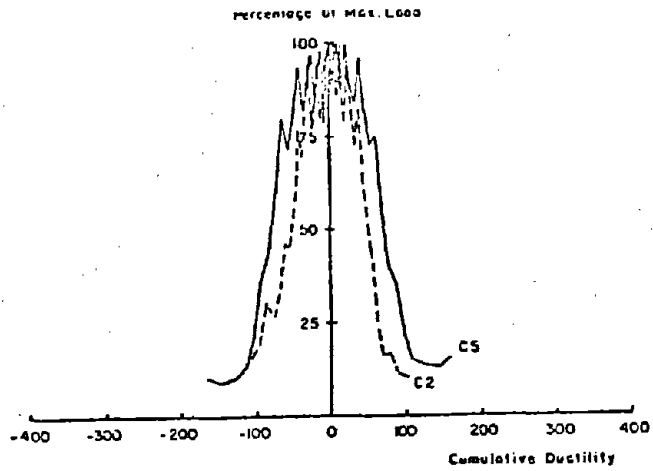
Energy dissipation provides a measure of the inelastic performance of a structure under load reversals. Energy dissipated is the difference between that expended during load application and that recovered during unloading. Energy dissipation is thus defined as the area enclosed by the load versus deflection loops. This is illustrated in Fig. 24. Using the energy dissipation derived from the measured load versus



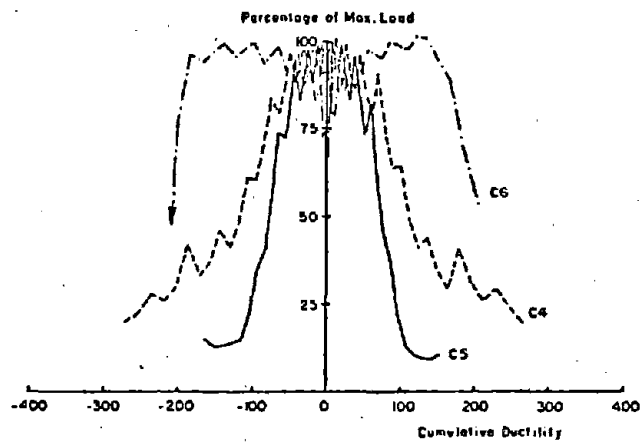
$$\mu_i = \frac{\Delta_i}{\Delta_y}$$

$$\text{Cum. Deflection Ductility Ratio} = \sum_{i=1}^n \mu_i$$

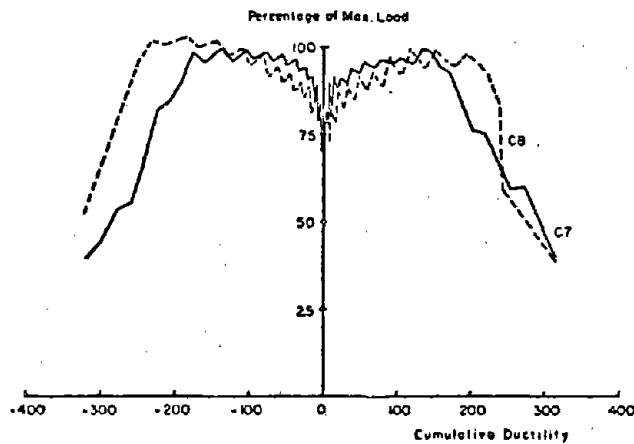
Fig. 22 Cumulative Deflection Ductility Ratio



a) Effect of Core Size for Short-span Beams



b) Effect of Reinforcement for Short-span Beams



c) Effect of Reinforcement for Long-span Beams

Fig. 23 Load versus Cumulative Deflection Ductility

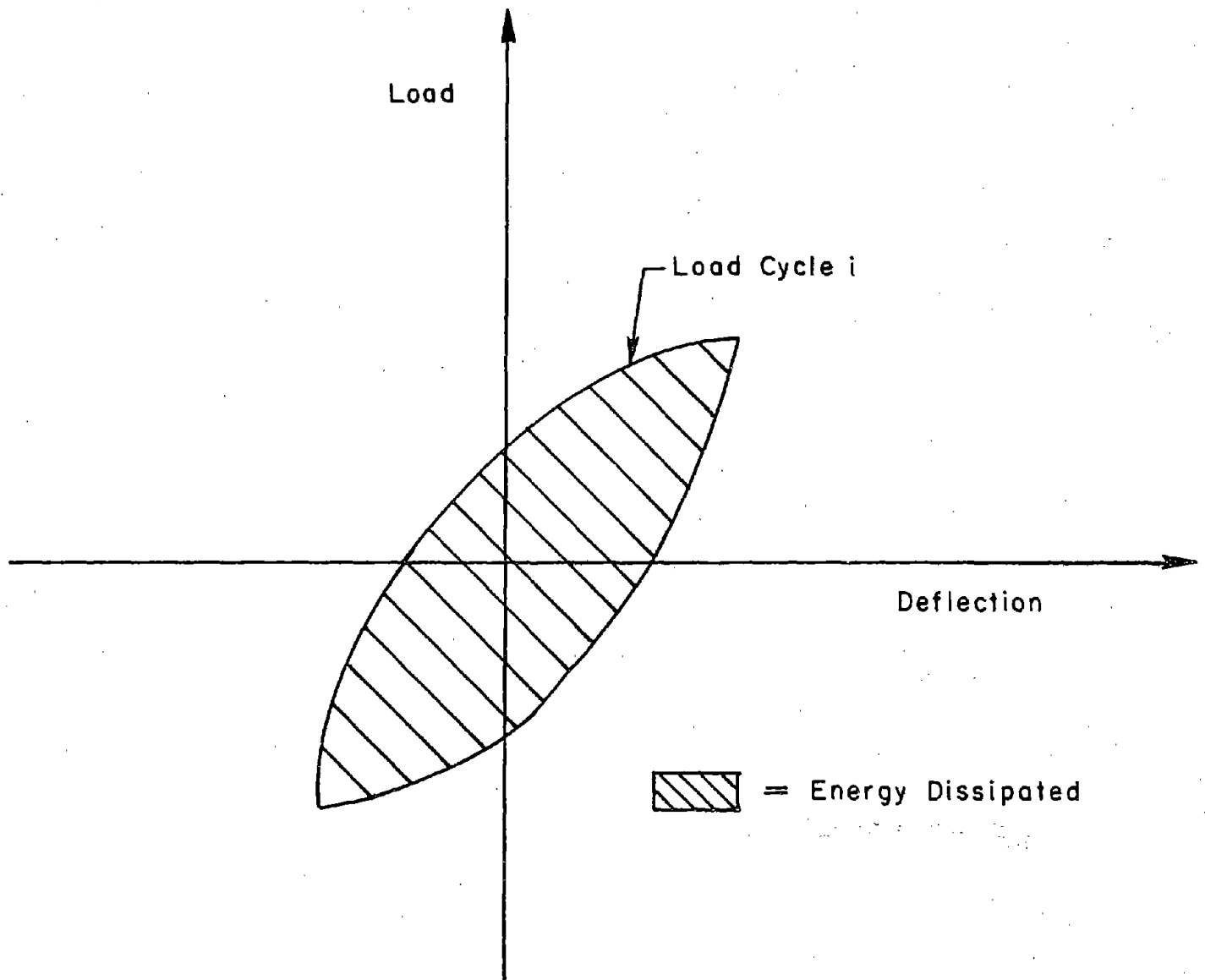


Fig. 24 Energy Dissipation



deflection relationships of the test specimens provides a convenient reference for quantifying their performance. Essentially, for equivalent loads and deflections, specimens dissipating the most energy would be considered to have the best performance.

Figures 25 and 26 illustrate the "stability" of the load versus deflection loops for the specimens tested. In the loading sequence, three complete cycles of load or deflection were applied at each load deflection increment. Figures 25 and 26 show the cumulative energy dissipated for the first, second, and third cycles of each increment. Energy dissipation is plotted against displacement ductility ratio. Displacement ductility ratio is defined as the deflection at each increment divided by the yield deflection.

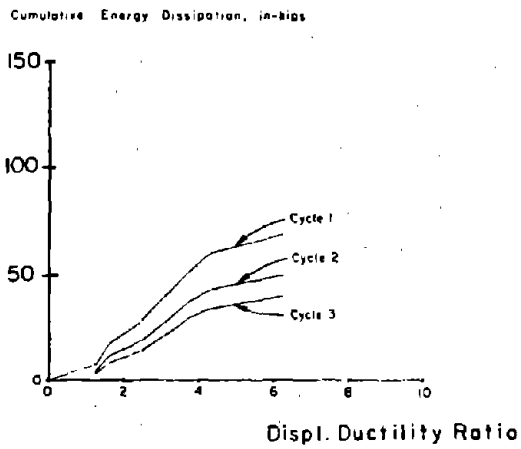
If the three loops within each increment had identical areas for each cycle, it would mean that there was no loss of energy dissipation capacity. As can be seen, this was nearly the case for Specimens C6 and C8 which had full-length diagonals. The wider differentials between successive cycles within each load increment for the other beams indicates that more severe deterioration of these beams had occurred. These curves illustrate more clearly what was indicated in the load versus deflection relationships presented earlier.

Figures 25 and 26, while indicative of performance for each specimen, do not directly relate the various specimens. To do this the cumulative energy dissipated was normalized by the product of the yield load and yield deflection as follows:

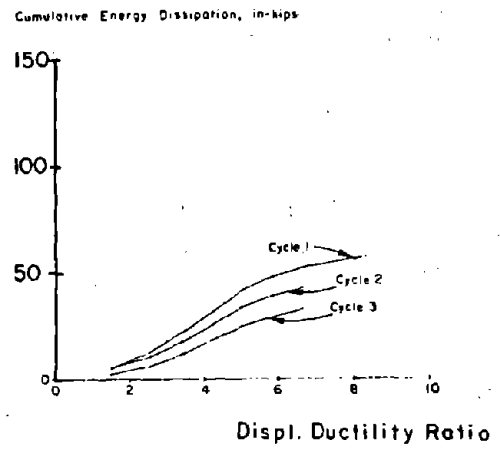
$$E_{mn} = \frac{1}{P_Y \Delta_Y} \sum_{i=1}^n e_i \quad (2)$$

where:

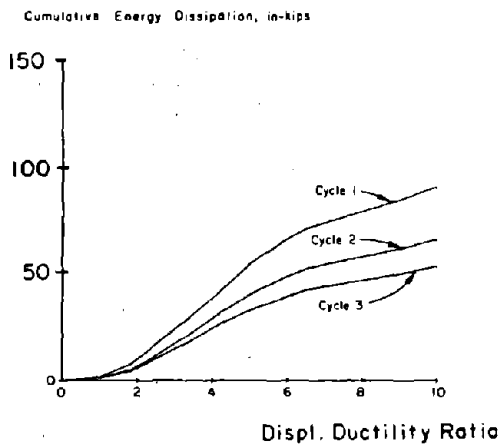
- $E_{mn}$  = normalized cumulative energy dissipated
- $P_Y$  = yield load (kips/kN)
- $\Delta_Y$  = yield deflection (in./mm)
- $e_i$  = energy dissipated in i-th load cycle (kip-in./kN-mm)
- $i$  = load cycle



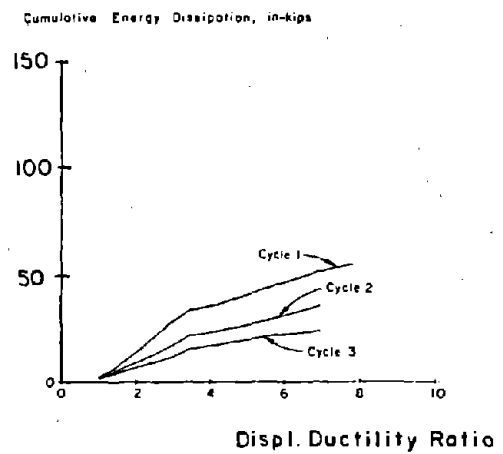
a) Specimen C2



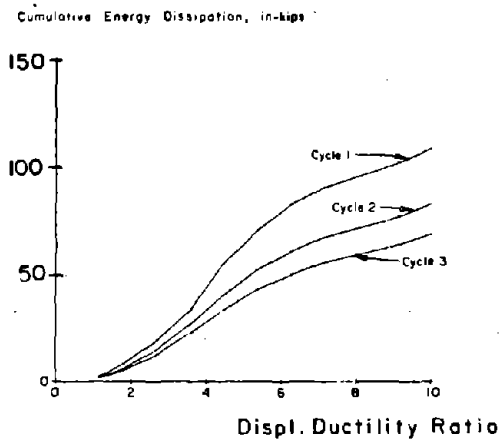
b) Specimen C5



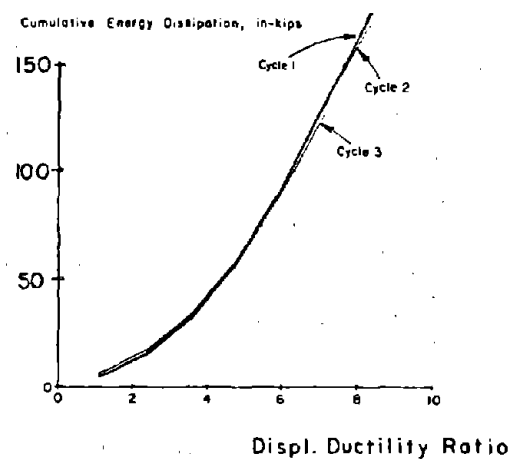
c) Specimen C1



d) Specimen C3

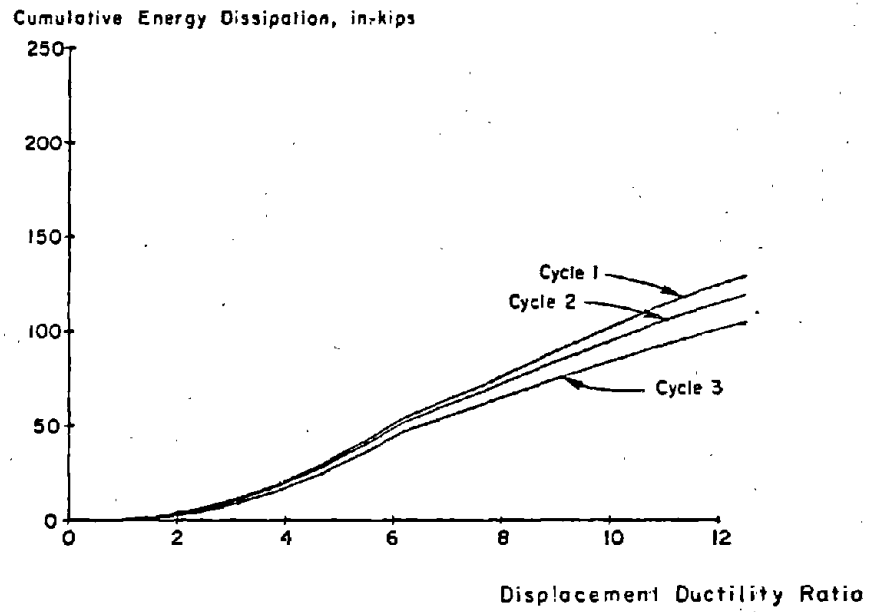


e) Specimen C4

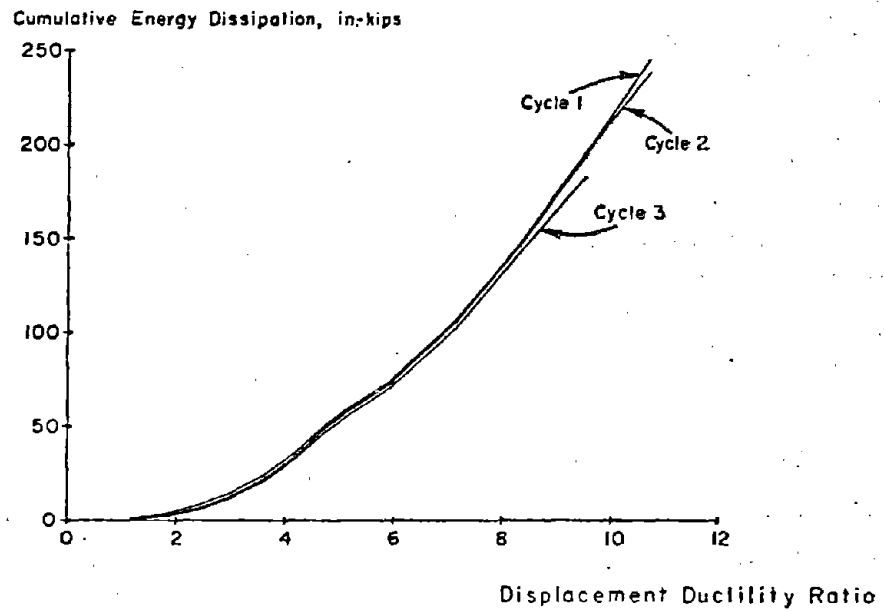


f) Specimen C6

Fig. 25 Energy Dissipation versus Displacement Ductility Ratio for Short-Span Beams



a) Specimen C7



b) Specimen C8

Fig. 26 Energy Dissipation versus Displacement Ductility Ratio for Long-Span Beams

Figures 27 and 28 show the normalized cumulative energy dissipated versus number of cycles for the short- and long-span beams, respectively. All load cycles are included in the cumulative energy determination. Since the specimens had similar load histories, these curves provide a comparative measure of the energy dissipation capacity of the test specimens.

Energy dissipation versus ductility relationships confirm the results previously indicated. For short-span beams, Specimen C6 with full-length diagonals provided the greatest energy dissipation capacity. Special diagonals within the hinging regions improved energy dissipation capacity but not enough to justify their complexity and cost.

For the long-span beams the full-length diagonals did not provide significant additional energy dissipation capacity.

Normalized Cumulative Energy Dissipation

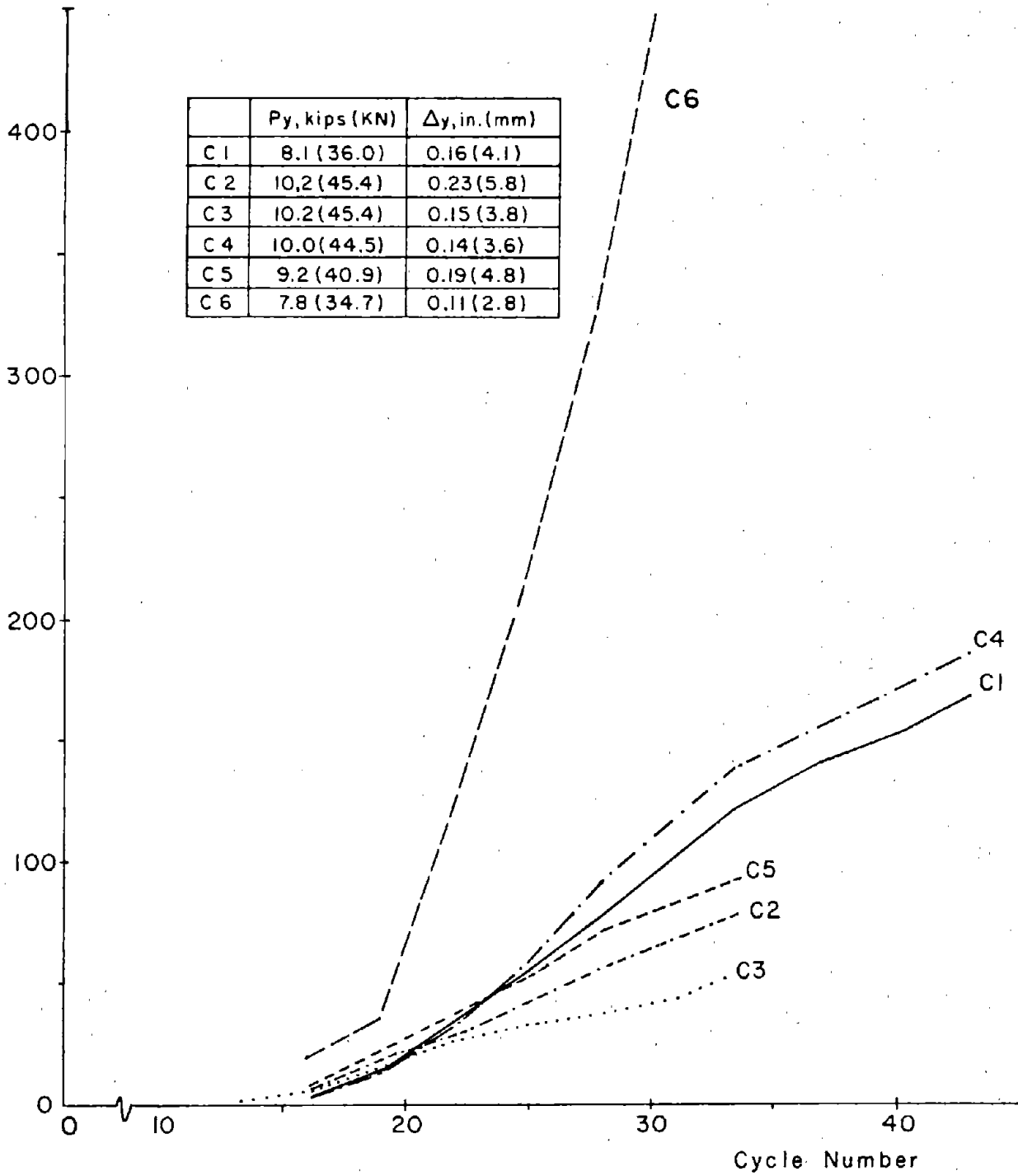


Fig. 27 Normalized Cumulative Energy Dissipation versus Cycle Number for Short-Span Beams

Normalized Cumulative Energy Dissipation

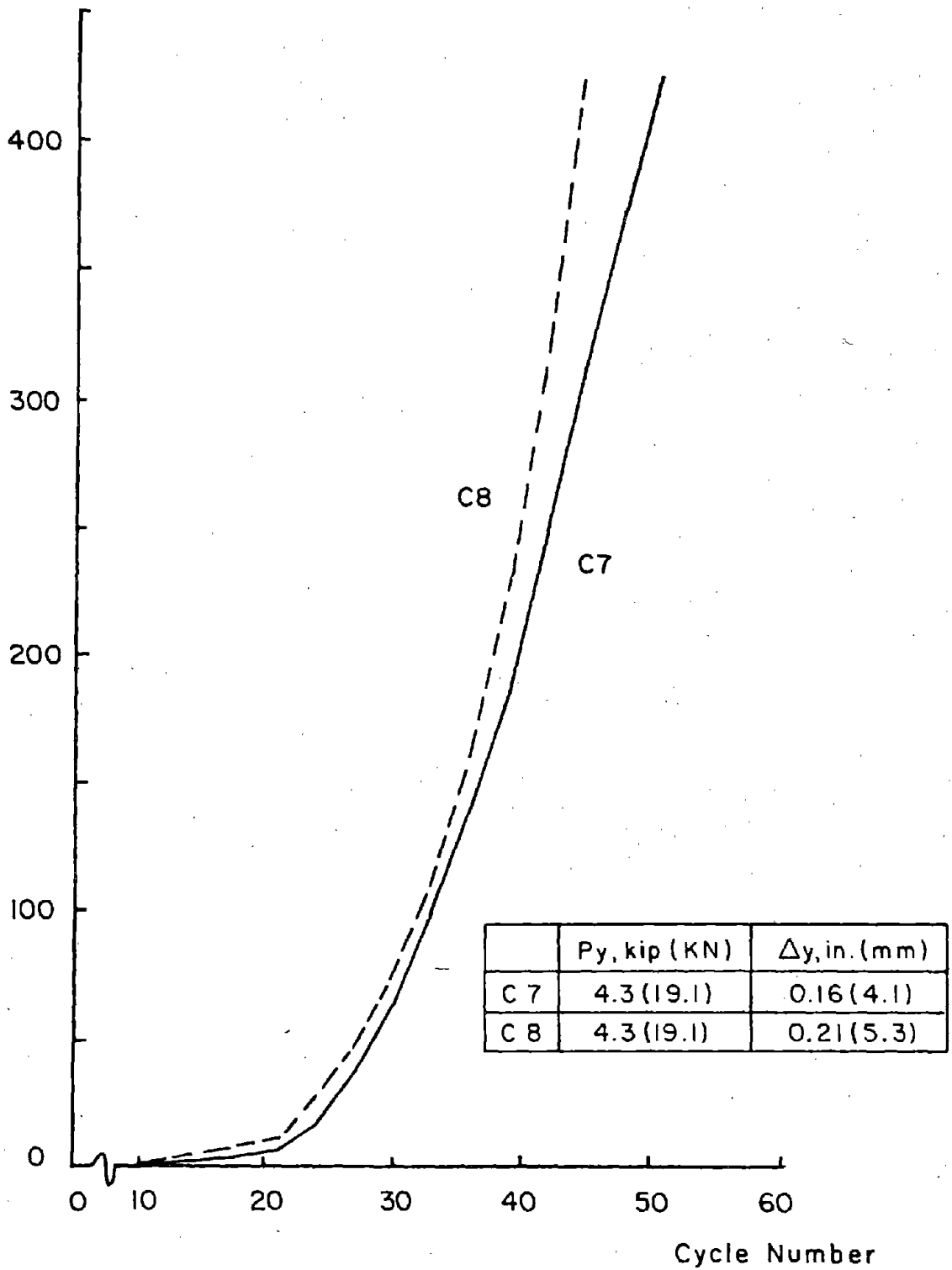


Fig. 28 Normalized Cumulative Energy versus Ductility for Long-Span Beams

## SUMMARY AND CONCLUSIONS

Eight model reinforced concrete coupling beam specimens were subjected to reversing loads representing those that would occur in beams of coupled structural walls during a severe earthquake. The beams were constructed at approximately 1/3-scale. Effects of selected variables on hysteretic response were determined. Controlled variables included shear span-to-effective depth ratio of the beams, reinforcement details, and size of the confined concrete core. The variables are summarized in Table 1.

The beams had shear span-to-effective depth ratios of either 1.4 or 2.8. These corresponded to shear span-to-depth ratios of 2.5 and 5.0. Maximum nominal shear stresses on short-span beams ranged from  $7\sqrt{f'_c}$  psi ( $0.58\sqrt{f'_c}$  MPa) for beams with conventional reinforcement to  $11\sqrt{f'_c}$  psi ( $0.91\sqrt{f'_c}$  MPa) for beams with full-length diagonal reinforcement. Equivalent shear stresses for long-span beams were  $4\sqrt{f'_c}$  and  $5\sqrt{f'_c}$  psi ( $0.33\sqrt{f'_c}$  and  $0.42\sqrt{f'_c}$  MPa), respectively.

Load versus deflection relationships, strength, energy dissipation and ductility were the basic parameters used to evaluate performance of the test specimens. The following conclusions are based on the test results.

### Conventional Longitudinal Reinforcement

Inelastic response of coupling beams with conventional reinforcement was limited by sliding shear deterioration at the beam-wall intersection. This was the case even though transverse hoops were provided to carry the entire shear without yielding. Since sliding shear cracks propagated between transverse reinforcement, the hoops eventually became ineffective. Development of sliding shear is dependent on load history. Deterioration is a function of the cycle number and the intensity of applied loads. As such, any generalization of the results must consider load history. Both the number of cycles and load intensity used in the laboratory tests can be considered as representative of extremely severe earthquake conditions on the most critically stressed beam in a coupled wall system.

Specimen C5, which had short-span beams, sustained an overall rotation of 0.025. At this rotation increment more than 80% of the maximum load was maintained for three complete cycles. Yield rotation for Specimen C5 was 0.01 rad.

Specimen C7, which had long-span beams, sustained an overall rotation of 0.04 rad. Yield rotation for this specimen was 0.005 rad.

Tests indicate that improved inelastic performance was obtained by increasing the size of the concrete core. The confined core of coupling beams should be made as large as possible within the limits of cover requirements.

#### Diagonal Reinforcement in Hinging Regions

Diagonal reinforcement within hinging regions at the ends of the beams improved performance, but not enough to justify the added complexity and cost. To use this type of reinforcement, extreme care must be exercised in selection and construction of details, particularly at locations of bends in the reinforcement. Based on the laboratory tests, it does not appear that this detail would be an economical solution.

#### Full-Length Diagonal Reinforcement

Beams with full-length diagonal reinforcement had the best strength, ductility, and energy dissipation characteristics of any of those tested.

Specimen C6, which has short-span beams, sustained an overall rotation of 0.05 rad. Yield rotation for this specimen was 0.01 rad.

Specimen C8, which had long-span beams, sustained an overall rotation of 0.06 rad. Yield rotation was 0.01 rad. Improvement in hysteretic response using full-length diagonals for long-span beams was not as significant as for short-span beams. In addition, gravity loads within the span take on greater significance for longer span beams. These loads cannot be resisted efficiently by diagonal reinforcement. Considering these findings, straight diagonal bars do not appear to be



justified for beams with shear span-to-effective depth ratios of 2.8 or more. Tests using this type of reinforcement have not been carried out on coupling beams with shear span-to-effective depth ratios between 1.4 and 2.8.

If full-length diagonals are used, the diagonal bars must be properly anchored in the adjoining wall. The diagonals must be restrained over their full length to prevent buckling.

Since this type of detail effectively developed strain hardening of the reinforcement, the actual capacity of the beams should be considered in designing a structural wall system. A design based on yield level would not properly allow for the forces that can be imparted to the walls by the beams.

#### Final Remarks

The results of these tests have clearly indicated the relative influence of special reinforcement details on inelastic hysteretic response of coupling beams. This does not, however, justify the use of one system over another for all situations. The response characteristics and energy dissipation capacity attainable in the beams must be matched with that required for the structure and design conditions being considered.

For example, for very short beams under severe earthquake loads, full-length diagonals may provide the best solution. However, in other situations conventionally reinforced beams might be adequate. Also, consideration must be given to the fact that not all beams over the height of a coupled wall system are subjected to the same load histories.

### ACKNOWLEDGMENTS

This investigation was carried out in the Structural Development Section of the Portland Cement Association. Fabrication and testing of the specimens were performed by the Technical Staff of the Section under the direction of Laboratory Foreman B. W. Fullhart.

The work was part of a combined analytical and experimental investigation sponsored by the National Science Foundation under Grant No. ENV74-14766 and by the Portland Cement Association. M. Fintel is Overall Project Director. The opinions, findings, and conclusions expressed in this publication are those of the authors and do not necessarily reflect the views of the National Science Foundation.

## REFERENCES

1. Brown, R.H., and Jirsa, J.O., "Reinforced Concrete Beams Under Load Reversals," Journal of the American Concrete Institute, Proc. Vol. 68, No. 5, May 1971, pp. 380-390.
2. Paulay, T. and Binney, J.R., "Diagonally Reinforced Coupling Beams of Shear Walls," Publication SP-42, Shear in Reinforced Concrete, American Concrete Institute, Detroit, 1974, pp. 579-598.
3. Bertero, V.V. and Popov, E.P., "Hysteretic Behavior of Reinforced Concrete Flexural Members with Special Web Reinforcement," Proceedings, U. S. National Conference on Earthquake Engineering, Ann Arbor, June 1975, pp. 316-326.
4. Wight, J.K. and Sozen, M.A., "Strength Decay of RC Columns Under Shear Reversals," Journal of the Structural Division, American Society of Civil Engineers, Vol. 101, No. ST5, May 1975, pp. 1053-1065.
5. ACI Committee 318, Building Code Requirements for Reinforced Concrete, ACI Standard 318-71, American Concrete Institute, Detroit, 1971, 78 pp.
6. Bachmann, H., "Influence of Shear and Bond on Rotational Capacity of Reinforced Concrete Beams," Publications, International Association for Bridge and Structural Engineering, Vol. 30, Part II, Zurich, 1970, pp. 11-28.
7. Park, R. and Paulay, T., "Reinforced Concrete Structures," John Wiley & Son, Inc., New York, 1975 pp. 307-309.
8. "Standard Specification for Deformed and Plain Billet-Steel Bars for Concrete Reinforcement," A615-76a, American Society for Testing and Materials, Philadelphia, PA.
9. Hognestad, Eivind; Hanson, N.W.; Kriz, L.B. and Kurvitis, O., "Facilities and Test Methods of PCA Structural Laboratory," Development Department, Bulletin D33, Portland Cement Association, Research and Development Laboratories, 1959.
10. Pfrang, E.O., Siess, C.P., and Sozen, M.A., "Load-Moment-Curvature Characteristics of Reinforced Concrete Cross Section," Journal of the American Concrete Institute, Vol. 61, No. 7, July 1964, pp. 763-778.
11. Kent, D.C. and Park, R., "Flexural Members with Confined Concrete," Journal of the Structural Division, ASCE, Vol. 97, No. ST7, July 1971, pp. 1969-1990.
12. Popov, E.P., Introduction to Mechanics of Solids, Prentice-Hall, Englewood Cliffs, 1968, p. 408.



## APPENDIX A - EXPERIMENTAL PROGRAM

Details of the experimental program including specimen geometry, reinforcement details, material properties, fabrication, and testing are given in this Appendix.

### Test Specimens

Eight specimens representing approximately 1/3-scale models of coupling beams were tested. Each specimen consisted of two coupling beams framing into rigid abutment walls at each end as shown in Fig. A-1. The end conditions imposed by the abutments simulated those in a structural wall system.

Coupling beams had rectangular cross sections 4-in. (102 mm) wide and 6.67-in. (169 mm) deep. The beams had lengths of either 16.67-in. (423 mm) or 33.33-in. (846 mm), corresponding to span-to-depth ratios of 2.5 and 5.0, respectively. The L-shaped abutments were 4-in. (102 mm) thick.

### Details of Reinforcement

Steel reinforcement details are presented in Figs. A-2 through A-7.

#### Specimens C2, C5 and C7

Primary reinforcement in Specimens C2, C5, and C7, consisted of four straight longitudinal 6-mm bars, top and bottom. Reinforcement details are shown in Fig. A-2 and A-3. Specimens C2 and C5 had shear span-to-effective depth ratios of 1.4. The shear span-to-effective depth ratio for Specimen C7 was 2.8. Specimens C5 and C7 had confined concrete core size about 33% larger than that of Specimen C2. To obtain the increase in core size without bending the bars, it was necessary to place the straight flexural bars in the coupling beams outside the reinforcement in the abutment walls. Therefore, these bars were not anchored in confined concrete. This anchorage detail, although satisfactory for the test specimen, is not recommended for field practice.

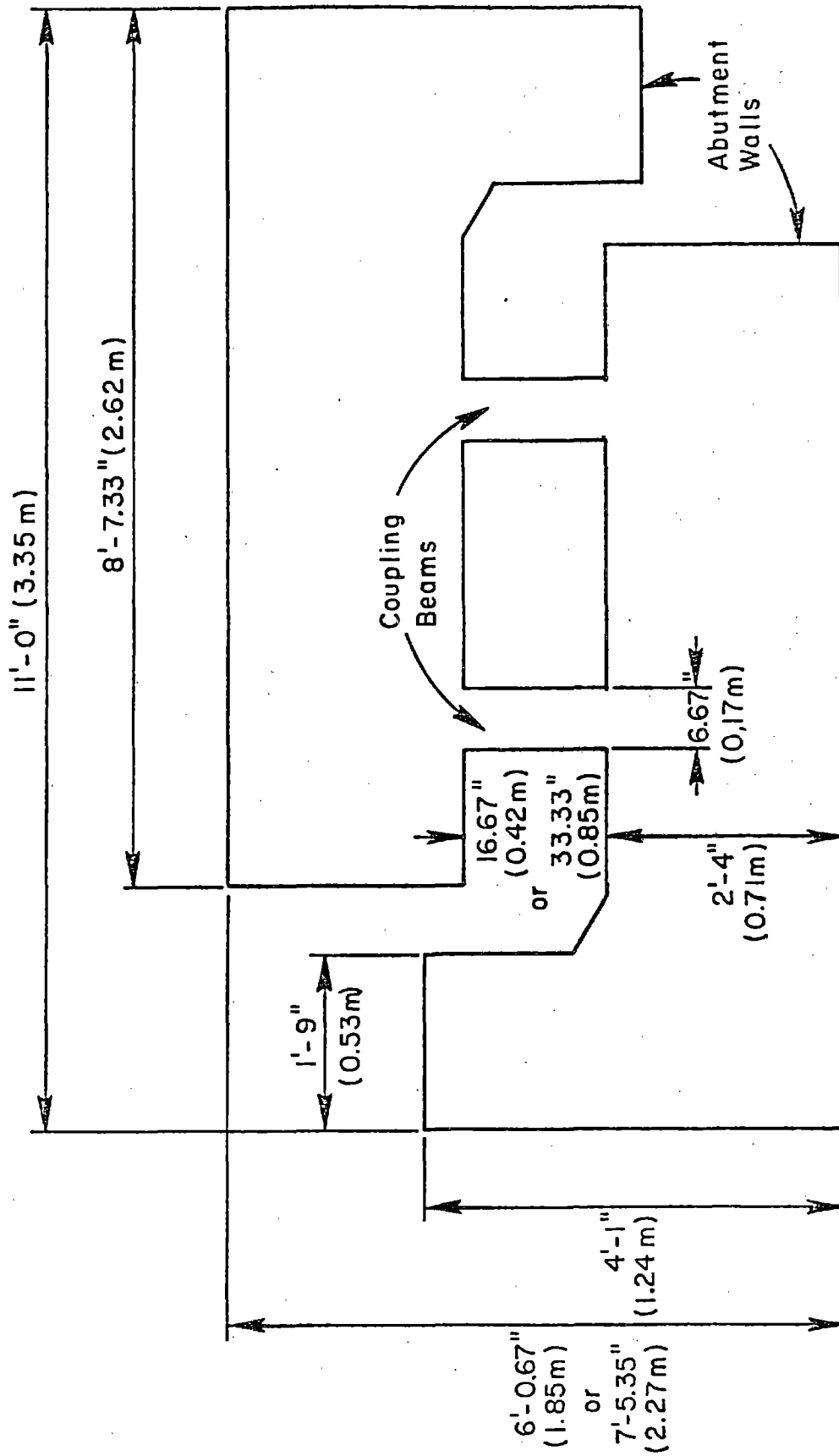
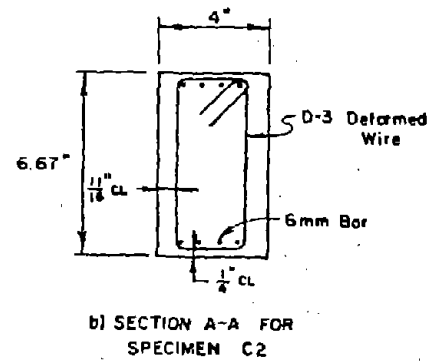
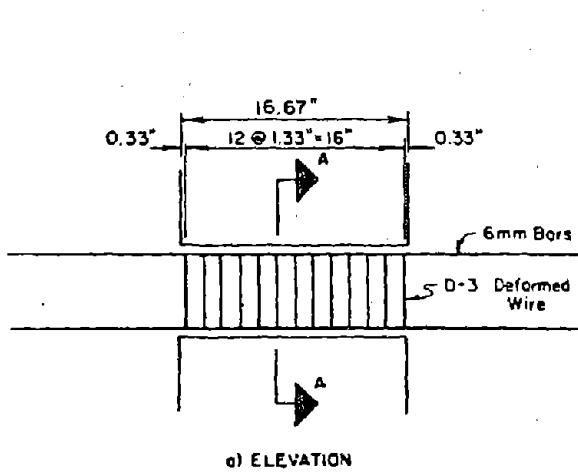
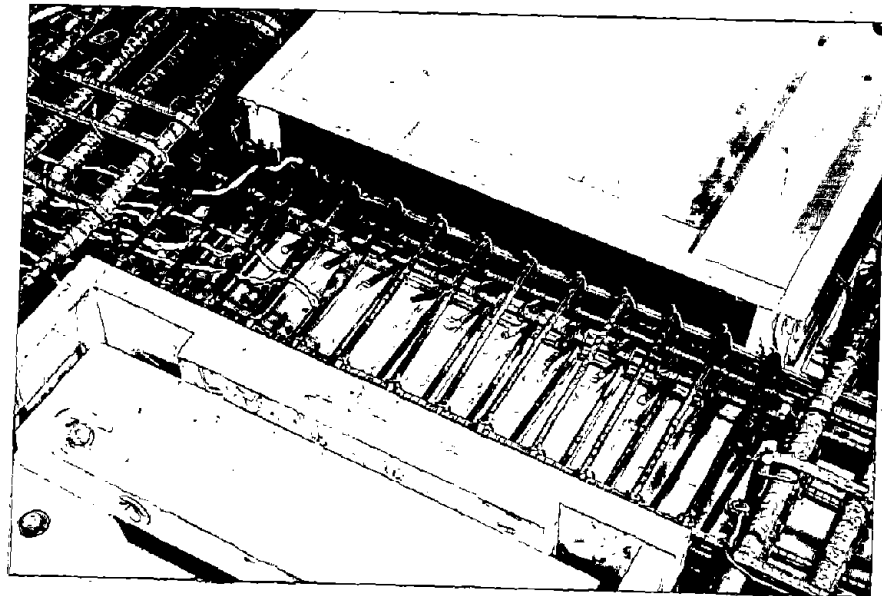
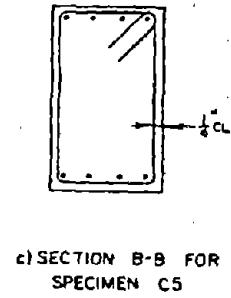


Fig. A-1 Test Specimen

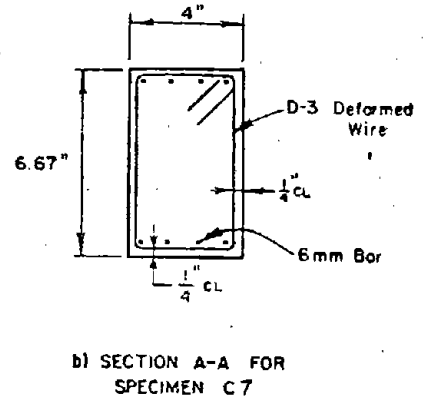
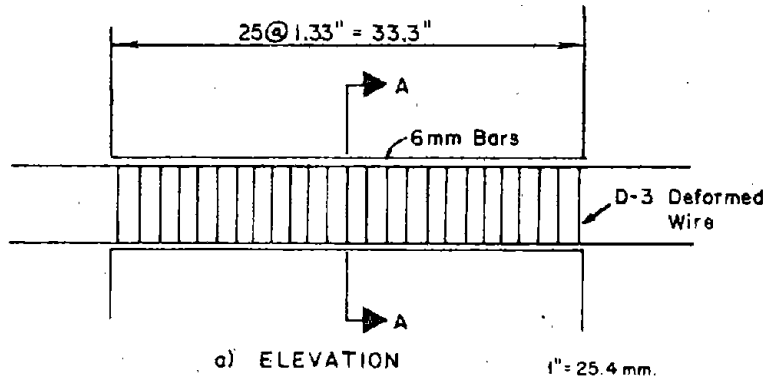


1" = 25.4 mm.



d) Reinforcement Cage

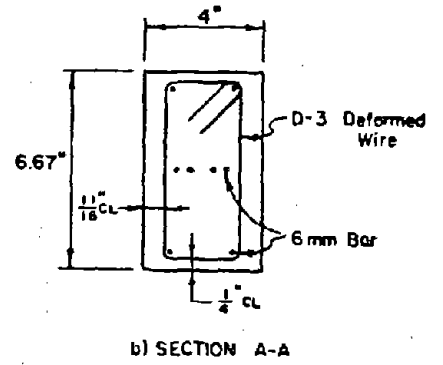
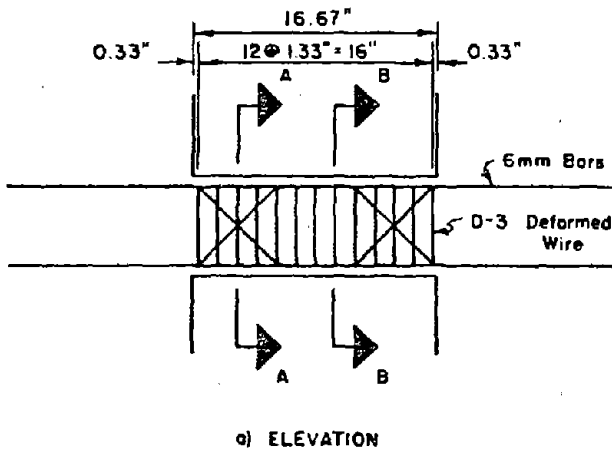
Fig. A-2 Reinforcement for Specimens C2 and C5



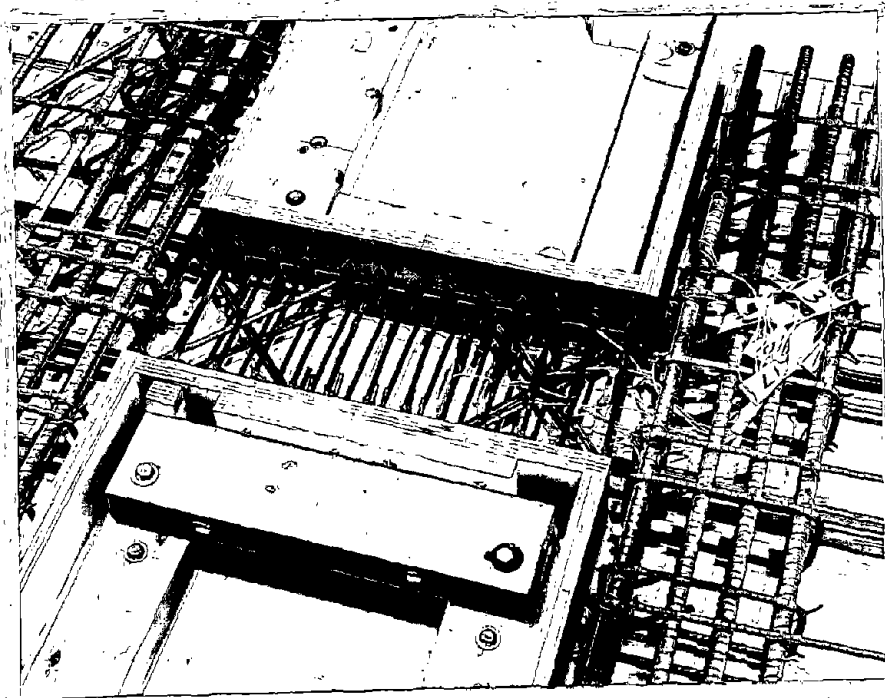
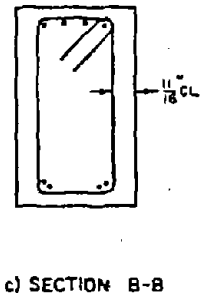
c) Reinforcement Cage

Fig. A-3 Reinforcement for Specimen C7



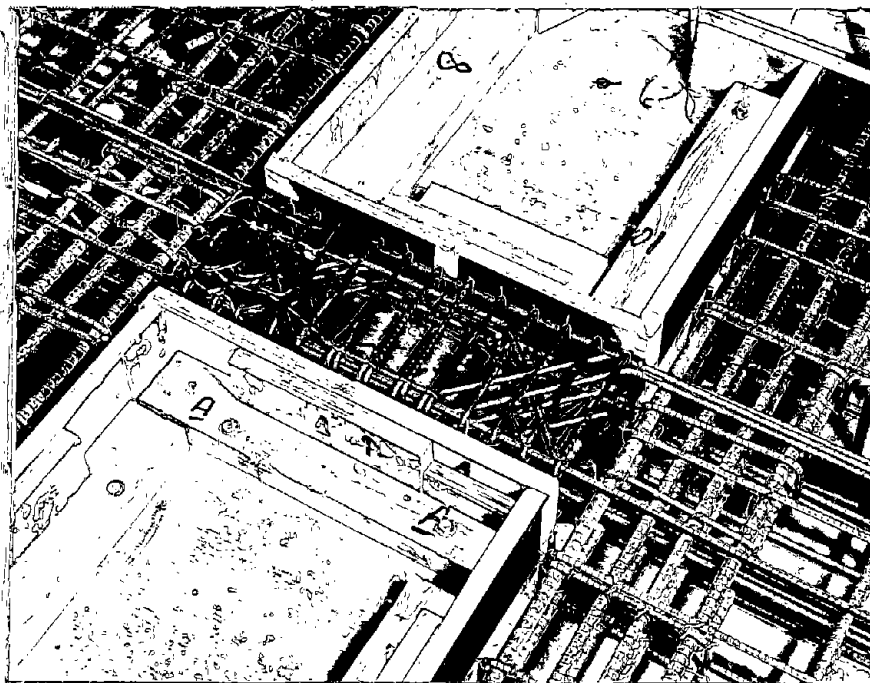
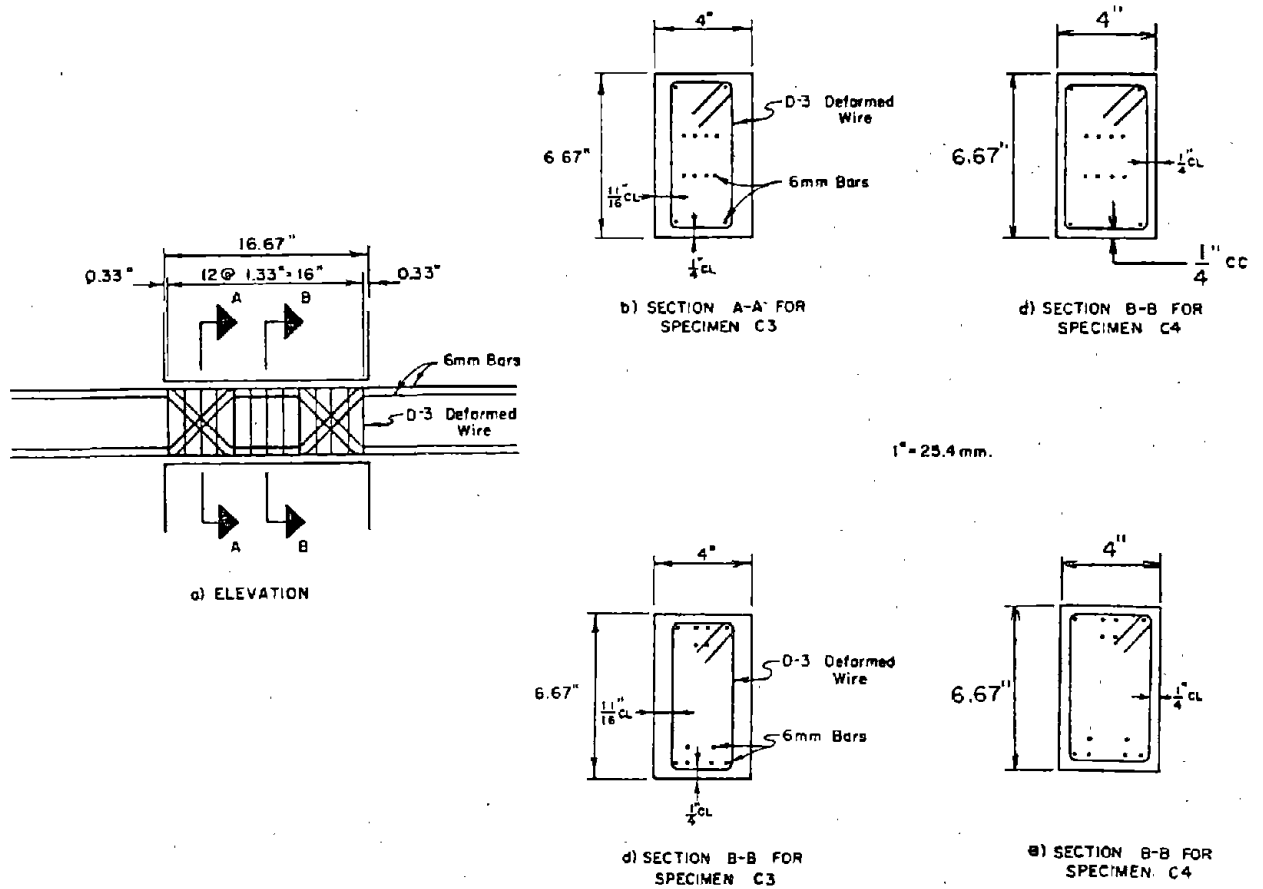


1" = 25.4 mm.



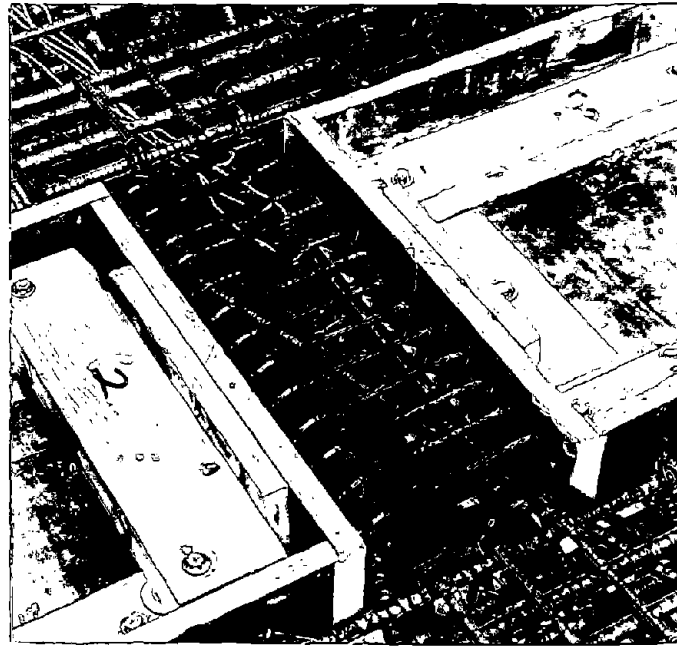
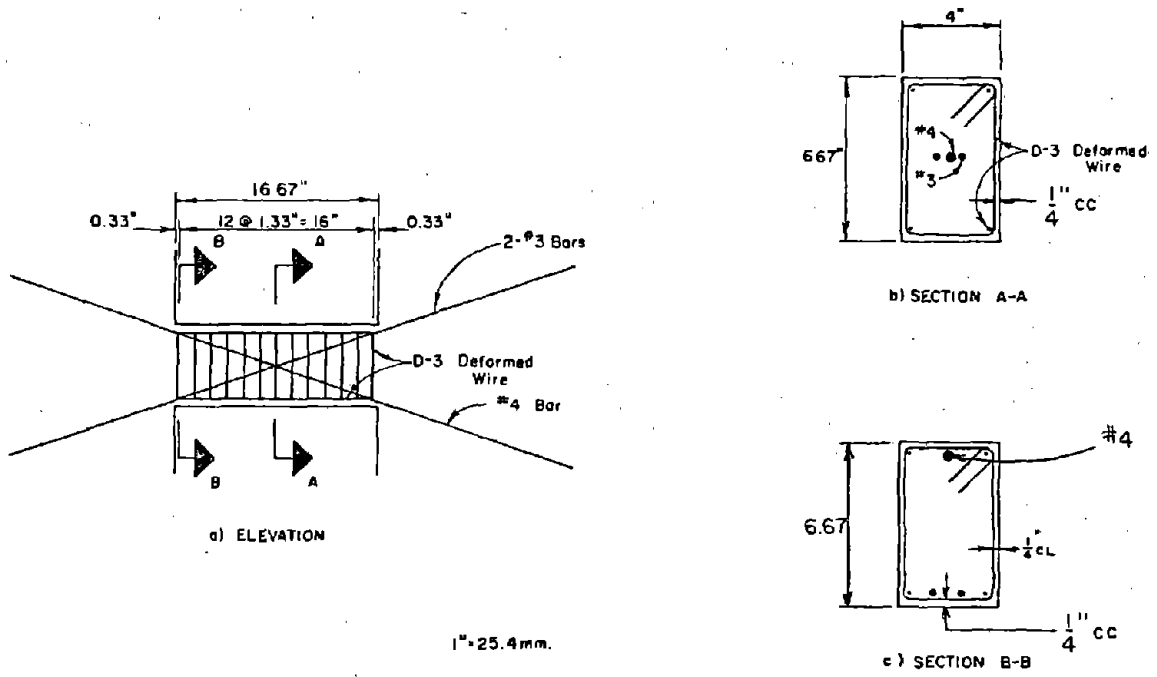
d) Reinforcement Cage

Fig. A-4 Reinforcement for Specimen C1



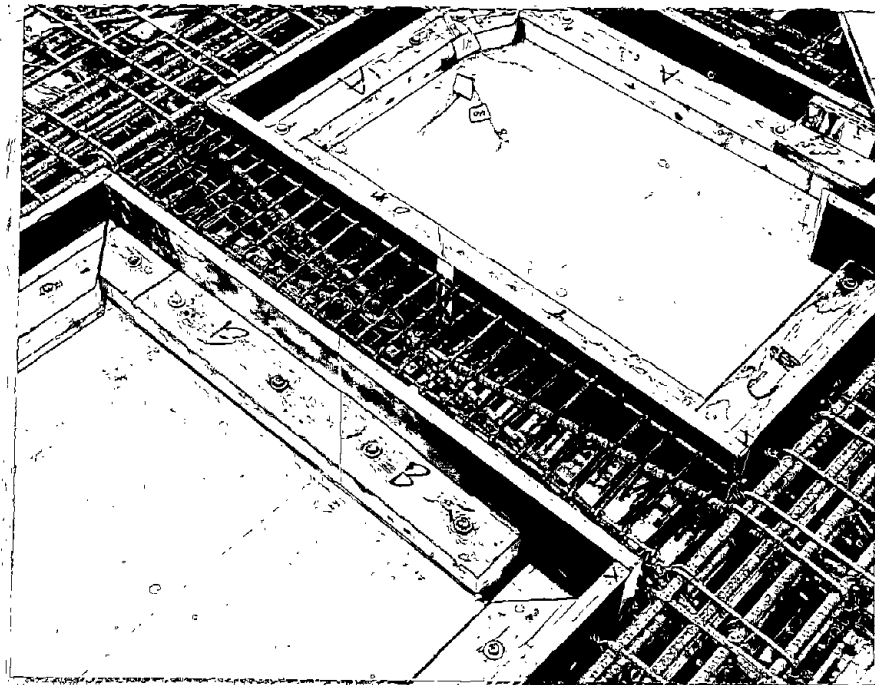
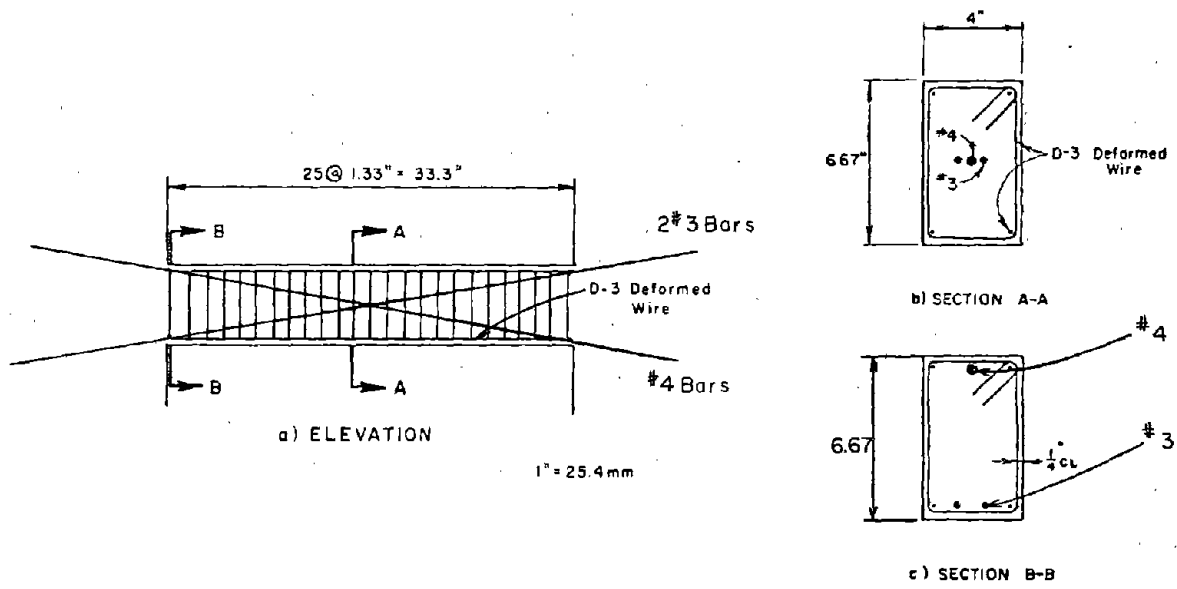
f) Reinforcement Cage

Fig. A-5 Reinforcement for Specimens C3 and C4



d) Reinforcement Cage

Fig. A-6 Reinforcement for Specimen C6



d) Reinforcement Cage

Fig. A-7 Reinforcement for Specimen C8

### Specimen C1

Diagonal reinforcement was provided for Specimen C1 as shown in Fig. A-4. Two 6 mm bars top and bottom were bent at 45 degrees starting at the face of the wall at each end of the beam.

### Specimens C3 and C4

Diagonals were provided in the hinging regions of Specimens C3 and C4 as shown in Fig. A-5. Four 6-mm bars were bent at 45 degrees top and bottom. Specimens C3 and C4 were similar except for the size of the confined concrete core. Specimen C4 had a core area 33% greater than Specimen C3 as shown in Fig. A-5(b) and (c). The larger core size required that the top and bottom reinforcing bars in the coupling beams be placed outside the steel in the rigid abutments. This anchorage detail is not recommended for field practice.

### Specimens C6 and C8

Primary reinforcement for Specimens C6 and C8 consisted of full-length diagonals as shown in Figs. A-6 and A-7. Diagonals were two No. 3 bars in one direction and one No. 4 in the other. Symmetry was maintained by passing the No. 4 bar between the No. 3 bars at midspan. Two 6 mm longitudinal bars were provided for tying hoops in place. These bars were not anchored in the abutment walls.

## Materials

Concrete and reinforcing steel properties for the test specimens are summarized in Table A-1.

Concrete used was designed to have compressive strength of 3,000 psi (20.7 MPa). The mix consisted of Type I cement, sand, and aggregate with a maximum size of 3/8 in. (9.5 mm). Material properties were determined from tests on 6x12-in. (153x305 mm) cylinders. Concrete properties are contained in Table A-1 and a representative stress versus strain curve is shown in Fig. A-8.

For the reinforcement, No. 3 and No. 4 bars conformed to ASTM Designation A615 Grade 60.<sup>(8)</sup> Deformed 6-mm hot rolled

TABLE A-1 - MATERIAL PROPERTIES

Specimen No.	D-3* Deformed Wire (ksi)			6 mm** Bar (ksi)			No. 3 Bar (ksi)			No. 4 Bar (ksi)			Concrete	
	$f_y$	$f_{su}$	$E_s$	$f_y$	$f_{su}$	$E_s$	$f_y$	$f_{su}$	$E_s$	$f_y$	$f_{su}$	$E_s$	$f'_c$ (psi)	$E_c$ (ksi)
C1	70.0	76.3	32,400	69.2	98.0	31,400	--	--	--	--	--	--	2,940	3,180
C2	69.3	75.0	30,000	74.9	99.8	30,000	--	--	--	--	--	--	3,050	2,910
C3	69.3	75.1	29,400	73.6	98.8	30,600	--	--	--	--	--	--	2,970	3,040
C4	70.8	75.0	31,300	66.0	89.7	30,000	--	--	--	--	--	--	3,490	3,170
C5	71.1	75.1	31,100	66.3	88.8	30,000	--	--	--	--	--	--	3,140	2,730
C6	71.4	75.1	31,000	--	--	--	70.7	104.7	30,200	59.2	103.2	31,000	2,620	2,780
C7	62.1	72.5	26,700	66.5	87.8	30,800	--	--	--	--	--	--	3,710	3,050
C8	71.0	81.7	28,300	--	--	--	82.5	125.1	28,600	62.8	102.5	28,500	3,470	3,100

\*Area = 0.03 sq. in. (19 sq. mm)  $f_y$  = yield strength of steel  $f'_c$  = compressive strength of concrete  
 \*\*Area = 0.05 sq. in. (32 sq. mm)  $f_{su}$  = tensile strength of steel  $E_c$  = mod. of elasticity of concrete  
 1,000 psi = 1 ksi = 6.895 MPa  $E_s$  = mod. of elasticity of steel

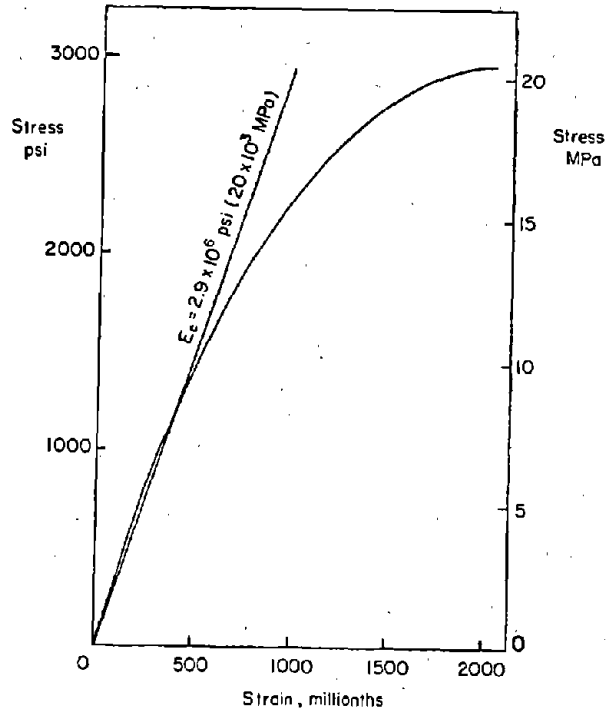


Fig. A-8 Representative Stress versus Strain Relationship for Concrete

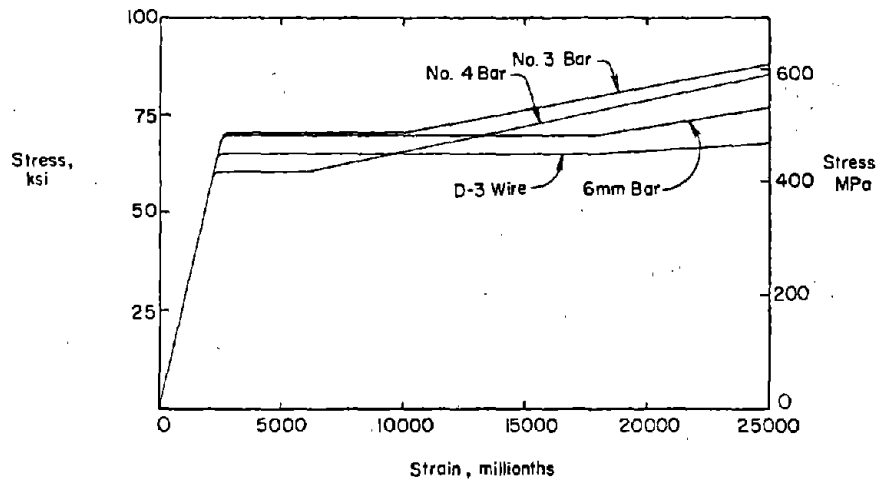


Fig. A-9 Representative Stress versus Strain Relationships for Reinforcement

bars with properties similar to Grade 60 were also used as primary reinforcement. Deformed wire, size D-3, was used for transverse hoops. This wire was heat treated to obtain stress-strain characteristics similar to Grade 60. Physical properties of the reinforcement used in the test specimens are given in Table A-1. Representative stress versus strain relationships are shown in Fig. A-9.

#### Fabrication

Specimens were cast in a horizontal position using the forming system shown in Fig. A-10. Reinforcing cages for the abutments and coupling beams were constructed separately and then placed together in the form. Before casting, lifting eyes and inserts for attaching external instrumentation were placed in position.

Each specimen was cast in four batches. Concrete for both coupling beams in each specimen was taken from the same batch. After casting, the specimens were covered with a sheet of polyethylene plastic and allowed to cure for four days. Control cylinders were cured in a similar manner. Specimens were then stripped and moved to the test location. Testing usually began on the fourteenth day after casting.

#### Supporting and Loading Systems

Specimens were placed parallel to the laboratory floor<sup>(9)</sup> and supported on thrust bearings as illustrated in Fig. A-11. Blocks to resist applied forces were post-tensioned to the laboratory floor on each side of the specimen. One end of the specimen was fixed. Hydraulic rams were used to apply load at the opposite end. The line of action of the applied forces passed through the mid-span of the coupling beams. This minimized the possibility of axial forces occurring in the beams.

Magnitude of the applied forces was controlled by a hydraulic pump. A four-way valve was used in the hydraulic line to direct pressure to one of two rams to either push or pull on



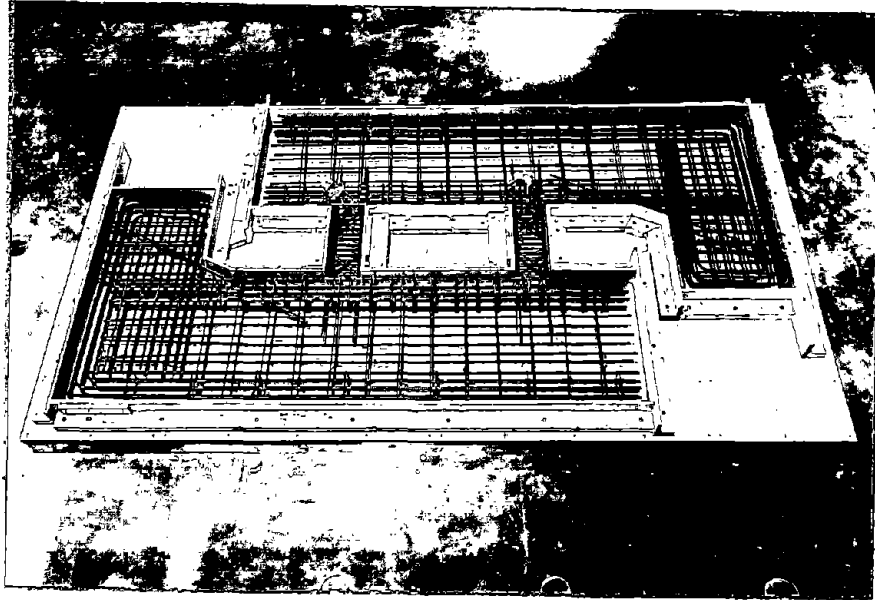


Fig. A-10 Specimen Prior to Casting

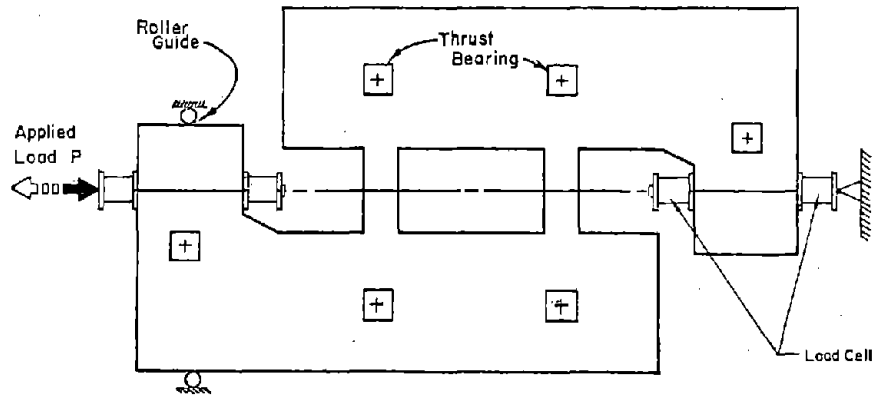


Fig. A-11 Test Setup

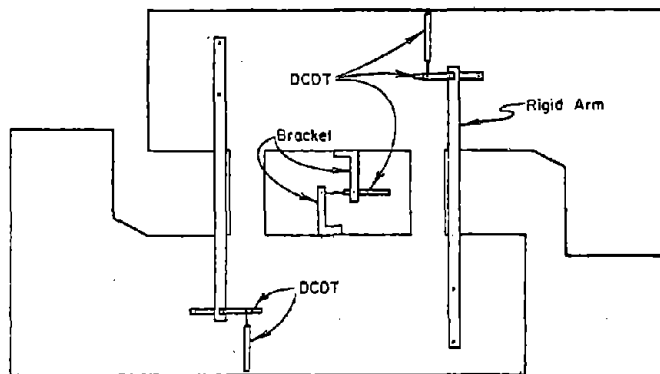


Fig. A-12 External Instrumentation

the specimen. Lateral movement at the live end of the specimens was prevented by roller guides bearing against blocks stressed to the laboratory floor.

#### Instrumentation

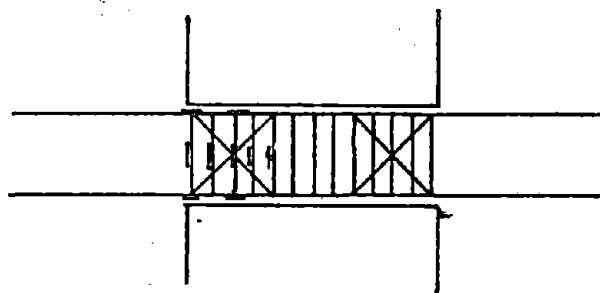
Test specimens were instrumented to measure applied and resisted loads, deflections, and steel strains. Readings from each sensing device were recorded by a digital data acquisition systems interfaced with desk top micro computer. Data were stored on cassettes.

Loads were recorded by load cells<sup>(9)</sup> located at both the fixed and live ends of the specimens. This arrangement provided a means for determining losses caused by friction in the thrust-bearing supports. Loss was generally less than 2% of the applied loads.

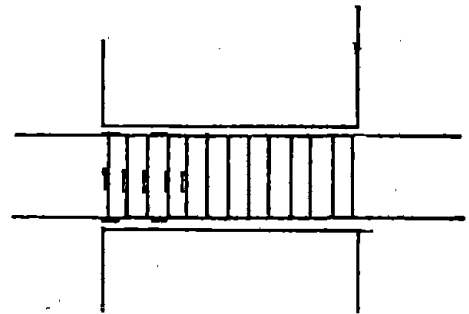
Lateral displacements in most specimens were recorded at three locations. The gages used had a sensitivity of 0.001 in. (0.03 mm). One gage was attached to brackets on the inside face of each rigid abutment midway between the coupling beams as shown in Fig. A-12. Two additional gages were installed at the end of each coupling beam. All three gages measured the relative lateral displacement of the ends of the coupling beams. Gages were also installed to measure axial deformations at each coupling beam location.

A continuous record of load versus deflection was also recorded by an X-Y plotter. Load was measured by calibrated pressure cells. Deflections were taken as the relative lateral movement between the abutment walls.

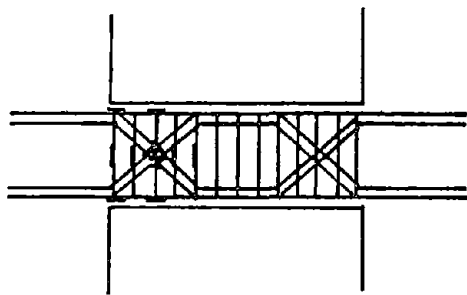
Electrical resistance strain gages were attached to the reinforcing steel in all specimens. Strains were measured on the flexural steel, diagonal steel, and hoops. Locations of strain gages are shown in Fig. A-13.



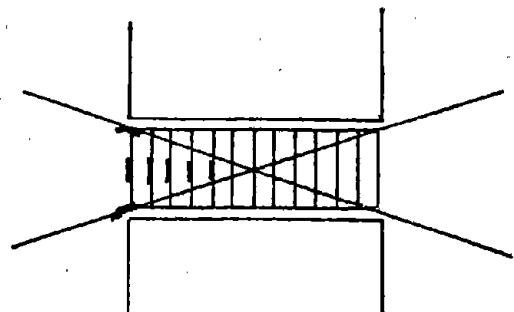
a) Specimen C1



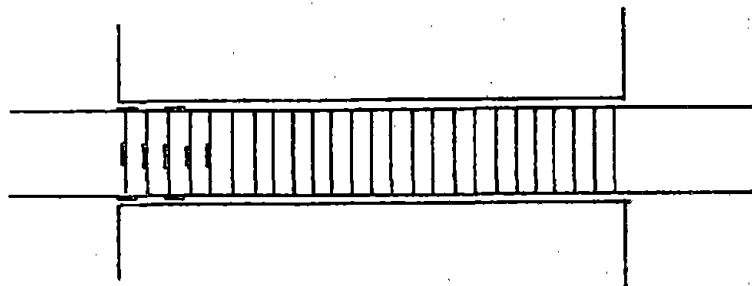
b) Specimen C2 and C5



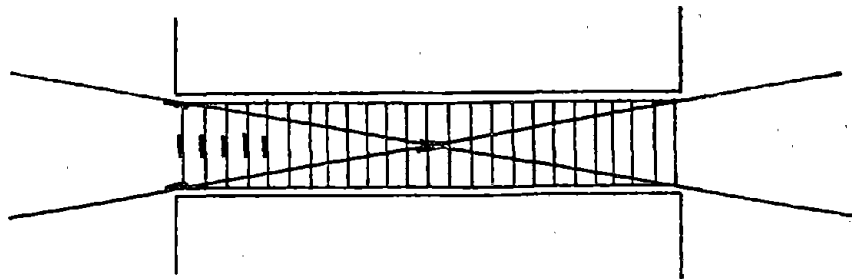
c) Specimens C3 and C4



d) Specimen C6



e) Specimen C7



f) Specimen C8

Fig. A-13 Location of Strain Gages

### Test Procedure

Prior to yield, loading was controlled by the magnitude of applied forces. After yielding, loading was controlled by the imposed deflection on specimens.

Three complete loading cycles were applied for each pre-determined level of force or displacement. The three cycles together are termed a "load increment." Each cycle started and ended with zero force applied.

The first cycle of each increment was applied in steps termed load stages. Data were recorded at each load stage. On the second and third cycle data were recorded only at peak loads or displacements.

Testing was terminated either when a significant loss of capacity occurred or when specimens experienced bar fracture.

After each load stage, specimens were inspected visually for cracking and evidence of distress. Cracks were marked with a felt tip pen. Photographs were taken at the end of each load stage to provide a record of crack development.



## APPENDIX B - TEST RESULTS

In this Appendix the behavior of each test specimen is described in detail. Load and deflection histories, and measured steel strains are presented. The data plots use straight lines between the load stages. The numbers on each plot are the cycle number. The segmental load versus deflection plot represents the first cycle of each loading increment.

### Specimen C1

Reinforcement details and section dimensions for Specimen C1 are shown in Fig. A-4. Diagonal reinforcement was provided in the hinging regions. Load and deflection histories of this specimen are given in Fig. B-1.

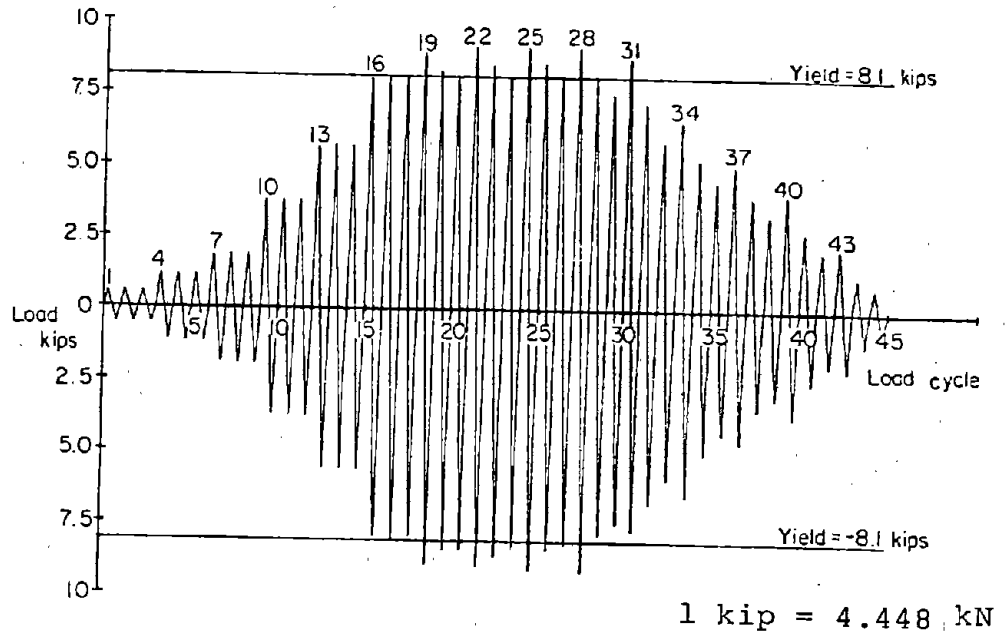
Cracking in this specimen was first observed in the tension zones at the ends of each beam during the seventh load cycle at an applied load of 3.3 kips (14.7 kN) per beam. Yielding of the flexural reinforcement occurred during the seventeenth load cycle at a load of 8.1 kips (36.0 kN) per beam. The recorded deflection at yield was 0.16-in. (4 mm). Flexural cracks at the yield load extended across the full depth of each beam at the ends. Flexure-shear cracks were also observed at sections located between 3 and 6-in. (76 and 154 mm) from the ends of the beams.

A segmental plot of load versus deflection between the ends of coupling beams is shown in Fig. B-2. Measured reinforcement strains are presented in Figs. B-3 through B-9.

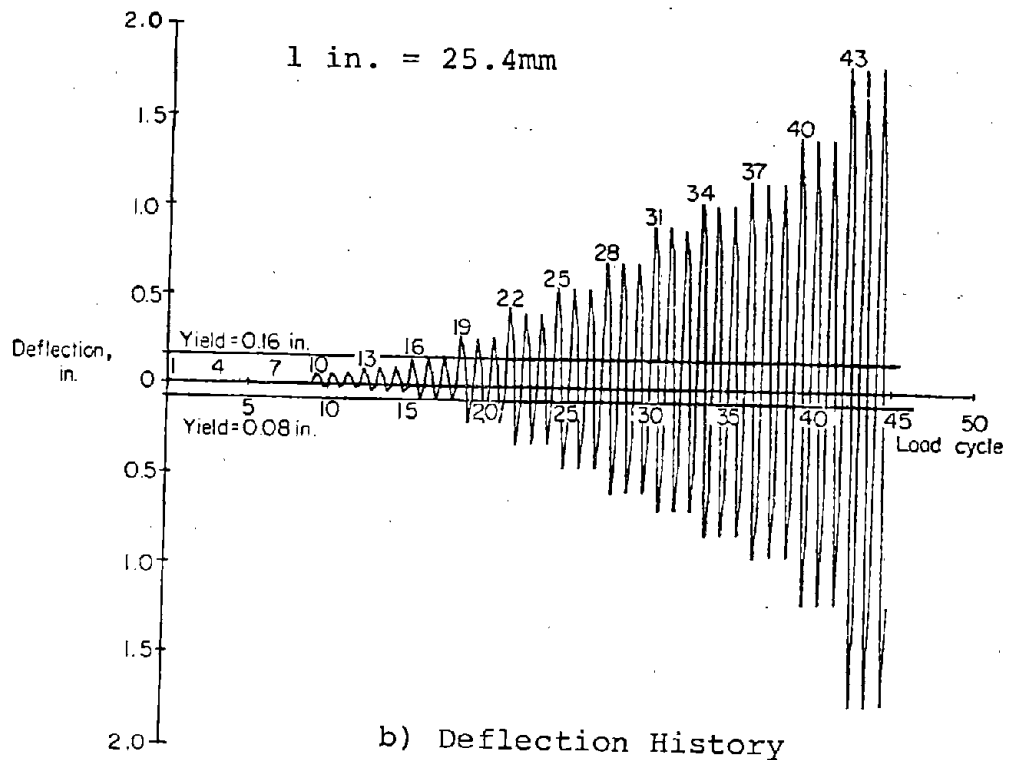
Yielding of the diagonal reinforcement occurred at a load of 8.9 kips (39.6 kN) per beam during the third inelastic load cycle.

A maximum load of 9.2 kips (40.9 kN) per beam was carried by the specimen during the ninth inelastic load cycle. The nominal shear stress at this load was  $7.0 \sqrt{f'_c}$  psi ( $0.58 \sqrt{f'_c}$  MPa). The corresponding deflection was measured as 0.55-in. (14 mm).

Concrete cover in the hinging regions began spalling at an applied load of 9.1 kips (40.5 kN) per beam. This occurred at



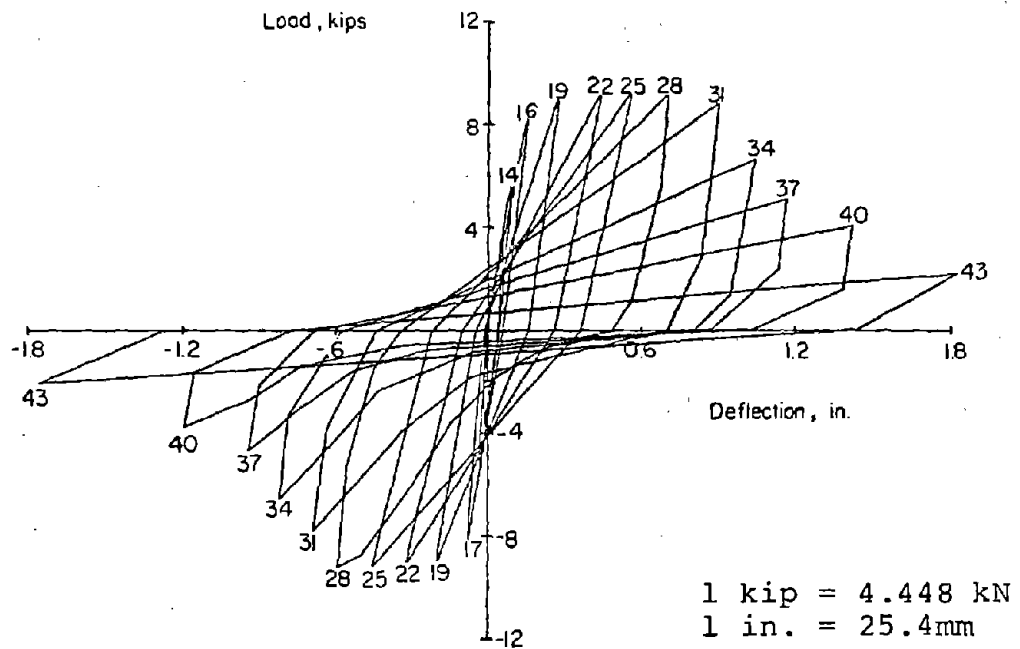
a) Load History



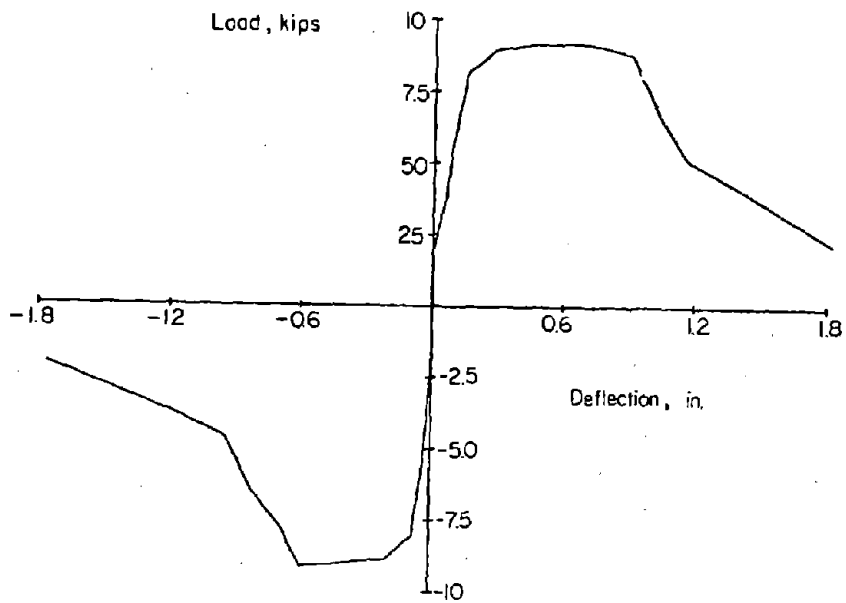
b) Deflection History

Fig. B-1 Loading History for Specimen C1





a) Segmental Plot



b) Envelope

Fig. B-2 Load versus Deflection Relationships for Specimen C1

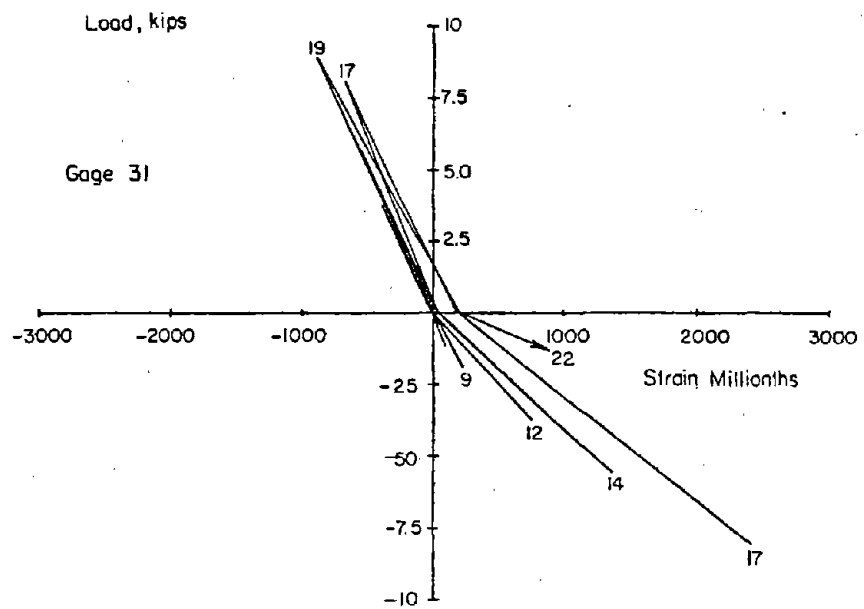
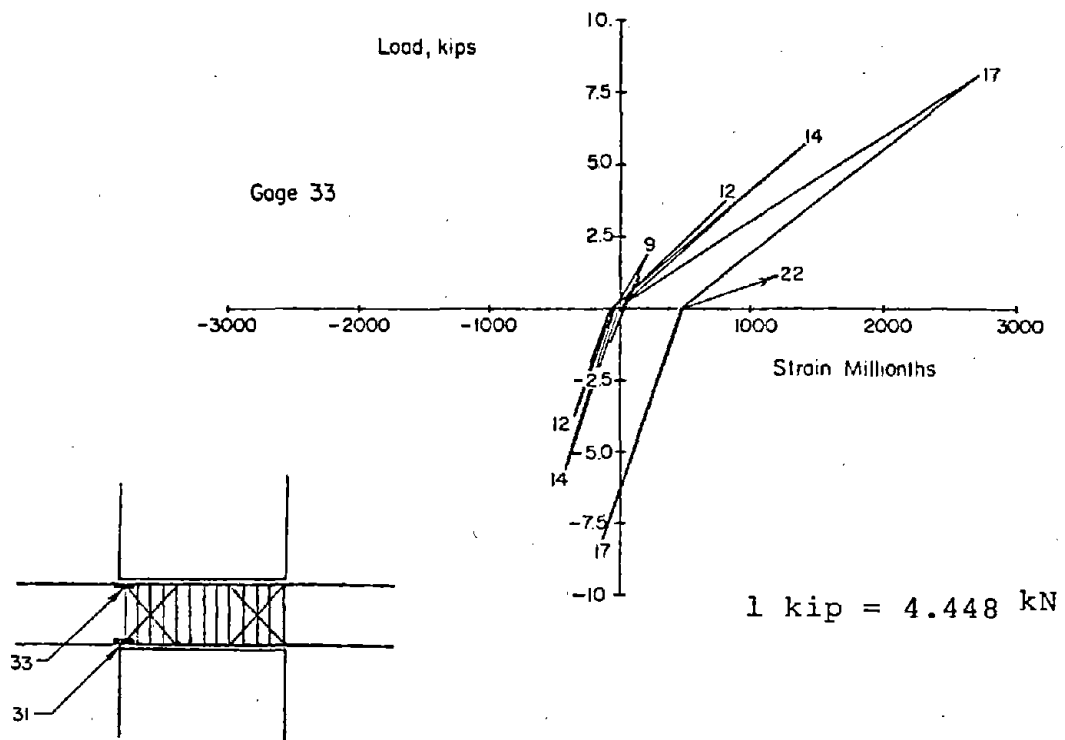


Fig. B-3 Load versus Flexural Steel Strains  
for Specimen C1 (East Beam)

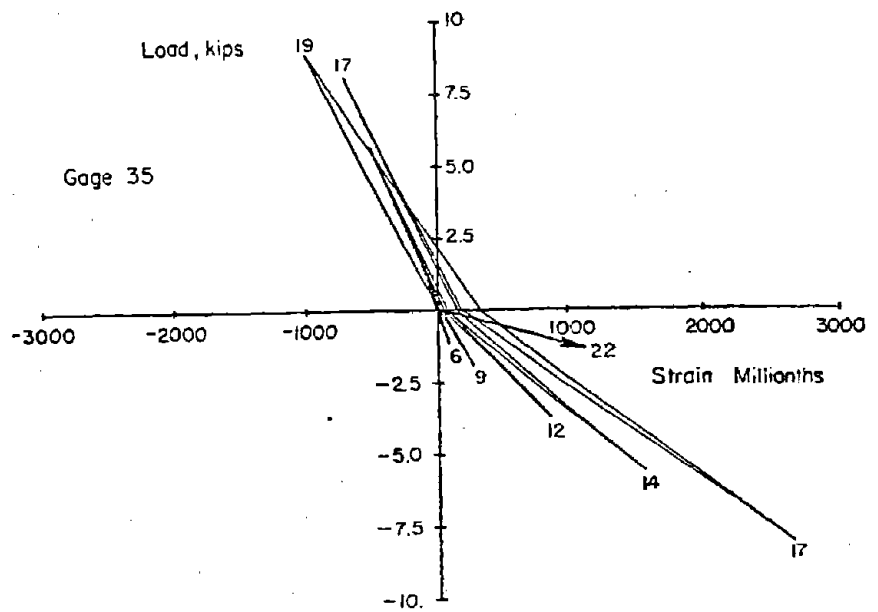
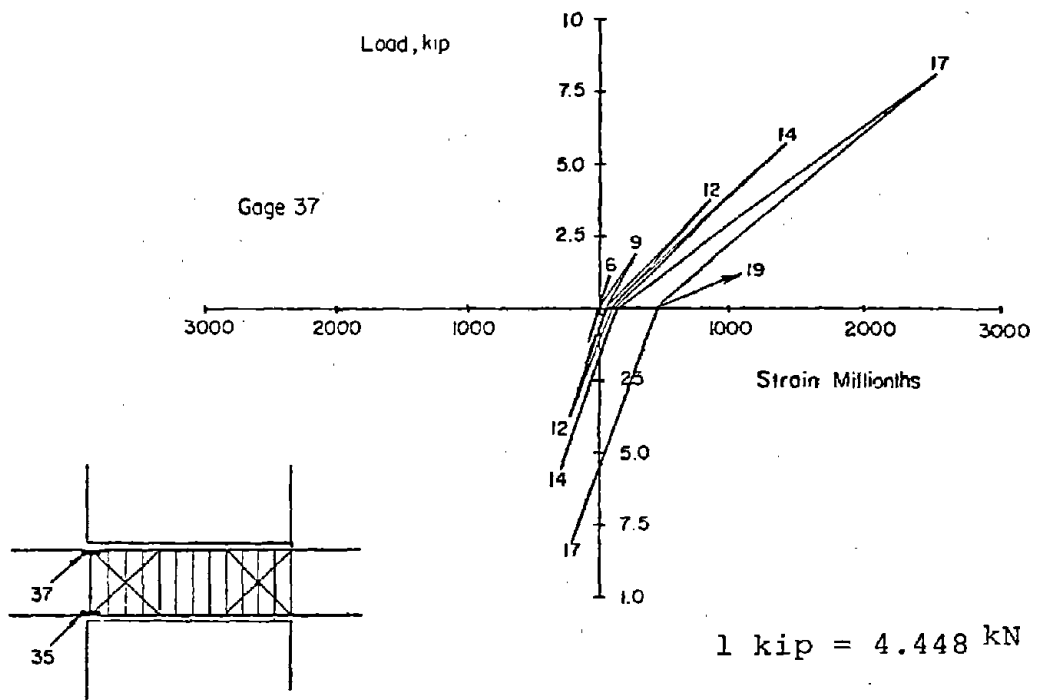


Fig. B-4 Load versus Flexural Steel Strains for Specimen C1 (West Beam)

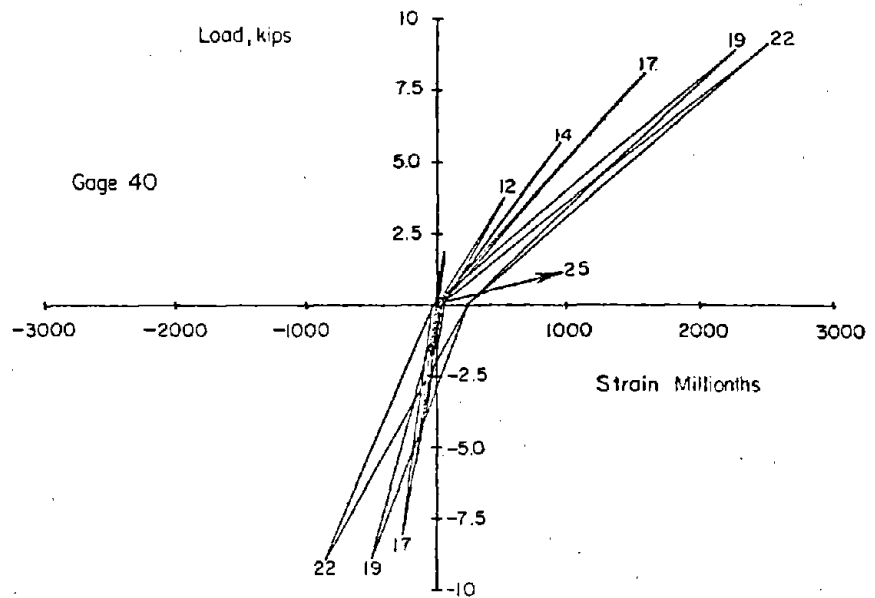
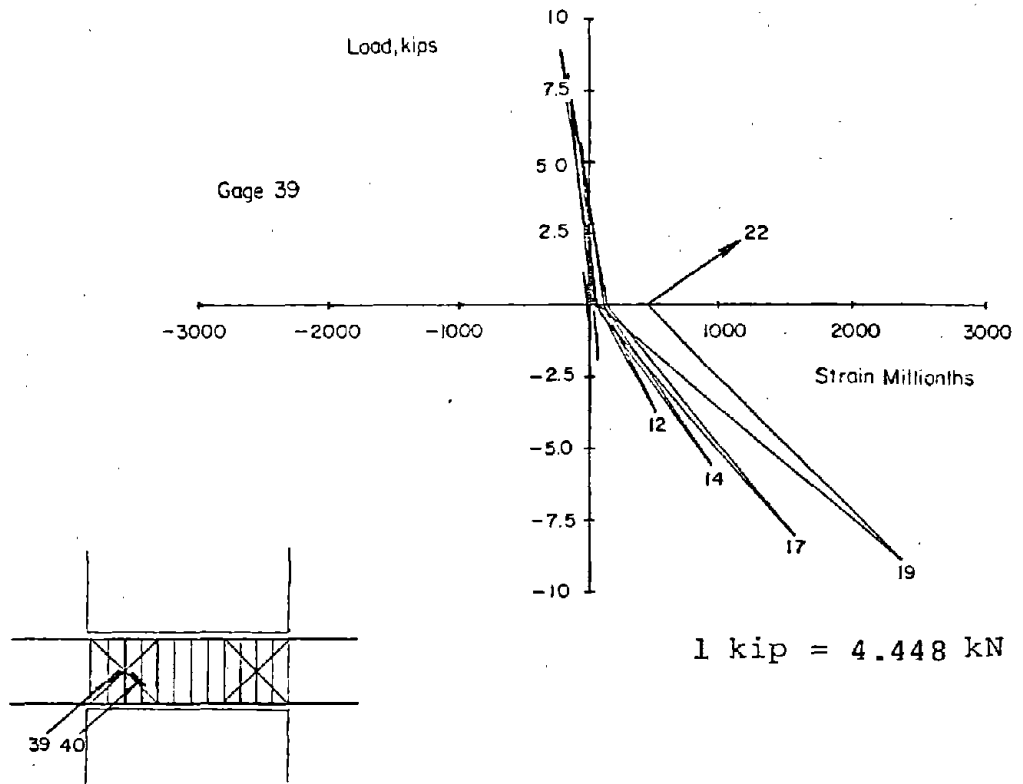


Fig. B-5 Load versus Diagonal Steel Strains for Specimen C1 (East Beam)

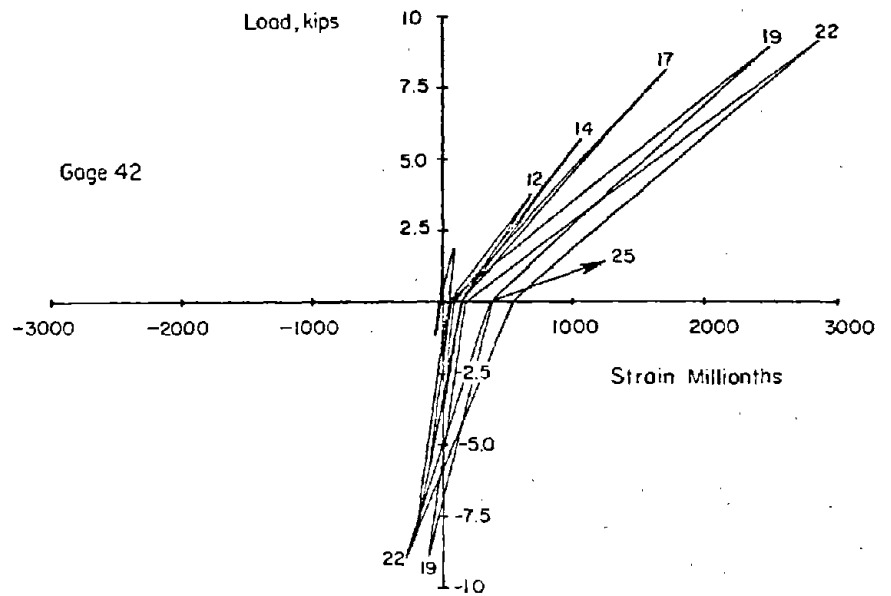
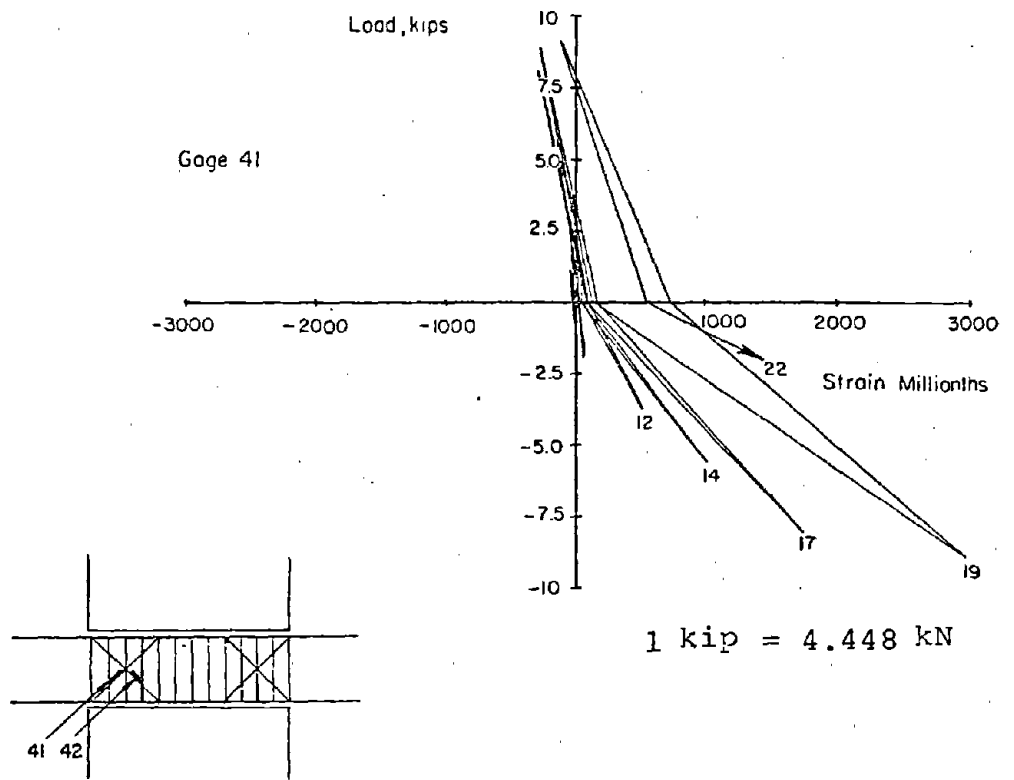


Fig. B-6 Load versus Diagonal Steel Strains for Specimen C1 (West Beams)

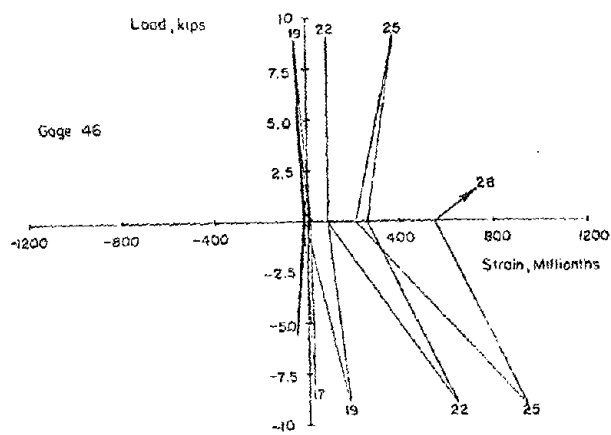
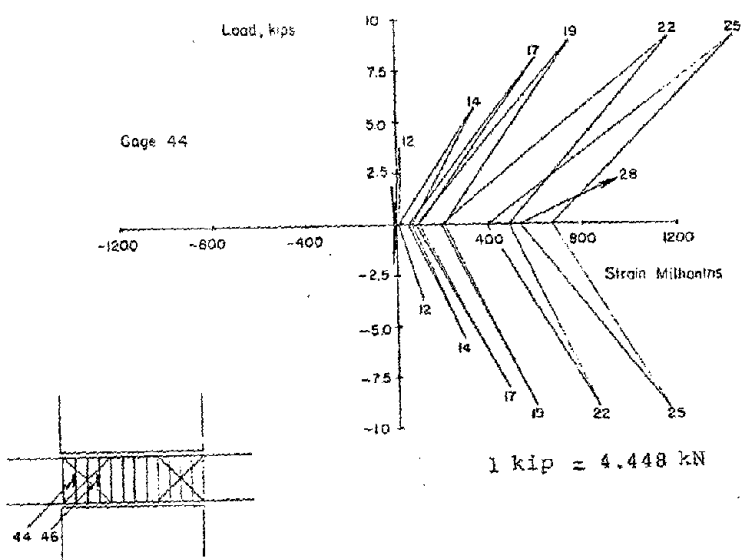


Fig. B-7 Load versus Hoop Steel Strains for Specimen C1 (East Beam)

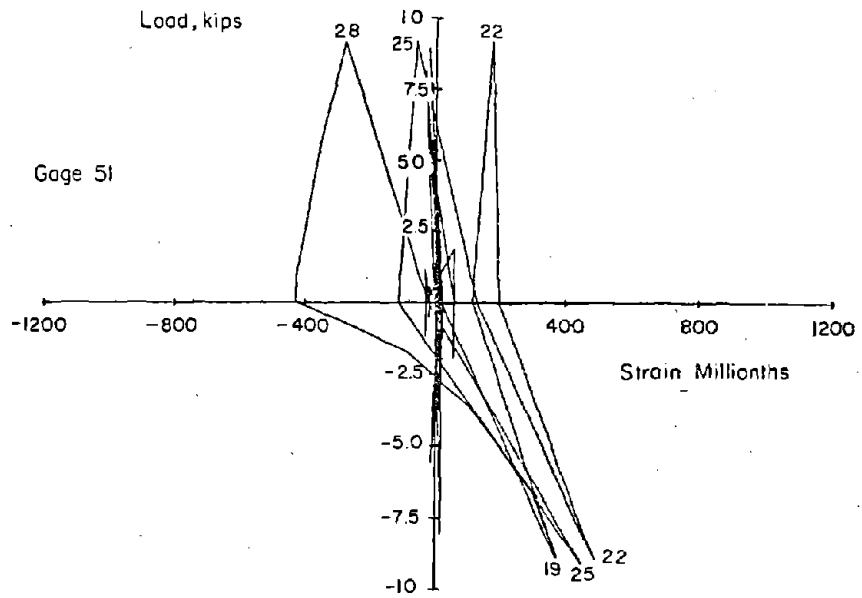
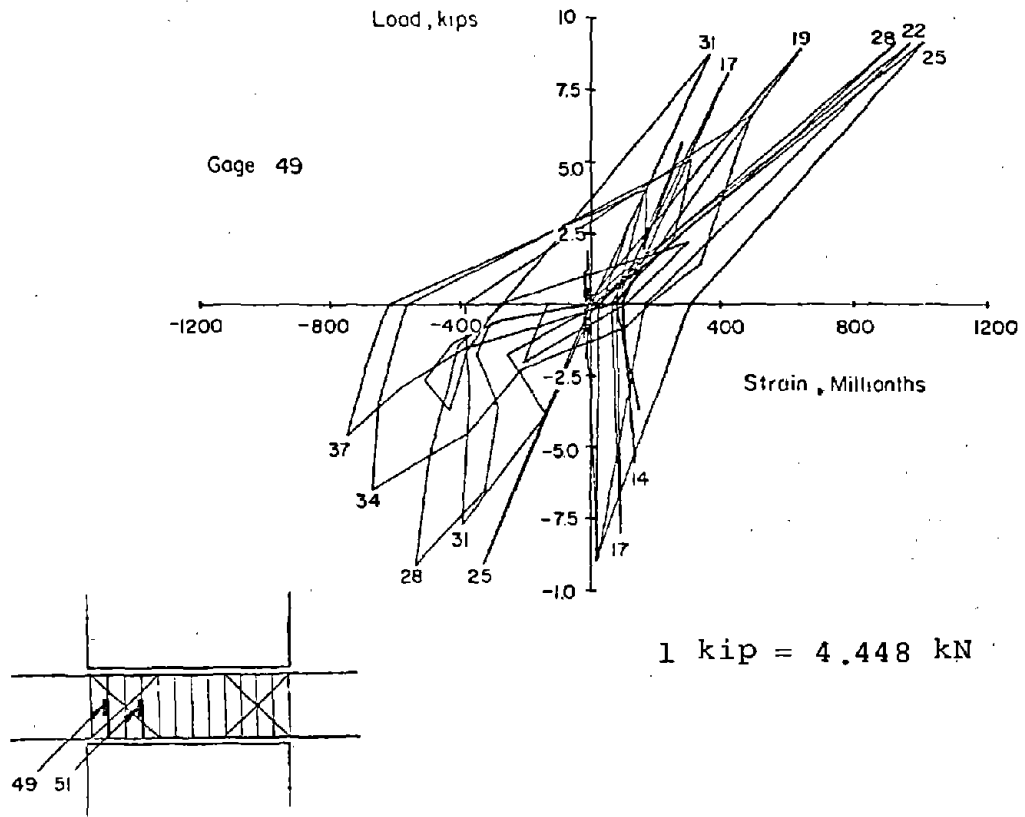
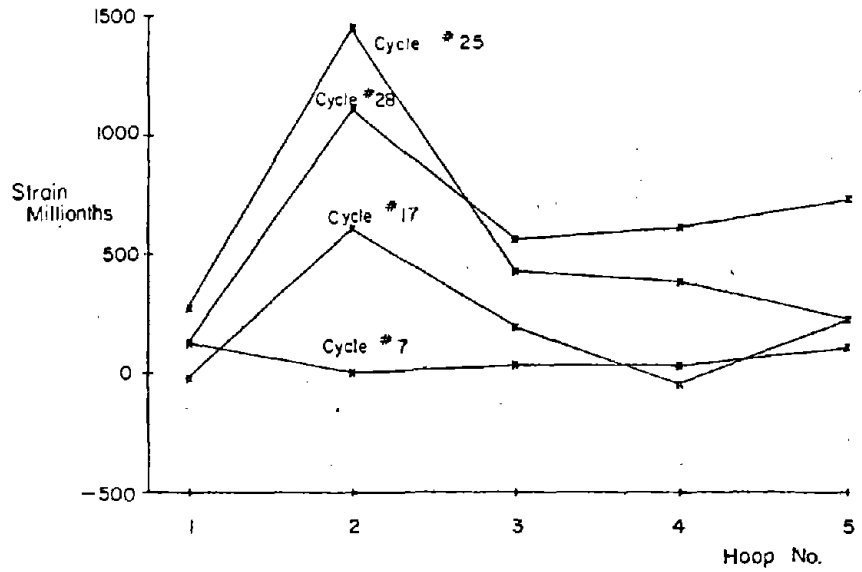
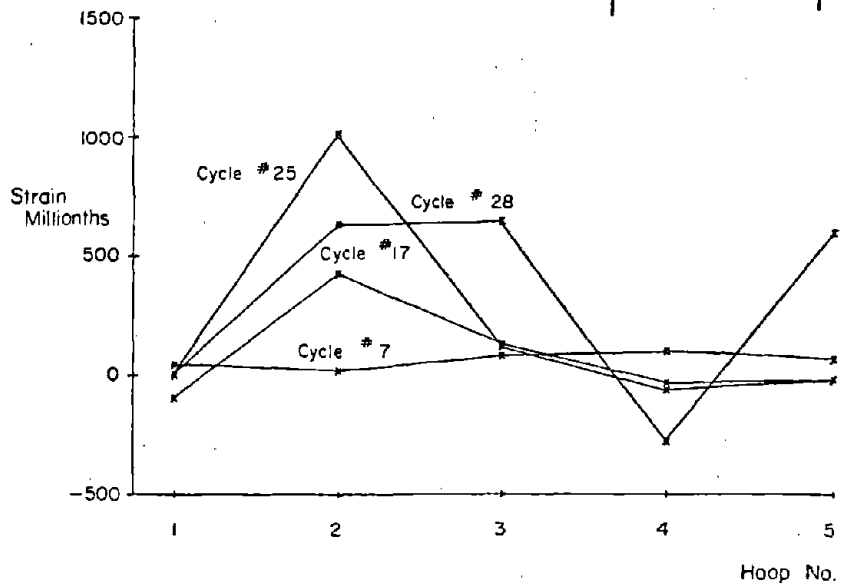
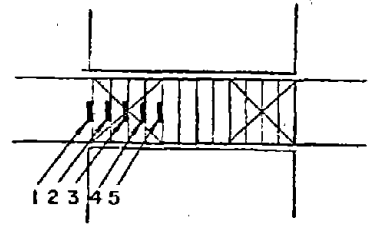


Fig. B-8 Load versus Hoop Steel Strains for Specimen C1 (West Beam)



a) East Beam



b) West Beam

Fig. B-9 Hoop Steel Strains for Specimen C1



a deflection of 0.71-in. (18 mm) during the twelfth inelastic load cycle.

Spalling concrete in the shell around the confined core exposed the reinforcement. Deterioration of the concrete inside the confined core was also observed in the hinging regions.

In the final loading cycle at the maximum imposed deflection of 1.82-in. (46 mm), a load of 0.9 kips (4.0 kN) per beam was recorded. The test was terminated after this cycle. A total of 29 inelastic cycles were applied to the specimen.

### Specimen C2

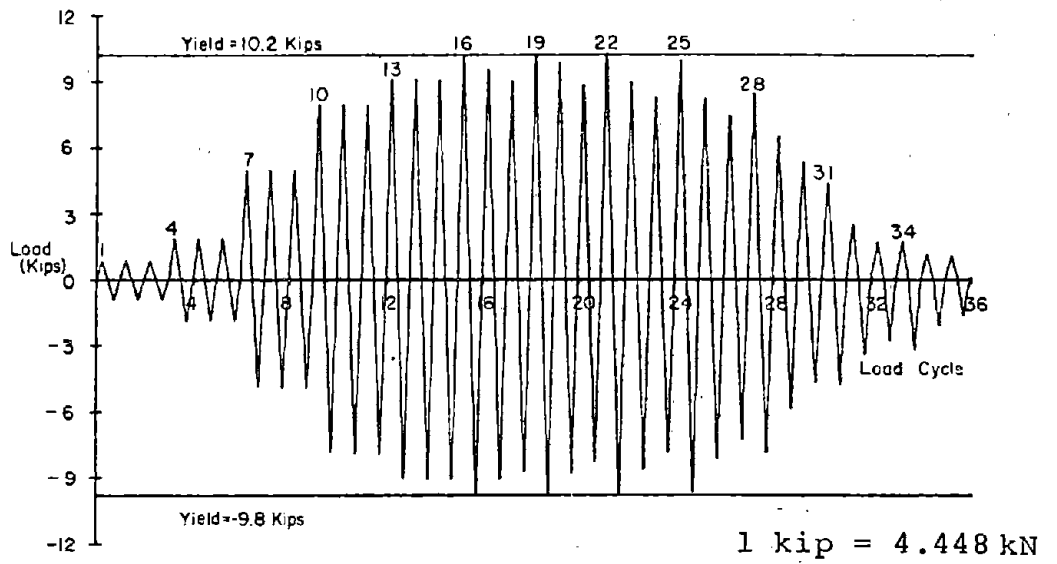
Details for Specimen C2 are shown in Fig. A-2. Load and deflection histories for Specimen C2 are shown in Fig. B-10. Plots of load versus deflection during the test are given in Fig. B-11. Strain data are given in Figs. B-12 through B-16.

First cracking in this specimen occurred during the fourth load cycle at a load of 1.9 kips (8.5 kN) per beam. Yielding of the flexural reinforcement was recorded during the sixteenth load cycle at a load of 10.2 kips (45.4 kN) per beam. Deflection at first yield reached 0.23-in. (6 mm). The reversing loads caused flexural cracks extending across the full depth of the beams at the ends. Diagonal cracking in both directions also appeared in the end regions of both beams.

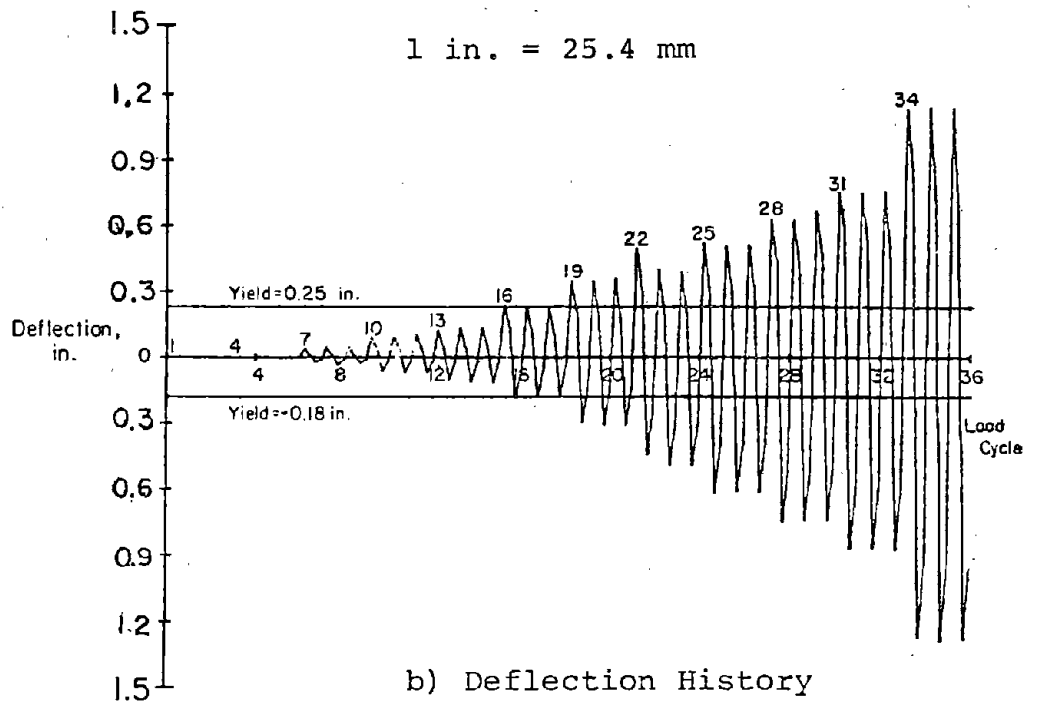
The maximum load of 10.3 kips (45.8 kN) per beam carried by Specimen C2 occurred during the seventh inelastic load cycle. Nominal shear stress at this load was  $7.7 \sqrt{f'_c}$  psi ( $0.64 \sqrt{f'_c}$  MPa). Deflection at this load was measured as 0.41-in. (10 mm).

Spalling of the concrete shell surrounding the confined core began in the hinging region at a load of 5.9 kips (26.2 kN) per beam during the fourteenth inelastic load cycle. Deflection at this load was 0.74-in. (19 mm).

During the final cycle, the capacity of the specimen at an imposed deflection of 1.28-in. (32 mm) was 1.7 kips (7.6 kN) per beam. A total of 21 inelastic load cycles were applied to the specimen.

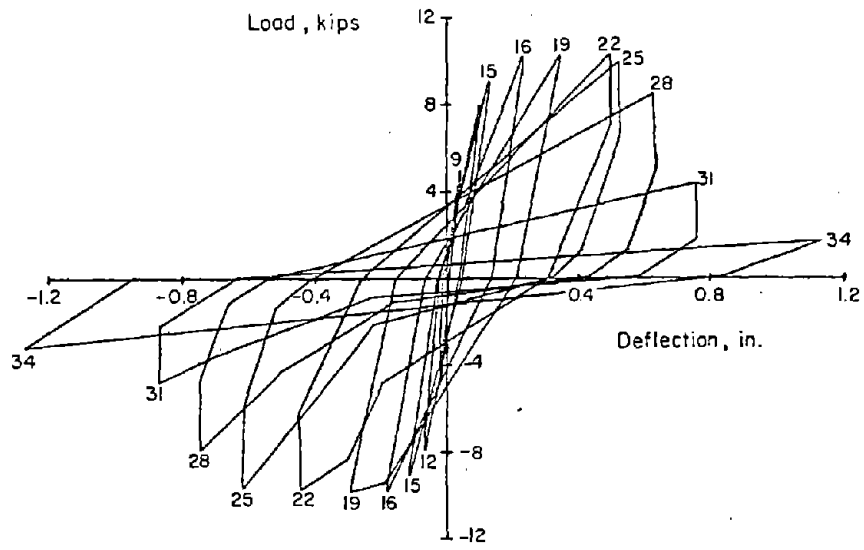


a) Load History



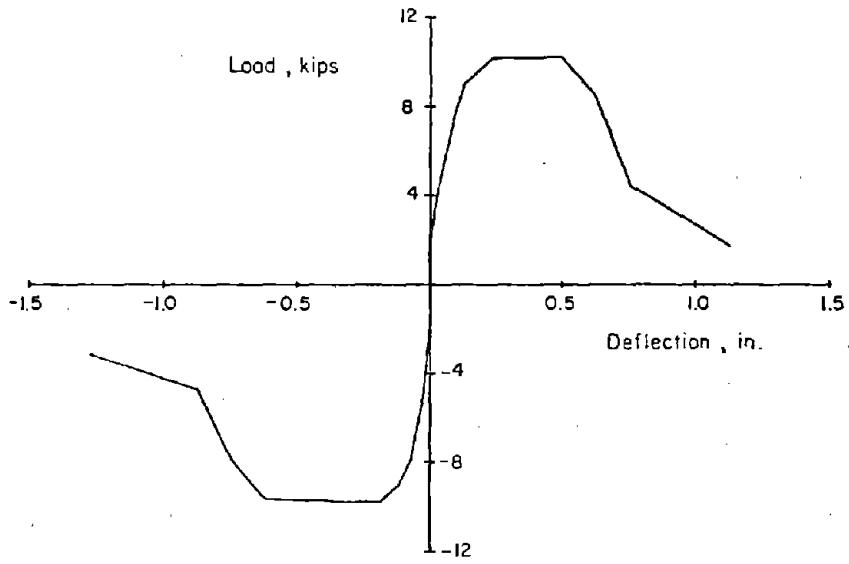
b) Deflection History

Fig. B-10 Loading History for Specimen C2



a) Segmental Plot

1 in. = 25.4 mm  
 1 kip = 4.448 kN



b) Envelope

Fig. B-11 Load versus Deflection Relationships for Specimen C2

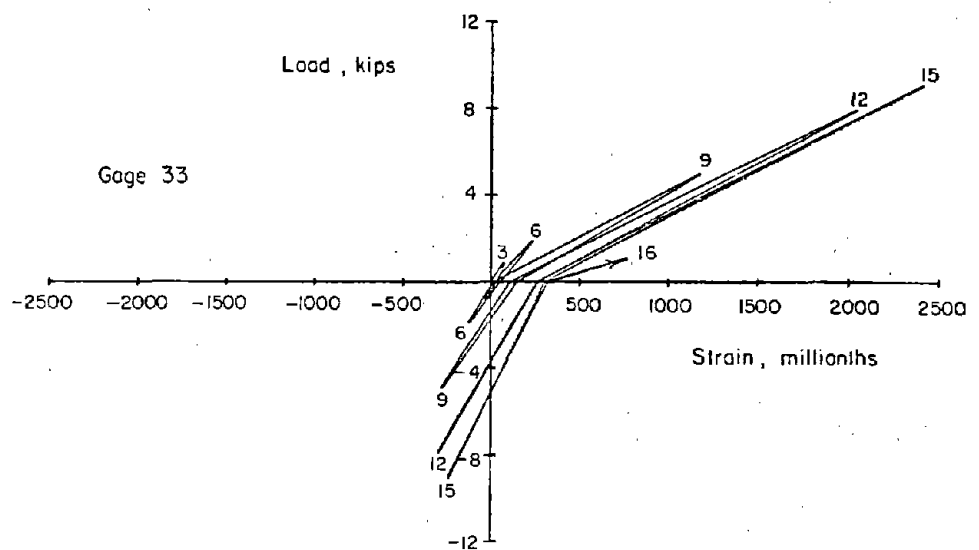
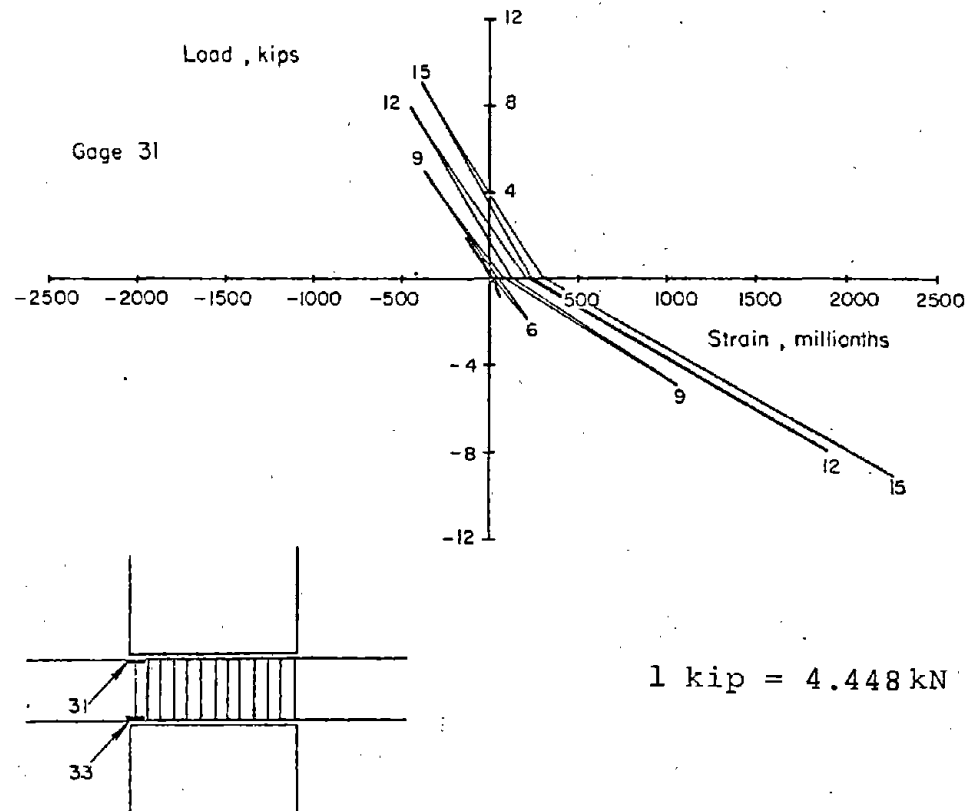
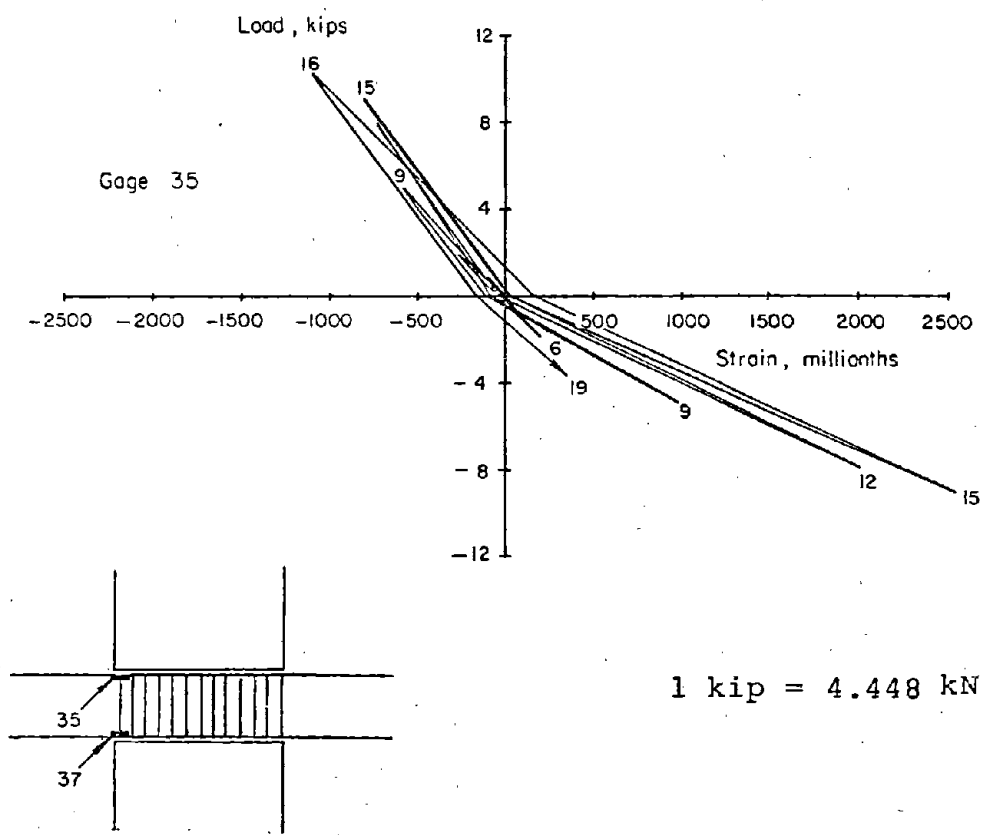


Fig. B-12 Load versus Flexural Steel Strains  
for Specimen C2 (East Beam)



1 kip = 4.448 kN

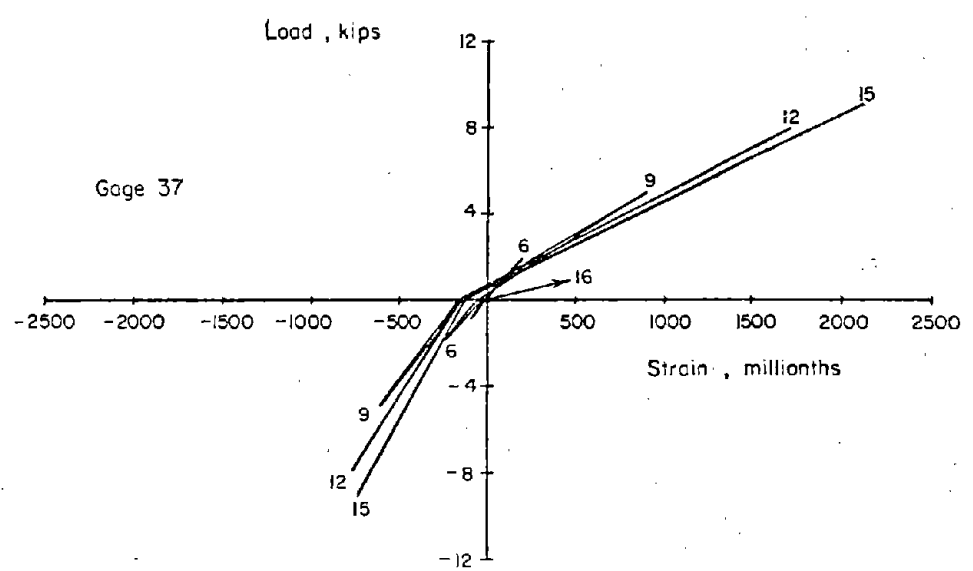


Fig. B-13 Load versus Flexural Steel Strains for Specimen C2 (West Beam)

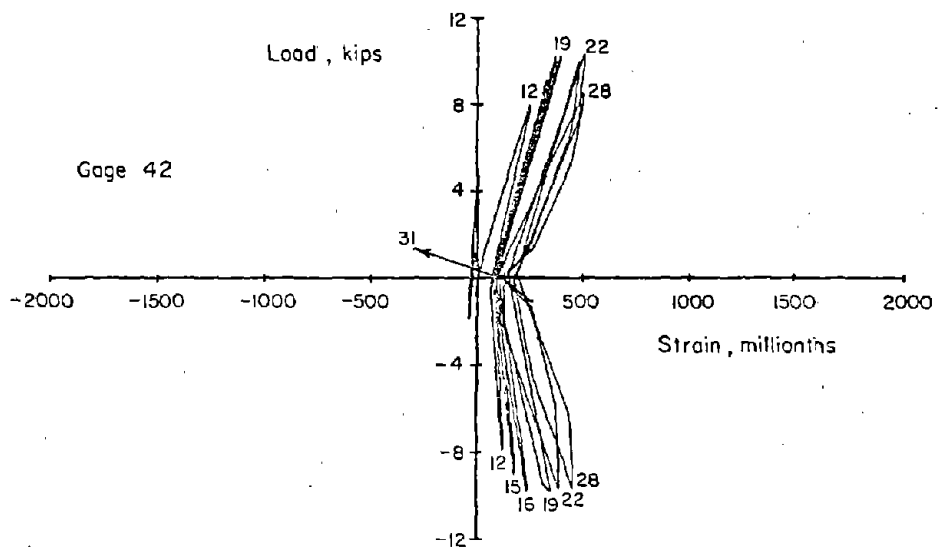
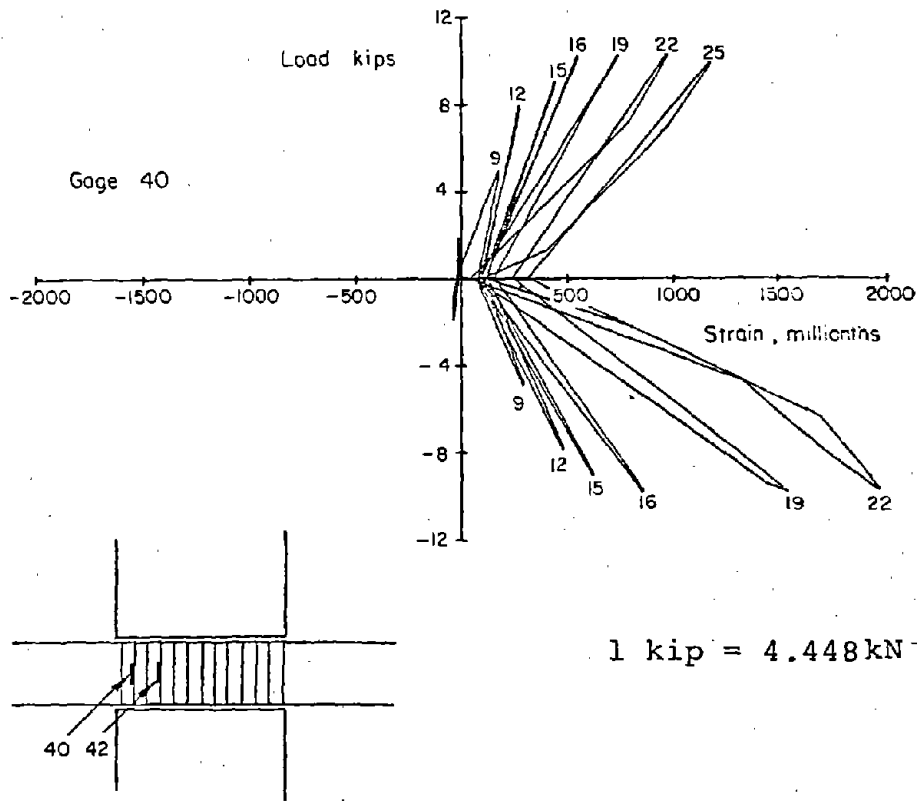
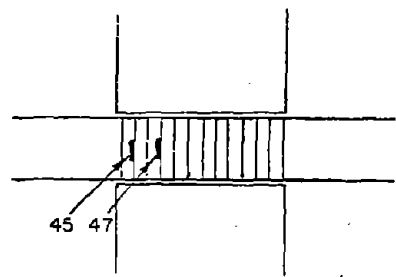
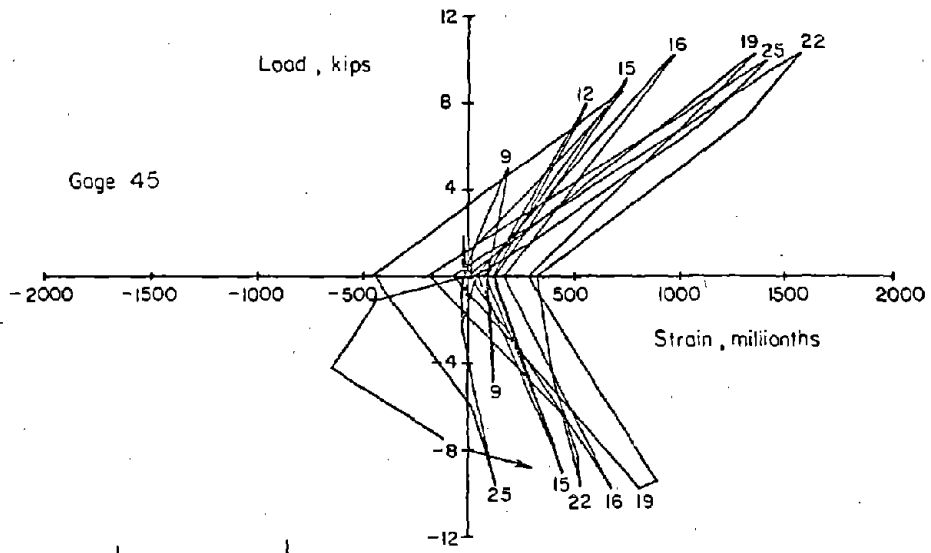


Fig. B-14 Load versus Hoop Steel Strains for Specimen C2 (East Beam)



1 kip = 4.448 kN

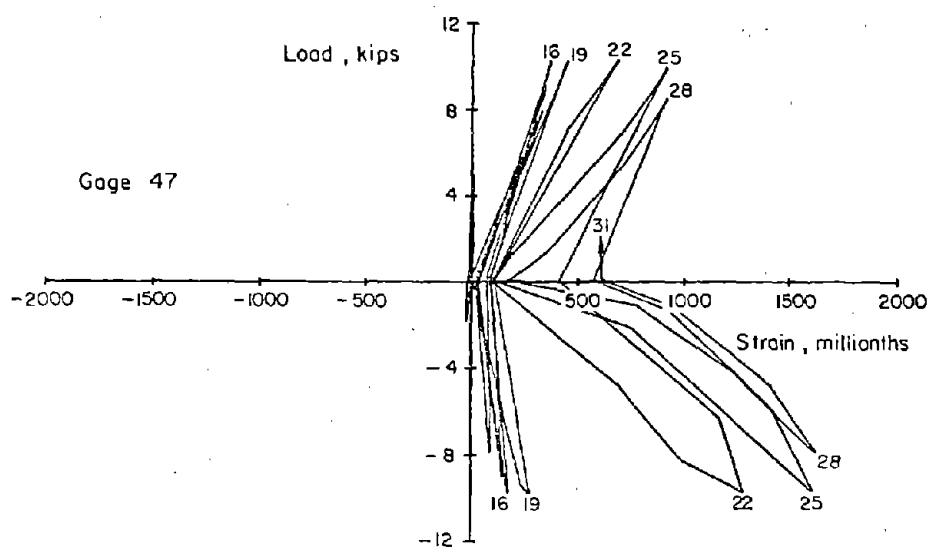
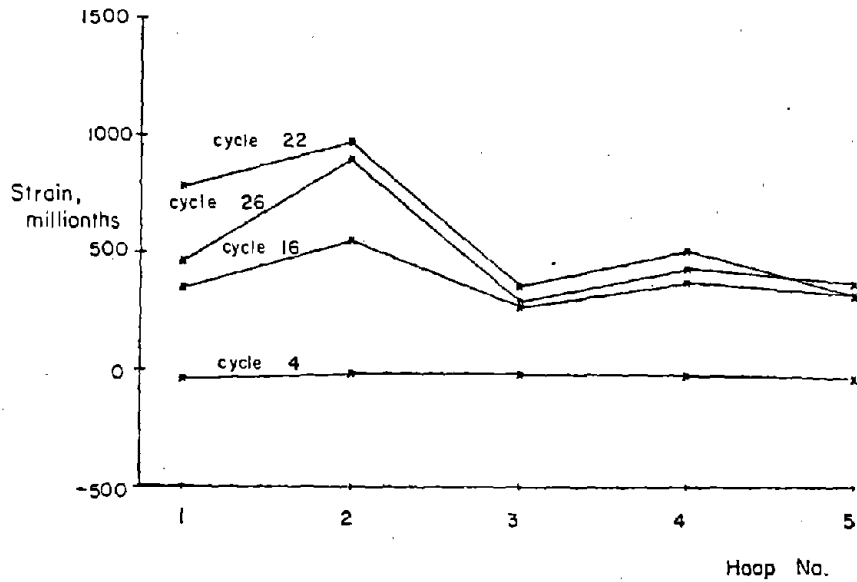
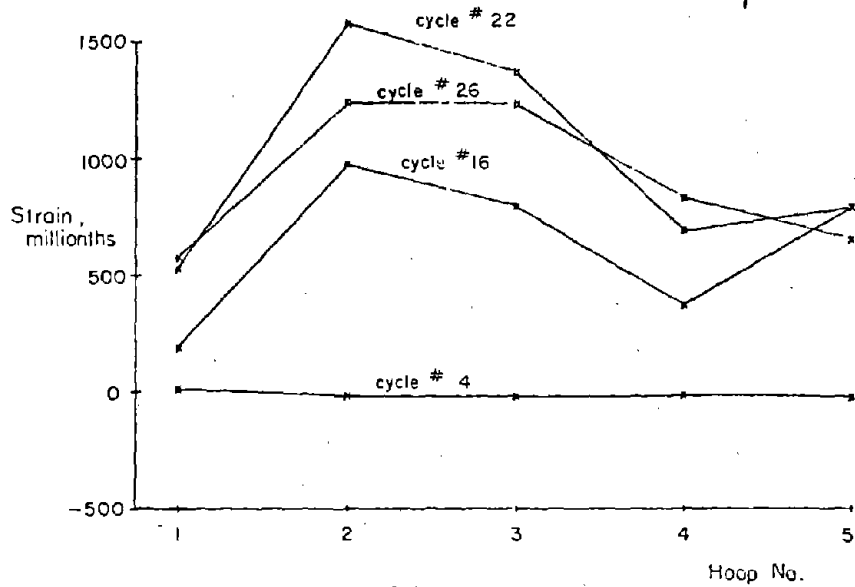
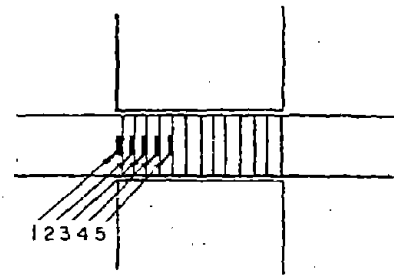


Fig. B-15 Load versus Hoop Steel Strains for Specimen C2 (West Beam)



a) East Beam



b) West Beam

Fig. B-16 Hoop Steel Strains for Specimen C2



Loss of strength appeared to be caused primarily by sliding at the interface between the beam and the face of the abutment wall.

### Specimen C3

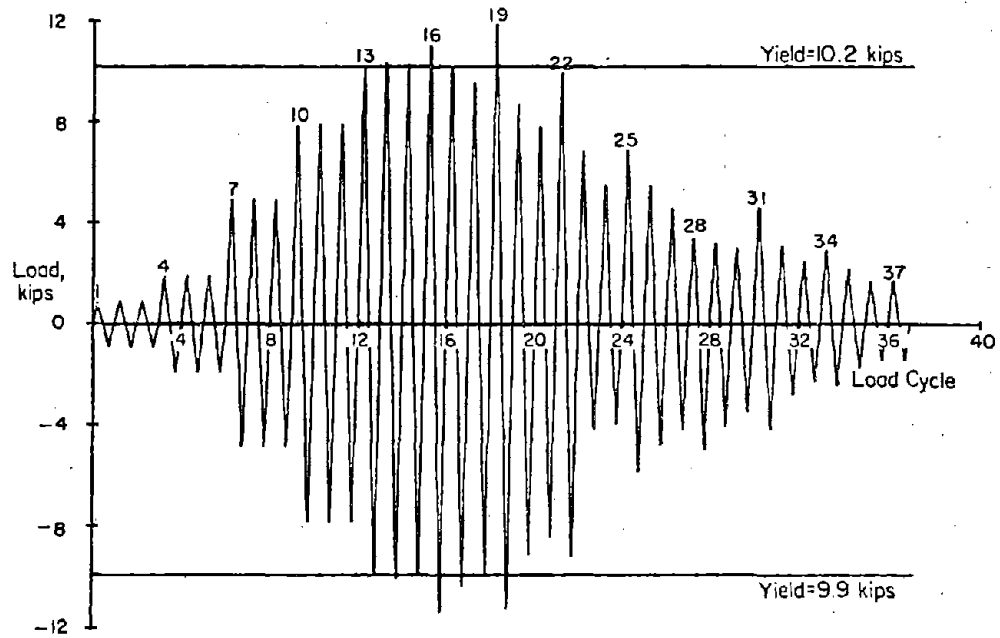
Specimen C3 contained double diagonal reinforcement in the hinging regions of the beams, as shown in Fig. A-5. Load and deflections histories and plots of load versus deflection are shown in Figs. B-17 and Fig. B-18, respectively. Strain data are presented in Figs. B-19 through B-25.

Cracking in this specimen first occurred during the seventh load cycle at a load of 2.9 kips (12.9 kN) per beam. Yielding of the main flexural reinforcement occurred during the thirteenth load cycle at a load of 10.2 kips (45.5 kN) per beam and a deflection of 0.15-in. (4 mm). At this level, flexural cracks in each beam extended across the full depth at the ends. Furthermore, a diagonal crack extending across more than half the depth at approximately the 1/3-point in the span of the east beam was also observed.

Maximum load carried by the specimen was 11.8 kips (52.5 kN) per beam during the seventh inelastic load cycle. Nominal shear stress at this load was  $9.0 \sqrt{f'_c}$  psi ( $0.75 \sqrt{f'_c}$  MPa). The deflection recorded at this load was 0.36-in. (9.1 mm). Yielding of the diagonal reinforcement also occurred during this load cycle at a load of 11.2 kips (49.8 kN) per beam. Cracking was more severe in the east beam.

Spalling of the concrete shell surrounding the confined core began at a load of 18.3 kips (81.4 kN) during the tenth inelastic load cycle. Deflection at this load was 0.74-in. (19 mm).

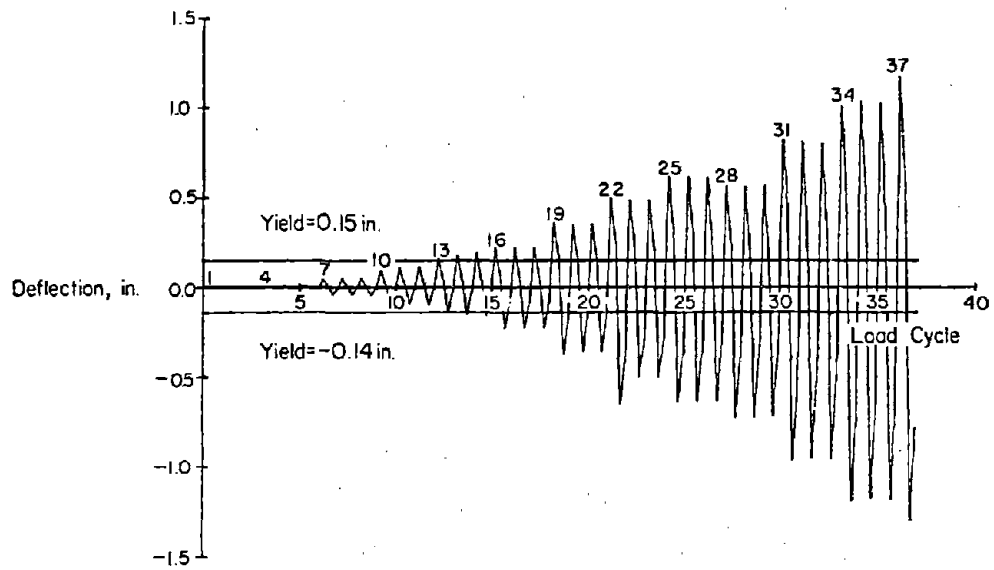
During the final load cycle at an imposed deflection of 1.45 in. (37 mm), the specimen carried a load of 1.4 kips (6.2



a) Load History

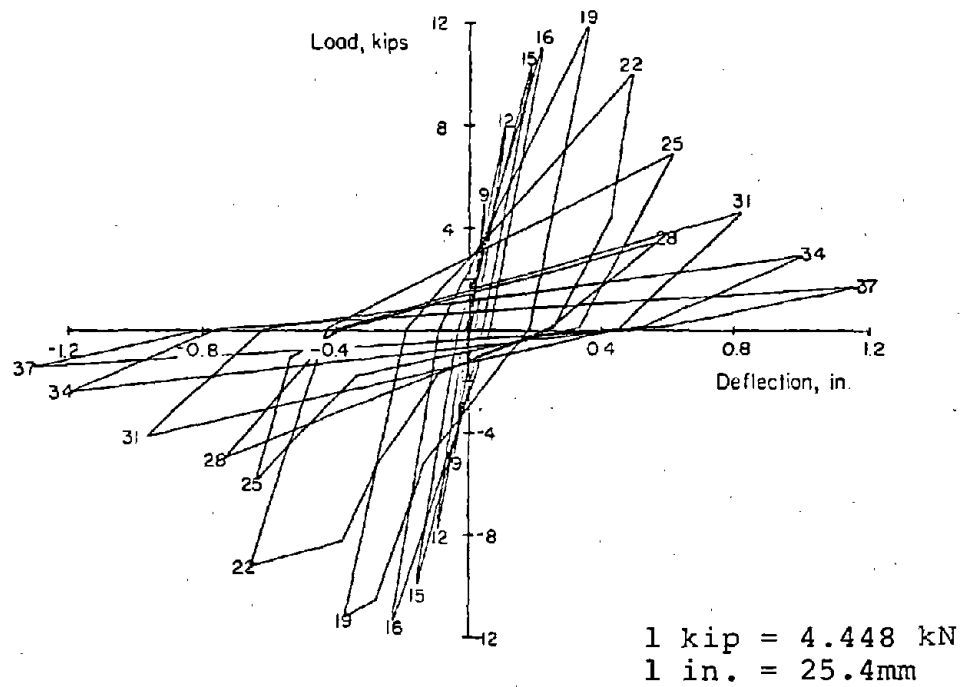
1 kip = 4.448 kN

1 in. = 25.4mm

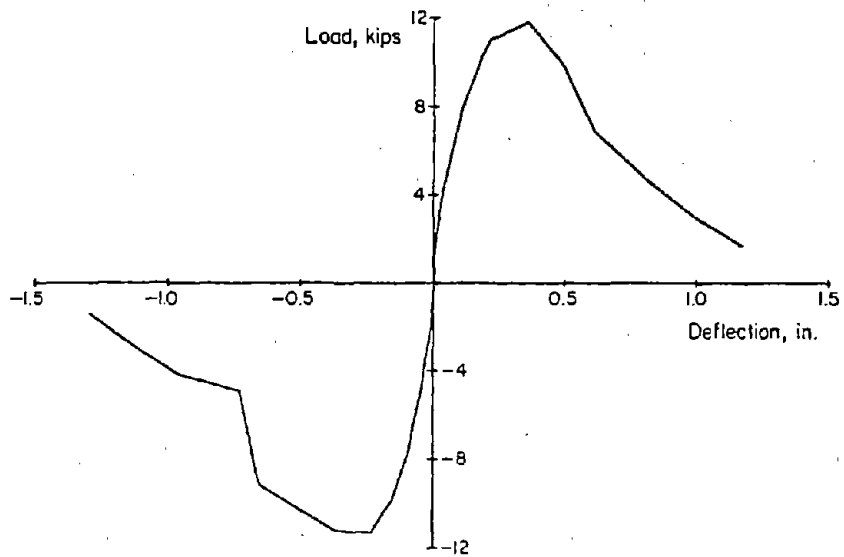


b) Deflection History

Fig. B-17 Loading History for Specimen C3



a) Segmental Plot



b) Envelope

Fig. B-18 Load versus Deflection Relationships for Specimen C3

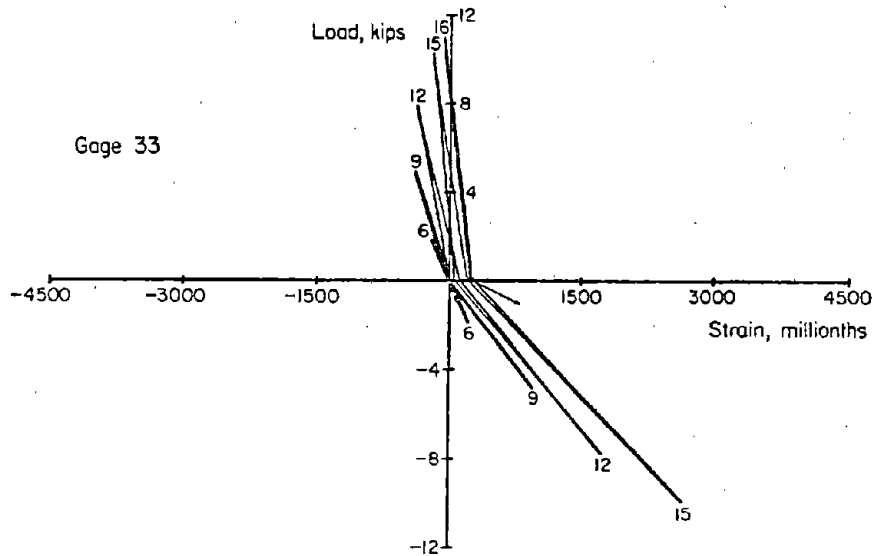
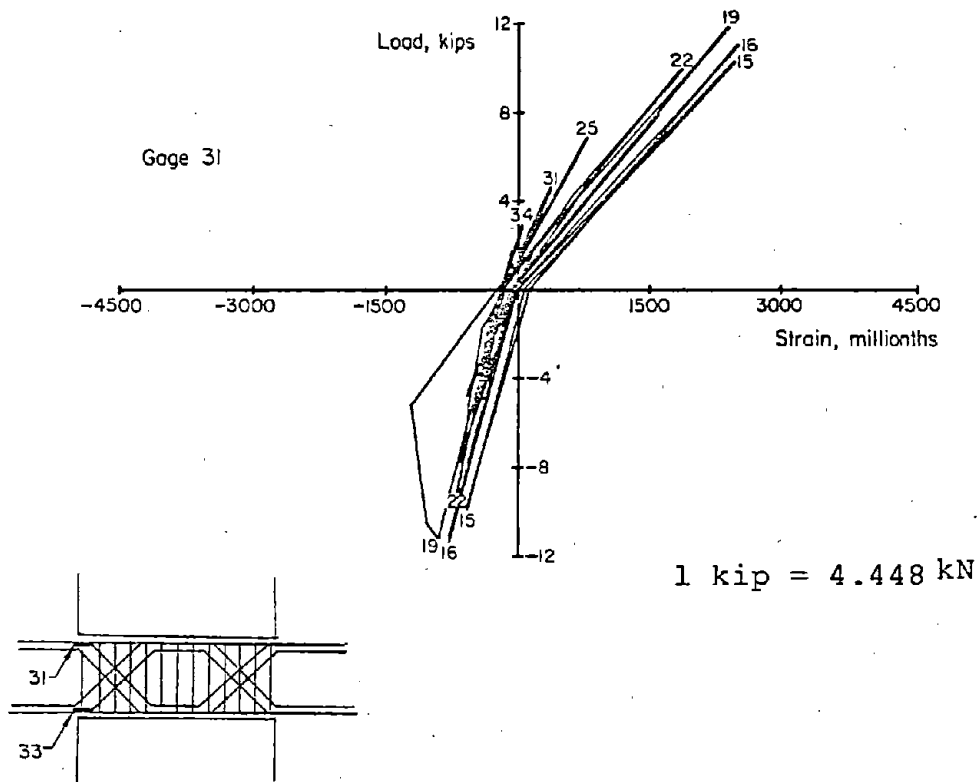


Fig. B-19 Load versus Flexural Steel Strains for Specimen C3 (East Beam)

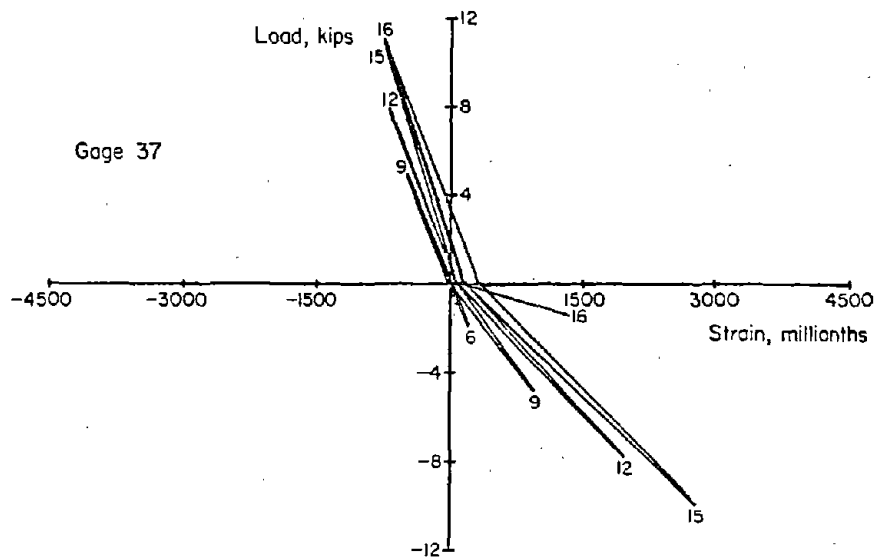
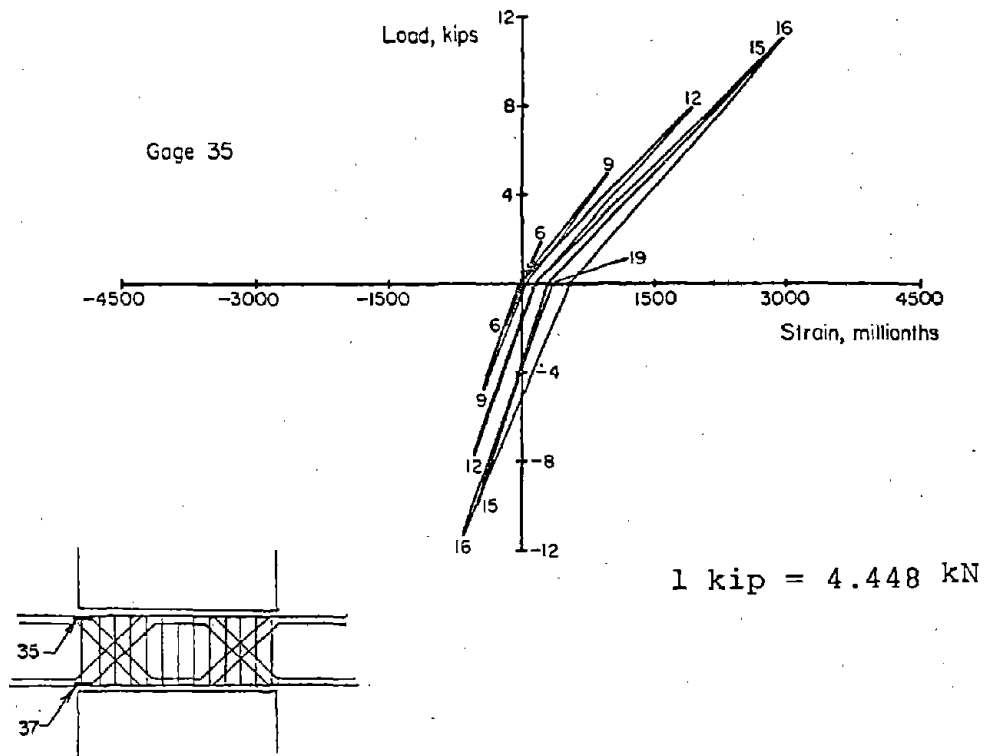


Fig. B-20 Load versus Flexural Steel Strains for Specimen C3 (West Beam)

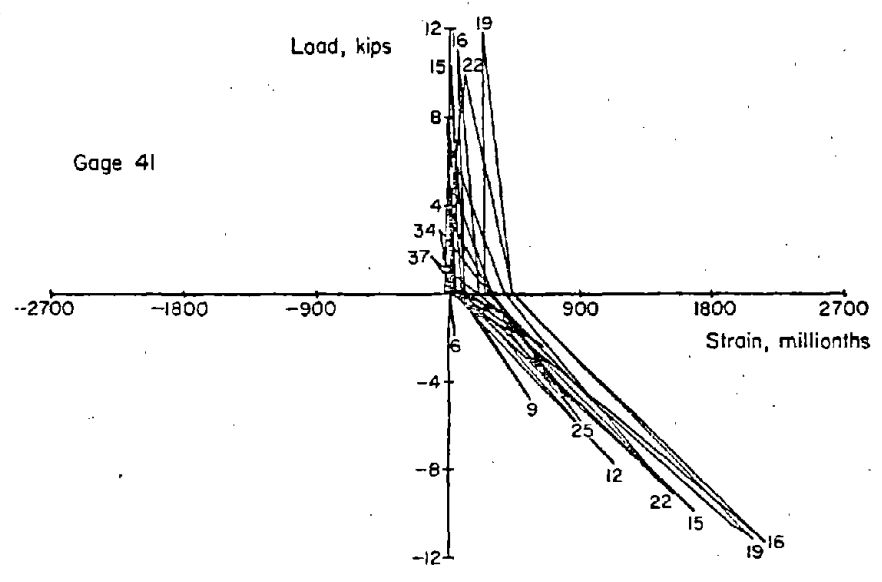
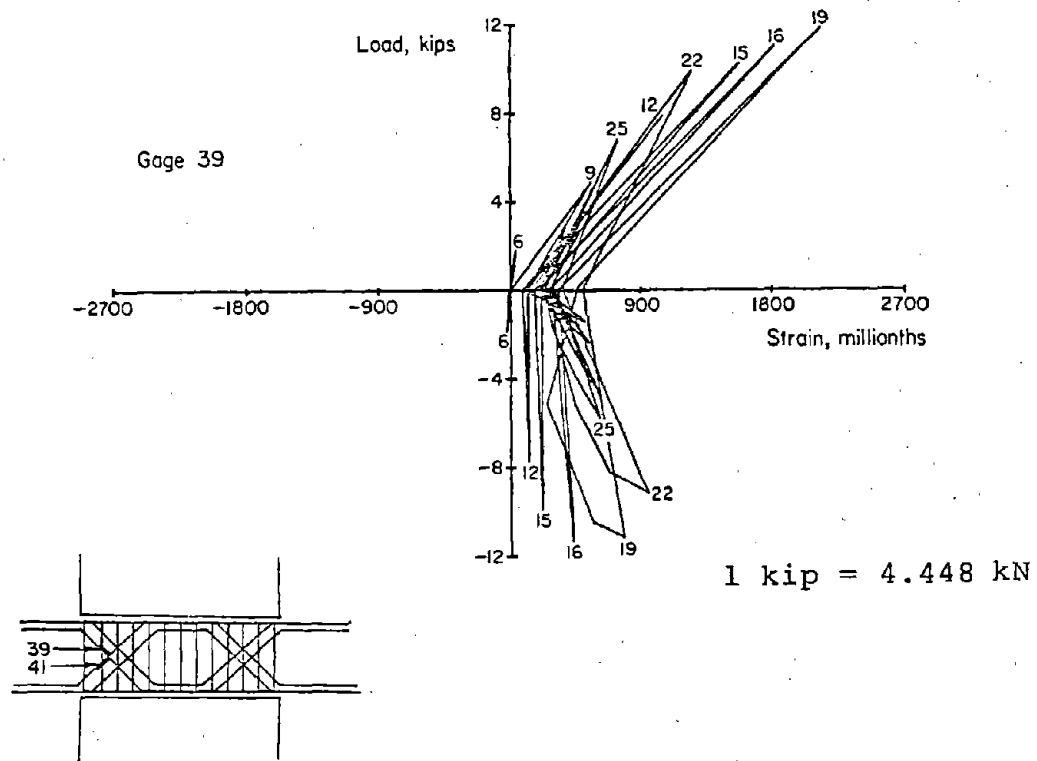


Fig. B-21 Load versus Diagonal Steel Strains for Specimen C3 (East Beam)

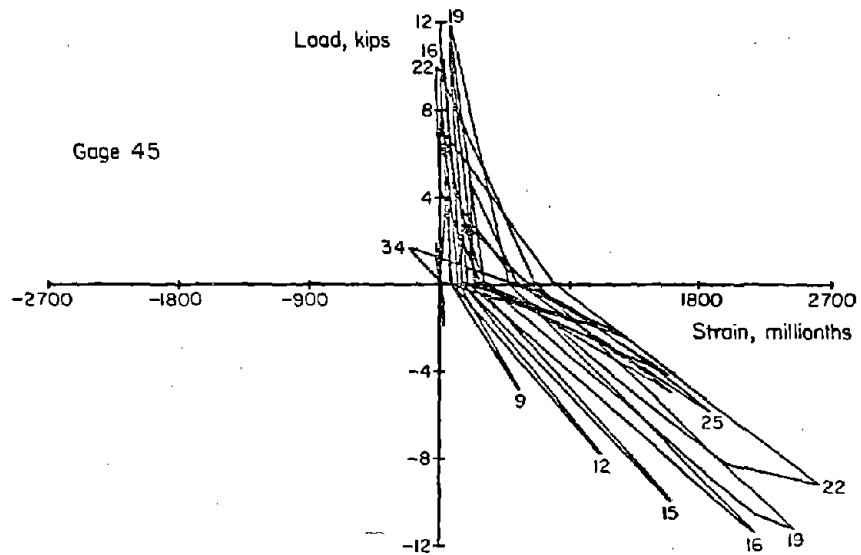
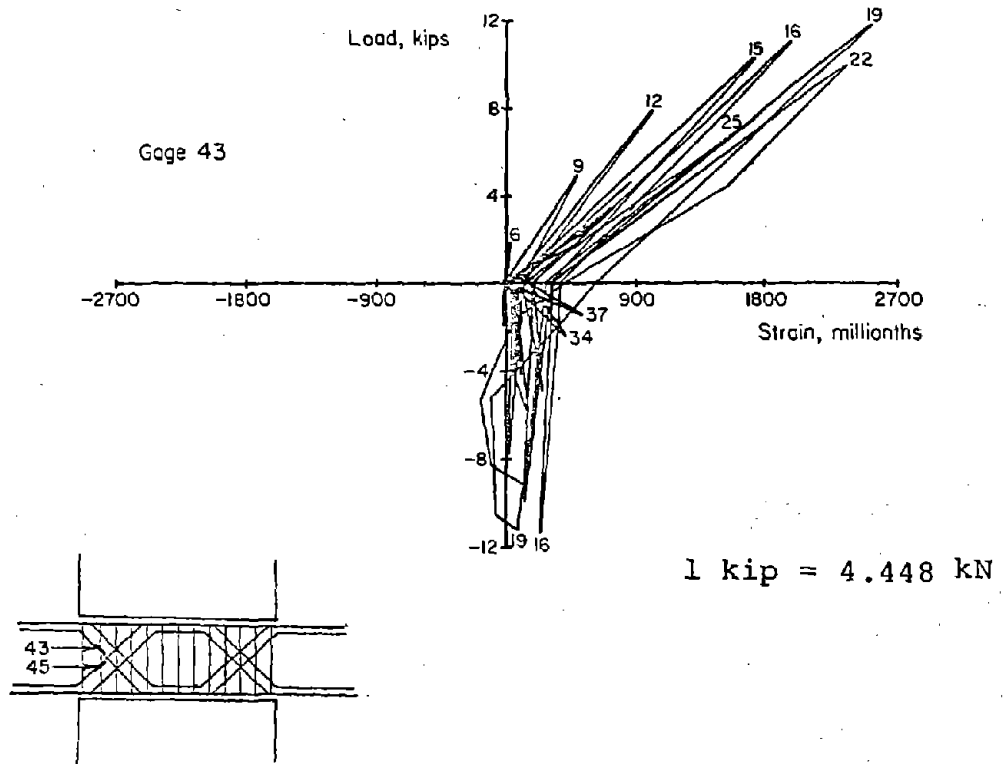


Fig. B-22 Load versus Diagonal Steel Strains  
for Specimen C3 (West Beam)

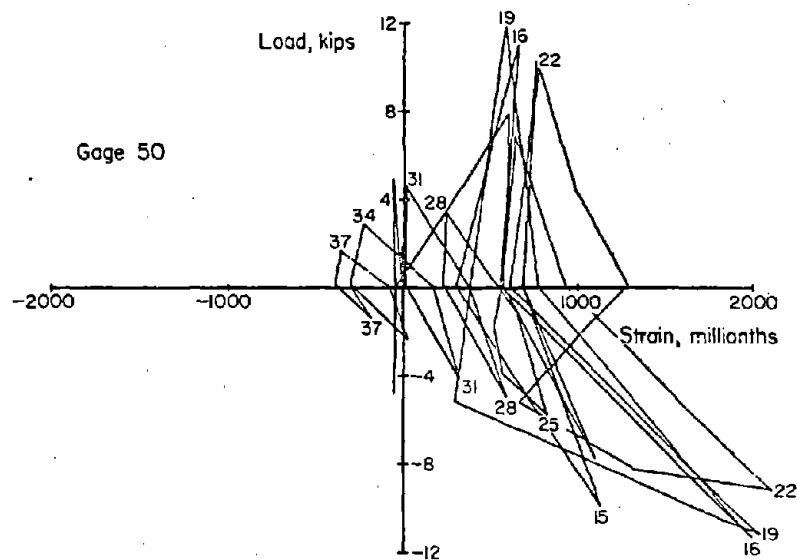
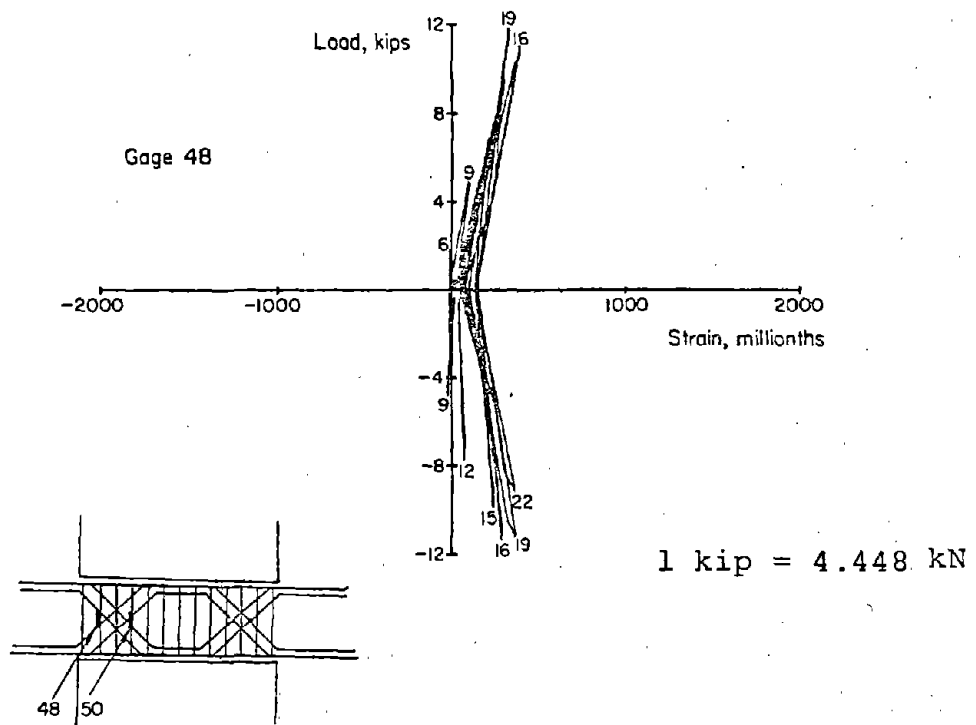


Fig. B-23 Load versus Hoop Steel Strains for Specimen C3 (East Beam)



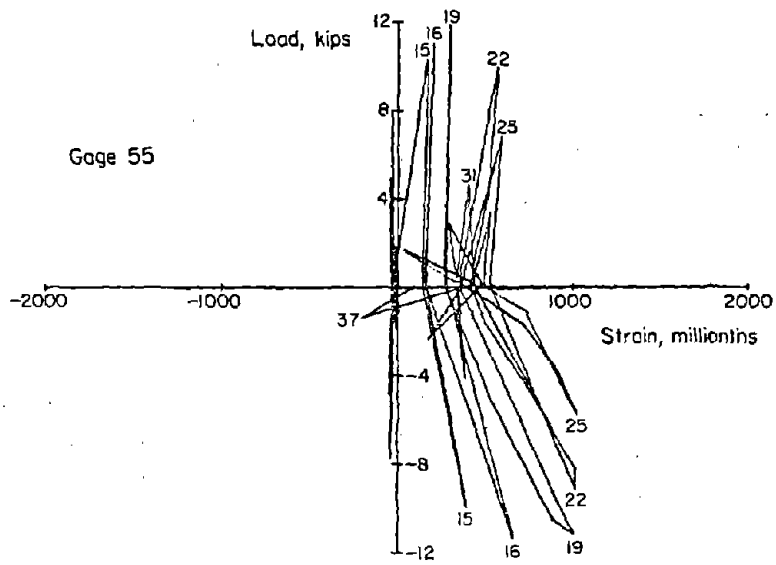
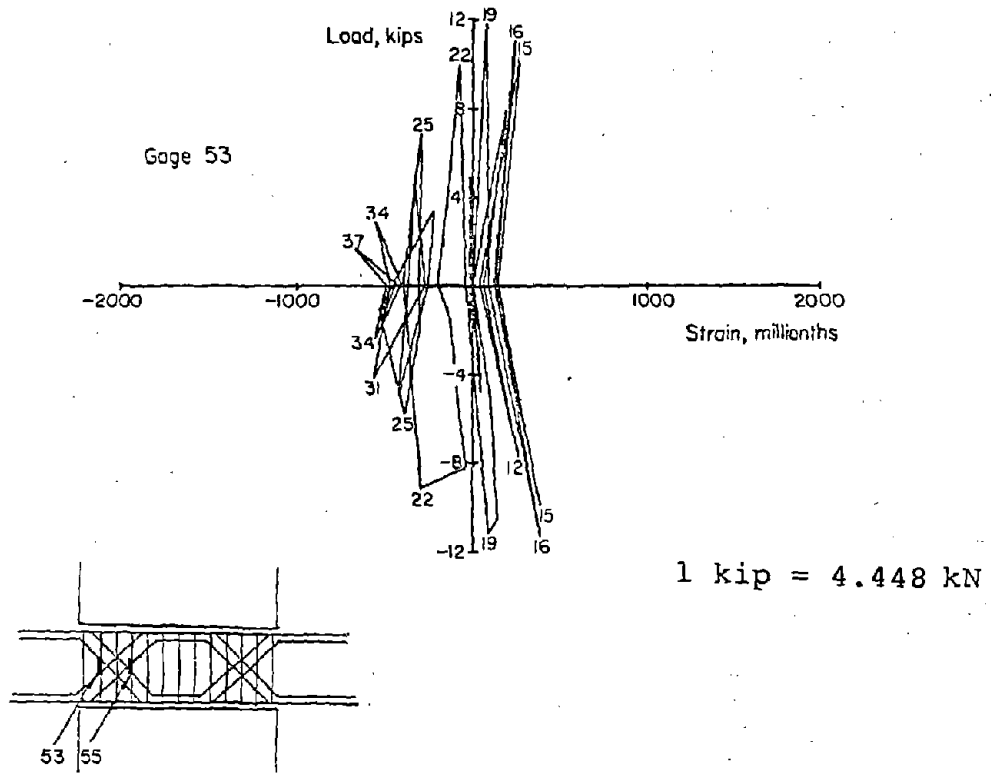
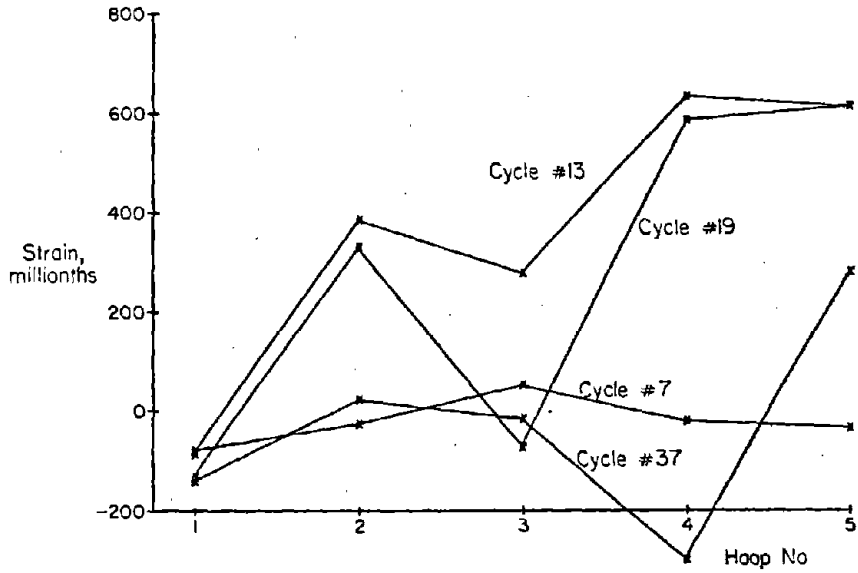
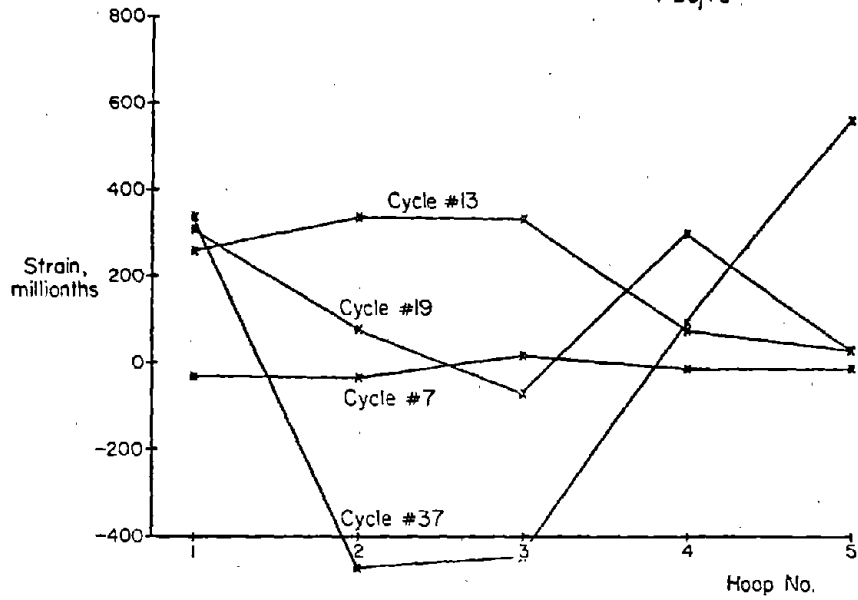
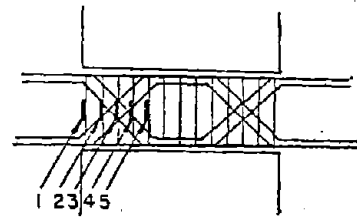


Fig. B-24 Load versus Hoop Steel Strains for Specimen C3 (West Beam)



a) East Beam



b) West Beam

Fig. B-25 Hoop Steel Strains for Specimen C3

kN) per beam. A total of 25 inelastic load cycles were applied to the specimen.

Observed behavior of the two beams was quite different after the maximum load was reached. The diagonal crack that formed in the east beam caused complete deterioration of the concrete core in the center of the span. The west beam behaved in a manner similar to Specimen C1. Deterioration occurred in the hinging regions at the ends of the beam.

#### Specimen C4

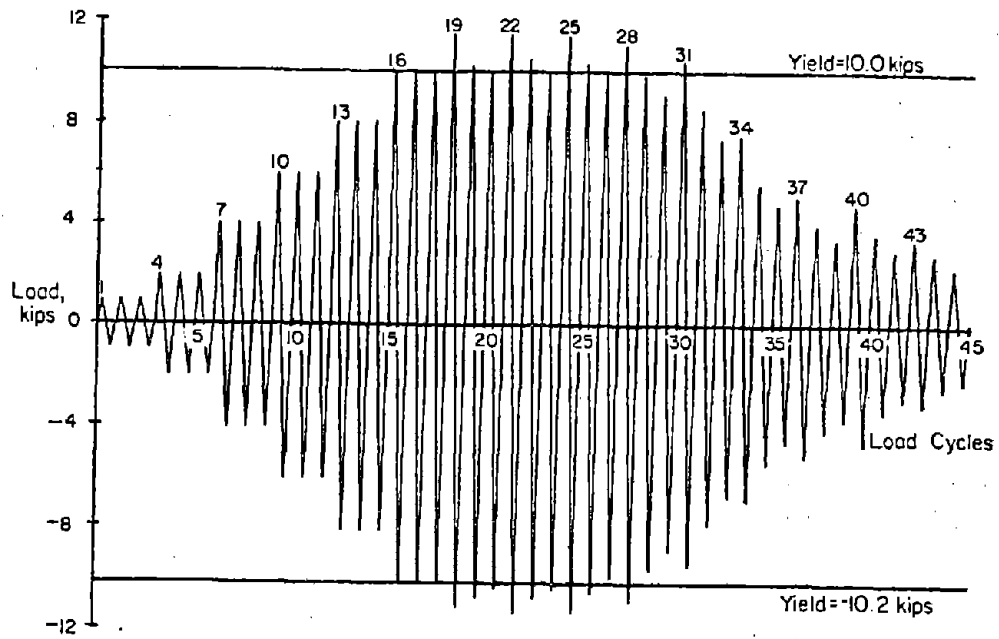
Specimen C4 was similar to Specimen C3 except for the larger confined concrete core size as shown in Fig. A-5. Load and deflection histories for Specimen C4 are given in Fig. B-26. The relationship of load versus deflection is shown in Fig. B-27. Strain data are presented in Figs. B-28 through B-34.

Cracking was first observed in this specimen during the seventh load cycle at a load of 4.0 kips (17.8 kN) per beam. Flexural reinforcement yielding occurred during the sixteenth load cycle at a deflection of 0.14-in. (4 mm). At this load, flexural cracks extended across the full depth at the ends of both beams. Diagonal cracks had also formed at approximately the 1/4-points of the span in both beams. Yielding of the diagonal reinforcement occurred at a load of 11.4 kips (50.7 kN) per beam during the fourth inelastic load cycle.

A peak load of 11.5 kips (51.2 kN) per beam was recorded for Specimen C4 during the seventh inelastic load cycle. Nominal shear stress at this load was  $8.0 \sqrt{f'_c}$  psi ( $0.66 \sqrt{f'_c}$  MPa). Deflection at this load was 0.40-in. (10 mm).

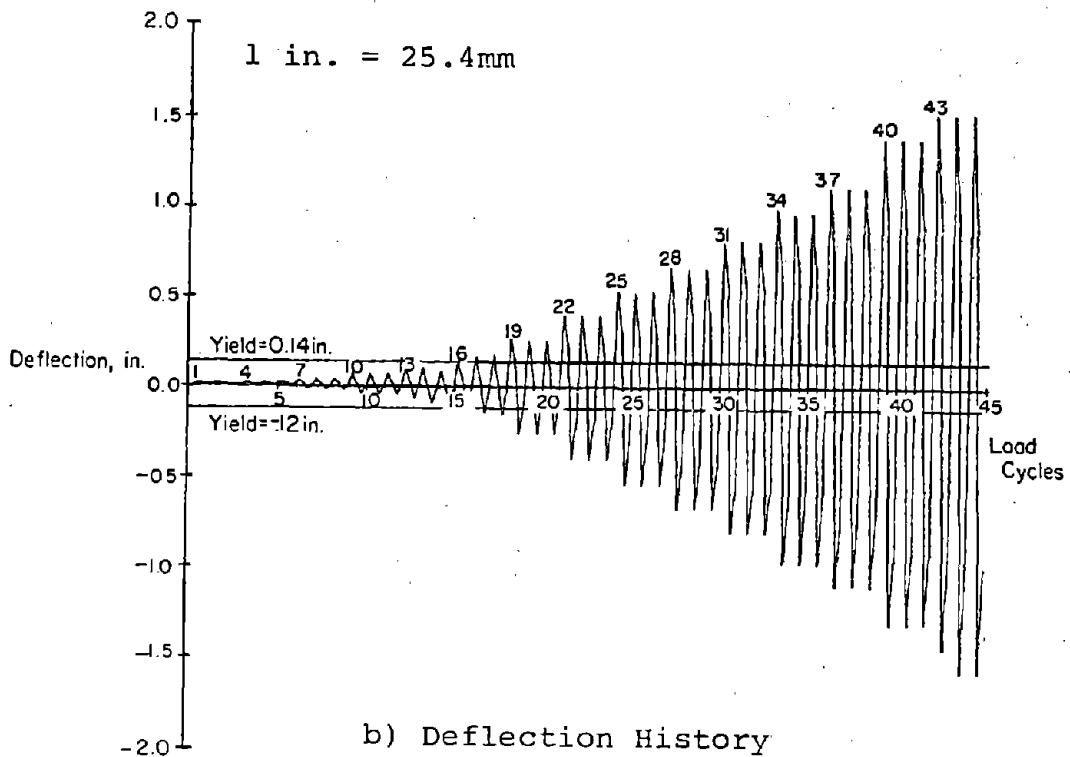
A maximum deflection of 1.57-in. (40 mm) was imposed on the specimen during the seventh inelastic load cycle. The measured load was 2.4 kips (10.7 kN) per beam.

Spalling of the concrete shell in the hinging region was first observed at a load of 10.9 kips (48.5 kN) per beam during the thirteenth inelastic load cycle. The corresponding deflection was 0.67-in. (17 mm).



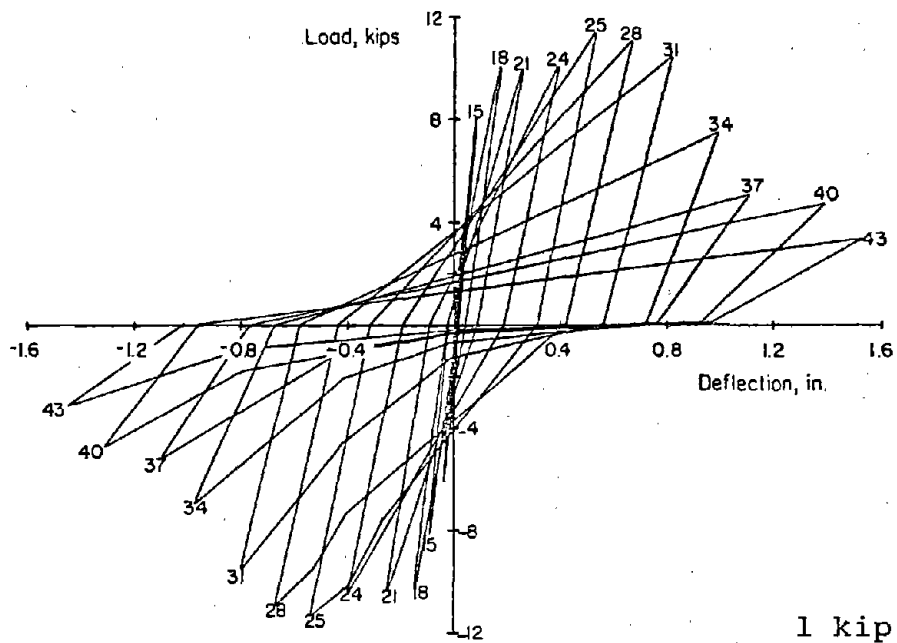
1 kip = 4.448 kN

a) Load History

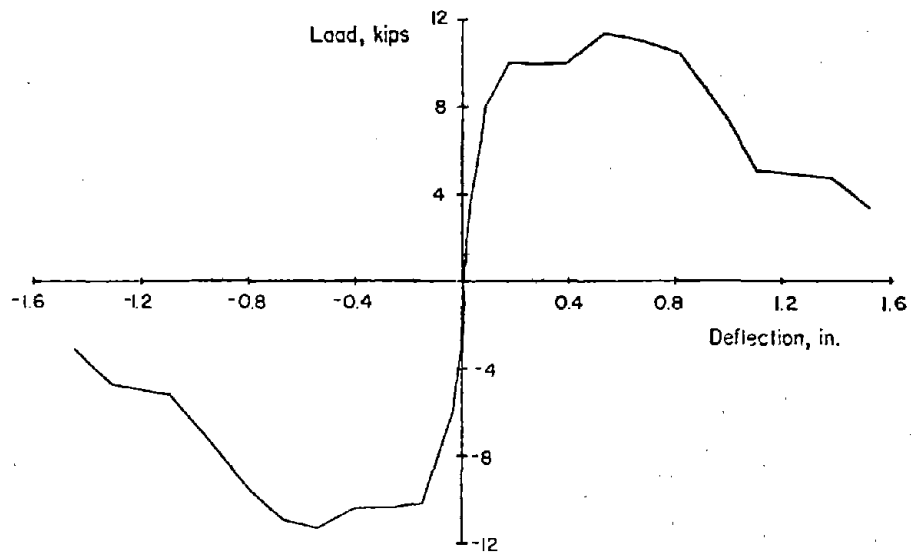


b) Deflection History

Fig. B-26 Loading History for Specimen C4



a) Segmental Plot



b) Envelope

Fig. B-27 Load versus Deflection Relationship for Specimen C4

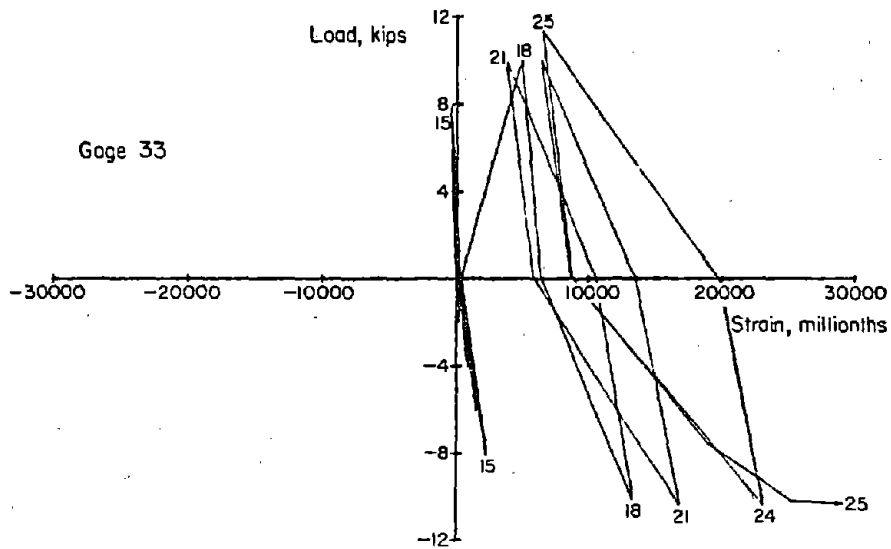
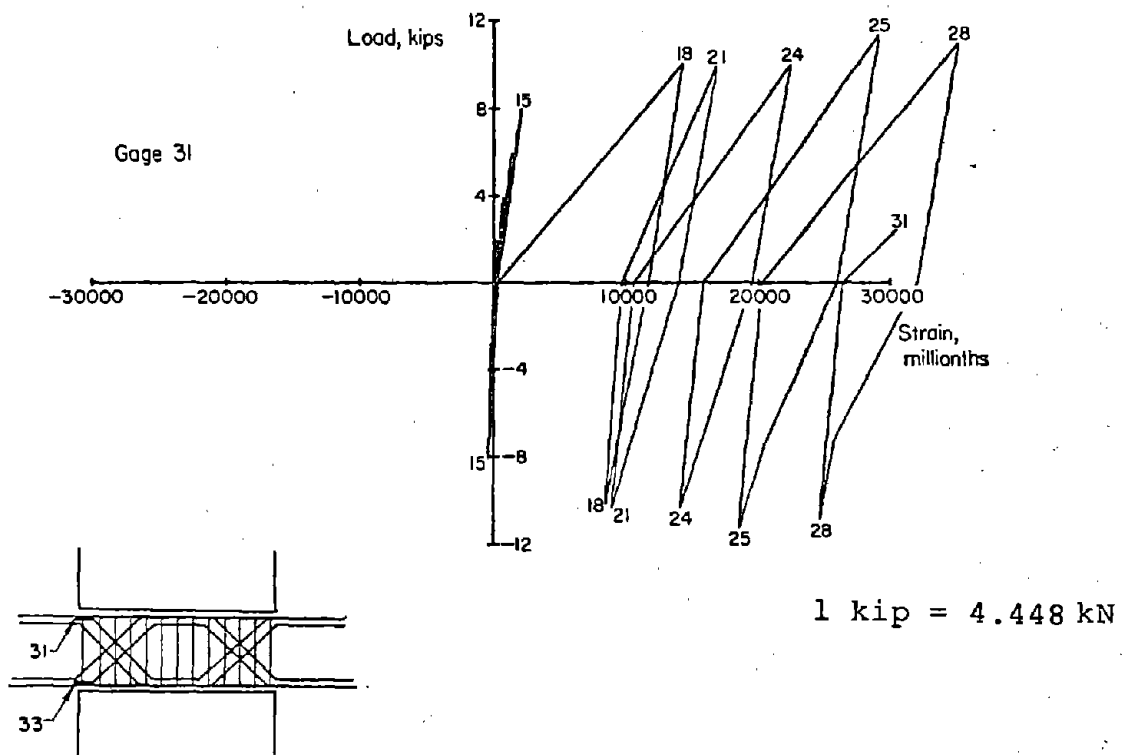


Fig. B-28 Load versus Flexural Steel Strains for Specimen C4 (East Beam)

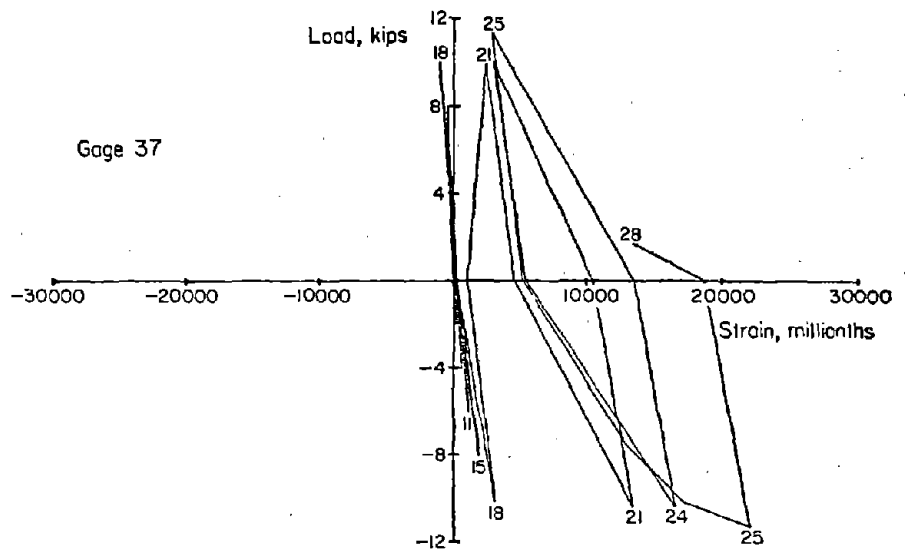
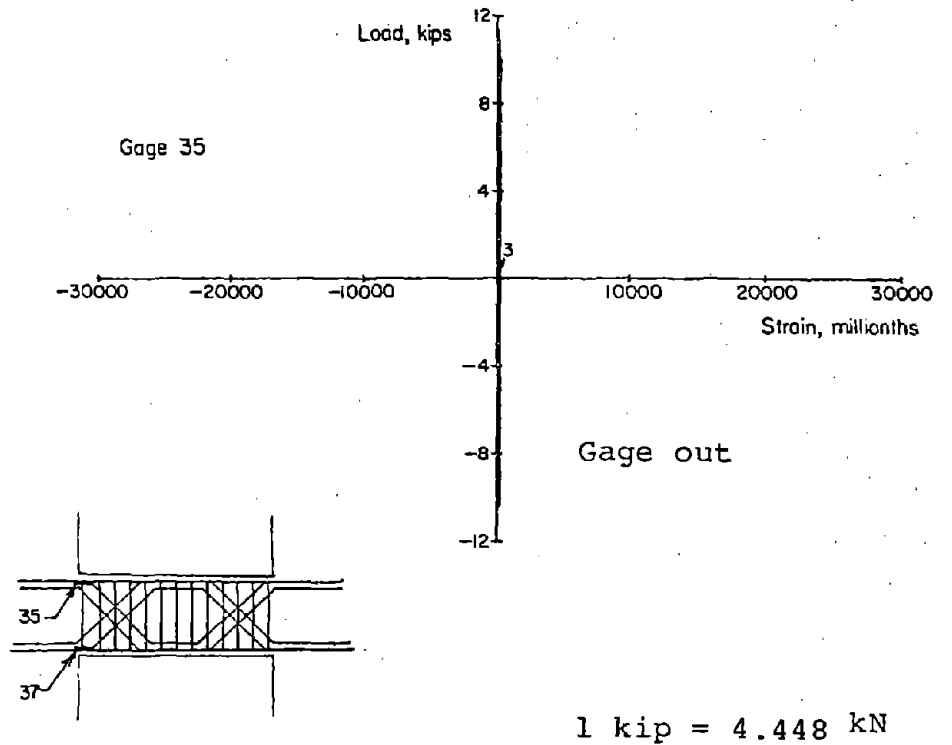


Fig. B-29 Load versus Flexural Steel Strains for Specimen C4 (West Beam)

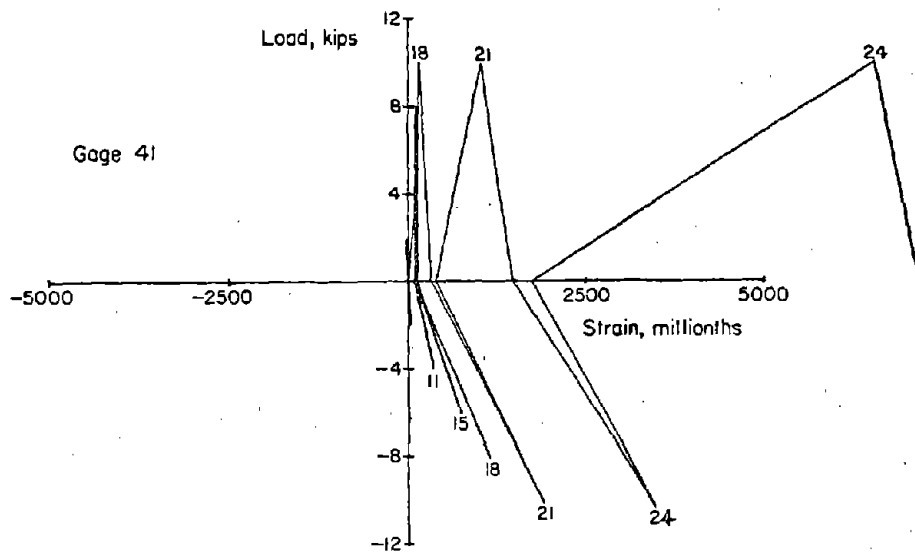
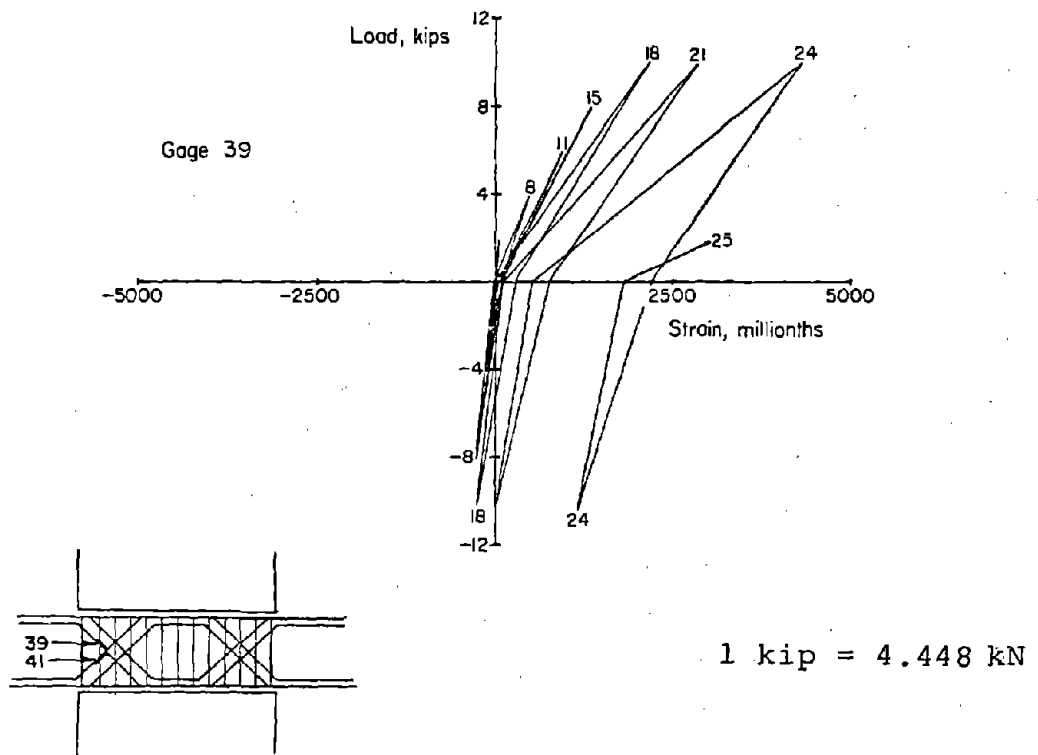


Fig. B-30 Load versus Diagonal Steel Strains for Specimen C4 (East Beam)



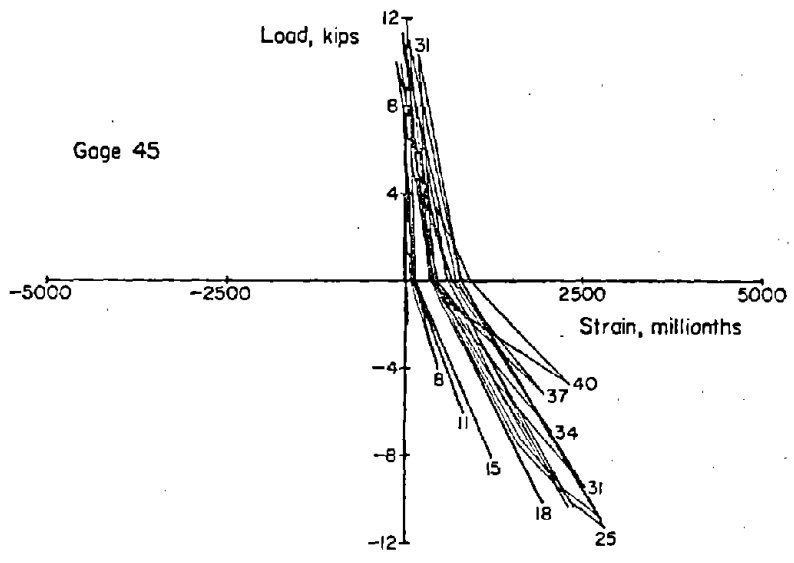
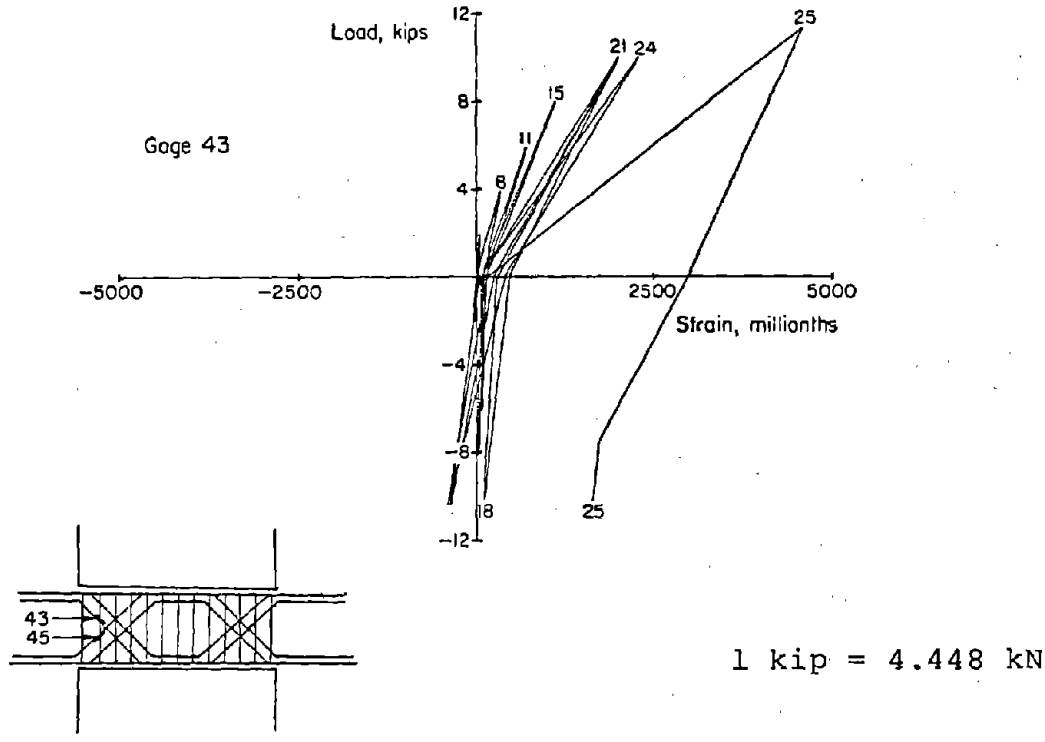


Fig. B-31 Load versus Diagonal Steel Strains for Specimen C4 (West Beam)

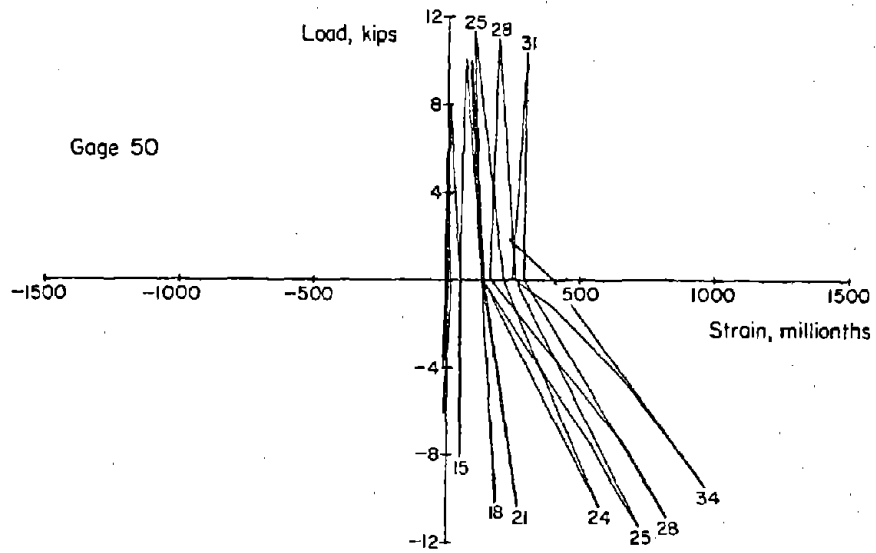
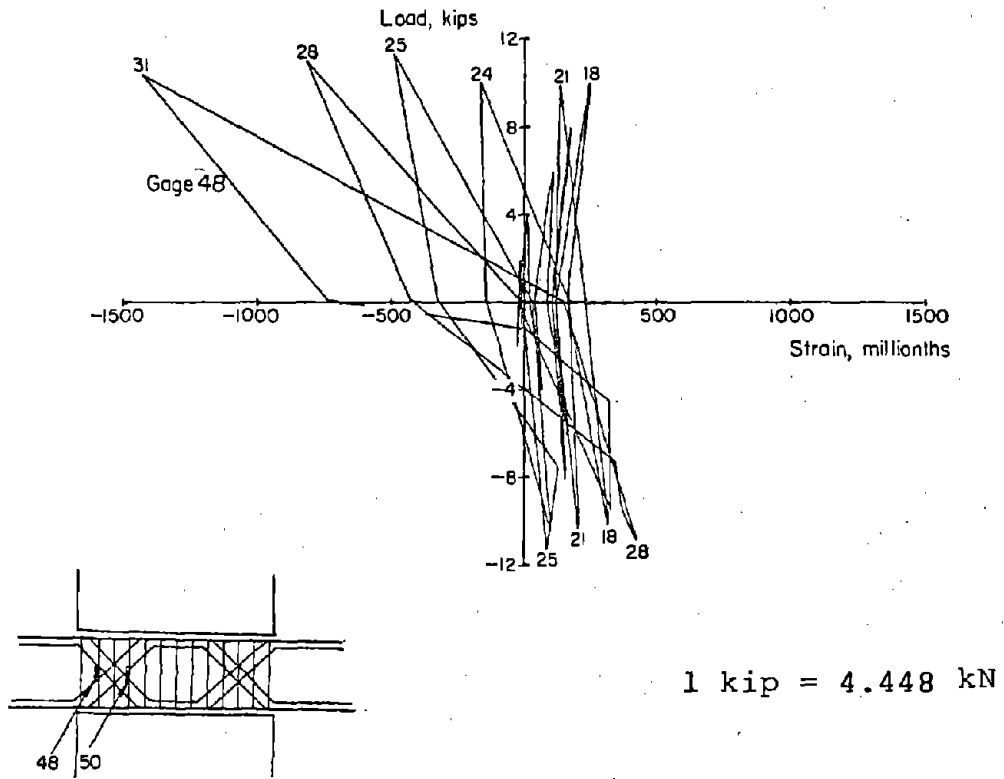


Fig. B-32 Load versus Hoop Steel Strains for Specimen C4 (East Beam)

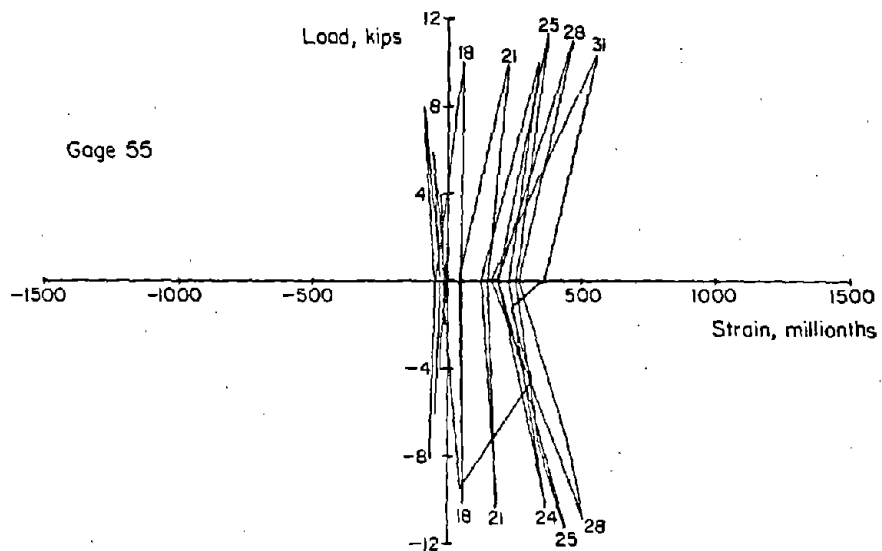
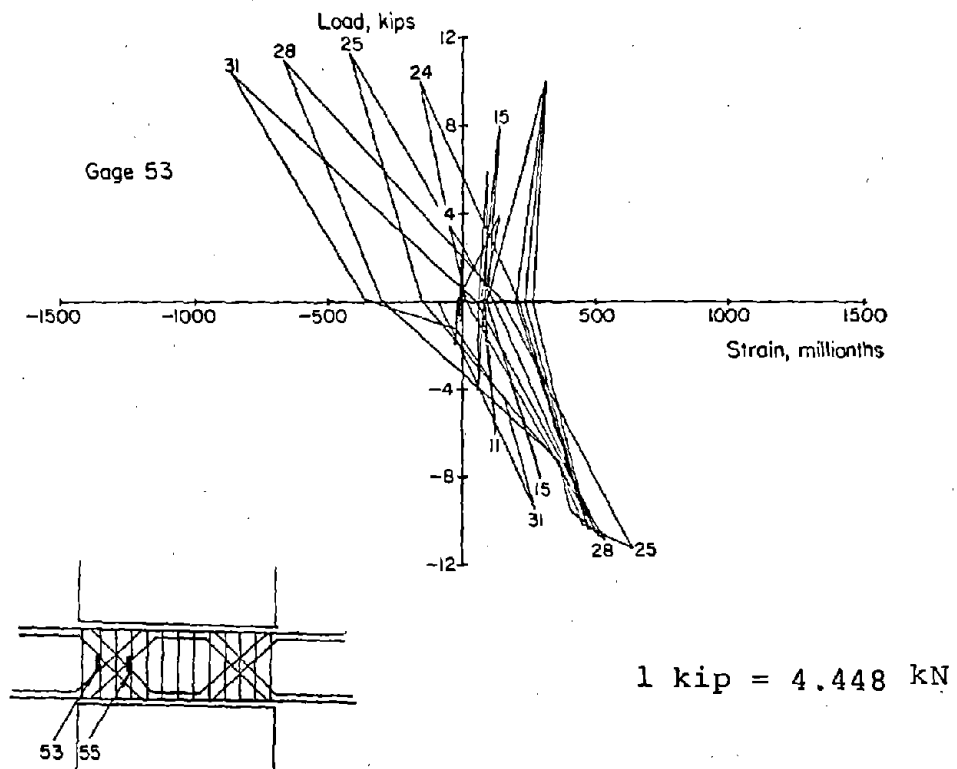
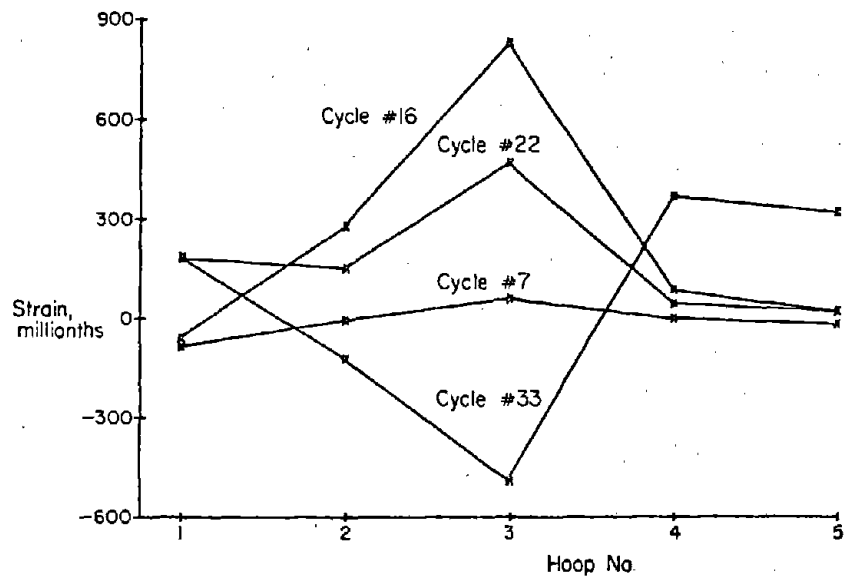
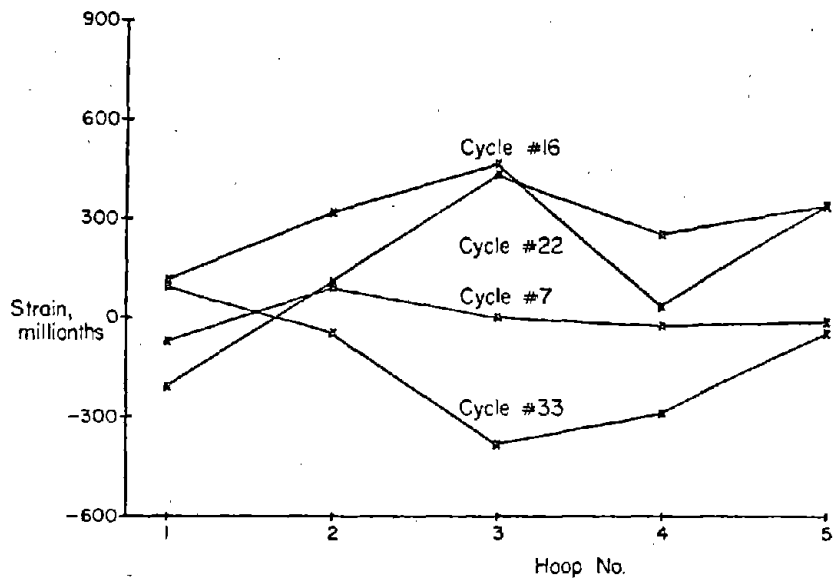
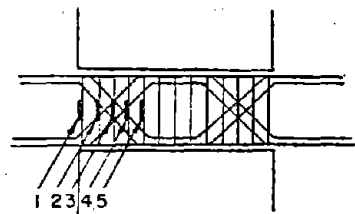


Fig. B-33 Load versus Hoop Steel Strains for Specimen C4 (West Beam)



a) East Beam



b) West Beam

Fig. B-34 Hoop Steel Strains for Specimen C4

More cracks were visible in the abutment walls near the beam ends than in previous specimens. These were associated with stresses in the embedment zone of the coupling beam flexural steel. These cracks appeared prior to yield. However, no bond failure was observed. For this specimen, the primary beam reinforcement was embedded in the shell surrounding the confined concrete in the abutment walls.

#### Specimen C5

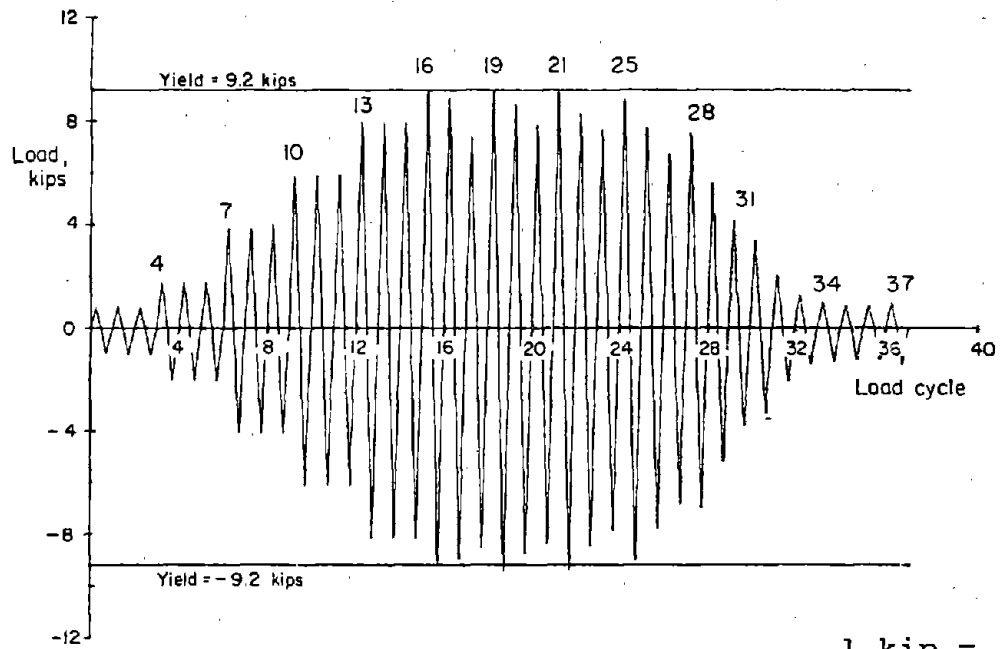
Specimen C5 was similar to Specimen C2 except for a larger confined concrete core size as indicated in Fig. A-2. Load and deflection histories are given in Fig. B-35. Plots of load versus deflection are shown in Fig. B-36. Strain data are given in Figs. B-37 through B-41.

First cracking in this specimen occurred during the seventh load cycle at a load of 3.7 kips (16.5 kN) per beam. Yielding took place during the sixteenth load cycle at an applied load of 9.2 kips (40.9 kN) per beam. The measured deflection at yield was 0.19-in. (5 mm). Full depth flexural cracks and some diagonal cracks had formed at yield load.

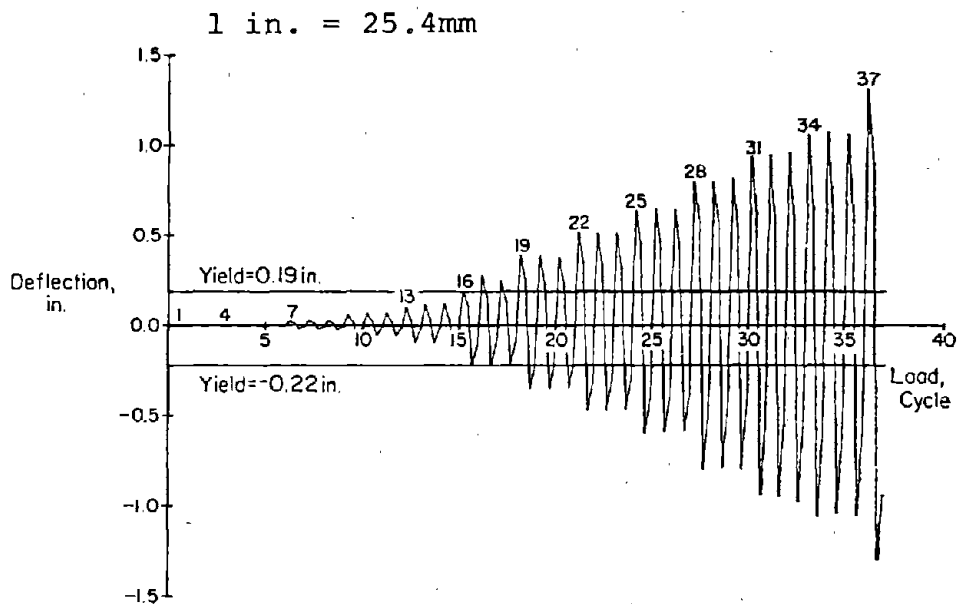
The maximum load carried by Specimen C5 was 9.4 kips (41.8 kN) per beam during the fourth inelastic load cycle. Nominal shear stress at this load was  $6.8 \sqrt{f'_c}$  psi ( $0.56 \sqrt{f'_c}$  MPa). Deflection at this load level was 0.59-in. (15 mm).

The test was terminated after 22 inelastic load cycles had been applied to the specimen. Maximum deflection was 1.30-in. (33 mm). The final load applied to the specimen was 1.4 kips (6.2 kN) per beam.

Observed deterioration of concrete in each of these beams occurred at one end. Extensive crushing of the confined concrete in the core of the west beam was observed. Failure was attributed to "sliding shear" at the interface between the beam ends and the face of the abutment wall. Cracking in the abutment walls near the ends of the beams was less severe in this specimen than in Specimen C4.

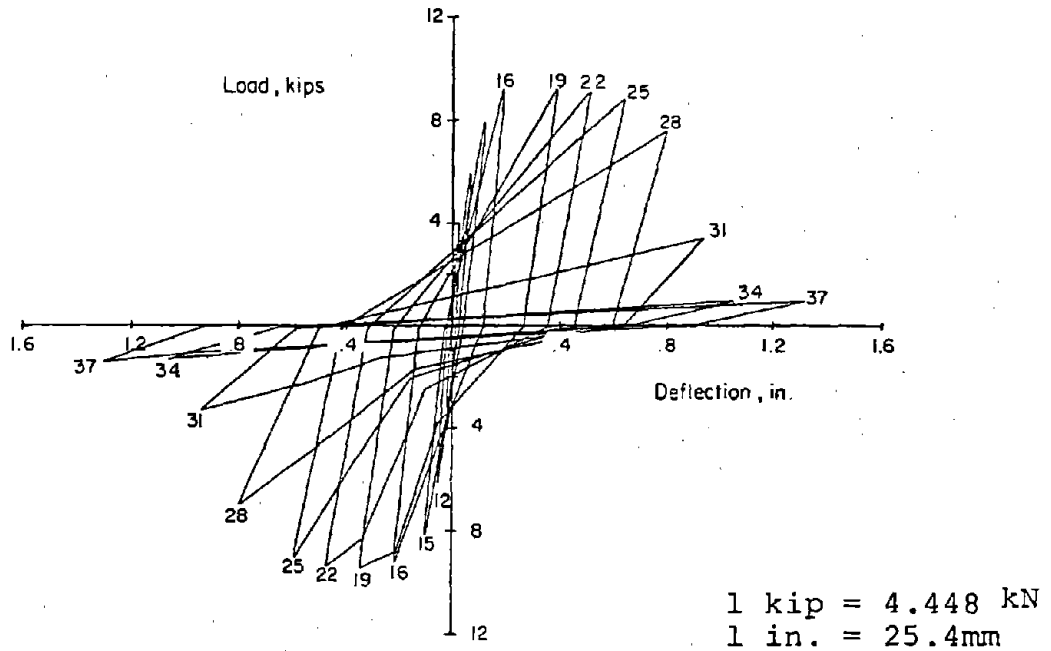


a) Load History

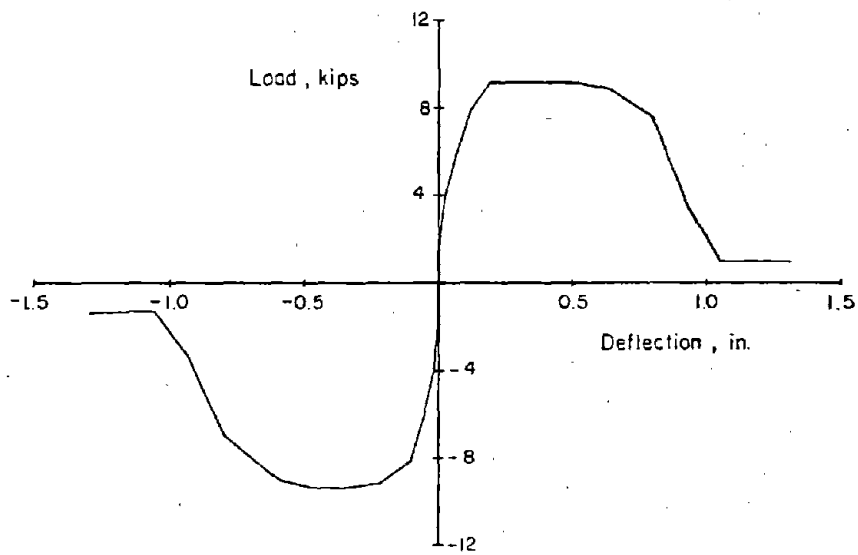


b) Deflection History

Fig. B-35 Loading History for Specimen C5

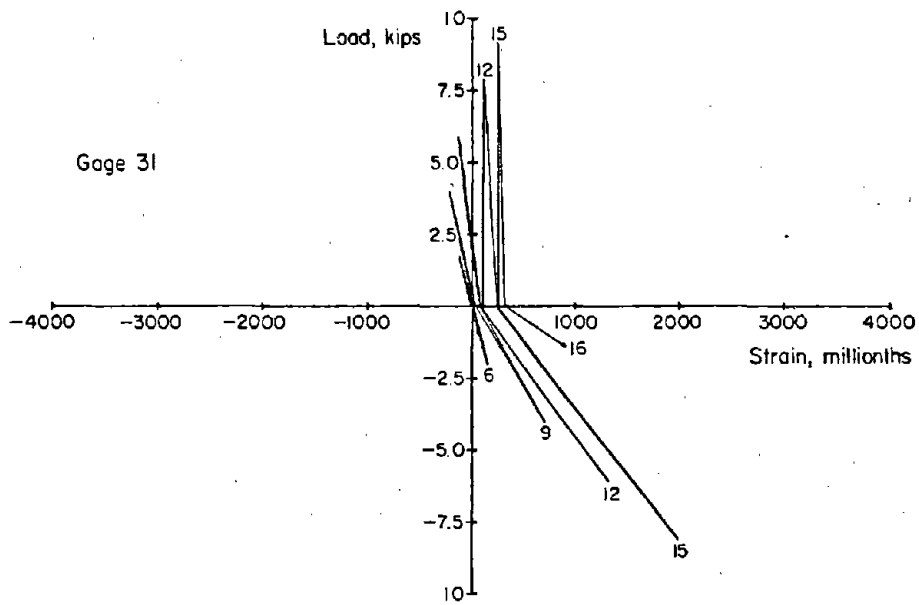


a) Segmental Plot



b) Envelope

Fig. B-36 Load versus Deflection Relationships for Specimen C5



1 kip = 4.448 kN

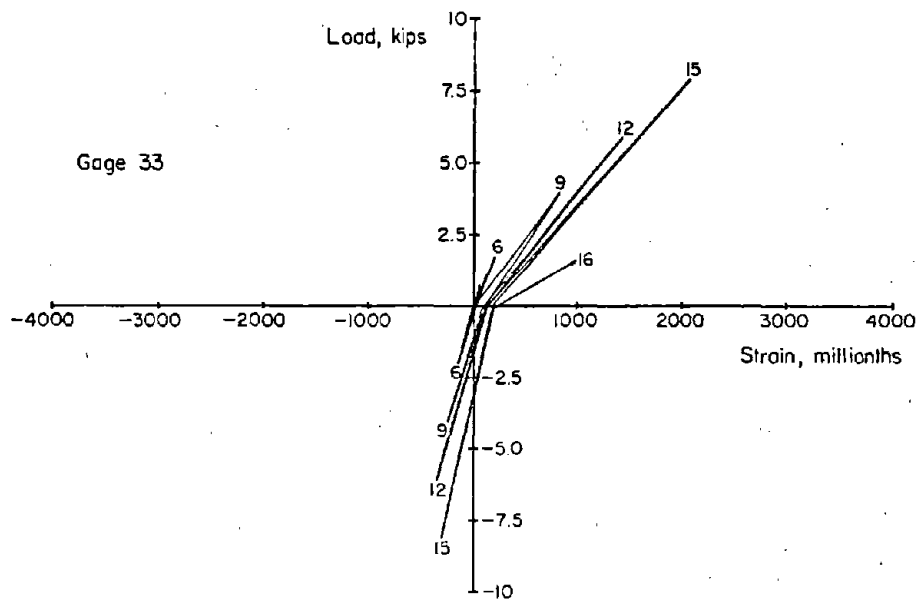
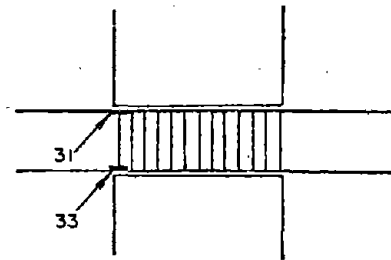
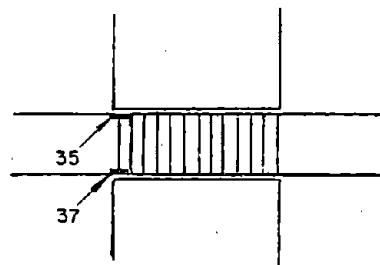
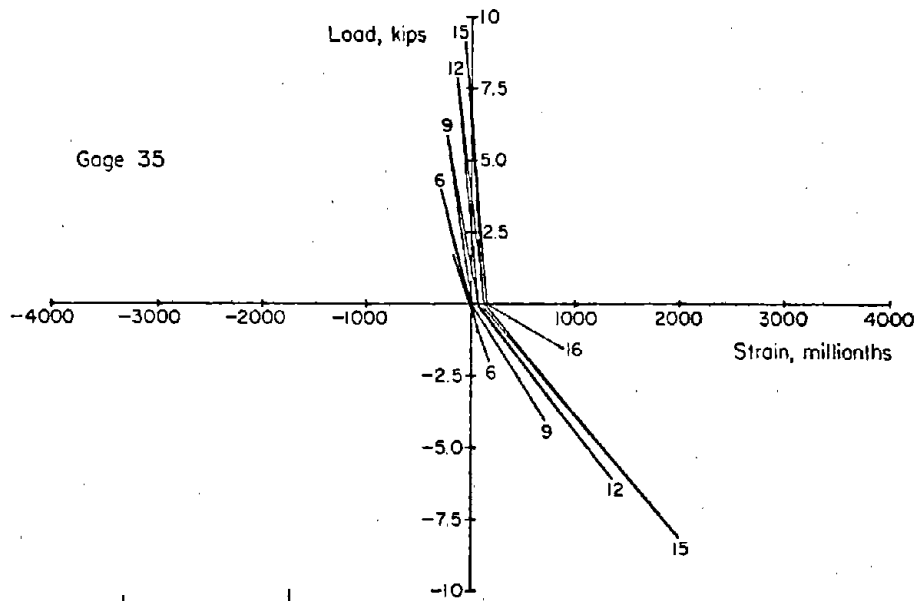


Fig. B-37 Load versus Flexural Steel Strains for Specimen C5 (East Beam)





1 kip = 4.448 kN

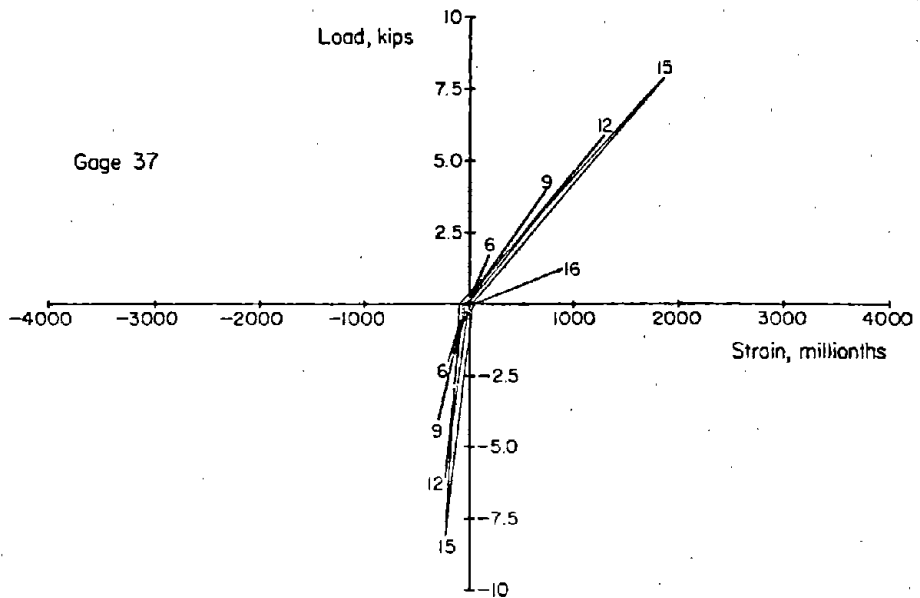


Fig. B-38 Load versus Flexural Steel Strains for Specimen C5 (West Beam)

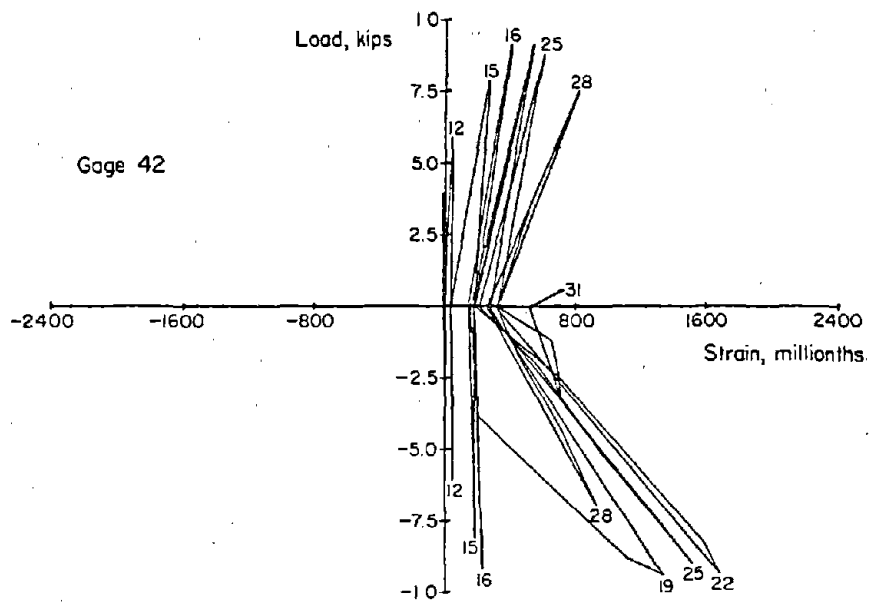
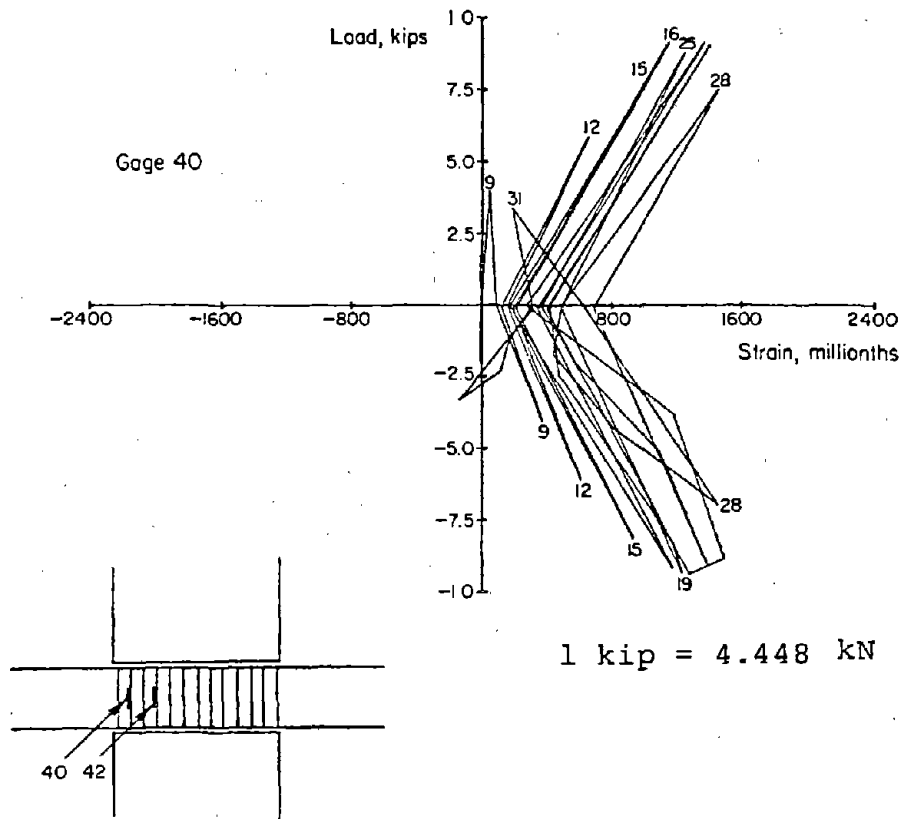


Fig. B-39 Load versus Hoop Steel Strains for Specimen C5 (East Beam)

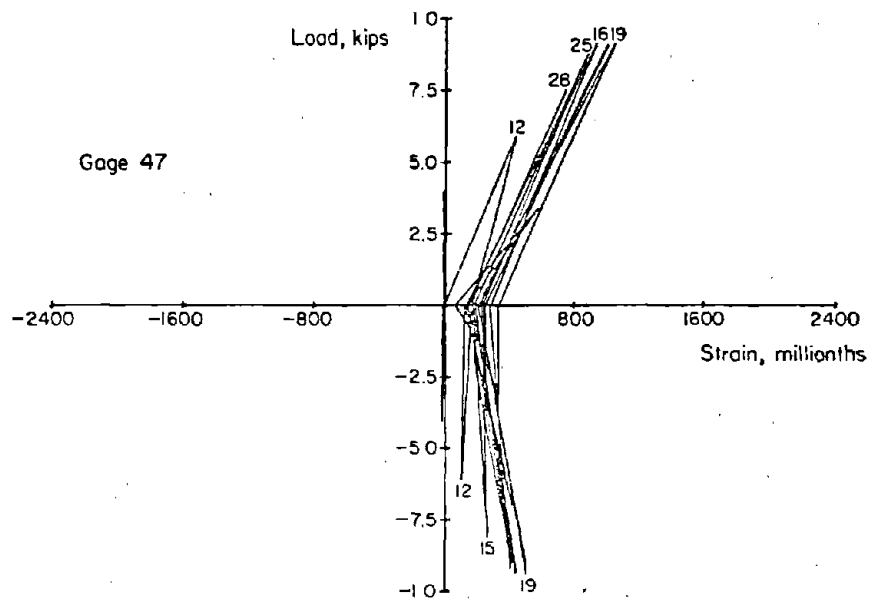
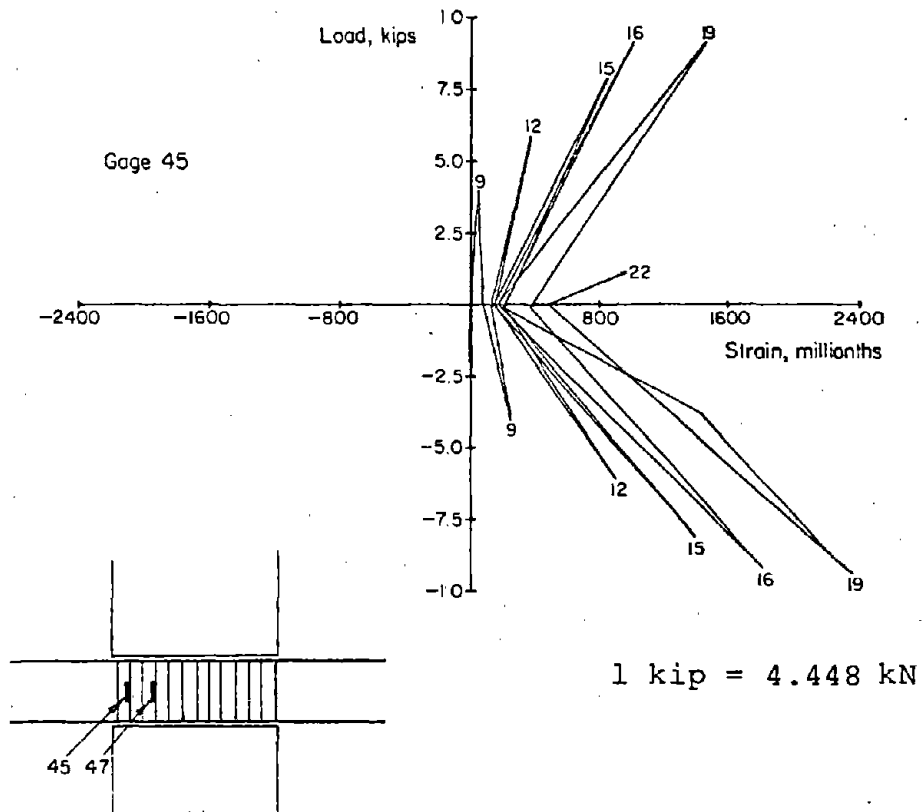
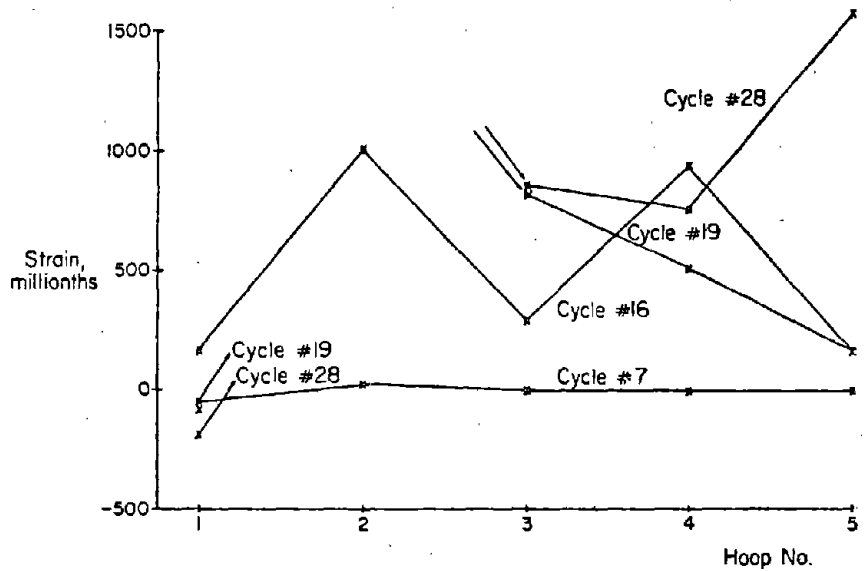
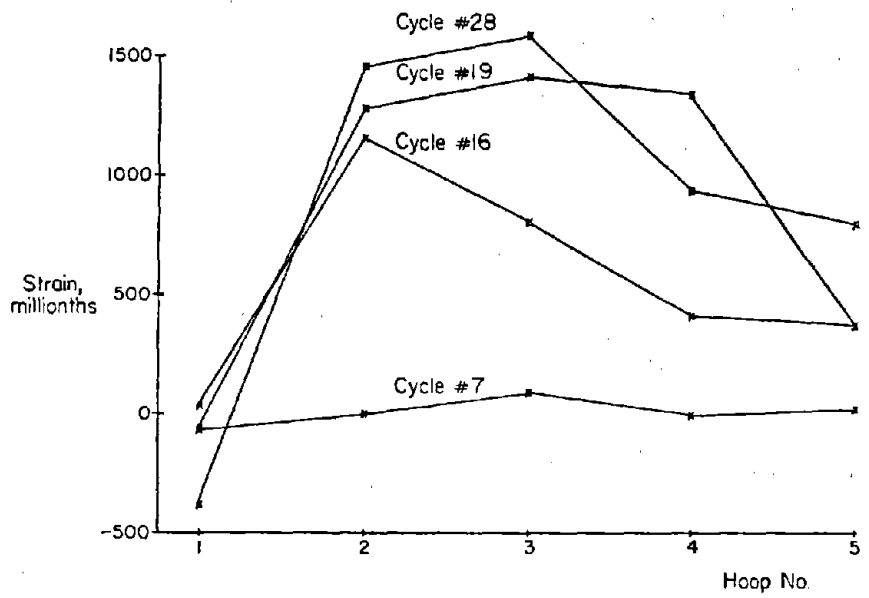
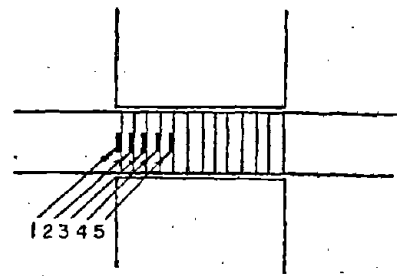


Fig. B-40 Load versus Hoop Steel Strains  
for Specimen C5 (West Beam)



a) East Beam



b) West Beam

Fig. B-41 Hoop Steel Strains for Specimen C5

### Specimen C6

Specimen C6 was tested with diagonal steel as primary reinforcement, as shown in Fig. A-6. Load and deflection histories are given in Fig. B-42. Plots of load versus deflection are shown in Fig. B-43. Strain data are presented in Figs. B-44 through B-48.

First cracking in this specimen occurred during the seventh load cycle at an applied load of 3.7 kips (16.5 kN) per beam. Yielding in the primary reinforcement occurred during the thirteenth load cycle at an applied load of 7.8 kips (34.7 kN) per beam. Deflection at yield was 0.11-in. (3 mm). Full depth cracks and some diagonal cracks had formed at the yield load.

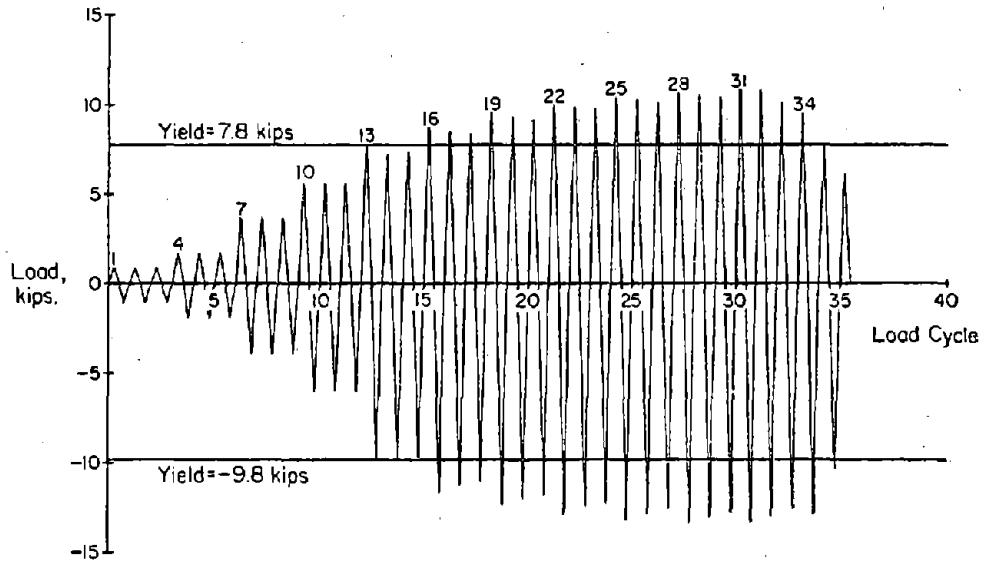
Spalling of the concrete shell was first observed during the tenth inelastic load cycle at a load of 8.8 kips (39.1 kN) per beam. Deflection at this load level was 0.35-in. (9 mm).

The maximum load carried by Specimen C6 was 13.4 kips (59.6 kN) per beam during the sixteenth inelastic load cycle. Nominal shear stress at this load was  $10.9 \sqrt{f'_c}$  psi ( $0.91 \sqrt{f'_c}$  MPa). Deflection at this load level was 0.75-in. (19 mm).

As load was being applied in the positive direction during the twenty-first inelastic load cycle, further twisting was observed in the east beam about its longitudinal axis. Deflection at this level was 0.88 in. (22 mm). Examination of the specimen after the test revealed that the diagonal reinforcement was approximately 1/4-in. (6.4 mm) off center at one end of the beam. The internal forces in the beam were, therefore, not symmetric and caused the beam to twist.

As load was applied during the twenty-second inelastic load cycle, further twisting of the east beam occurred and twisting of the west beam was observed. As deflection was increased to 1.00 in. (25 mm), buckling of the exposed No. 3 bars at the end of the beam was observed. The first decrease in load capacity occurred during this load cycle.

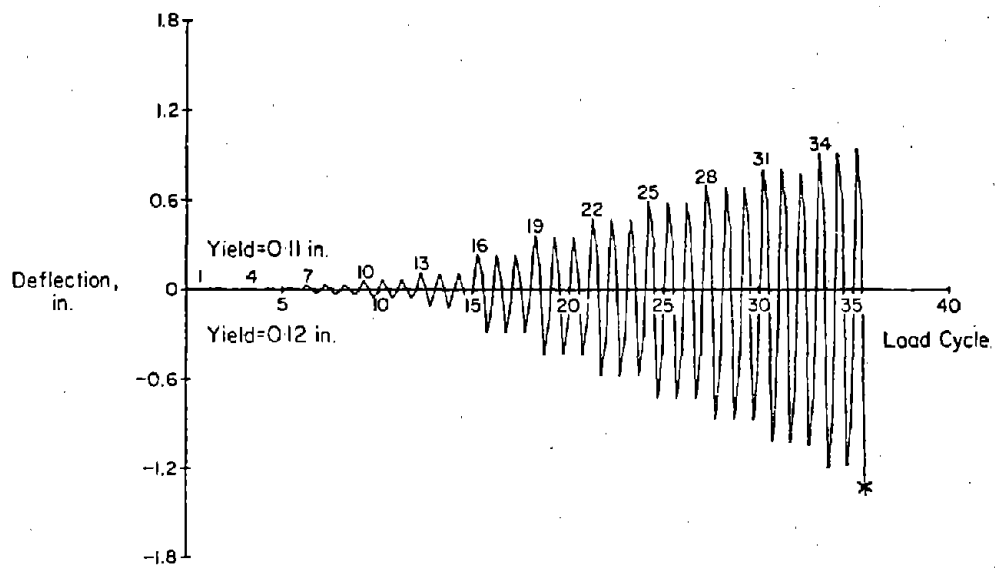
During application of load in the negative direction at the twenty-third inelastic load cycle, fracture of a No. 3 bar



a) Load History

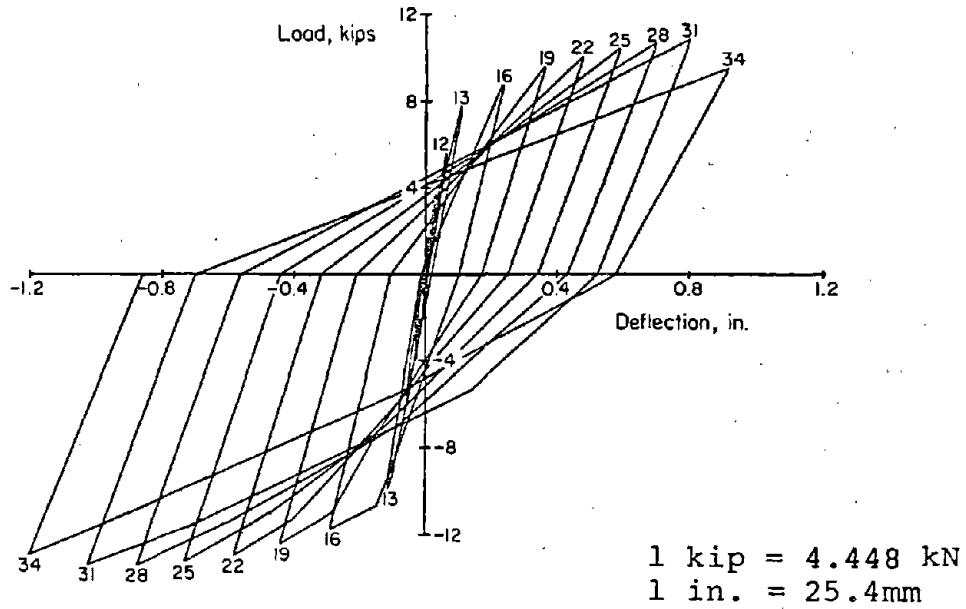
1 kip = 4.448 kN

1 in. = 25.4mm

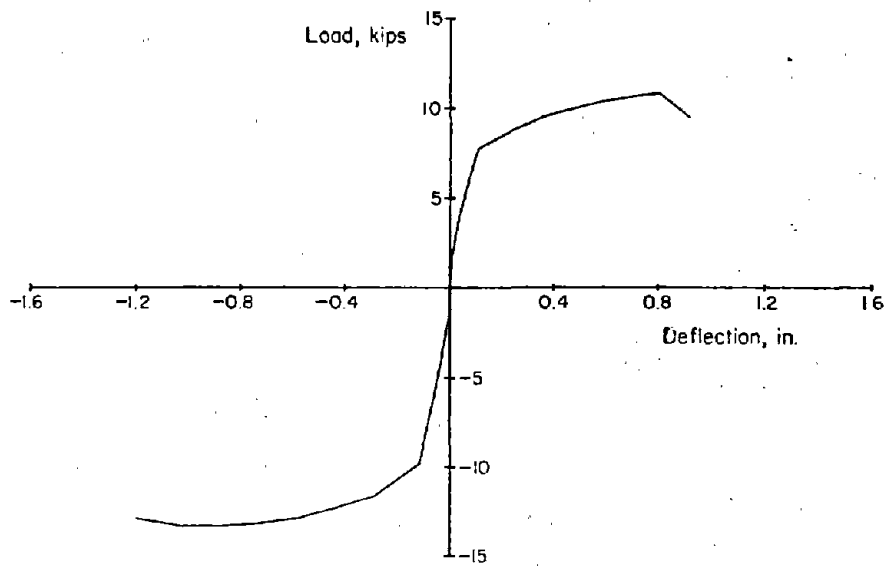


b) Deflection History

Fig. B-42 Loading History for Specimen C6

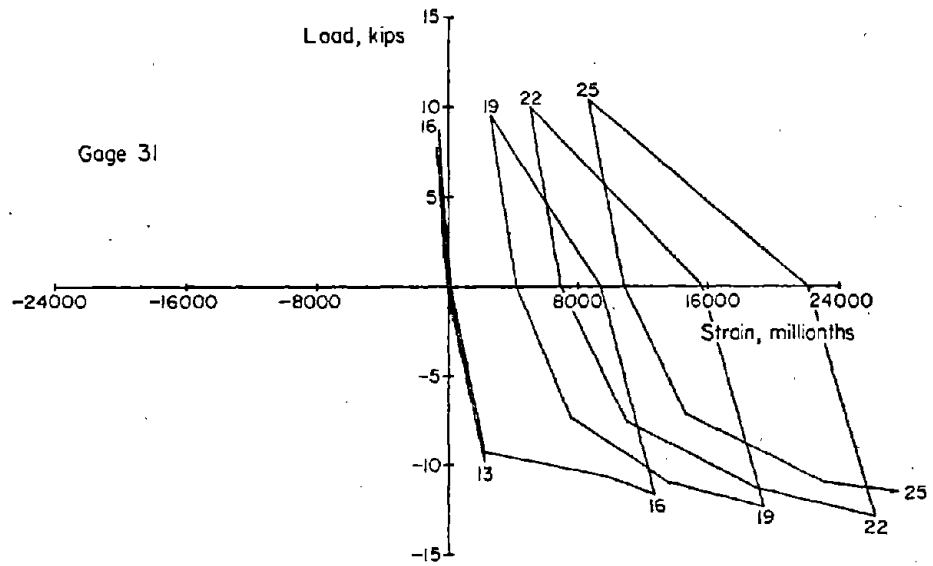


a) Segmental Plot



b) Envelope

Fig. B-43 Load versus Deflection Relationships for Specimen C6



1 kip = 4.448 kN

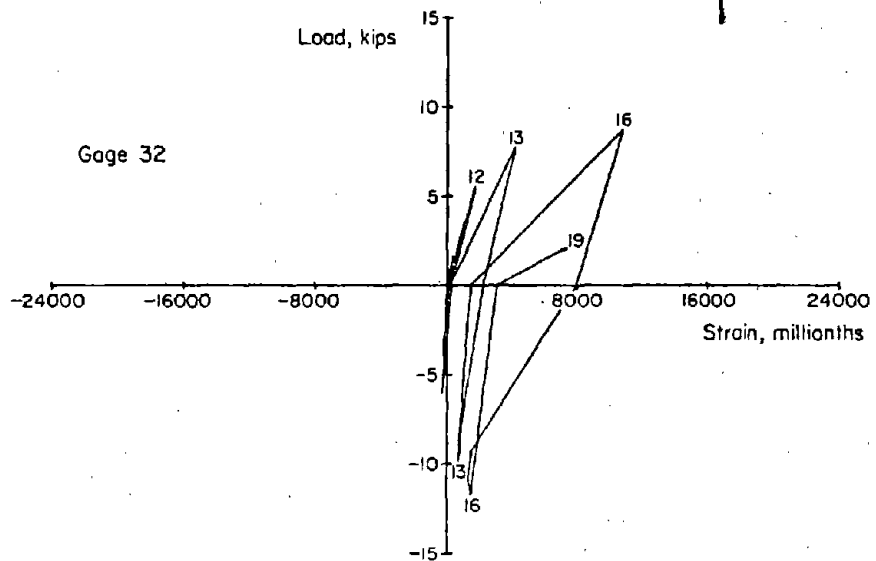
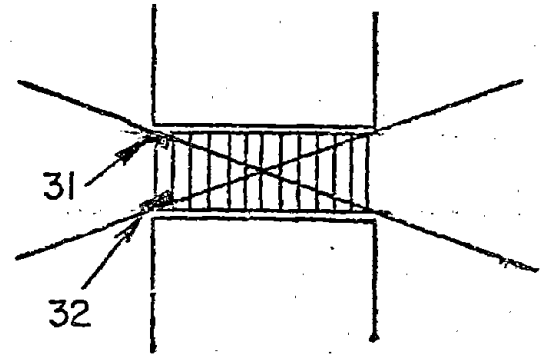
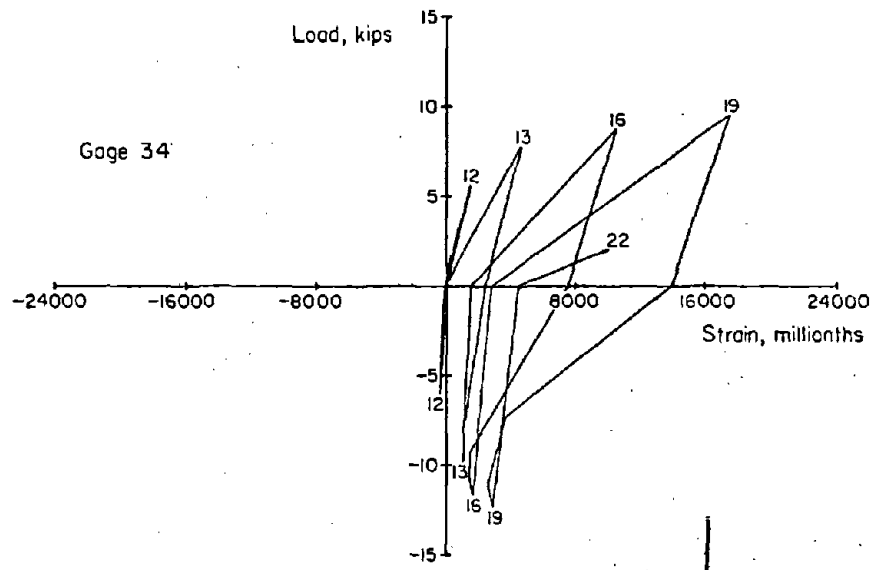


Fig. B-44 Load versus Diagonal Steel Strains for Specimen C6 (East Beam)





1 kip = 4.448 kN

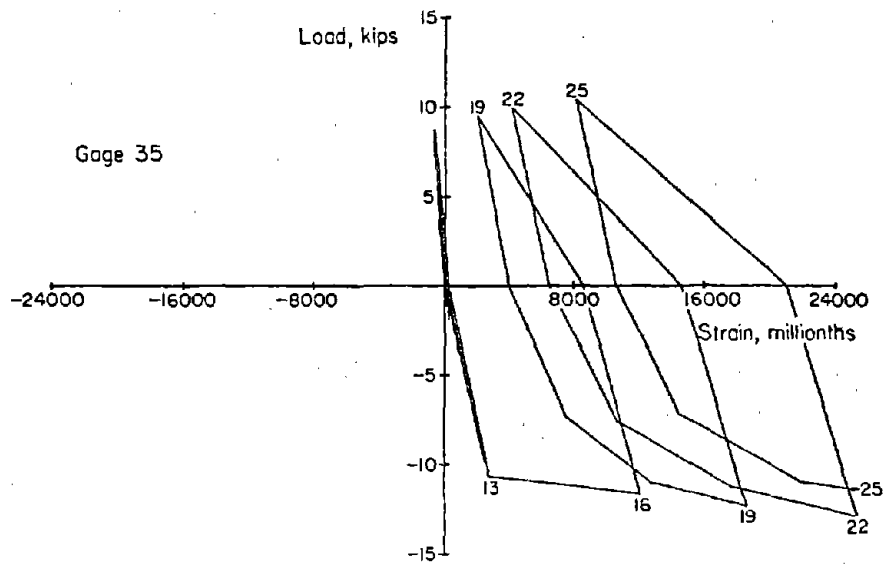
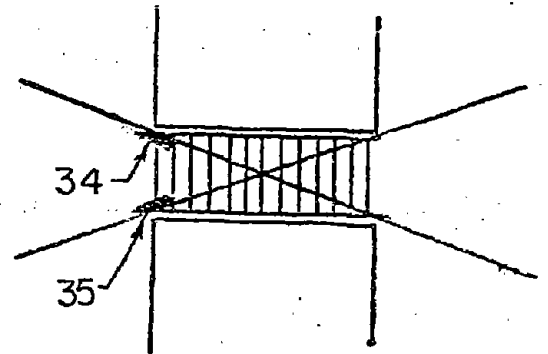
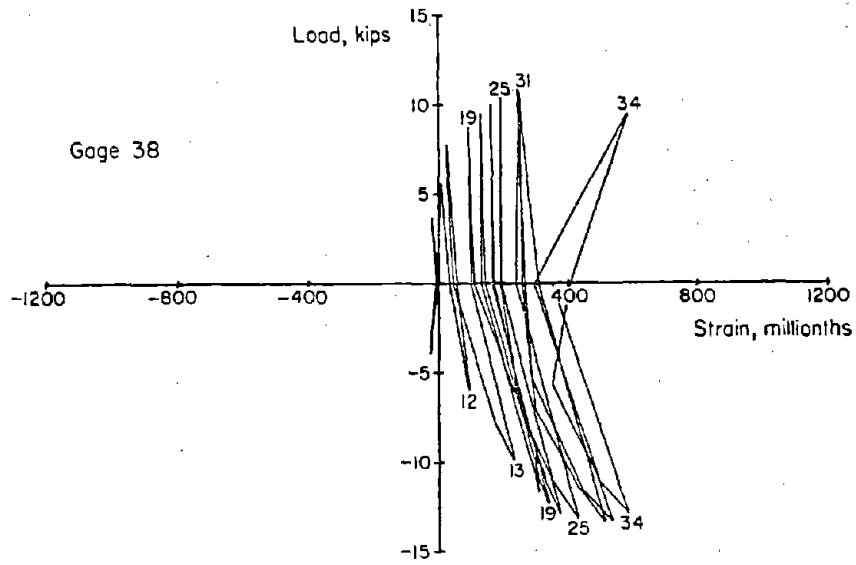


Fig. B-45 Load versus Diagonal Steel Strains for Specimen C6 (West Beam)



1 kip = 4.448 kN

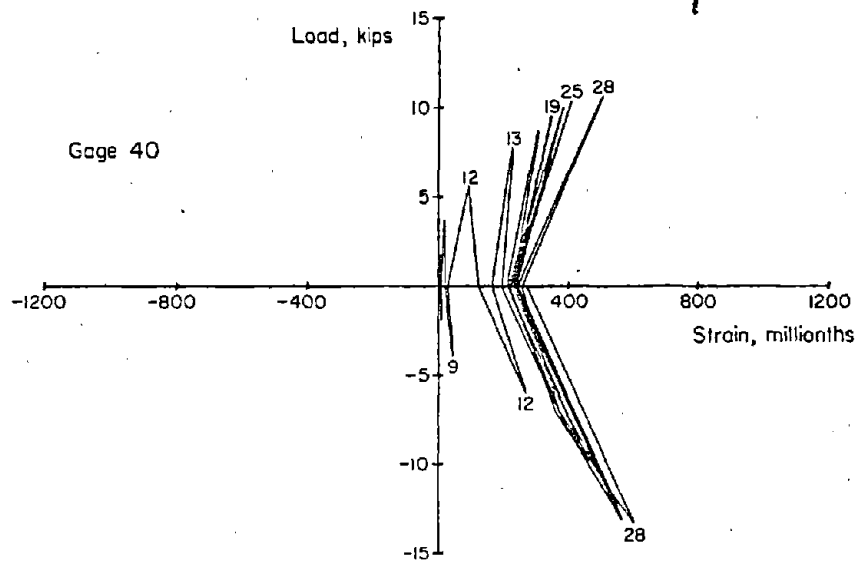
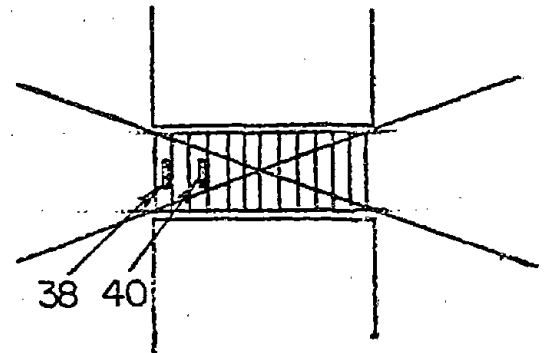
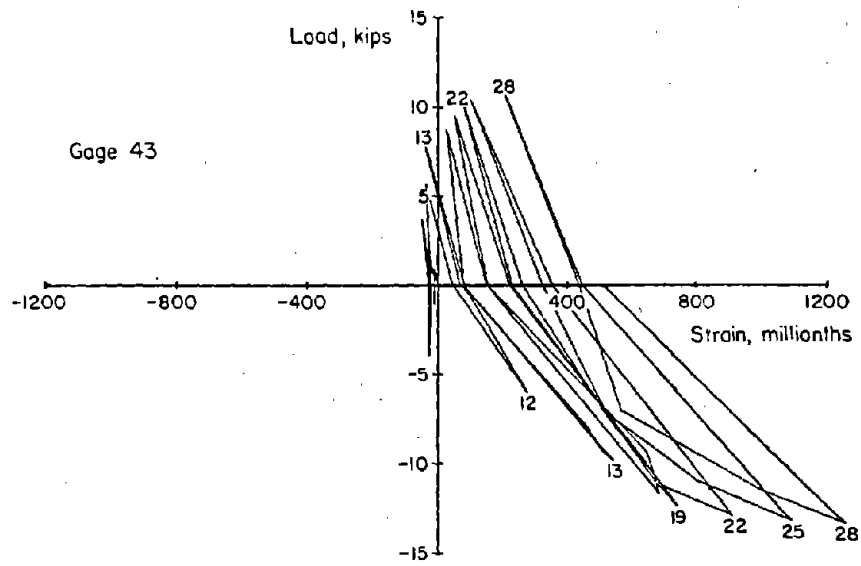


Fig. B-46 Load versus Hoop Steel Strains for Specimen C6 (East Beam)



1 kip = 4.448 kN

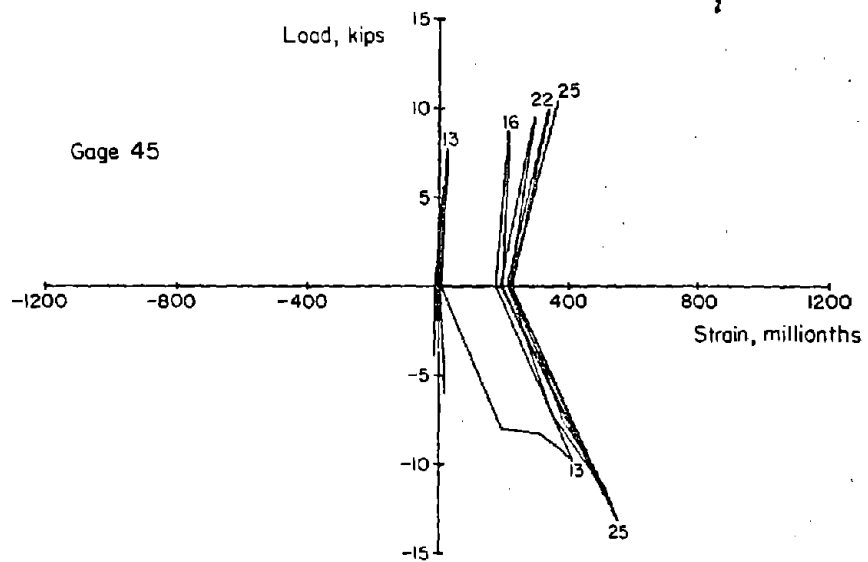
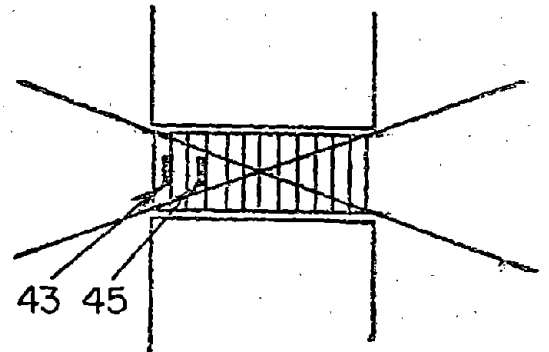
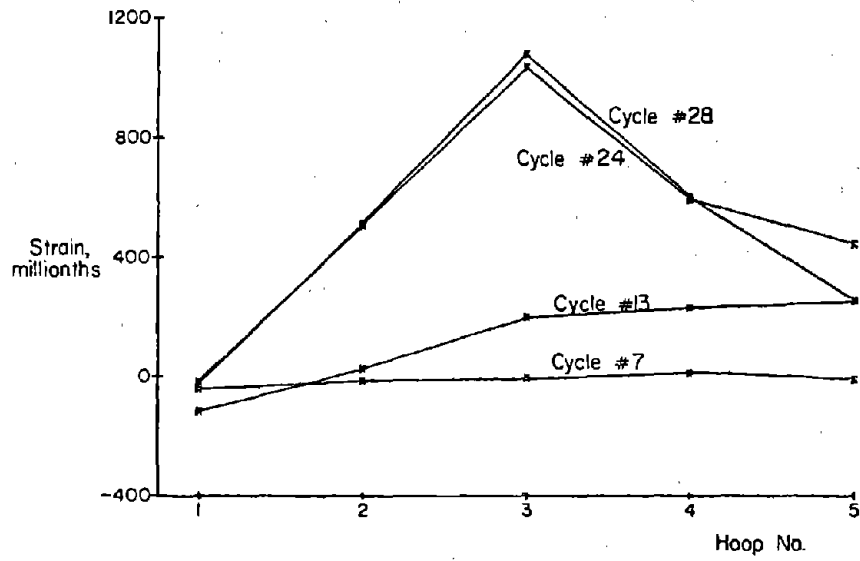
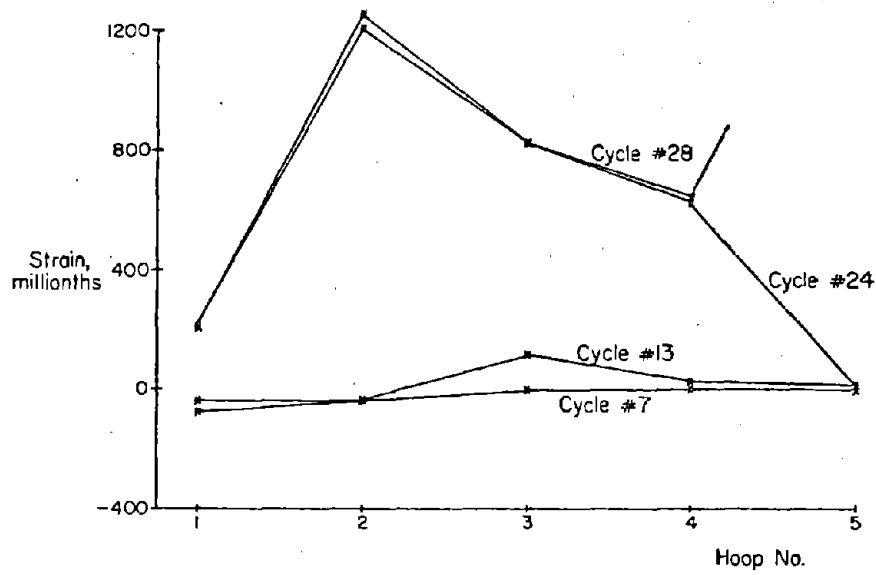
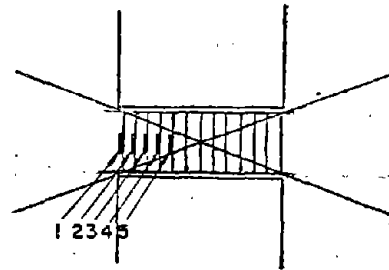


Fig. B-47 Load versus Hoop Steel Strains for Specimen C6 (West Beam)



a) East Beam



b) West Beam

Fig. B-48 Hoop Steel Strains for Specimen C6

occurred on the north side of the east beam. A maximum deflection of 1.00-in. (25 mm) was imposed during this load cycle. Applied load had dropped to 10.4 kips (46.3 kN) per beam. The test was terminated during the twenty-fourth inelastic load cycle when the remaining No. 3 bar in the east beam fractured.

#### Specimen C7

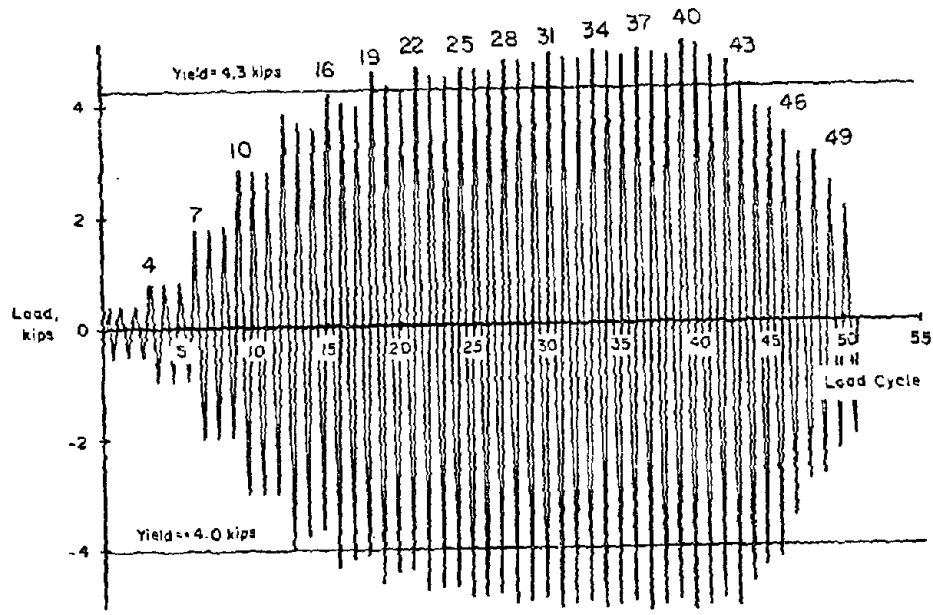
Details of Specimen C7 are shown in Fig. A-3. This specimen had a span length of 33.3-in., resulting in a span-to-depth ratio of 5.0. Load and deflection histories are given in Fig. B-49. Plots of load versus deflection are shown in Fig. B-50. Steel strains are presented in Figs. B-51 through B-55.

First cracking in this specimen occurred during the seventh load cycle at a load of 1.8 kips (8.0 kN) per beam. Yielding of the flexural reinforcement took place during the thirteenth load cycle at an applied load of 4.3 kips (19.1 kN) per beam, with a corresponding deflection of 0.16-in. (4.1 mm). A maximum load of 5.2 kips (23.3 kN) per beam was carried by the specimen during the twenty-seventh inelastic load cycle. The measured deflection at maximum load was 1.25 in. (32 mm). The nominal shear stress at this load was  $3.5 \sqrt{f'_c}$  psi ( $0.29 \sqrt{f'_c}$  MPa). This is approximately one-half of the peak shear stress of Specimens C2 and C5.

Spalling of the concrete shell was first observed in the hinging region during the seventeenth inelastic load cycle. Maximum load and deflection recorded during this cycle were 4.9 kips (21.8 kN) per beam and 0.63-in. (16 mm), respectively.

The test was terminated after thirty-eight inelastic load cycles because of deflection limitations in the test setup. The imposed deflection at the last load cycle was 2.0-in. (51 mm). The final load applied to the specimen was 2.0 kips (8.9 kN) per beam.

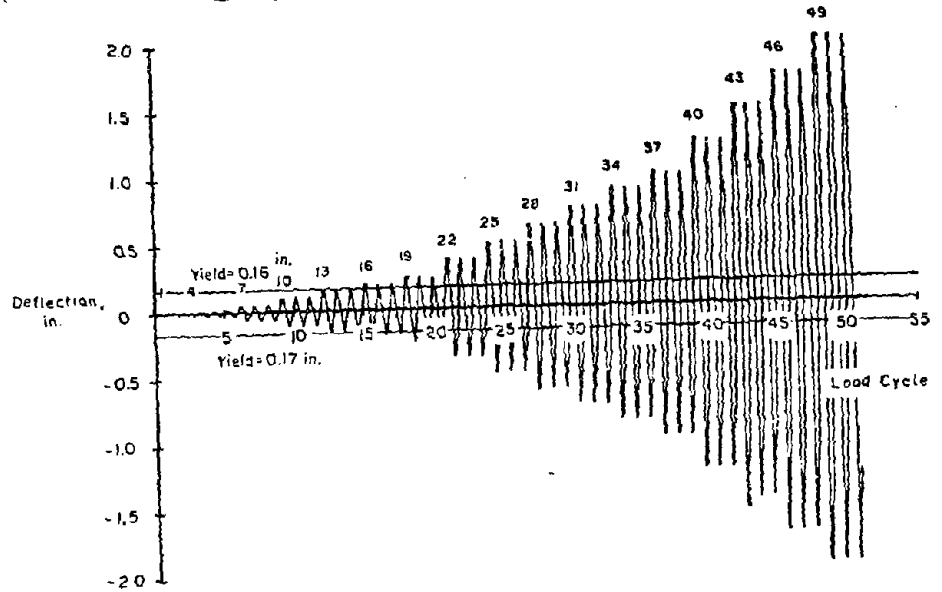
Concrete deterioration occurred primarily at the ends of beams. Flexure-shear cracks were observed in the regions between the one-third points and the ends of the beams. Loss



1 kip = 4.448

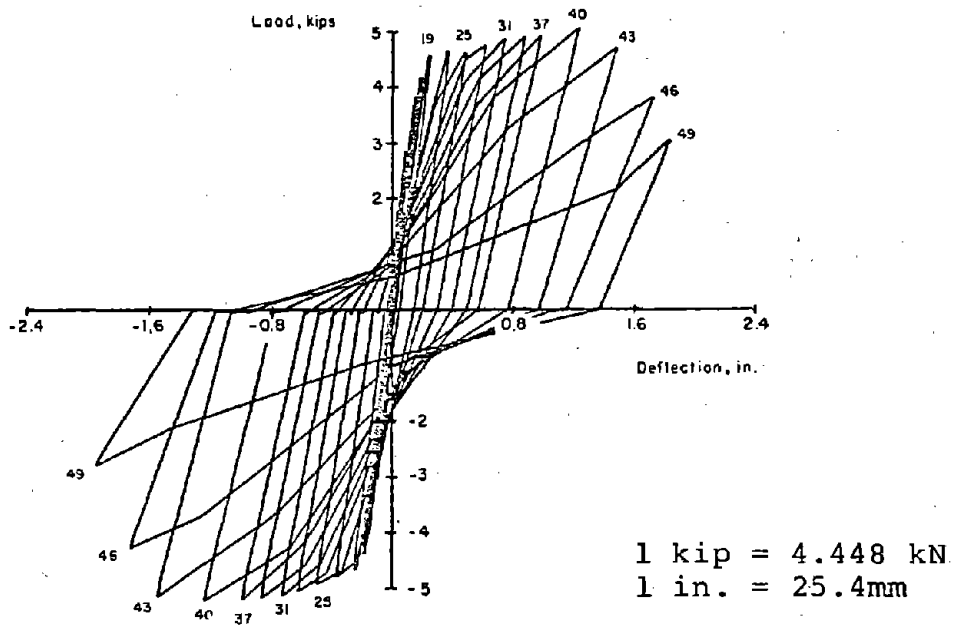
a) Load History

1 in. = 25.4mm

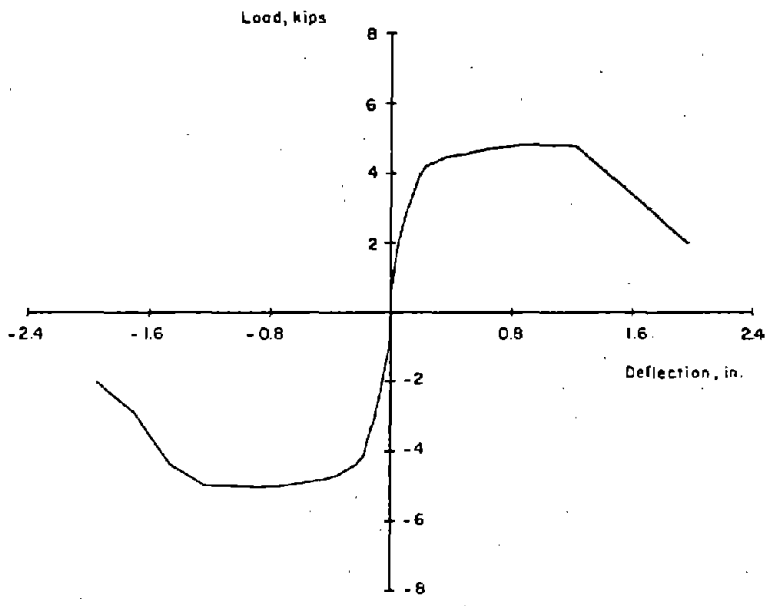


b) Deflection History

Fig. B-49 Loading History For Specimen C7



a) Segmental Plot



b) Envelope

Fig. B-50 Load versus Deflection Relationships for Specimen C7

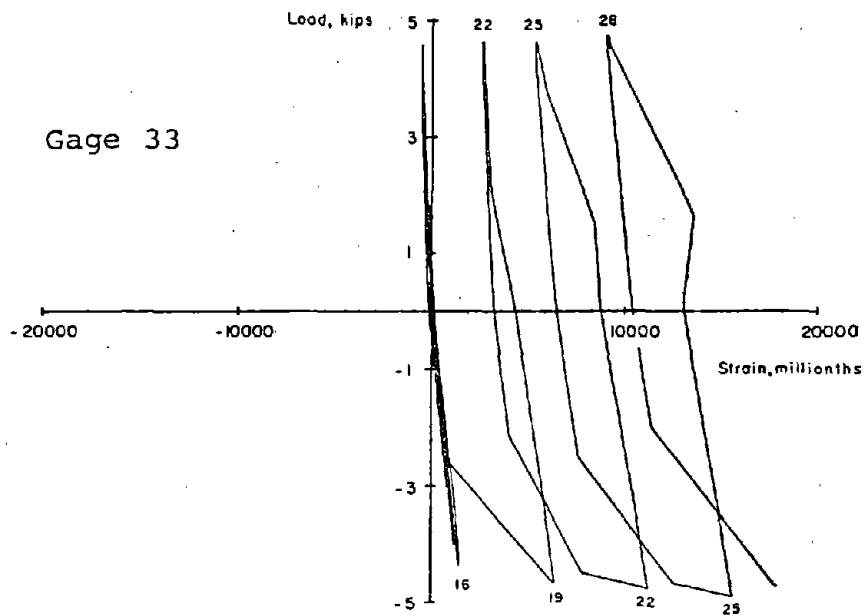
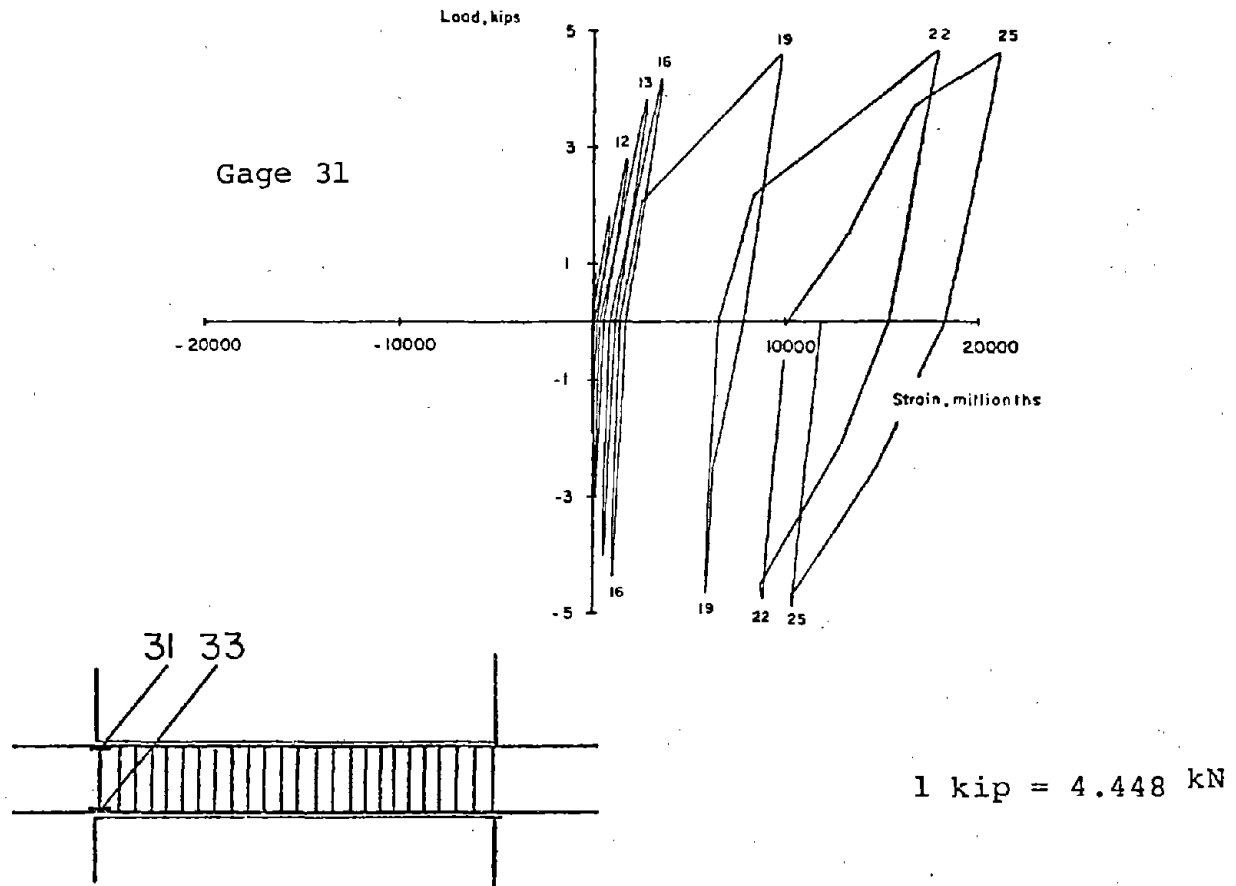


Fig. B-51 Load versus Flexural Steel Strains for Specimen C7 (East Beam)



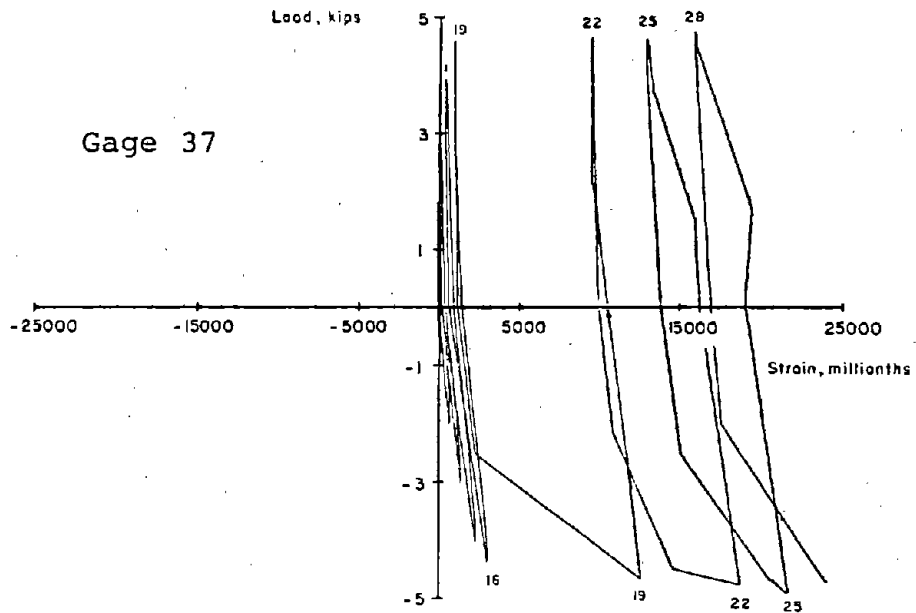
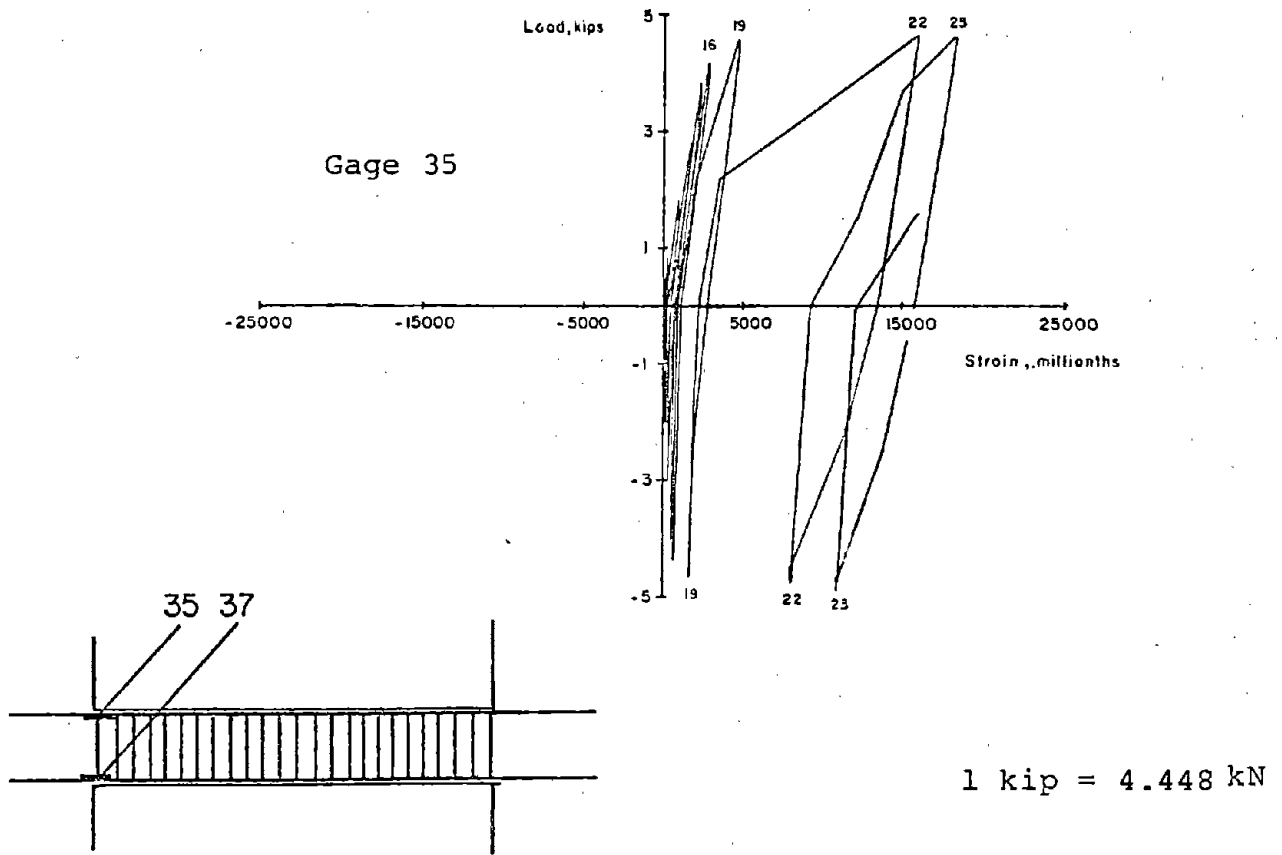
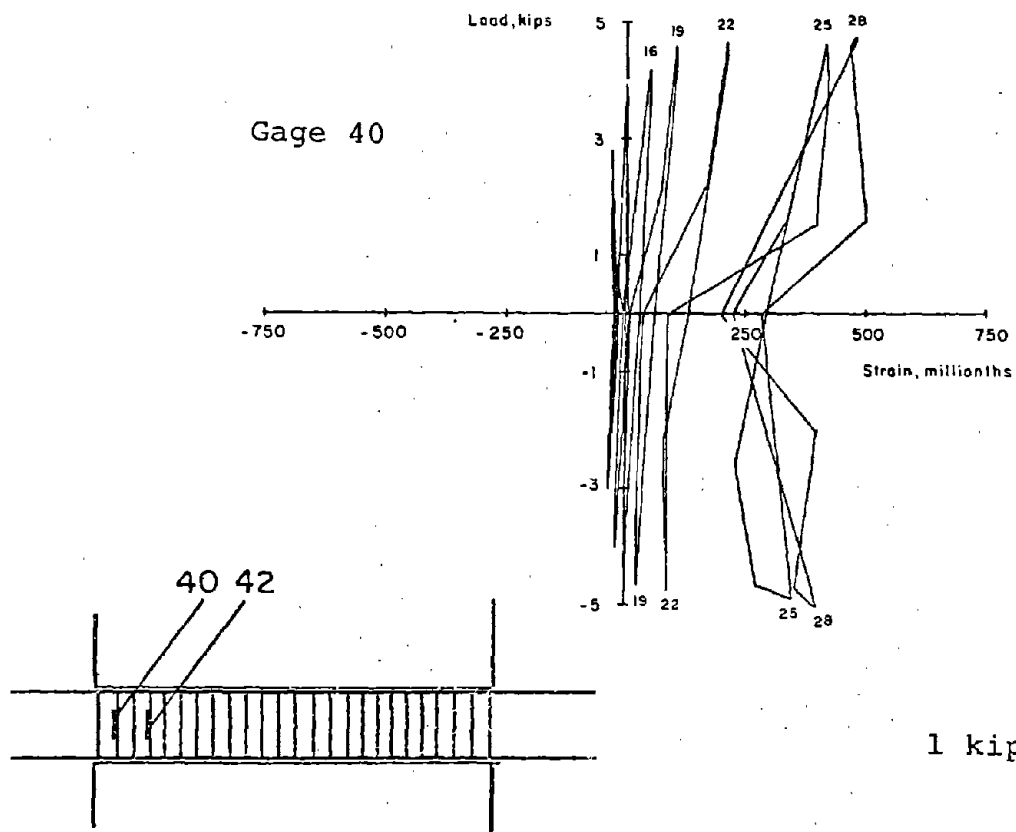


Fig. B-52 Load versus Flexural Steel Strains for Specimen C7 (West Beam)



1 kip = 4.448 kN

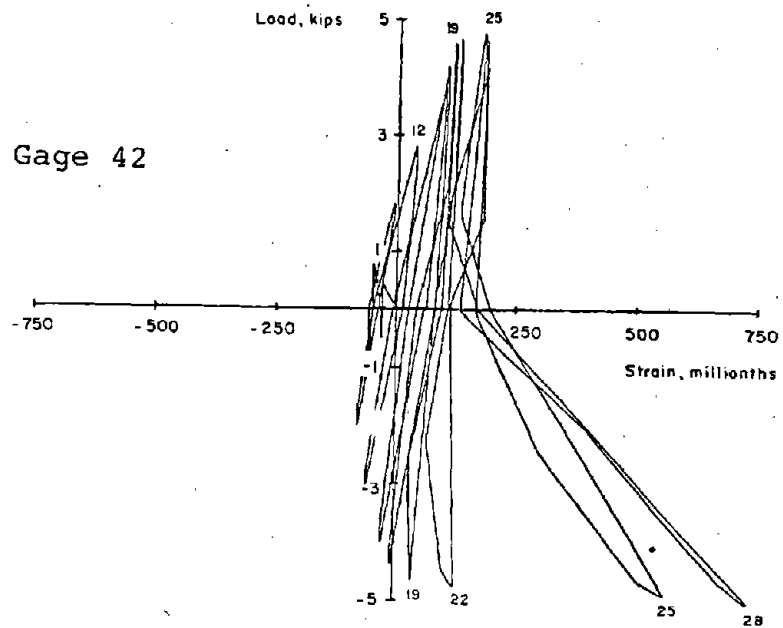


Fig. B-53 Load versus Hoop Steel Strains for Specimen C7 (East Beam)

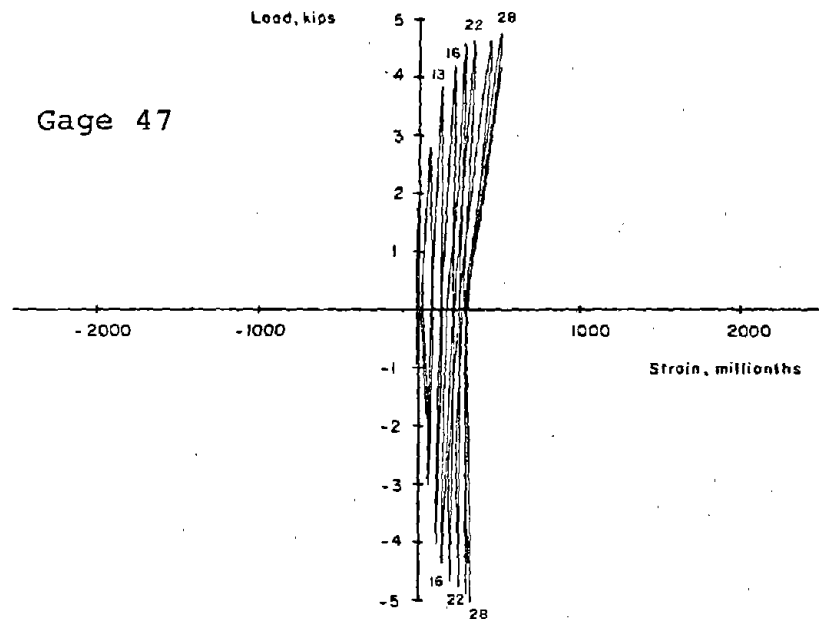
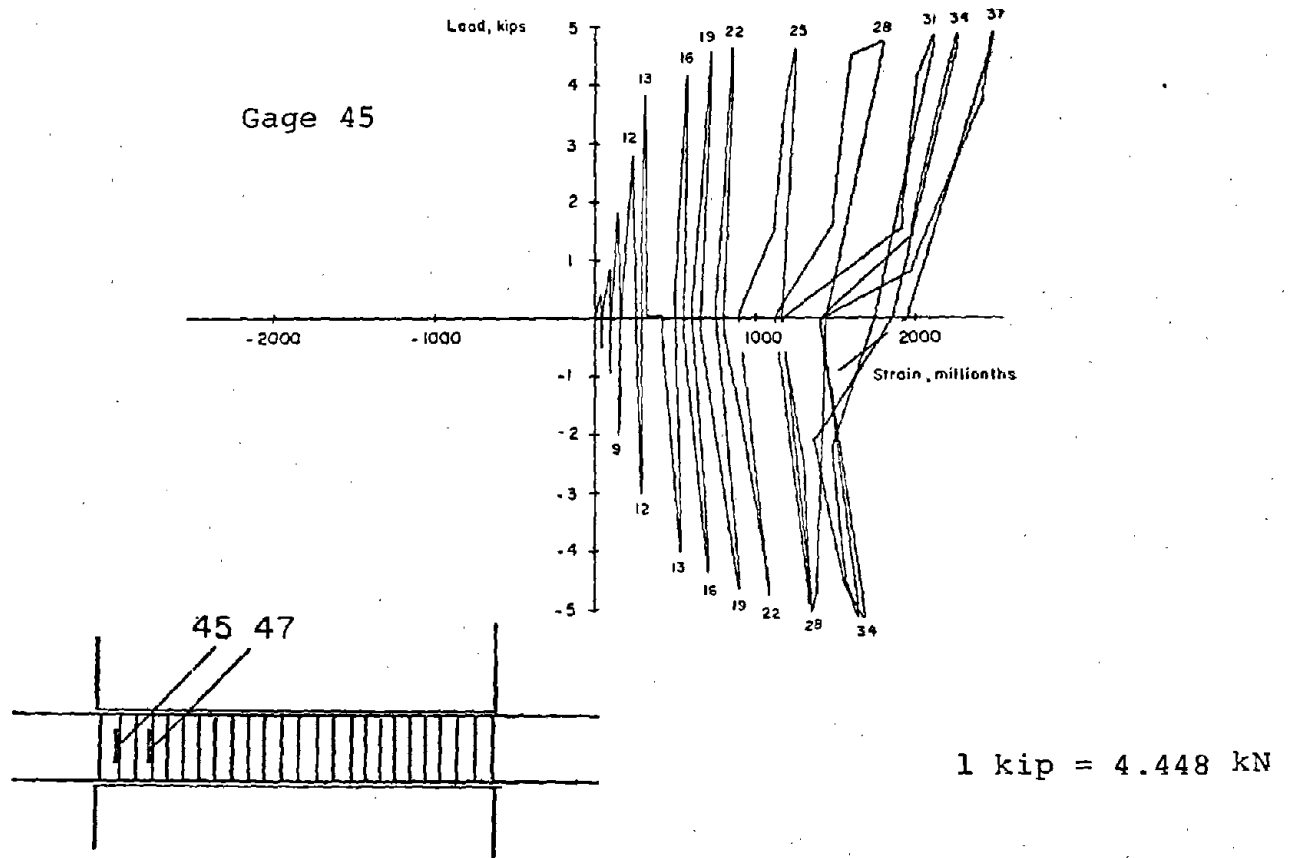
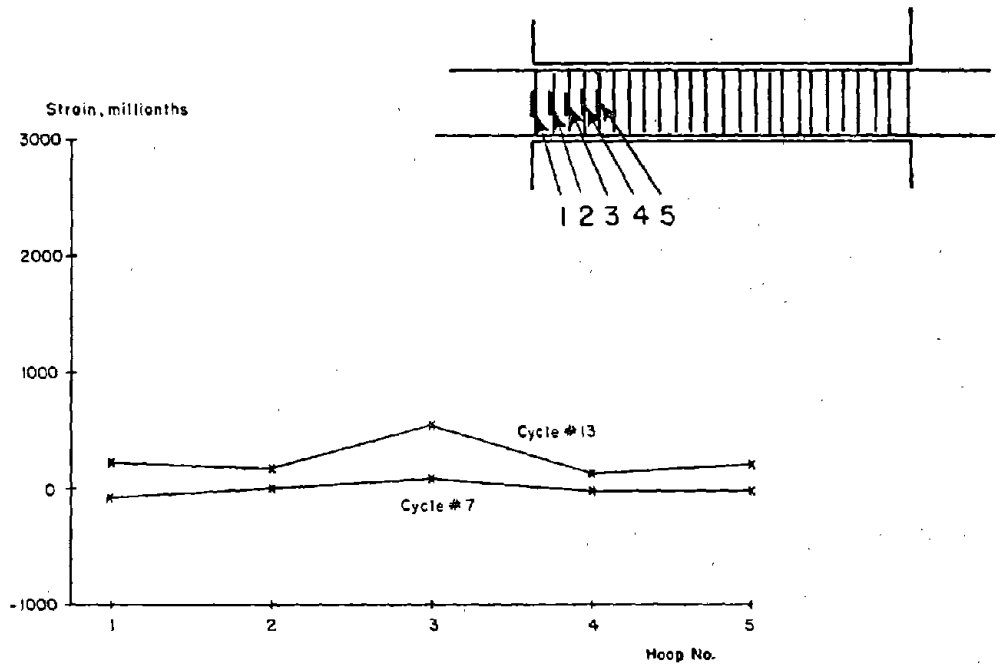
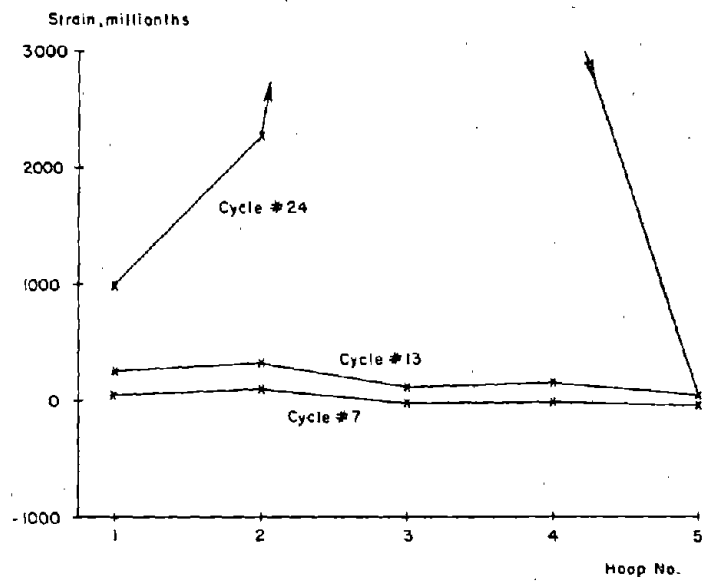


Fig. B-54 Load versus Hoop Steel Strains for Specimen C7 (West Beam)



a) East Beam



b) West Beam

Fig. B-55 Hoop Steel Strain for Specimen C7

of capacity was attributed to "sliding shear" at the interface between the ends of beams and the face of the abutment wall.

#### Specimen C8

Specimen C8 had a span length of 33.3-in. (846 mm) corresponding to span-to-depth ratio of 5.0. Reinforcement details are shown in Fig. A-7. Load and deflection histories are given in Fig. B-56. Plots of load versus deflection are shown in Fig. B-57. Strain data are presented in Figs. B-58 through B-62.

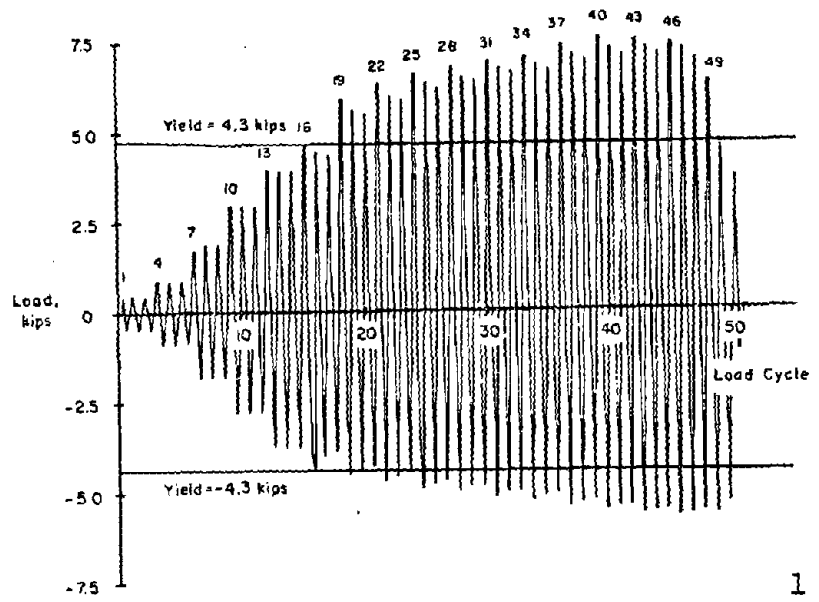
First cracking in this specimen occurred during the fifth load cycle at an applied load of 0.5 kips (2.2 kN) per beam. Yielding of the diagonal reinforcement took place during the sixteenth load cycle at a load of 4.6 kips (20.5 kN) per beam. Deflection at yield was 0.21-in. (5 mm).

Concrete spalling was observed in the hinging region during the seventeenth inelastic load cycle at a load of 5.0 kips (22.2 kN) per beam. Deflection at this load level was 0.88-in. (22 mm).

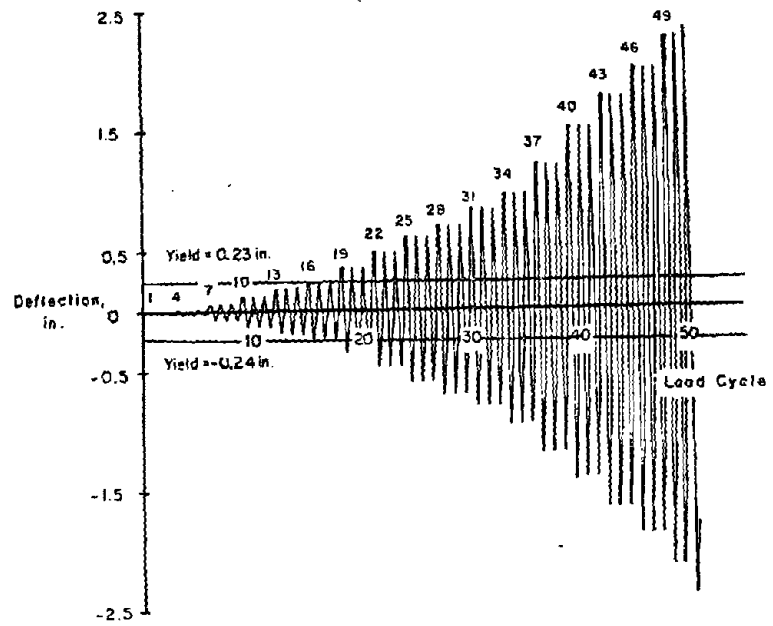
Load capacity of Specimen C8 was 7.5 kips (33.3 kN) per beam during the twenty-fourth inelastic cycle. This corresponds to a maximum nominal shear stress of  $5.3 \sqrt{f'_c}$  psi ( $0.44 \sqrt{f'_c}$  MPa). This was about half of that for Specimen C6. Recorded deflection at this load was 1.5-in. (38.1 mm).

As load was being applied in the positive direction during the thirty-second inelastic cycle, twisting was observed in the east beam. Deflection at this load level was 2.0-in. (51 mm). Examination of the specimen after testing indicated that the diagonal reinforcement was off center by about 1/4-in. at the south end of this beam. This resulted in unsymmetric forces, causing the beam to twist.

As load was applied during the thirty-third inelastic load cycle, further twisting in the east beam and slight twisting in the west beam was observed.

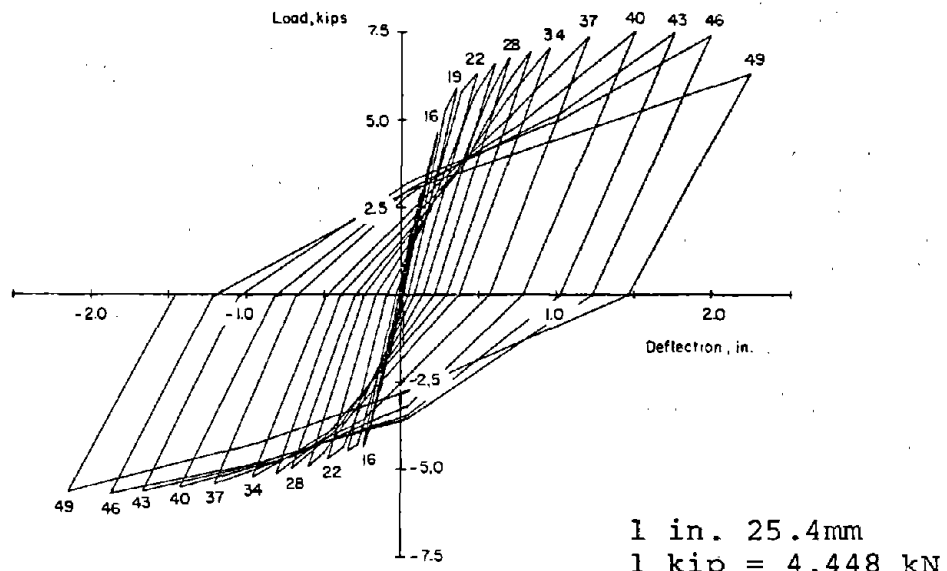


a) Load History

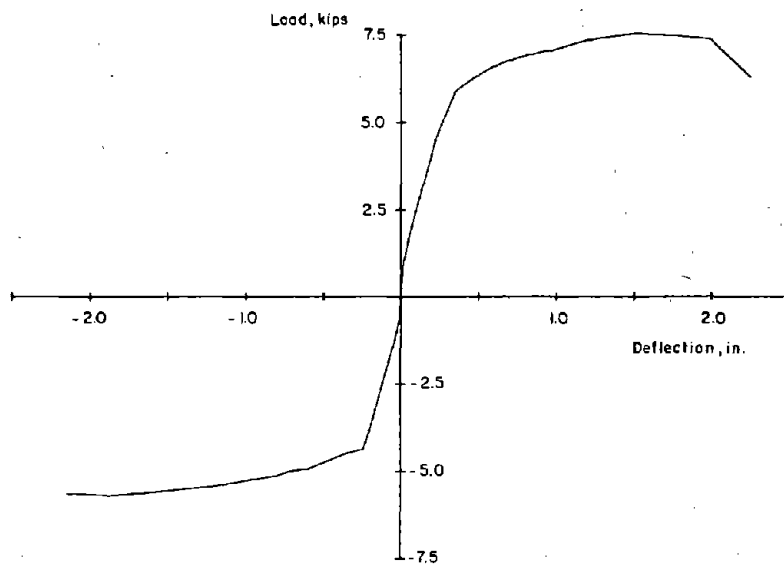


b) Deflection History

Fig. B-56 Loading History for Specimen C8



a) Segmental Plot



b) Envelope

Fig. B-57 Load versus Deflection Relationship for Specimen C8

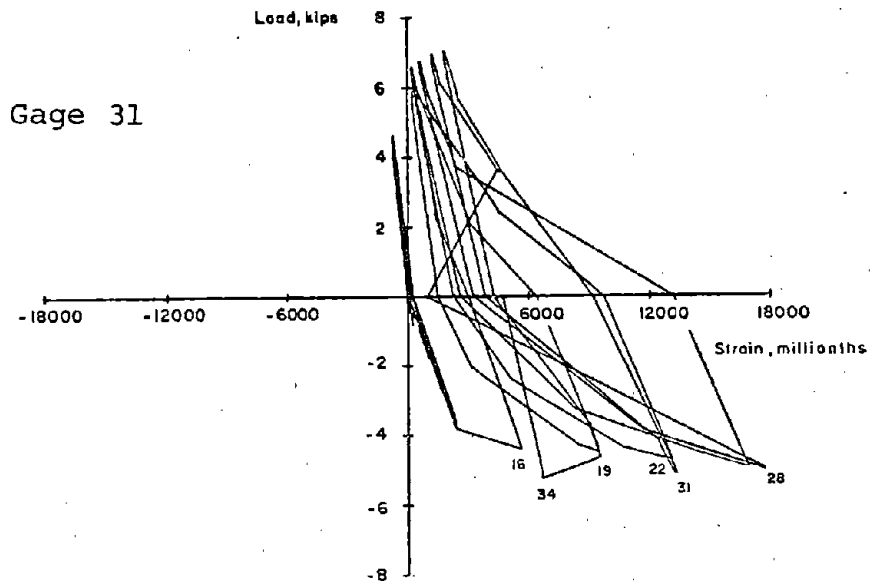
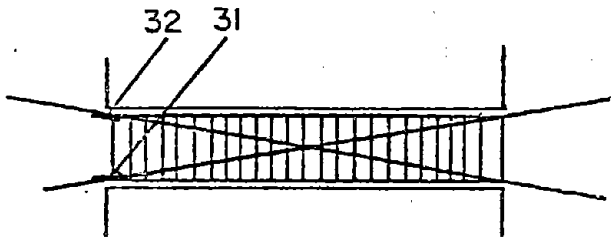
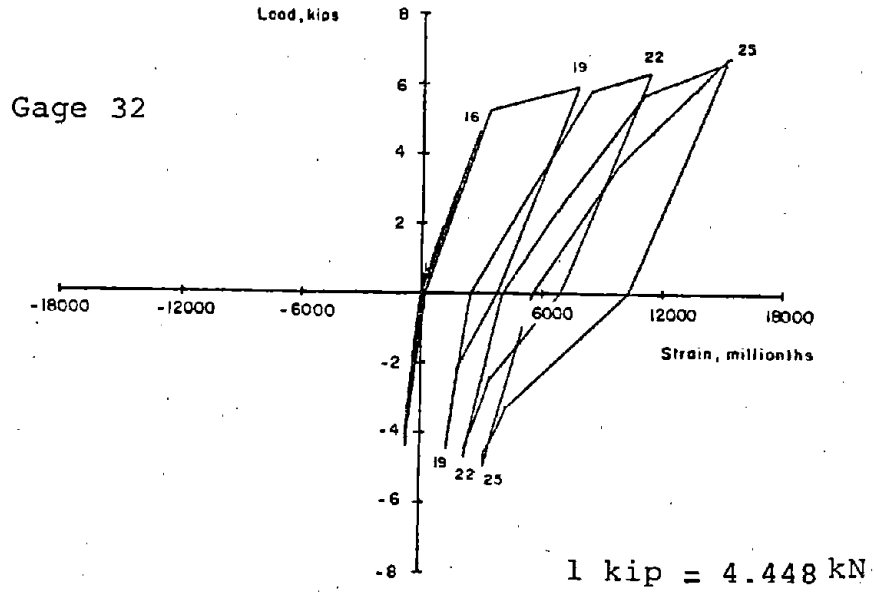


Fig. B-58 Load versus Diagonal Steel Strains for Specimen C8 (East Beam)



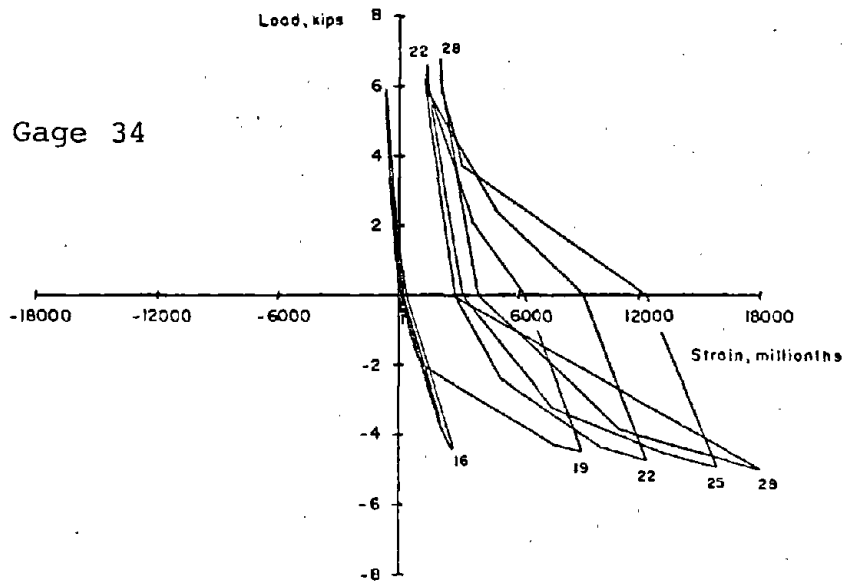
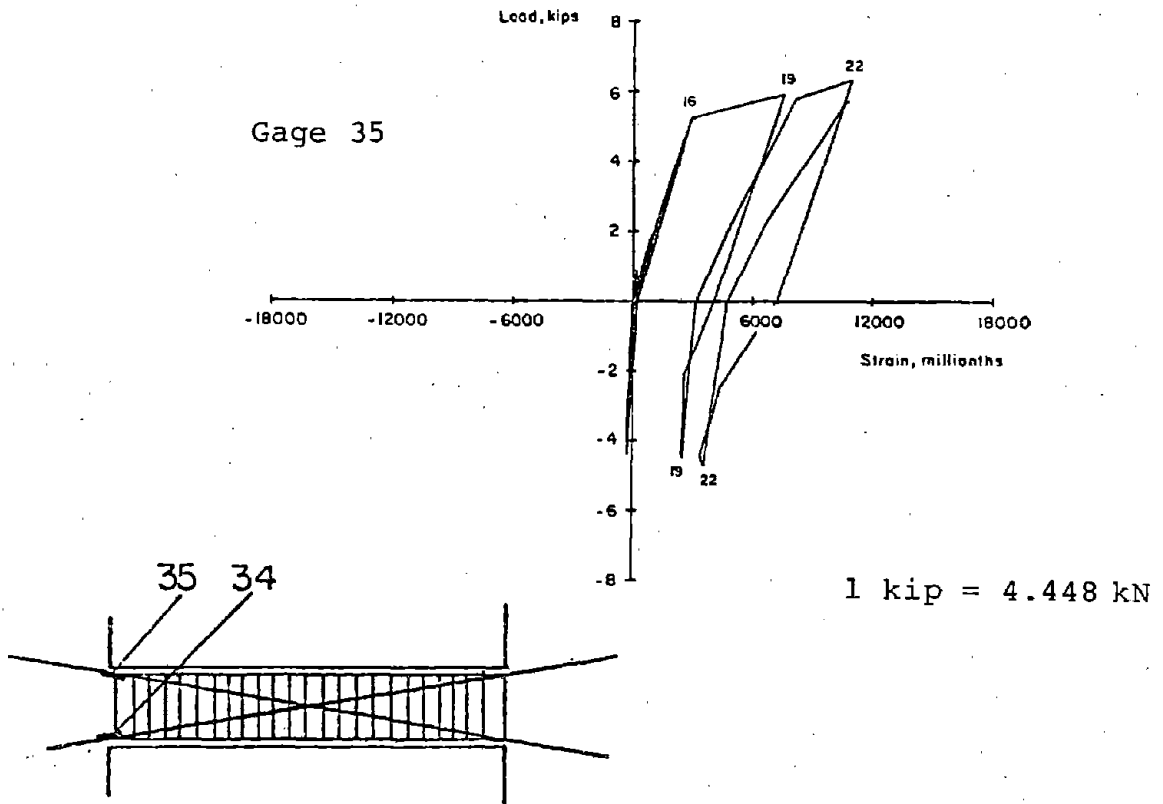
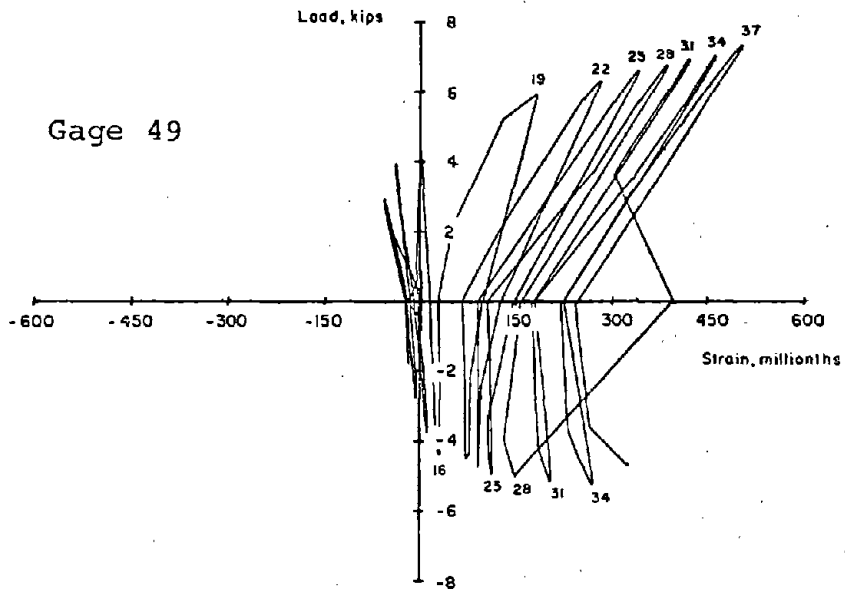


Fig. B-59 Load versus Diagonal Steel Strains for Specimen C8 (West Beam)



1 kip = 4.448 kN

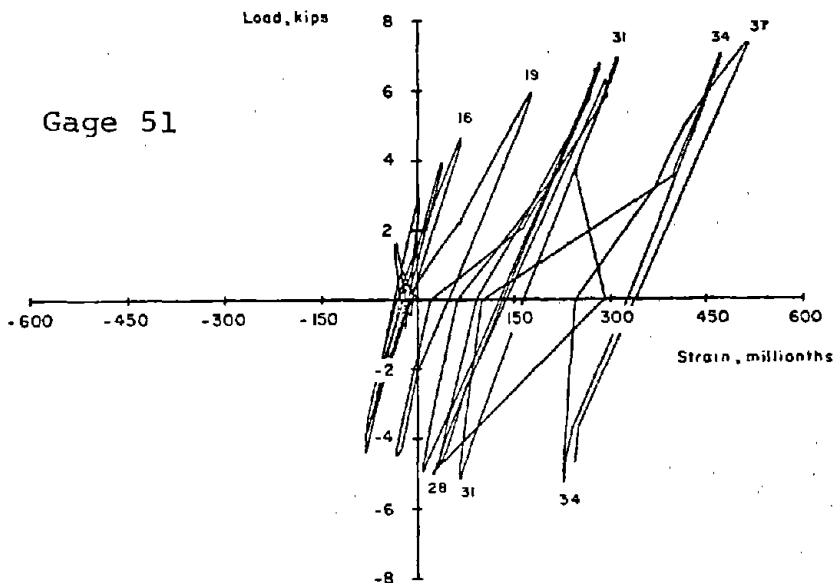
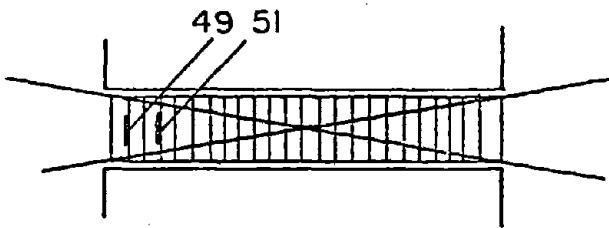
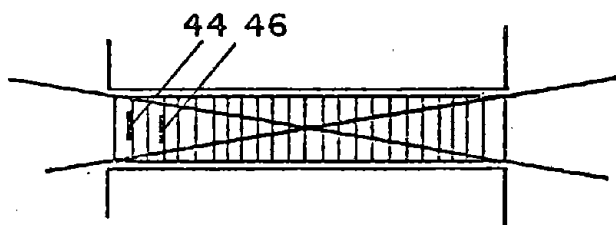
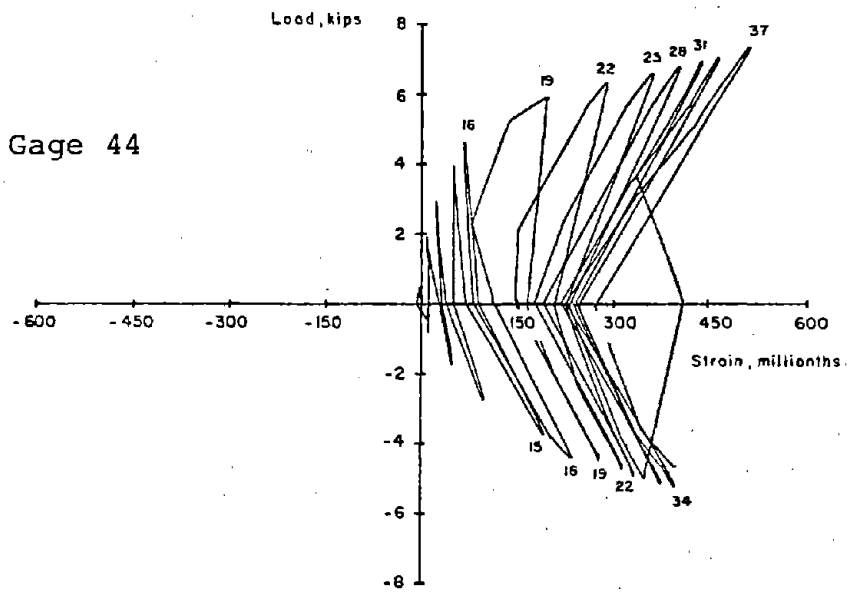


Fig. B-60 Load versus Hoop Steel Strains for Specimen C8 (West Beam)



1 kip = 4.448 kN

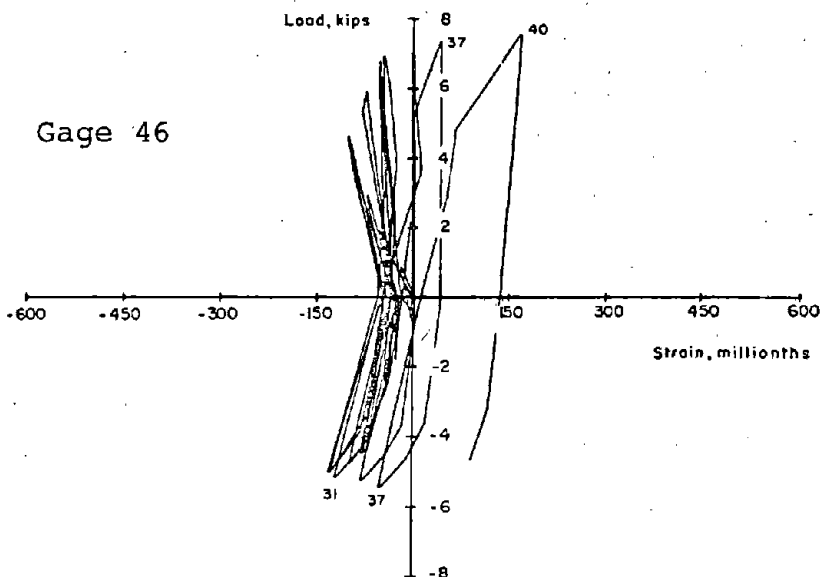
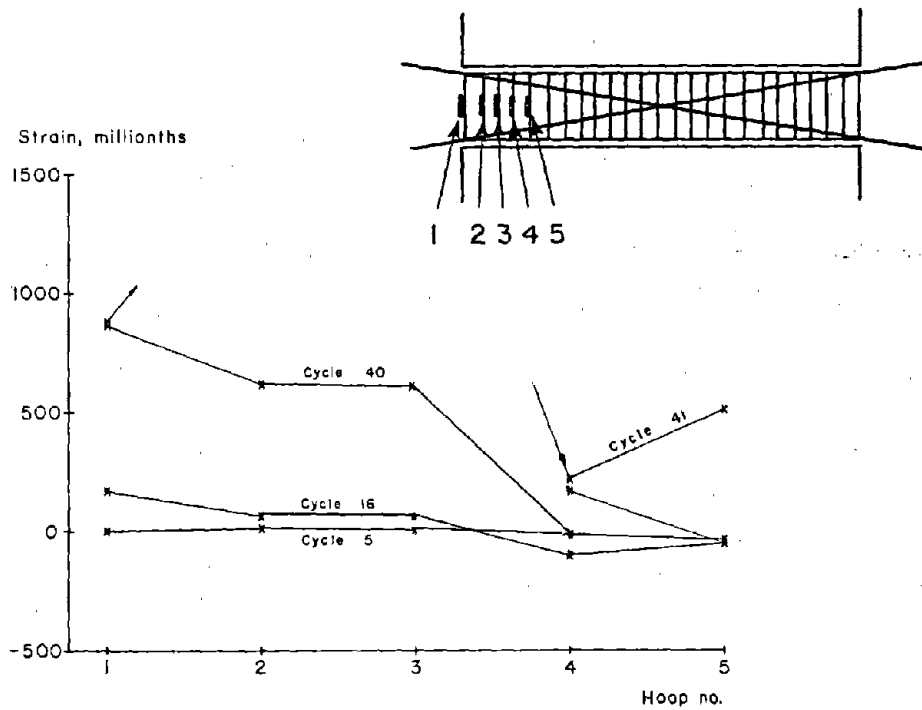
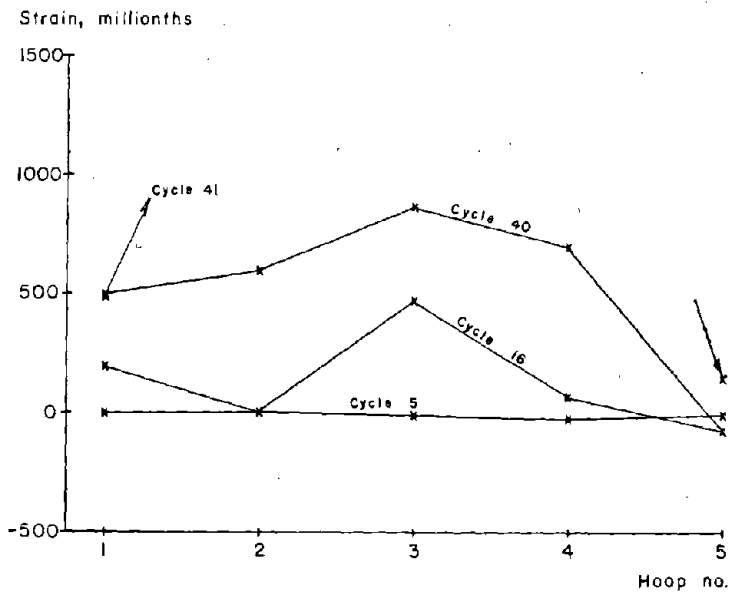


Fig. B-61 Load versus Hoop Steel Strains for Specimen C8 (East Beam)



a) East Beam



b) West Beam

Fig. 62 Hoop Steel Strain for Specimen C8

During application of load in the negative direction of the thirty-fifth inelastic load cycle, the No. 4 bar diagonal reinforcement of the east beam fractured. The test was terminated at this cycle. Maximum deflection imposed was 2.3 in. (57 mm). Applied load had dropped to 3.3 kips (14.9 kN) per beam.



## APPENDIX C - CALCULATION OF LOAD VERSUS DEFLECTION ENVELOPES

To understand the behavior of coupling beams under reversing loads, a comparison with behavior under monotonic loading conditions is useful. Since cost and time prohibited monotonic tests, calculated estimates of the load versus deflection relationships were made. Because of the complexities involved in calculating deflections for short beams and for beams with special reinforcement details, the results should be considered first order approximations. They do, however, give insight into the factors affecting deformations of the coupling beams.

### Basic Calculations

Calculations consisted of first estimating the moment versus curvature relationships for the beam cross sections. Then deflections caused by the applied forces were estimated from the moment versus curvature relationships. Only flexural deformations were considered. Shearing distortions and fixed end rotations caused by reinforcement slip were not included.

To obtain the calculated moment versus curvature relationships, a computer analysis of each cross section was performed. Analysis of sections was based on satisfying applicable conditions of equilibrium and strain compatibility.<sup>(10)</sup> A linear distribution of strain over the section was assumed. Measured material properties were used. The analysis considered complete stress-strain relationships for concrete and steel, including strain hardening of the reinforcement and the effect of confinement in the concrete compression block. The Kent and Park<sup>(11)</sup> relationship was used for the confined concrete stress versus strain relationship as shown in Fig. C-1. Reinforcing steel curves were idealized as shown in Fig. C-2.

Once the moment versus curvature relationships were obtained for the beam sections, deflections were estimated using ordinary principles of structural mechanics.<sup>(12)</sup> For specimens with special reinforcement details, section properties were idealized as shown in Figs. C-3 and C-4.

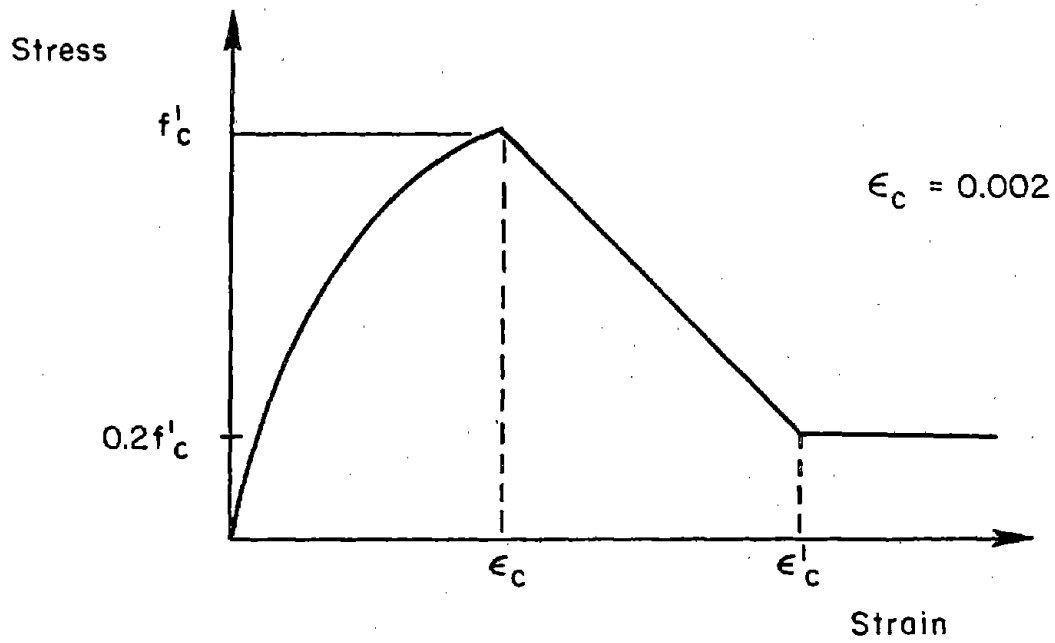


Fig. C-1 Idealized Stress versus Strain Relationship for Confined Concrete

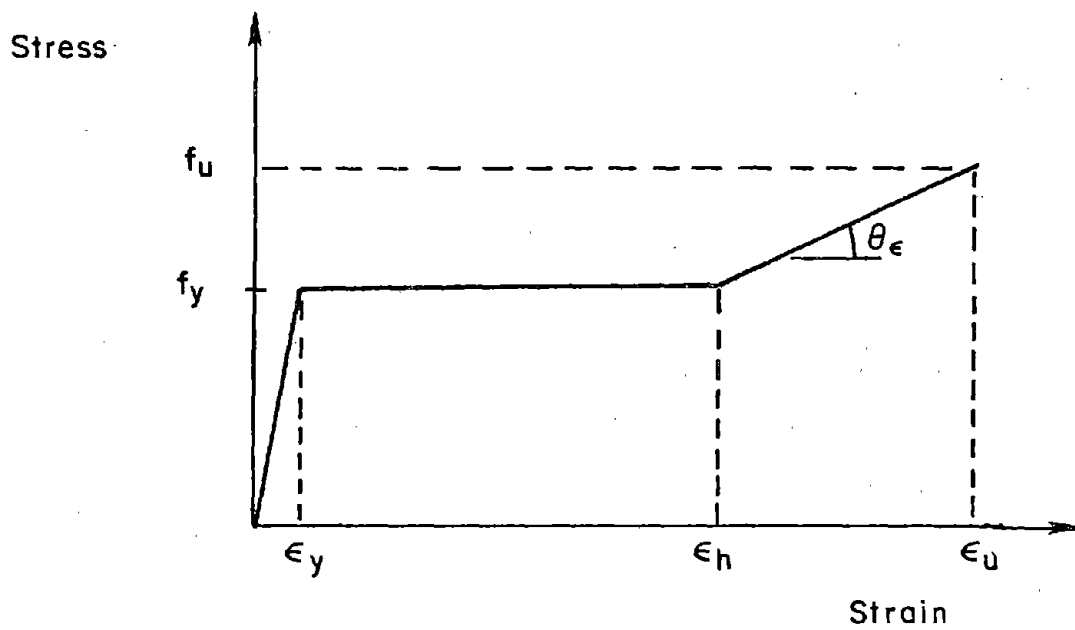


Fig. C-2 Idealized Stress versus Strain Relationship for Reinforcing Steel



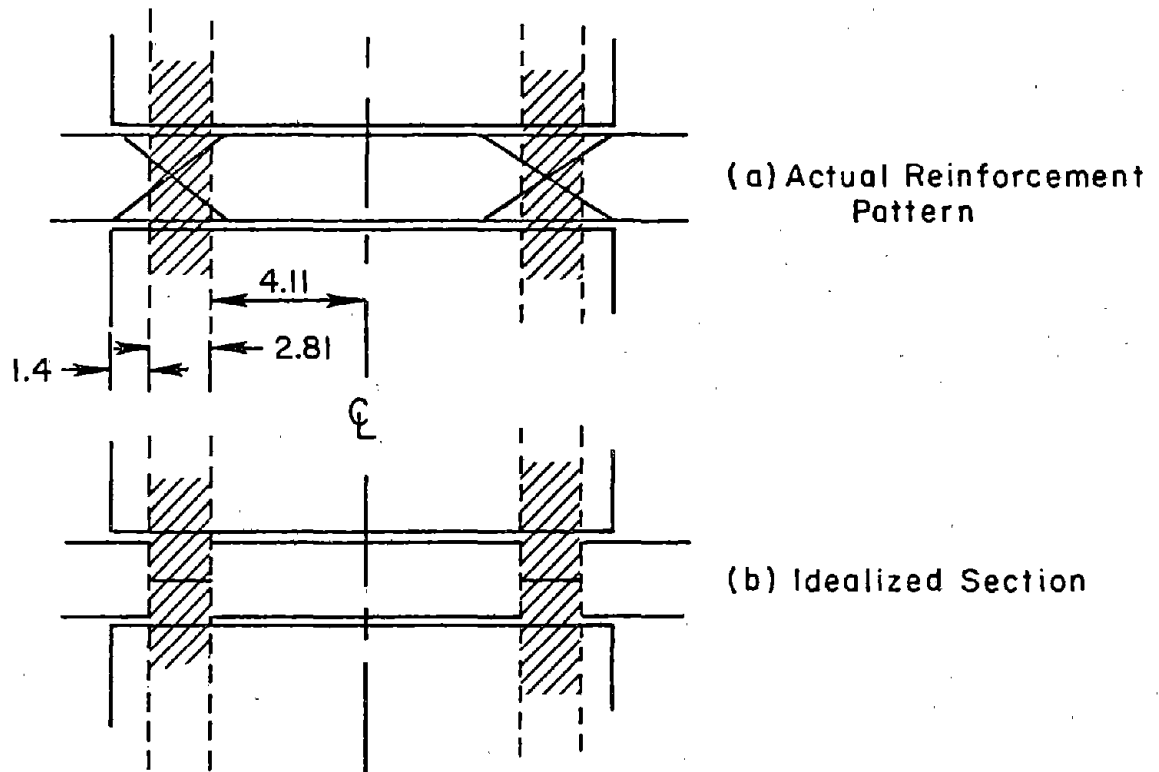


Fig. C-3 Idealized Sections for Specimens with Diagonals in Hinging Regions

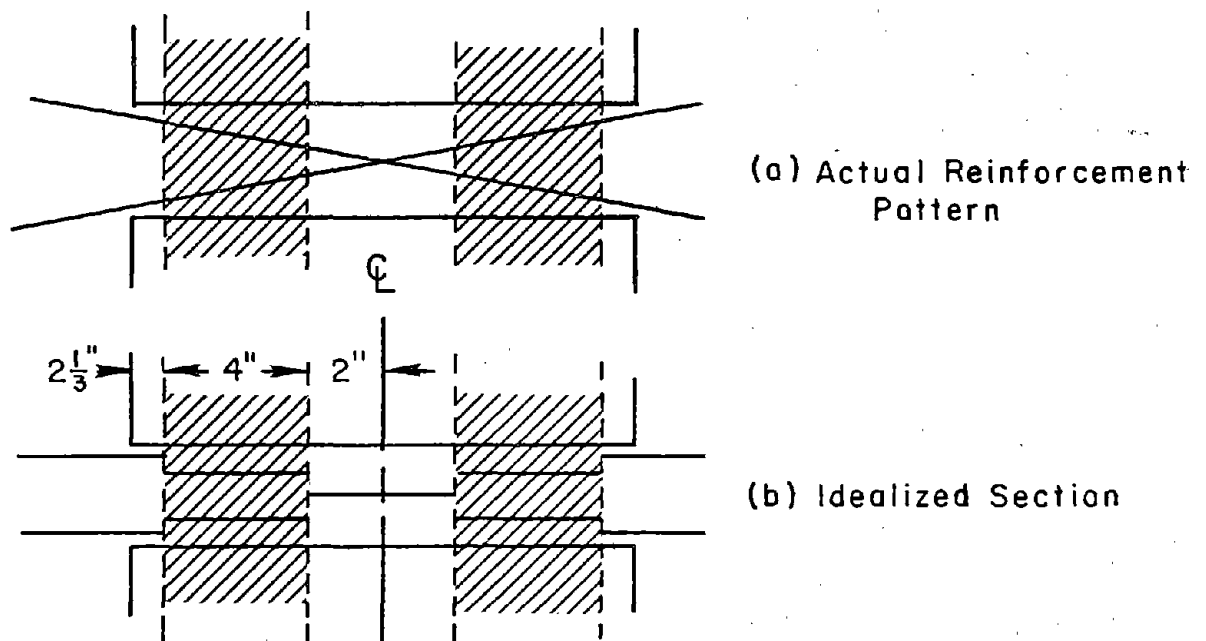


Fig. C-4 Idealized Sections for Specimens with Full-Length Diagonals

### Modified Calculations

In reinforced concrete flexural members inelastic curvature spreads over a "hinge length". Therefore, the theoretical curvature distribution corresponding to the actual moment distribution is not exactly representative of actual conditions. In addition, diagonal cracking affects the spread of the hinging region. This is particularly apparent in short-span beams such as those tested.

Bachmann's method<sup>(6,7)</sup> was used to include the effect of diagonal shear cracking on the spread of the hinging region. This method was only used for the short-span beams with conventional reinforcement, Specimens C2 and C5. With this method, an effective moment distribution is determined from the tension in the flexural steel. The calculated curvature is then related to this effective moment distribution.

The calculations described above were performed only to obtain an estimate of monotonic behavior. In both the basic and modified methods, no attempt was made to include the effects of bond slip and variation of steel strain between cracks. In the method used for diagonally cracked specimens, only the tensile strains are directly related to the effective moment distribution and plane sections do not remain plane. The calculated curvature is only approximately related to the effective moment at a section. Therefore, the calculated monotonic deflections should only be considered approximate values. However, the calculated monotonic strengths should be accurate estimates.

#### APPENDIX D - NOTATION

- $A_s$  = Cross-section area of reinforcement  
 $C$  = Compressive force  
 $C_n$  = Cumulative deflection ductility at  $n^{\text{th}}$  load cycle  
 $d$  = Effective depth of beam  
 $\Delta_i$  = Deflection at  $i^{\text{th}}$  load cycle with respect to the previous zero load position  
 $\Delta_y$  = Yield deflection  
 $e_v$  = Distance of the resultant stirrup shear force acting from the wall  
 $e_i$  = Cumulative energy dissipated in the  $i^{\text{th}}$  load cycle  
 $\epsilon_c$  = Concrete strain at ultimate strength  
 $\epsilon'_c$  = Concrete strain at  $0.2 f'_c$   
 $\epsilon_y$  = Yield strain  
 $\epsilon_n$  = Strain of steel when strain hardening occurred  
 $\epsilon_u$  = Strain of steel at ultimate load  
 $E_{mn}$  = Normalized cumulative energy dissipated  
 $j_d$  = Distance between compression and tension reinforcement in a beam  
 $f'_c$  = Ultimate compressive strength of concrete  
 $f_s$  = Stress in diagonal reinforcement  
 $\phi_y$  = Curvature at yield  
 $\phi_u$  = Curvature at ultimate  
 $M_{\text{cracking}}$  = Cracking moment  
 $M_y$  = Moment at yield  
 $M_u$  = Ultimate moment  
 $P_y$  = Yield load  
 $V_u$  = Maximum shear force  
 $z$  = Distance from support to point of counter flexure

